REGENERATED DESICCANT DEVICES FOR COOLING STORED GRAINS

by

LI CHEN

Thesis Submitted in Fulfilment of the Requirements
for the Degree of
Doctor of Philosophy

SCHOOL OF THE BUILT ENVIRONMENT
VICTORIA UNIVERSITY
MELBOURNE
AUSTRALIA

AUGUST, 2003

TO MY FAMILY, TEACHERS AND FRIENDS

STATEMENT

This thesis contains no material which has been previously submitted for any other degree or diploma in any University, and to the best of the author's knowledge and belief, the thesis contains no material previously published or written by another person, except where due reference has been made in the text.

Li Chen
School of the Built Environment
Victoria University
Melbourne
Australia

ABSTRACT

About 10% of all food grains that are harvested are ruined by insects and moulds during storage. One method of protecting stored grains is to cool them, as this reduces biological activities such as insect pest reproduction and mould growth. Cooling grains also reduces that rate at which moisture migrates from warm regions of a bulk of grain to cooler regions. There is resurgence in interest in physical methods of pest control, which is a result of the increasing restrictions on the use of chemically based control programs. Cooling can be achieved by forcing ambient air through grains, but the enthalpy of such air is often too high, particularly in tropical and subtropical climates, to achieve a sufficient degree of cooling. This thesis describes an augmentation of ambient aeration, which uses a desiccant device placed in a heat exchanger to produce the air that has a sufficiently low enthalpy to cool grains to safe storage temperatures.

The research is based on an understanding of the heat and mass transfer processes that occur in aerated grain silos. A manifestation of this understanding is the conservation equations of heat and mass transfer are formulated, and a three-dimensional mathematical model is presented for the behaviour of thermophysical processes occurring in a conical bottomed fitted with linear aeration ducts. This analysis is implemented by calculating the air flow field within the silo. The air flow field is three dimensional and it is determined by solving continuity's equation. We also formulated the equations for calculating the appropriate boundary conditions. The numerical solution of the model is obtained basis on the control-volume method by using an explicit upwind-difference scheme.

Sets of experimental recorded data obtained by CSIRO in Wongan Hills, Western Australia, are used to validate the mathematical model. The results of validation show that the calculated grain temperatures agree with the recorded data very well along the centerline of the silo and the more accurate methods of simulating the headspace and the wall of the silo need to be implemented in the model. In this thesis, this was achieved using the measured experimental data.

A detailed theoretical analysis of the conditions of the air leaving the desiccant devices is obtained for both cooling and regeneration processes. Two prototypes of a desiccant cooling system were built in Ararat, Victoria. The experimental testing was carried out in both the laboratory and field. The performance of the desiccant system was measured by the cooling degree in two silos. The experimental results show that 1) the wet-bulb temperature of ambient air can be reduced by 5 ~ 7°C during the cooling process, 2) the desiccant device can be regenerated completely in six hours with a regeneration temperature 65°C, 3) the average grain temperatures reduced by 11°C in both the wheat and canola silos.

The regression process of the recorded experimental data resulted in two empirical formulae for the performance of the desiccant cooling system. Combining with the degree of the regeneration of the desiccant the formulae can be used to calculate the condition of the air leaving the desiccant device during the cooling processes. The simulation study of the experimental recorded data shows that the calculated grain temperatures capture the recorded data very well along the centerline of the silo. The simulations have been used to demonstrate the efficacy of the time-proportioning algorithm to control the desiccant cooling system. The likely degree of improved cooling in the silos has been demonstrated by means of a mathematical model.

ACKNOWLEDGEMENT

I would like to express my gratitude to numerous people who have contributed to this project.

First of all, my most sincere gratitude goes to my supervisor Associate Professor. Graham R. Thorpe, for his generous assistance, invaluable encouragement and continuous support during the period of my candidature.

Thanks all staff members of A.F. Gason Pty Ltd at Ararat, Victoria, for supporting the field experimental study for this project.

Special gratitude goes to my husband Harry, my son Robin, my parents and my brother for their love and moral support during this project.

The financial support of Victoria University is gratefully acknowledged.

Finally, I would like to take this opportunity to express my thanks to Associate Professor Michael Sek, Professor Mike Xie and other faculty members and fellow friends of the School of the Built Environment.

TABLE OF CONTENTS

NOMENCLATURE

A	Convection-diffusion coefficient that is function of the Peclet number, P
A_{a_w}	Constant in equation (1.2) and (1.3)
A_B	General convection-diffusion coefficient at node **B**
A_E	General convection-diffusion coefficient at node **E**
A_N	General convection-diffusion coefficient at node **N**
A_P	General convection-diffusion coefficient at node **P**
A_p	Coefficient in equation (2.82)
A_{pest}	Coefficient in equation (1.5)
A_{pr}	Coefficient
A_S	General convection-diffusion coefficient at node **S**
A_{silo}	Area of silo, m^2
A_T	General convection-diffusion coefficient at node **T**
A_W	General convection-diffusion coefficient at node **W**
a	Constant
a_{pr}	Constant that depends on the permeability of the grain, the viscosity of air and the distance of two nodes
a_w	Water activity, the fractional relative humidity of interganualar air
b	Constant
b_p	Constant term in discretization equations
B	General coefficient
B_{a_w}	Constant in equation (1.2) and (1.3)

B_p	Coefficient in equation (2.82)
B_{pest}	Coefficient in equation (1.5)
c	Specific heat, J/kg/K
c_1	Specific heat of free water vapour, J / kg / K
c_2	Specific heat of carbon dioxide, J / kg / K
c_3	Specific heat of oxygen, J / kg / K
c_4	Specific heat of nitrogen and other non-reaction gases of intergranular air, J / kg / K
c_a	Specific heat of dry air, J / kg / K
c_σ	Specific heat of dry grain, J / kg / K
c_{s1}	Constant in equation (1.7)
c_{s2}	Constant in equation (1.7), °C^{-1}
C_{a_w}	Constant in equation (1.2) and (1.3)
C_{pest}	Concentration of pesticides
C^0_{pest}	The initial applied concentration of pesticides
d	Constant
d_{ist}	Radial distance of the node (i, j, k) from the vertical center-line of the silo, m
d_{ist1}	Radial shorter distances of the linear duct from the vertical center-line of the silo, m
d_{ist2}	Radial longer distances of the linear duct from the vertical center-line of the silo, m
d_{duct}	Diameter of the duct, m
D_b	General diffusion coefficient in discretization equations at the bottom surface of the control volume
D_e	General diffusion coefficient in discretization equations at the east surface of the control volume
D_n	General diffusion coefficient in discretization equations at the north surface of the control volume
D_s	General diffusion coefficient in discretization equations at the south

	surface of the control volume
D_t	General diffusion coefficient in discretization equations at the top surface of the control volume
D_w	General diffusion coefficient in discretization equations at the west surface of the control volume
dt	Time interval in numerical solutions, s
f	Weighting factor, between 0 to 1
f_{peak}	Calculation function of the grain temperature at the upper surface in the silo, °C
f_{sur}	Calculation function of surface temperature of the silo, °C
F_b	Flow rate through the control-volume bottom face, kg/m^{2}s
F_e	Flow rate through the control-volume east face, kg/m^{2}s
F_n	Flow rate through the control-volume north face, kg/m^{2}s
F_s	Flow rate through the control-volume south face, kg/m^{2}s
F_t	Flow rate through the control-volume top face, kg/m^{2}s
F_w	Flow rate through the control-volume west face, kg/m^{2}s
h_{base}	Height of cone base of the silo, m
h_{bulk}	Height of the grain bulk above the aeration duct, m
h_i	Enthalpy refer to the corresponding chemical species, $i=$ 1, 2, 3, 4, J/kg, $i=$ 1, 2, 3, 4
h_{ijgh}	Height of the node (i, j, k) on the hopper bottom, m
h_s	Latent heat of vaporization of water in grain, J / kg
h_{top}	Height of the natural conical top, m
h_v	Latent heat of vaporization of free water, J / kg
h_{wall}	Height of a silo wall, m
h_W	Differential heat of wetting of grain per unit mass of water, J/kg
h_γ	Enthalpy of moist air, J/kg$_{\text{dry air}}$
h_σ	Enthalpy of dry grain, J/kg
h_σ^0	Reference enthalpy of dry grain, J/kg

H	Enthalpy of moist grain, J/kg
H_w	Integral heat of wetting of grain, J / kg
k	Constant, °C $^{-1}$
k_{eff}	Effective thermal conductivity of bed of grain, W/m/K
k_{ind}	Label of nodes according to its types in numerical solutions
k_v	Constant in Equation (1.7)
kk	Count
K	Constant
L_{duct}	Total length of the duct, m
m	Maintenance coefficient, J/s
M	Moisture content of grain as a percentage, wet basis, %
n	Count
ni	Number of nodes in x-direction that setup as an odd number
n_{imid}	Mid-point between 1 and ni
nj	Number of nodes in y-direction that setup as an odd number
n_{jmid}	Mid-point between 1 and nj
nk	Number of nodes in z-direction that setup as an odd number
n_{r1}	Node number in x-direction corresponding to the end of the duct near to the centre of the silo
n_{r1}	Node number in x-direction corresponding to the end of the duct further away from the center of the silo
N	The number of insect in a silo
N_0	The initial number of insect in a silo
p	Pressure, Pa
p_0	Vapour pressure of water, Pa
p_1	Pressure in control-volume 1, Pa
p_2	Pressure in control-volume 2, Pa
p_3	Pressure in control-volume 3, Pa
p_4	Pressure in control-volume 4, Pa
p_5	Pressure in control-volume 5, Pa

p_{duct}	Pressure in the aeration duct, Pa
p_n	Pressure to the impermeable boundaries, Pa
p^*	Vapour pressure at the face of a control-volume, Pa
p_1^*	Vapour pressure at the face **1** of a control-volume, Pa
p_2^*	Vapour pressure at the face **2** of a control-volume, Pa
p_3^*	Vapour pressure at the face **3** of a control-volume, Pa
p_4^*	Vapour pressure at the face **4** of a control-volume, Pa
p_5^*	Vapour pressure at the face **5** of a control-volume, Pa
p_E^*	Vapour pressure at the face **E** of a control-volume, Pa
p_P^*	Vapour pressure at the face **P** of a control-volume, Pa
p_W^*	Vapour pressure at the face **W** of a control-volume, Pa
p'	Pressure correction, Pa
p_1'	Pressure correction at the face **1** of a control-volume, Pa
p_2'	Pressure correction at the face **2** of a control-volume, Pa
p_3'	Pressure correction at the face **3** of a control-volume, Pa
p_4'	Pressure correction at the face **4** of a control-volume, Pa
p_5'	Pressure correction at the face **5** of a control-volume, Pa
p_E'	Pressure correction at the face **E** of a control-volume, Pa
p_P'	Pressure correction at the face **P** of a control-volume, Pa
p_W'	Pressure correction at the face **W** of a control-volume, Pa
p_s	Saturation vapour pressure of water, Pa
P	Peclet number that is the ratio of the strengths of convection and diffusion at the control-volume faces
P_b	Peclet number that is the ratio of the strengths of convection and diffusion at the control-volume bottom face
P_e	Peclet number that is the ratio of the strengths of convection and diffusion at the control-volume east face
P_n	Peclet number that is the ratio of the strengths of convection and diffusion at the control-volume north face
P_s	Peclet number that is the ratio of the strengths of convection and

	diffusion at the control-volume south face
P_t	Peclet number that is the ratio of the strengths of convection and diffusion at the control-volume top face
P_w	Peclet number that is the ratio of the strengths of convection and diffusion at the control-volume west face
Q	Total heat generated per unit mass of grain, J/kg
Q_f	Volume flow rate of air through the silo, m^3/s
R_{node}	Radius of a circular silo, m
R_p	Specific empirical constant in equations (3.101), (3.102), (3.103), (3.104), (3.105), (3.108) and (3.112)
R_s	Solar radiation, $\mathrm{W/m}^2$
R_{silo}	Radius of a circular silo, m
r_{e1}	Radial shorter distances of the east linear duct from the vertical center-line of the silo, m
r_{e2}	Radial longer distances of the east linear duct from the vertical center-line of the silo, m
s_5	Mass variation of dry grain, kg/kg / day
S	General source term in governing equations
S_1	Mass variation of water vapour, $\mathrm{kg/m}^3/s$
S_2	Mass variation of carbon dioxide, $\mathrm{kg/m}^3/s$
S_3	Mass variation of oxygen, $\mathrm{kg/m}^3/s$
S_4	Mass variation of nitrogen and other non-reaction gases of intergranular air, $\mathrm{kg/m}^3/s$
S_5	Mass variation of dry grain, $\mathrm{kg/m}^3/s$, $S_5 = \dfrac{s_5 \rho_\sigma}{3600 \times 24}$
S_p	Source term at node **P**
$SWBT$	Wet-bulb temperature of intergranular air in moisture equilibrium with the grain, °C
t	Time, s
$t_{\frac{1}{2}}$	Time for a given pesticide's concentration of residue to decay to half that concentration, week

t_{50}	Time for seed viability to decline from 100% to 50%, day
t_h	Time of day, hour
t_{mon}	Time used in empirical equations that governs insect population growth, month
t_{pest}	Time used in empirical equations that governs rate of decay pesticides, week.
t_s	Safe storage time, s
T	Equilibrium temperature, °C
T_a	Air temperature, °C
T_{amb}	Ambient dry-bulb temperature, °C
$T_{d_{max}}$	Maximum daily temperature, °C
$T_{d_{min}}$	Minimum daily temperature, °C
$\overline{T}_d$	Average daily temperature, °C
T_{duct}	Grain temperature at the duct boundary which is equilibrium with aerated air, °C
T_B	Temperature at grid point, **B**, °C
T_E	Temperature at grid point, **E**, °C
T_{head}	Air temperature in the headspace of a silo, °C
$T_{i,j,k}$	Grain temperature at the grid (i,j,k), °C
T_{max}	Maximum temperature, °C
T_N	Temperature at grid point, **N**, °C
T_{set}^{0}	Old setpoint of the controller, °C
T_{set}^{on}	New setpoint of the controller for switching on, °C
T_{set}^{off}	New setpoint of the controller for switching off, °C
T_S	Temperature at grid point, **S**, °C
T_S	Temperature at grid point, **S**, °C
T_{SWBT}	Wet-bulb temperature of intergranular air in moisture equilibrium with the grain, °C
T_T	Temperature at grid point, **T**, °C

T_W	Temperature at grid point, **W**, °C
T_σ	Grain temperature, °C
$T_{\sigma_{wb}}$	Grain wet-bulb temperature in moisture equilibrium with the interstitial air, °C
$T_{\sigma_{wb}}^{0}$	Grain wet-bulb temperature threshold in Equation 1.4, °C
$T_{\sigma_{wb}}^{\max}$	The maximum limit of grain wet-bulb temperature that can be used in Equation 1.4, °C
$\mathbf{v}$	General velocity vector, m/s
$\mathbf{v}_1$	Velocity vector of water vapour, m/s
$\mathbf{v}_2$	Velocity vector of carbon dioxide, m/s
$\mathbf{v}_3$	Velocity vector of oxygen, m/s
$\mathbf{v}_4$	Velocity vector of nitrogen and other non-reaction gases of intergranular air, m/s
$\mathbf{v}_a$	Velocity vector of intergranular dry air, m/s
$\mathbf{v}_\gamma$	Mass average velocity vector of intergranular air, m/s
v_e	Mass average component of velocity of intergranular air through east face, **e**, of the control-volume in **x**-direction, m/s
v_x	Mass average component of velocity of intergranular air in x-direction in the control-volume, m/s
v_w	Mass average component of velocity of intergranular air through west face, **w**, of the control-volume in **x**-direction, m/s
v^*	Guessed component of mass average velocity of intergranular air in x-direction in the control-volume, m/s
v_e^*	Guessed component of mass average velocity of intergranular air through east face, **e**, of the control-volume in **x**-direction, m/s
v_w^*	Guessed component of mass average velocity of intergranular air through west face, **w**, of the control-volume in **x**-direction, m/s
v'	Velocity correction of intergranular air in x-direction in the control-volume, m/s
v_e'	Velocity correction of intergranular air through east face, **e**, of the control-volume in **x**-direction, m/s

v'_w	Velocity correction of intergranular air through west face, **w**, of the control-volume in **x**-direction, m / s
u_n	Mass component of average velocity of intergranular air through north face of the control-volume in **y**-direction, m / s
u_s	Mass component of average velocity of intergranular air through south face of the control-volume in **y**-direction, m / s
u_y	Mass component of average velocity of intergranular air in y-direction in the control-volume, m / s
w	Humidity ratio of the intergranular air in equilibrium with grain, $kg / kg_{dry\ air}$
w_b	Mass average velocity of intergranular air through bottom face of the control-volume in **z**-direction, m / s
w_t	Mass average velocity of intergranular air through top face of the control-volume in **z**-direction, m / s
w_0	Constant
w_z	Mass average velocity of intergranular air in z-direction in the control-volume, m / s
W	Moisture content of grain as a fractional dry basis, kg/kg
W_{duct}	Moisture content of grain at the duct boundary which is equilibrium with aerated air, dry basis, kg/kg
$W_{i,j,k}$	Grain moisture content at the grid (i, j, k), kg/kg
W_{silica}	Moisture content of silica gel as a fractional, dry basis, kg/kg
X_{max}	Maximum mould population sustainable per unit mass of grain, kg^{-1}
δx	x-direction distance between two adjacent grid points, m
yl	Diameter of the silo, m

Greek symbols

α_B	Coefficient in the discretization equations

α_E	Coefficient in the discretization equations
α_N	Coefficient in the discretization equations
α_P	Coefficient in the discretization equations
α_S	Coefficient in the discretization equations
α_T	Coefficient in the discretization equations
α_W	Coefficient in the discretization equations
Δh	Heat of oxidation of 1 kg of grain substrate, J/kg
ΔH	Heat of oxidation of one molar mass of cellulosic material at room temperature, J/mol
Δp_{linear}	Pressure drop arising from of linear term in pressure gradient equations, Pa
Δt	Time step used in numerical integration, s
ΔT	The change in temperature, °C
ΔT_{cool}	The change of dry-bulb temperature of the process air after desiccant cooling processes, °C
$\Delta T_{WB_{cool}}$	The change of wet-bulb temperature of the process air after desiccant cooling processes, °C
Δx	x-direction width of control volume, m
δx	x-direction distance between two adjacent grid points, m
yl	Diameter of the silo, m
Δy	y-direction width of control volume, m
δy	y-direction distance between two adjacent grid points, m
Δz	z-direction width of control volume, m
δz	z-direction distance between two adjacent grid points, m
Γ	General diffusion coefficient,
ε_γ	Void fraction of bulk grain (porosity)
ε_p	Occupancy fraction of grain Kerri in the bulk
θ_1	Angle of cone base of a silo, degree
θ_2	Angle of natural conical top of grain in a silo, degree
ρ	Density of the matter discussed in discretization equations, kg / m^3_{air}

ρ_1	Mass of water vapour per unit mass of interganualr air, kg / m^3_{air}
ρ_2	Mass of carbon dioxi de per unit mass of interganualr air, kg / m^3_{air}
ρ_3	Mass of oxygen per unit mass of interganualr air, kg / m^3_{air}
ρ_4	Mass of nitrogen and other non-reaction gases per unit mass of intergranular air, kg / m^3_{air}
ρ_a	Density of intergranular dry air, kg / m^3
ρ_γ	Density of intergranular air, kg / m^3
ρ_σ	Bulk density of dry grain, kg / m^3
ϕ	Air relative humidity (percentage), %
ϕ_{duct}	Air relative humidity at the outlet of aeration duct in a silo, %
ϕ_{head}	Air relative humidity in the head space of a silo when aeration, %
$\phi_{initial}$	Initial relative humidity of the air leaving the desiccant unit during the cooling processes, %
Φ	General dependent variable in governing equations

Subscripts

a	Refers to intergranular dry air
B	Neighbour in the negative z direction, i.e., at the bottom
b	Control-volume face between nodes **P** and **B**
E	Neighbour in the negative x direction, i.e., on the east side
e	Control-volume face between nodes **P** and **E**
i	Number of grids in x-direction
j	Number of grids in y-direction
k	Number of grids in z-direction
N	Neighbour in the negative y direction, i.e., on the north side
n	Control-volume face between nodes **P** and **N**
P	Central grid point under consideration
S	Neighbour in the negative y direction, i.e., on the south side
s	Control-volume face between nodes **P** and **S**
T	Neighbour in the negative z direction, i.e., at the top

t	Control-volume face between nodes **P** and **T**
W	Neighbour in the negative x direction, i.e., on the west side
w	Control-volume face between nodes **P** and **W**
γ	Refers to intergranular moist air
σ	Refers to grains

Superscripts

0	Old value (at time t) of the temperature or moisture content

Special symbol

$[[A, B, C, ...]]$	Largest value of A, B, C, ...

LIST OF FIGURES

LIST OF TABLES

CHAPTER 1

INTRODUCTION

In 1997, the annual world production of cereal grains was around 2096 million tones, an amount that constituted 50% of the quantity of global agricultural and fish production (FAO, 1998). About 900 million tonnes of grain are currently in storage through the world at any given time, nearly one half of annual world production (Jayas *et al.*, 1995). Protection of this commodity is critical to alleviating human hunger, since cereal grains are the largest energy resource for human beings in that 50% of their energy supply is from cereals (FAO, 1998).

During storage, grain has to be stored in good condition for prolonged periods of time, and free from spoilage caused by live insect pests and mould growth. One strategy of achieving these aims is to cool the grains with aeration to temperatures at which insects are unable to breed and moulds are unable to grow. As noted by many and quantified by Thorpe *et al.* (1992a, b), aeration achieves an intergranular wet-bulb temperature in equilibrium with the inlet air. The work of Sutherland *et al* (1971) indicates that under certain climatic conditions such as in the tropics or sub-tropics, ambient aeration cannot cool the grains to the desirable temperatures because of the high ambient wet-bulb temperatures. In these situations, air conditioning methods need to be introduced into aeration to enhance stored grain cooling; one of those methods is desiccant dehumidification.

Desiccant cooling and dehumidification have received much attention as viable alternatives for the air conditioning (Pesaran, 1992 and ASHRAE, 1992) and been successfully used in commercial and residential buildings. Although the principle of desiccant dehumidifiers cooling stored grains as revealed by Thorpe (1982) very few works on desiccant cooling stored grains have been reported in the literature (Rodda *et al.*, 1977, Chau, 1982; Miller, 1984, Thorpe, 1985, Ahmad *et al.*, 1996), and no results reported on the comprehensive design, operation, assessment and optimization of a desiccant dehumidifier cooling system for stored grains. This represents a serious gap in the knowledge required for the efficient cooling stored grains with the latest air-conditioning technology.

In response to this issue, we have studied a desiccant cooling device which is a novel air-conditioning system for stored grain aeration. The experimental and computational investigation reported in this thesis will be valuable in developing a fundamental understanding of desiccant cooling techniques and it will also lead to practical computation and design modeling used to implement stored grain aeration systems.

To achieve these aims, descriptive materials are needed to understand how the cool stored grains are preserved with changing the grain thermophysical conditions and protecting the grain from spoilage. Those include psychrometrical properties of air and grain, and the quantification of those factors that result in grain spoilage. A brief review of theory and practice relevant to technologies of aeration cooling for stored grains have been highlighted.

1.1 Psychrometrics

Psychrometrics is the quantitative description for the thermophysical properties of mixtures of air and water vapour. In this thesis we use psychrometrics to quantify the processes and results of stored grain cooling because the temperature and moisture content are the key determinants of good grain storage.

1.1.1 Psychrometrical definitions

Air is a mixture of dry air and water vapour, namely *moist air*. The properties of this mixture of gases can be specified by any two of the properties: *temperature* (dry-bulb temperature, °C), *humidity* (humidity ratio, g/kg $_{\text{dry air}}$, or relative humidity, %) and *saturation* (wet-bulb temperature, °C or dew point, °C) (ASHRAE, 1997). The thermophysical properties of stored grains can be described in terms of *temperature* (°C) and *moisture content* (% wet basis, or % dry basis).

The condition of intergranular air that resides in the spaces between the grain kernels is assumed to be the air that is in thermodynamic equilibrium with grain (Sutherland *et al.*, 1971). Grain storage technologists often use two terms to help define the moisture content of this intergranular air. One term is *water activity* (a widely used term) and the other is peculiar piece of jargon, namely the *seed wet-bulb temperature, SWBT* (°C) (Wilson, 1993). The water activity is the fractional relative humidity of intergranular air in equilibrium with the grain. The grain wet-bulb temperature is the value of the wet-bulb temperature of intergranular air in equilibrium with the grain.

To define thermophysical properties within an aerated grain silo, Sutherland *et al.* (1971) recommended that both thermal and moisture equilibrium relationships are believed to be maintained, or very closed approximated, for the air flowing between the grain kernels at the low flow rates used for aeration. Thorpe *et al.* (1992a, 1992b) established the conditions that must be satisfied if thermodynamic equilibrium may be assumed, and showed that the thermal equilibrium between the intergranular air and the grain is almost always achieved but moisture equilibrium is attained only under more restricted conditions.

We note that the calculation of thermophysical properties of air and grains within an aerated grain silo is one of critical issues in this thesis. So far the assumption of both thermal and moisture equilibrium of grain and intergranular air maintained in a silo containing grains is widely used in the literature, and we make use of this assumption in the study and validate it in Chapter 4.

1.1.2 Calculation of equilibrium isotherms for bulked grains

The widely used quantified analysis on equilibrium isotherms of bulk grains is used for calculations of water activity with empirical models. In general, the water activity,

a_w, can be expressed as follows

$$a_w = f(T_\sigma, W) \tag{1.1}$$

where T_σ is the grain temperature and W is the moisture content of grain expressed on a fractional dry basis.

The American Society of Agricultural Engineers (ASAE, 1998) accepted five standard equations in the ASAE Standards D245.5 OCT95, namely the modified Henderson, Chung-Pfost, Halsey, Oswin equations and Guggenhein-Anderson-deBoer (GAB) equation. Wilson (1993) developed psychromatric charts for the common grain species of Australian bases on Hunter's isosteric equation (Hunter, 1987) that show the equilibrium relationship as lines of equilibrium grain moisture concentration, M, (wet-basis).

So far, none of the proposed models has been adequate over the entire range of relative humidity (Cenkoski *et al.*, 1995). It was indicated by Chen *et al.* (1989) that the modified Henderson and Chung-Pfost equations are good models for starchy grains and fibrous materials. For high oil and protein products the modified Halsey equation is more suitable. The modified Oswin equation appears to be suitable for popcorn, corncobs, whole pods of peanuts and some varieties of corn.

In Australia, the main stored grains are wheat and barley that both are starchy grain species, and some oilseeds such as canola or sunflower seeds along with legumes also need to be stored. Hence, in this thesis we use the modified Chung-Pfost and modified Halsey equations for equilibrium calculations.

Modified Chung-Pfost Equation

$$a_w = \exp\left[-\frac{A}{T_\sigma + C}\exp(-100BW)\right] \tag{1.2}$$

Modified Halsey Equation

$$a_w = \exp\left[-\frac{\exp(A - BT_\sigma)}{(100W)^C}\right] \tag{1.3}$$

where a_w is the water activity of grain, T_σ is the temperature of grain in °C, W is the moisture content of grain (dry basis), and A_{a_w}, B_{a_w}, and C_{a_w} are constants listed in table 1.1.

Table 1.1 Isotherm equation constants for agricultural products

Commodity	Equation	A_{a_w}	B_{a_w}	C_{a_w}
Barley	Modified Chung-Pfost	475.12	0.14843	71.996
Corn (Shelled)	Modified Chung-Pfost	374.34	0.18662	31.696
Oats	Modified Chung-Pfost	442.85	0.21228	35.803
Rice	Modified Chung-Pfost	412.02	0.17528	39.016
Wheat	Modified Chung-Pfost	377.52	0.16456	35.59
Canola	Modified Halsey	3.0026	-0.0048967	1.7607
Peanuts	Modified Halsey	3.6616	0.1756	2.2375
Soybeans	Modified Halsey	2.87	-0.0054	1.38
Sunflower seed	Modified Halsey	2.7663	-0.0149	1.8375

Source: ASAE, 1998

When equations (1.2) and (1.3) are inverted, they can be used to calculate the grain moisture content, W, corresponding to a given dry-bulb temperature, T_σ, and a given water activity, a_w, (or relative humidity, ϕ).

In order to obtain an easy-to-understand and user-friendly explanation of the aeration processes, we also used the grain psychrometric charts (Wilson, 1993) for qualitative analysis.

1.2 Spoilage of stored grain

Stores must be provided for most of the grain harvested until it is needed for consumption, since grain production is seasonal and consumption is continuous. However stored grains are subject to predation by moulds, insects and mites. As a result, the stored grains will reduce in value and even become completely ruined by spoilage arising from mould growth and insect development.

1.2.1 Insects pests

The largest single threat to stored grains is the multitude of insects. They can cause losses in weight and quality (impurities such as frass, cocoons and fragments of insects, reduction of nutritional value, reduction in germination power), and insects also alter the environment in which they develop to encourage other deteriorative factors such as moulds (Harein *et al.*, 1992).

For insects living in stored grains, the growth of insects largely relies on the temperature and moisture content of the surrounding air for their supply of heat and water. Imagine that when we make the surrounding air cool or dry, or both, so the insects cannot get enough growth input, the insects are unable be to breed or even survive and the insect pests can not occur in grain storage. This is the critical to preserving stored grain with environmentally benign methods.

In spite of the restricted conditions in the laboratory which rarely occur in the real grain storages, we have used such data to estimate the insect population growth with a general empirical model, equation (1.4), presented by Desmarchelier (1993) with the laboratory data on the intrinsic rates of increase of eight species of *Coleoptera*. A multiple, N/N_0, in a specific time period (month, week or day) is used to define the insect population growth where N is the number of insects in a silo and N_0 is the initial number. N/N_0 can be calculated as follows.

$$\log_{10}(N/N_0) = k\left(T_{\sigma_{wb}} - T^0_{\sigma_{wb}}\right)t_{mon}, \qquad T_{max} > T_{\sigma_{wb}} > T^0_{\sigma_{wb}} \qquad (1.4)$$

where $T_{\sigma_{wb}}$ is the grain wet-bulb temperature, k is a constant, and $T^0_{\sigma_{wb}}$ is the grain wet-bulb temperature threshold. The constants are specific to grain insect species and for the nine species that are commonly found in Australian silos the values of k and $T^0_{\sigma_{wb}}$ are listed in table 1.2.

Table 1.2 Constants in equation 1.4 for insect population growth (Desmarchelier, 1993)

Species	Commodity used in experiment	Constant k, °C^{-1}	Wet-bulb temperature $T^0_{\sigma_{wb}}$, °C	Maximum wet-bulb temperature* $T^{max}_{\sigma_{wb}}$, °C
Sitophilus oryzae	wheat	0.089	9.0	24
Sitophilus zeamais	wheat	0.031	14.0	21
Sitophilus granarius	wheat	0.146	8.5	24
Rhyzopertha dominica	wheat	0.170	13.0	26
Tribolium castaneum	wheat	0.080	13.0	30
	sorghum	0.138	13.0	28
	flour	0.210	16.0	26
Oryzaephilus surinamensis	flour	0.130	16.0	28
Oryzaephilus mercator	flour	0.084	12.0	28
Lasioderma serricorne	flour	0.021	14.0	26

* The maximum limit of grain wet-bulb temperature that can be used in equation 1.4

The temperature threshold, $T^0_{\sigma_{wb}}$, can be explained as that the rate of growth can be zero or less if the grain wet-bulb temperature is below $T^0_{\sigma_{wb}}$. In general, the wet-bulb temperature of stored grain should be at or below $T^0_{\sigma_{wb}}$ to avoid pests occurring in the silo.

1.2.2 Moulds

Mould, or fungal, growth is a major problem in stored grains throughout the world and can lead to poor appearance of the products due to deterioration of colour, texture and taste, loss of seed germination ability, energy and nutritional loss, allergies in humans and domestic animals, infection, and production of secondary metabolites including mycotoxins, antibiotics, and pharmacologically active substances (Frisvad, 1995). The presence of any such secondary metabolites in food and feed is undesirable due to the poison produced by mycotoxins.

In general, moulding processes are strongly related to grain temperature and moisture content. Wilson (1993) noted that moulding normally occurs at moisture contents and temperatures in a region that is called a '*mould envelope*'. The ten common stored grains' mould envelopes have presented both in tables and figures (Wilson, 1993).

Figure 1.1 shows the mould envelope for barley. When the temperature or moisture content, or both, are reduced until the condition of grain outsides the mould

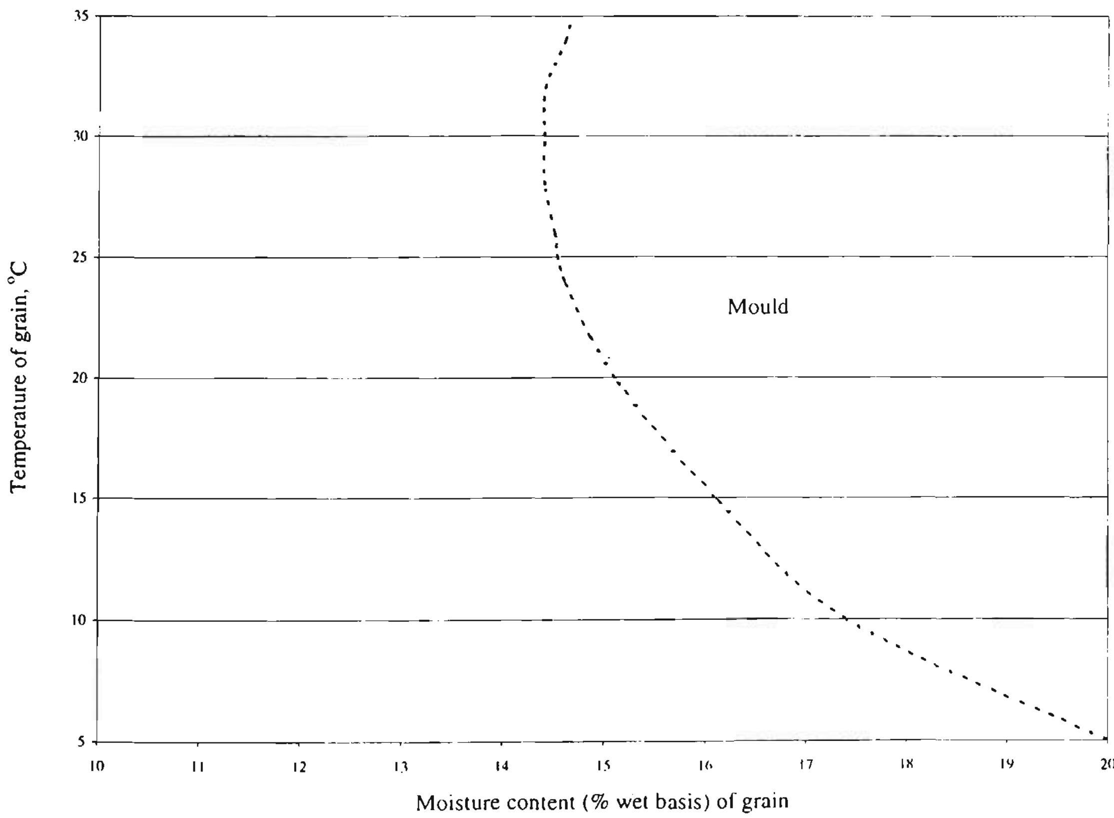

Figure 1.1 Mould envelope, barley

envelope the moulding process can be avoided in the silo.

In figure 1.1 we also can see that when moisture content of grain is small *e.g.* a value smaller than 14% wet basis, the moulding does not occur no matter what the grain temperature is. This situation indicates that most fungi require a water activity, a_w, of 0.7 at least to grow, an ' spoilage increases greatly above 0.8 (Wilson *et al.*, 1992). Therefore, moulding can be avoided when the grains are stored under the conditions with a water activity, a_w, below o.7.

1.2.3 Breakdown of pesticides

Grain protectants are chemicals applied to stored grain that will persist for extended periods at concentrations lethal to target insects so that the insects are killed. Due to their low cost, easy application and great effectiveness, chemical protectants are very commonly applied to stored grains worldwide.

In time, pesticides applied to grain decay. The rate of decay of pesticides can be quantified by the protectants' '*half-lives*', $t_{1/2}$, which is the time for a given pesticide's concentration to decay to a half of its initial concentration. Desmarchelier (1993) summarized experimental reports of six pesticides that the logarithms of protectants' '*half-lives*', $t_{1/2}$, week, are linear functions of the wet-bulb temperature of grain in equilibrium with intergranular air, $T_{\sigma_{wb}}$, given as

Table 1.3 Parameter values for protectants' 'half-lives'

Insecticide	A_{pest}	B_{pest}
Dichlorvos	0.00	0.050
Methacrifos	0.85	0.050
Malathion	0.95	0.051
Fenitrothion	1.18	0.038
Bioresmethrin	1.41	0.035

Source: Desmarchelier, 1993

$$\log_{10}(t_{1/2}) = A_{pest} + B_{pest}(20 - T_{\sigma_{wb}}) \tag{1.5}$$

where A_{pest} and B_{pest} are constants that are different for each pesticide and table 1.3 shows the their values for the five chemicals.

The relationship between the concentration of pesticides, C_{pest}, after a time, t_{pest}, week, is given by Desmarchelier (1993) as

$$C_{pest} = C_{pest}^{0} \exp\left(-0.30 \frac{t_{pest}}{t_{1/2}}\right) \tag{1.6}$$

where C_{pest}^{0} is the initial concentration of residue, and $t_{1/2}$ is the *half-life* of the pesticide, week.

It can be seen from equations (1.5) and (1.6) that when grain wet-bulb temperature, $T_{\sigma_{wb}}$, is reduced by reducing either the grain temperature or its moisture content, or both, the pesticides half-life, $t_{1/2}$, will increase. Consequently, the rate of reduction of C_{pest} will be slowed down and the time can be extended over which pesticide concentrations remain high enough to be effective against insects. It also permits a reduction in the amount of pesticide initially applied to the stored grains.

1.2.4 Loss of seed viability in stored grains

If food grains and oilseeds are stored for a sufficiently long period, certain changes in quality occur. In spite of major spoilages caused by insect pests and mould growth in stored grain, in this sub-section we discuss the loss of seed viability in ideally "*clean*" conditions; grains are free from insects and moulds. As far as possible, only the intrinsic property of the commodity is examined (Roberts, 1972).

For the seed of any grain that is intended for planting, it is of utmost importance that a high percentage of seeds will germinate when subjected to conditions conducive to germination. Furthermore, it is important that germination be vigorous and uniform for all seeds (Wilson, 1993).

A widely used model is developed by Roberts (1972), which relates loss of seed viability to storage temperatures and moisture contents, and the time of keeping 50% of seed viability, t_{50}, is used to describe the loss of seed viability as follows

$$\log(t_{50}) = k_v - c_{s1}W - c_{s2}T_\sigma \qquad (1.7)$$

where t_{50} is the time, days, for seed viability to decline from 100% to 50%, W is the moisture content of grain, dry basis, T_σ is grain temperature, k_v, c_{s1} and c_{s2} are constants listed in table 1.4.

Table 1.4 Roberts (1972) values for constants in equation (1.7)

Seed	k_v	c_{s1}	c_{s2}, °C^{-1}
Barley	6.745	0.172	0.075
Wheat	5.067	0.108	0.05
Rice	6.531	0.159	0.069
Peas	6.432	0.158	0.065
Faba beans	5.766	0.239	0.056

When the grain temperature, T_σ, or moisture content, W, or both, are reduced, the time of keeping 50% of seed viability, t_{50}, will increase.

1.2.5 Summary of spoilage in grain storage

From the previous discussions in this section, we can see clearly that all damaging biological activity will be slowed or even stopped when a low moisture content (or water activity) or a low temperature, or both are maintained in a grain store. Consequently, the storage duration is increased and the qualities of grain are maintained. Most of the biological activities are functions of the wet-bulb temperature of stored grain, hence, by reducing the temperature or moisture content, or both, the stored grain can have a low wet-bulb temperature that can prevent the grain being ruined by spoilage arising from mould growth and insect development.

1.3 Review of cooling grain by aeration

In Australia, most cereal grains need to be aerated by mechanically forcing cool ambient air through the grain mass in order to reduce the temperature of grain. Aeration is also an effective way to control moisture migration in grain silos (ASHRAE, 1995). However, in some climates the ambient air has a very high enthalpy that is not suitable to aeration and a conditioning system must be introduced to attain the low temperature of grain for the safe storage period.

1.3.1 The principal features of grain aeration

In this thesis, aeration refers to forcing *ambient* or *conditioned* air through *static* grain bulks. It has been pointed out by Sutherland *et al.* (1971) and Thorpe (1985) that the influence of aeration on the grain temperature and moisture content is not uniform throughout an entire grain bulk. To help define this non-uniform feature, grain storage technologies often use two terms: *temperature front* and *moisture front*, Those fronts are the regions where grain temperatures or moisture contents in the bulk change rapidly. In this thesis, the changes of temperature and moisture are caused by the aeration processes.

For an aeration process, the main objective is to ensure that a cooling front has traversed the entire grain bulk. Figure 1.2 shows the principal ideas of an aeration cooling process in a silo of warm grains. When the aeration air passes through the silo, there are heat and mass (moisture) transfers between the air and the grain and temperature fronts and moisture fronts are formed. Those fronts move through the grain as waves in the direction of the airflow (Thorpe, 1985).

Normally the movements of temperature and moisture fronts are not at the same speed; a moisture front is much slower than a temperature front; the speed of the temperature front is about 100 times of the moisture front (Thorpe, 1985). This indicates that a drying process needs a much longer time than a cooling process in a silo.

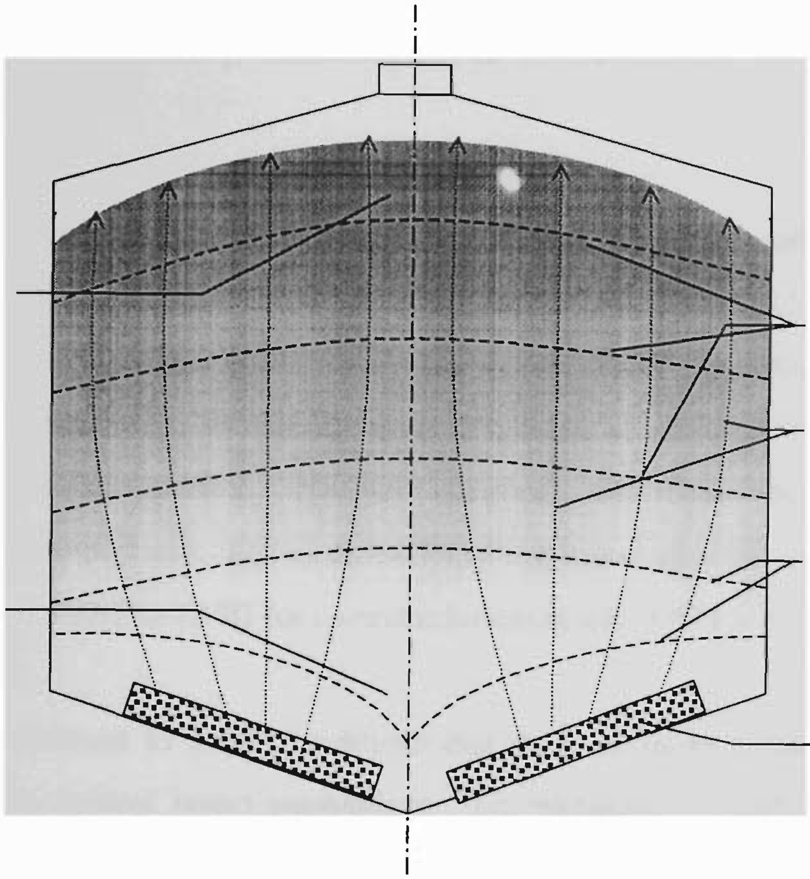

Figure 1.2 Schematic diagram of an aerated silo showing ducts, airflow vectors and temperature and moisture fronts

The capacity of an aeration system involves two components: *aeration rate* and *control action*. In Australia, aeration rates are usually expressed in litres per second per tonne (L/ s/ t) and referred to as *specific aeration rate*. The specific aeration rates can extend from 0.1 L /s /t to 30 L /s /t, although systems below 0.6 L /s /t and above 6 L /s /t are recent additions to the aeration scene in Australia (Darby, 1998). Normally aeration cooling needs a low specific aeration rate (*e.g.* 0.5 ~ 2.5 L /s /t) and aeration drying needs high specific aeration rates (*e.g.* 2.5 ~ 20.0 L /s /t) (Darby, 1998).

Control action identifies the ambient air selection process of an aeration system at the appropriate combination of ambient dry-bulb and wet-bulb temperatures (or relative humidity). Because the major causes of spoilage of stored grains are insect pests and moulding, Wilson (1993) recommended aeration control actions according to *Target SWBT*, where *SWBT* is the seed wet-bulb temperature of intergranular air in moisture equilibrium with the grain, and *Maximum aeration time* to control insect populations and mould growth. As mentioned in the previous section, we assumed moisture equilibrium is always maintained in an aerated silo so *SWBT* is the wet-bulb temperature of grain.

Australian experiences from aeration trials have showed that where the pest of *Sitophilus* species is not a problem, reducing the temperature of a chemically treated grain silo to 15 °C *Target SWBT*, prevents detectable re-infestation or growth of residual insect population. Where the pests of *Sitophilus* species are a problem, it is probably better to take additional care with chemicals and to cool the grain to a lower grain wet-bulb temperature, 12 °C. For controlling insect growth in untreated grain silos, the *Target SWBT* is 12 °C for commercial stores and 9 °C for on-farm stores.

It is also important to avoid conditions that promote mould growth when using *Target SWBT* to control insect populations. For example, in Australia wheat with 14% wet basis moisture content has to be stored at 13 °C wet-bulb temperature or below to avoid mould growth, and with 12% wet-basis moisture content the moulding is not a problem in stored wheat.

Aeration does not gradually cool all the grain in a store at the same time. Instead, a cooling front forms where the air flows into the grain. The grain will not have been cooled until the front has moved all of the way through the grain bulk. Spoilage occurs if the *Target SWBT* cannot be achieved within a time limit, the maximum allowable aeration time. In Australia, Wilson (1993) recommends that it is wise to set a maximum allowable aeration time at about five weeks to prevent moisture migration both in the chemically treated and untreated grains. The insect population growth is under the levels that are detectable in the first *five weeks* after receival in the untreated grain silos, and *three months* in treated grain silos.

1.3.2 Performance of grain aeration

The prediction of aeration performance should indicate which state the stored grains will reach, and when the aeration will be completed. An empirical method of determining temperature and moisture front velocities is provided by Wilson (1993). The results of this method show that both velocities are decided by the initial temperatures and moisture contents of the grain, and the air conditions and the flow rate used for aeration.

Because of the much slower movement of moisture fronts than temperature fronts, Sutherland *et al.*, (1971) approximated that the grain moisture content remains at the initial value during aeration processes, and grain temperature reaches the aeration air temperature finally. However, most of the grain stays at the so-called dwell state which is obtained, or approximately obtained, as the intersection of constant moisture content and wet-bulb temperature lines, as shown in figure 1.3. Sutherland *et al.*, (1971) also recommended a simple process in which the grain psychrometric charts are used to determine the final grain condition using the following method.

- The moisture content of grain remains approximately the same as the initial grain moisture content.
- The intergranular air condition is equal to the air inlet wet-bulb temperature.

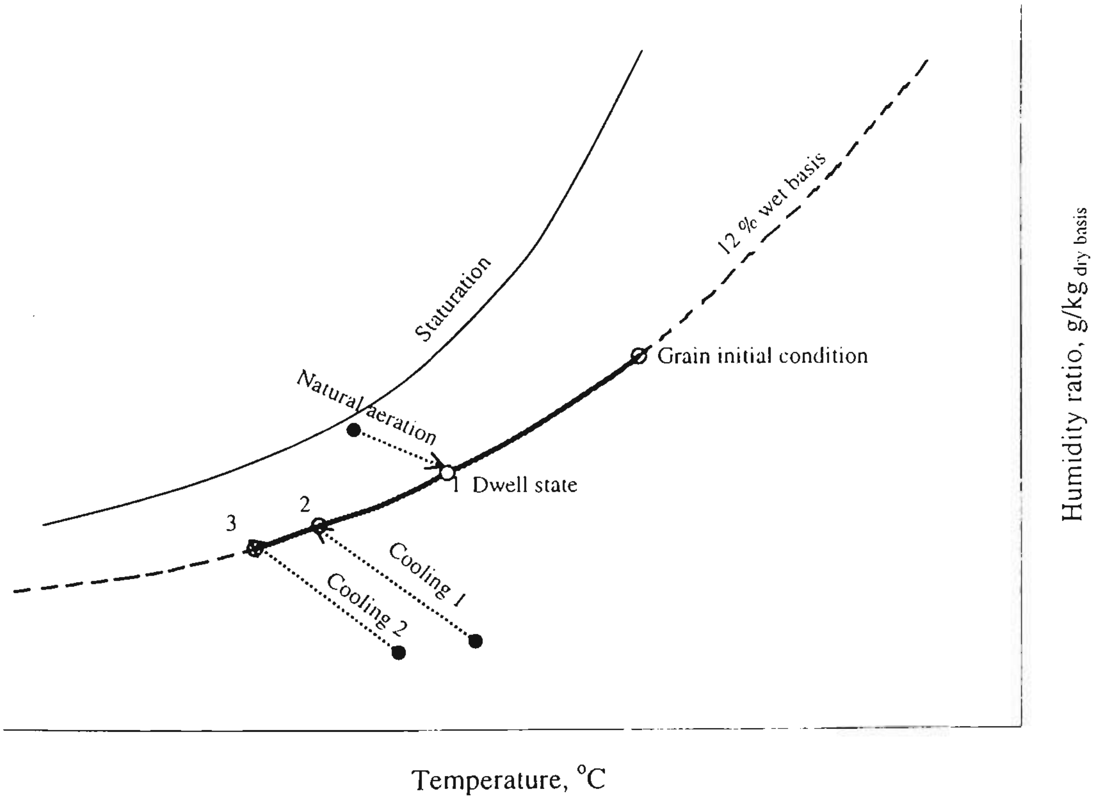

Figure 1.3 Thermodynamic states of aeration air passing through the wheat silo

Figure 1.3 shows three aeration processes, natural aeration, cooling 1 and cooling 2, on a psychrometric chart. The final dwell states of grain conditions, 1, 2, and 3, are located at the intersections of the constant wheat moisture content curve with inlet air wet-bulb temperature lines by using the equilibrium psychrometric chart. The dry-bulb temperature at the point of intersection is approximately the dry-bulb temperature of the final grain condition.

It should be noted that Sutherland *et al.*'s process (1971) is only applied for the steady continuous aeration in one-dimensional systems.

1.3.3 Conditioned aeration

It is impossible to reach 12°C or 9°C *SWBT*, the safe wet-bulb temperature for commercial or on-farm untreated grain storage, in five weeks in summer in the temperate climates of Australia (Wilson, 1993). In tropical climates, there is no time during the year that it can be attained. This leads to the fact that common aeration systems have to be used in conjunction with protectants to achieve the control of insect growth successfully.

For wet grains, spoilage still occurs in aerated stores even when they are chemically treated. Furthermore, insects develop resistance and consumers are concerned about toxins and pesticide residues, so many pesticides are being withdrawn from use because of high costs of developing new ones. And environmental considerations have made the production of certain pesticides illegal. Therefore, alternative, preferably non-chemical, or physical methods of effective pest control in stored grains, are now becoming more important (Maier, 1994 and Banks *et al.*, 1995).

Until now there were only three physical methods that are in widespread use for insect control: cold, exclusion and aridity (Banks *et al.*, 1995). Exclusion is not applicable for a built unsealed silo. It is also very hard to dry grains after loading in a silo because of the very large density of grain compared with the very low air flow rate of aeration. In this situation, cooling is a feasible practical alternative process.

There are three general cooling methods reported in the literature; ambient aeration, refrigeration (chilling) and desiccant dehumidification.

Grain refrigerators (chillers) have been commercialized in the USA and Europe since the 1980's (Maier, 1994). In Maier's (1994) field results, a 579-t wheat bin with an initial temperature of 30°C and moisture content of 14% wet basis, was cooled to 10°C in one week by a refrigerated aeration unit, in comparison to 15°C in 3 months and 10°C in 4.5 months by ambient aeration, and 15°C in 8 months and 13°C in 10 months with no aeration, between 1 July 1989 and 30 June 1990, Michigan, USA. Energy costs for cooling grain to 10 to 12°C is approximately 3.0 to 6.0 kWh per tonne of grain in areas with a temperate climate, and 8.0 to 12.0 kWh per tonne of grain under extreme tropical conditions (Brunner, 1996).

In the results of an Australian field trial (Masters *et al.* 1998), a 1215-tonne canola concrete vertical cell with an initial temperature 25°C, a moisture content 8% wet basis and an oil content 43% dry basis, was cooled by a McBea Refrigeration unit to 16°C in 9 days, in February 1998, Coomandook, South Australia. Energy costs in this field experiment were 2.7 kWh per tonne.

Another method of reducing the enthalpy of ambient air is by means of a solid desiccant as suggested by Chau (1982) and Thorpe (1981, 1985).

Thorpe (1994) indicated that the principle of grains cooling by aeration is that grain kernels need energy when they release water vapour, and the release of water vapour changes the grain moisture content by only a small amount, it is sufficient to cool grain. It means the latent load (moisture transfer) of grain kernels is large in comparison to the sensible load (heat transfer) when reducing grain temperature. A desiccant dehumidifier for cooling stored grains uses a very low relative humidity (low dew point) inlet air for grain aeration system and is more effective in moisture removing from grain kernels than conventional refrigeration so it has a greater evaporate cooling effect.

The other main reason for using a desiccant dehumidifier rather than conventional refrigeration is that the process of cooling grains can be optimized by choosing the air occurring the during the coldest periods of a day, since grains do not have to cool down in a few days (Thorpe, 1985). This usually coincides with the time of the lowest ambient temperature and highest relative humidity. In this situation, it is shown energy savings and the initial cost of equipment and maintenance are minimized (ASHRAE, 1997).

There are two Australian field trials reported in the literature on a novel desiccant system for cooling farm-stored grains (Ahmad, *et al.*, 1997). In a trial conducted at Walla Walla, NSW, a 104-tonne wheat on-farm silo containing *triticale* with an average initial temperature 22.5°C and an average initial moisture content 10.0% wet basis, was cooled to average grain temperature 19.3°C in 55 days. The energy costs in the Walla Walla experiment were 1.16 kWh per tonne for electricity and 2.0 kg per tonne for LPG. In the Moree trial, a 110-tonne sorghum on-farm silo with an average initial temperature 28.4°C, and an average initial moisture content 11.5% wet basis, was cooled to average grain temperature 14.6°C in 63 days. The energy costs in this experiment are 1.25 kWh per tonne for electricity and 2.75 kg per tonne for LPG. However, it should be noted that the system was operating far from its optimum in both trials.

Solar desiccant grain cooling devices have been developed over ten years. (Ismail *et al.*, 1991 and Ahmad *et al.*, 1996, 1998). It has been observed that a substantial reduction in humidity, e.g.11 g/kg $_{\text{dry air}}$ to 2.45g/kg $_{\text{dry air}}$ (Thorpe, 1996), could be obtained. A solar regenerated desiccant bed cooling system for grain silos was developed at Victoria University of Technology (Thorpe, 1996). Results of a series of experiments suggest that a system is capable of cooling 250 tonnes of wheat that are up to 10°C lower than obtainable using ambient aeration and the coefficient of performance (COP) of the system based on electrical power input is over nine. Commercial systems are being developed.

Ahmad *et al.* (1998) studied the use of a solar heater combined with a novel desiccant cooling system used in Walla Walla and Moree trials with a gas heater as the backup heating source. In a Warwick field trial, this solar desiccant cooling system cooled 50-tonne of barley in an on-farm silo to an average grain temperature 17.3°C in 33 days from an average initial grain temperature 32.1°C, and an average initial grain moisture content 11.9%. The energy costs in the Wawick experiment was 1.34 kWh per tonne for electricity and 1.5 kg per tonne for LPG. Again, the system was operating far from its optimum.

Ahmad *et al.* (1997) also summarized the previous studies of desiccant cooling for stored grain; the performance of the devices could be improved if the desiccant devices better approach isothermality during the absorption cycle. In addition, these desiccant cooling devices are not able to process high volume flow rates of aeration air.

1.3.4 Preliminary investigation

We wanted to know if stored grains are likely to be preserved as a result of desiccant cooling. In this preliminary investigation we predicted the biological properties such as insect population, breakdown pesticides and seed viability, in an aerated silo using desiccant cooling since the performance of the systems is decided on the basis that the biological properties of the grain are protected.

The desiccant cooling system used by Ahmad, *et al.* (1997, 1998) is pertinent to the study because this is the simplest model we could conceive in which the cool and moist ambient air during the night can be dried and the low temperature of night air can be maintained as well. Furthermore, Ahmad, *et al.* had presented the most comprehensive data recorded during the Warwick trial (Ahmad, *et al.*, 1998) that are shown in table 1.5.

We used the formulae introduced in section 1.2 to predict what may happen to biological properties in the silo from the Warwick trial. For the purpose of comparison, three storage strategies were examined, namely non-aeration, ambient aeration and cooling with the novel desiccant system. To predict the aeration performance the process suggested by Sutherland *et al.* (1971) was used and we approximated the initial grain condition will remain in non-aeration storage during the experimental period.

Table 1.5 Results of the Warwick grain cooling trial using the novel desiccant cooling system

Trial location	Warwick, Queensland
Trial period	1 December, 1997 ~ 2 January, 1998
Type of grain	Barley
Quantity of grain	50 tonnes
Initial average dry-bulb temperature of grain	32.1°C
Initial average wet-bulb temperature of grain	23.5°C
Initial moisture content of grain	11.9% wet basis
Final average dry-bulb temperature of grain	17.3°C
Final average wet-bulb temperature of grain	12.5°C
Final moisture content of grain	11.7% wet basis
Average air flow rate	2.2 L/s/T
Total cooling time	160 hours
Average dry-bulb temperature of ambient air during the cooling time	18.3°C
Average wet-bulb temperature of ambient air during the cooling time	16.3°C
Average relative humidity of ambient air during the cooling time	81.2%
Average dry-bulb temperature of conditioned air during the cooling time	20.4°C
Average wet-bulb temperature of conditioned air during the cooling time	9.6°C
Average relative humidity of conditioned air during the cooling time	21.3%
Electric energy consumed	1.34 kWh/tonne
LPG consumed	1.5 kg/tonne

Source: Ahmad, *et al.*, 1998

Firstly, we used equation (1.2) to calculate the initial and final states of the water activity of intergranular air, a_w, for the barley in table 1.5. Table 1.6 shows the grain (barley) conditions using the three different storage strategies.

Table 1.6 The conditions of grain in three storage strategies

Variable of grain	Storage condition		
	Non-aeration	Ambient aeration	Desiccant cooling
Dry-bulb temperature , °C	32.1	23.0	17.3
Wet-bulb temperature, °C	23.5	16.3	12.5
Moisture content, % wet basis	11.9	11.9	11.7
Moisture content,kg/kg dry basis	0.135	0.135	0.133
Water activity	0.54	0.54	0.48

Source: Ahmad, *et al.*, 1998

Table 1.7 The predicted monthly insect multiples

Species	Storage condition		
	Non-aeration	Ambient aeration	Desiccant cooling
	Dry-bulb 32.1°C Wet-bulb 23.5°C	Dry-bulb 23.0°C Wet-bulb 16.3°C	Dry-bulb 17.31°C Wet-bulb 12.5°C
Sitophilus oryzae	3.6	1.9	1.4
Sitophilus zeamais	1.2	n/a	n/a
Sitophilus granaius	8.9	3.1	1.8
Rhyzopertha dominica	5.0	1.8	n/a
Tribolium castaneum	6.0	1.5	n/a
Oryzaephilus surinamensis	2.6	n/a	n/a
Oryzaephilus mercator	2.6	1.4	n/a
Lasioderma serricorne	1.2	1.1	n/a

* Calculated with equation (1.4) and storage conditions in table 1.6

Using the data of storage conditions listed in table 1.6 and the equation (1.4) we calculated the multiple of insect development in the storage. Table 1.7 shows the predicted results of monthly insect increase at the three storage conditions.

It is shown that in the storage after the desiccant cooling process, most of insect species, 7 in 8 species, will not develop. On the other ha d, all of the 8 insect species will breed and develop in the storage under the non-aeration condition and 6 of 8 species will breed and develop in the ambient aeration silo. It is clear that the desiccant cooling using aeration is a potentially effective way to control the insect development in the grain storage.

Using the values of temperature and moisture content (wet basis) of the three storage conditions in table 1.6, we can observe from figure 1.1 that all three storage conditions were outside the mould envelope so that mould will not occur in storage. Also the water activities of all storage conditions were below 0.7 so mould will not occur. However, moisture migration in the non-aerated silo may occur as a result of temperature graduation.

Table 1.8 The predicted *'half-lives'* time of the protectants, weeks

Protectants	Storage condition		
	Non-aeration	Ambient aeration	Desiccant cooling
	Dry-bulb 32.1°C Wet-bulb 23.5°C	Dry-bulb 23.0°C Wet-bulb 16.3°C	Dry-bulb 17.31°C Wet-bulb 12.5°C
Dichlorvos	0.7	1.7	3.0
Methacrifos	5.2	12.3	21.1
Malathion	6.5	15.7	27.2
Fenitrothion	12.0	22.4	29.8
Bioresmethrin	20.7	37.8	55.3

* Calculated with equation (1.5) and storage conditions in table 1.6

Here we used the variable '*half-life*' to indicate the speed of breakdown of pesticides in which the longer '*half-life*' the protectant has, the slower speed of breakdown it has. Table 1.8 shows the '*half-lives*' of five protectants that are calculated with equation (1.5) and the storage conditions listed in table 1.6. We can see clearly that in table 1.8 all of five protectants had the increased '*half-time*' when aeration is applied to the grain storage and the degree of increase is larger in the silo with desiccant cooling aeration than the one with ambient aeration.

Table 1.9 shows the predicted storage times of keeping 50% of seed viability for those three storage conditions in table 1.6 in which equation (1.7) is used.

Table 1.9 The predicted time of keeping 50% of seed viability, barley.

	Storage condition		
	Non-aeration	Ambient aeration	Desiccant cooling
	Dry-bulb 32.1°C Wet-bulb 23.5°C	Dry-bulb 23.0°C Wet-bulb 16.3°C	Dry-bulb 17.31°C Wet-bulb 12.5°C
Days of 50 % viability	32	485	893

* Calculated with equation (1.7) and storage conditions in table 1.6

It is clear that after 32 days storage the seed viability may reduce to 50% under the initial storage conditions. On the other hand, it may take nearly 30 months storage with desiccant cooling aeration and 16 months with ambient aeration that the seed viability decreases to the same percentage, 50%. Desiccant cooling can preserve the viability of grain efficiently.

1.3.5 The limitations of previous studies in desiccant cooling

Although we see that the desiccant cooling has appeared working well to protect the stored grain from damage of spoilage, there are limitations found in the literature:

- Sutherland *et al.*'s process (1971) is only setup for predictions of one-dimensional and steady cases. Most of practical processes of grain aeration are three-dimensional and unsteady.

- There have been no studies that estimate the desiccant cooling performance by comparing with other storage strategies such as the natural aeration and aeration results under the same physical conditions.
- There are no comprehensive reports about the design and operating strategies of desiccant cooling for grain aeration.

This situation needs to be improved not only for the efficiency of stored grain cooling but also for the commercialized application of desiccant cooling technology in grain aeration.

1.4 Research approach

In response to the limitations mentioned in the previous section, the study in this thesis not only focuses on the mathematical modeling of an unsteady three-dimensional system occurring in an aerated silo, but also the experimental investigation of a novel desiccant cooling system that is designed and built especially for grain aeration.

The mathematical model we develop in this thesis will be used to predict the thermophysical properties in an aerated silo that offers the possibility to determine when aeration will be carried out and what conditions the stored grains will reach. The model also can be applied for situations in which physical measurements are impossible enabling a comparison study of different storage strategies. The study of mathematical modeling is presented in chapters 2, 3 and 4.

In Chapter 2, the thermodynamic procedure that occurs in an aerated grain silo is first described based on the fundamental theory of heat and mass transfer in porous media. Following first principles, we build up a set of partial differential equations governing heat (temperature) and mass (moisture) transfer in the bulk grains with consideration of transport both of air and water vapour. The governing equations are simplified with an order of magnitude analysis. The appropriate boundary conditions are discussed in detail. The equations formulated in Chapter 2 cannot be solved analytically. Thus, a numerical solution is expressed in Chapter 3.

A well-established numerical method, the control volume method (Patankar, 1980), is used in Chapter 3. The basic setup of a grid network and discretization equations is explained in detail. The governing partial differential equations are eventually converted into discretized equations with the simple linearized algebraic forms, as are the boundary condition equations. Those discretized equations have been developed into a computational program that enables us to calculate the thermophysical conditions in an aerated silo.

Here we ask a question whether or not the computational results of the program are satisfactory approximation to the practical situations. Validation of the program is reported in Chapter 4.

The process applied in Chapter 4 was to simulate the silo conditions from a field trial conducted by CSIRO Entomology at Wongan Hills, Western Australia, with the program. This simulation study enabled us to validate many considerations in the process of mathematical modeling such as equilibrium isotherms and boundary conditions.

The experimental study is described in chapters 5 and 6.

In Chapter 5, the mechanics and theoretical performance of the desiccant cooling are outlined. An experimental desiccant cooling system is designed and tested both in the laboratory and the field. There were two silos involved in the field experiments. The measurement procedure includes two sections. In the first section we are interested in the behaviour of the desiccant cooling unit. The measurement data of the desiccant cooling unit were processed and used to develop an empirical model for calculation of the condition of the air leaving the desiccant system during both the cooling and regeneration processes. The second section of experimental measurement was designed to determine the actual grain conditions in the aerated silos. Data on the actual stored grain conditions indicated the performance of the aeration system conducted with the desiccant cooling system and enabled validation of the mathematical model.

In Chapter 6, simulation study was used to develop a better performance in the wheat and canola silos of the Ararat field trial. The mathematical model was validated with the experimental recorded data of the Ararat trial. The empirical model obtained in Chapter 5 was used to calculate the condition of the air leaving the desiccant system during the desiccant and regeneration processes. An established operation method for cooling grain storage, namely time-proportioning control, was introduced in this chapter for a better operation schedule. Combining the mathematical model, the empirical model, the time-proportioning control and the recorded ambient and initial data from the Ararat field trial, improved cooling in the both wheat and canola silos was predicted.

The final conclusions were given in Chapter 7. It includes the contributions to knowledge of the thesis and suggestions for future research.

CHAPTER 2

THEORETICAL ANALYSIS

The idea for the desiccant grain cooling device was conceived as a result of considering Sutherland *et al.*'s analysis (1971). It can be observed from this work that grain aerated with cool dry air will reach a lower temperature than grain aerated with cool humid air. Although the work of Sutherland *et al.* (1971) is very useful it has three principal limitations, namely,

- It deals with only one-dimensional bulks of grain.
- The conditions of grain are spatially uniform.
- The inlet condition of the aeration air is constant.

In this work, we wish to consider the more realistic situation of a three-dimensional bulk of grain. In particular we shall consider a conical bottomed silo fitted with a linear aeration duct. To do this we formulate the equations that govern heat and mass (moisture) transfer in a three-dimensional bulk of grain. We also need to specify the boundary conditions as they apply to the surfaces of the silo and the inlet conditions of the air used to ventilate the grain. Mathematical descriptions are presented to account for non-uniform grain conditions in the silo, as well as arbitrarily changing boundary conditions.

The air flow field is inherently three dimensional, and it is determined by solving continuity equation. When this is done it implies that Darcy's law applies, *i.e.* the velocity of air is proportional to the pressure gradient, although this is an approximation.

However, it appears to give rise to small errors in calculating the flow field (Brooker, 1961 and Hunter, 1983).

2.1 Heat and mass transfer in bulk stored grains

2.1.1 A physical description of respiring grains

The actual physical, chemical and biological processes that occur in respiring grain bulks are very complicated. We shall make some simplifying assumptions that provide a useful starting point for analysis. Thorpe (1994b, 1995a, 1995b) has presented analyses of the heat and mass transfer phenomena that occur in aerated beds of respiring food grains. In his work, a bed of bridging grain is assumed for a fixed-volume element unit in which grains do not collapse, but the void fraction of that air increases when the grain substrate disappears as a result of it being consumed by fungi and insects. Within an elemental unit, the temperatures of grains and intergranular air are in equilibrium, and the grain moisture content is also in equilibrium with the intergranular air.

2.1.2 Equations governing heat and mass transfer in respiring grains

The respiration process in stored grains is represented by the oxidation of hexose, *i.e.*

$$C_6H_{12}O_6 + 6O_2 \rightarrow 6CO_2 + 6H_2O, \qquad \Delta H \qquad (2.1)$$

where ΔH is the heat of oxidation of one molar mass of cellulosic material at room temperature. This specification of temperature implies that the moisture is formed in its condensed state, *i.e.* liquid water. In physical chemistry, the heat of oxidation, ΔH, of the substrate is defined as the difference between the sum of the enthalpies of the products of reaction and sum of the enthalpies of the reactants.

It follows from Thorpe's work (1994b, 1995a, 1995b) that in rectangular coordinates the mass balances are expressed as:

Moisture

$$\frac{\partial}{\partial t}(\varepsilon_\sigma \rho_\sigma W)+\frac{\partial}{\partial t}(\varepsilon_\gamma \rho_1)+\nabla\cdot(\varepsilon_\gamma \rho_1 \mathbf{v}_1)=S_1 \tag{2.2}$$

Carbon dioxide

$$\frac{\partial}{\partial t}(\varepsilon_\gamma \rho_2)+\nabla\cdot(\varepsilon_\gamma \rho_2 \mathbf{v}_2)=S_2 \tag{2.3}$$

Oxygen

$$\frac{\partial}{\partial t}(\varepsilon_\gamma \rho_3)+\nabla\cdot(\varepsilon_\gamma \rho_3 \mathbf{v}_3)=S_3 \tag{2.4}$$

Nitrogen and other non-reacting gases

$$\frac{\partial}{\partial t}(\varepsilon_\gamma \rho_4)+\nabla\cdot(\varepsilon_\gamma \rho_4 \mathbf{v}_4)=S_4 \tag{2.5}$$

Mass balance on the solid substrate

$$\frac{\partial}{\partial t}(\varepsilon_\sigma \rho_\sigma)=S_5 \tag{2.6}$$

In the above equations the various densities, ρ_1, ρ_2, ρ_3 and ρ_4, refer to the masses of the corresponding chemical species. The density ρ_σ refers to the density of the dry matter in the grain kernels. The vector terms, $\mathbf{v}_1$, $\mathbf{v}_2$, $\mathbf{v}_3$, and $\mathbf{v}_4$, represent the velocities of the corresponding chemical species. The source terms, S_1, S_2, S_3, S_4, and S_5, represent the production or depletion of species arising from the respiration process.

The thermal energy continuity equation is written as

$$\frac{\partial}{\partial t}(\varepsilon_\sigma \rho_\sigma H_\sigma)+\sum_{i=1}^{4}\left\{\frac{\partial}{\partial t}(\varepsilon_\gamma \rho_i h_i)+\nabla(\varepsilon_\gamma \rho_i \mathbf{v}_i h_i)\right\}=k_{eff}\nabla^2 T \tag{2.7}$$

where the terms, h_i, indicate the enthalpies of the corresponding chemical species, and k_{eff} is the effective thermal conductivity of the bed of grain. The enthalpy of moist grain, H_σ, is the sum of the enthalpies of the dry substrate, h_σ, the free water, $W \cdot h_1$, and the integral heat of wetting, H_W, thus

$$\begin{aligned} H_\sigma &= h_\sigma + W \cdot h_1 + H_W \\ &= h_\sigma^0 + c_\sigma\left(T - T^0\right) + W\left[h_1^0 + c_1\left(T - T^0\right)\right] + H_W \end{aligned} \tag{2.8}$$

in which h^0 are the specific enthalpies at the reference temperature T^0.

Using the mass balance equations (2.2) to (2.6) we can write the above as

$$\begin{aligned} &\varepsilon_\sigma \rho_\sigma \frac{\partial H_\sigma}{\partial t} + H_\sigma \cdot S_5 + \sum_{i=1}^{4}\left(\varepsilon_\gamma \rho_i \frac{\partial h_i}{\partial t} + \varepsilon_\gamma \rho_i \mathbf{v}_i \cdot \nabla h_i\right) \\ &+ \sum_{i=1}^{4} h_i \cdot S_i - \frac{\partial\left(\varepsilon_\sigma \rho_\sigma W\right)}{\partial t} h_1 \\ &= k_{eff} \nabla^2 T \end{aligned} \tag{2.9}$$

In equation (2.9), the source terms, $H_\sigma \cdot S_5$ and $\sum_{i=1}^{4} h_i \cdot S_i$, actually correspond to the definition of the heat of oxidation in equation (2.1). Thus, the rate of liberation of heat per unit volume of grain, Q_r, is given by

$$-Q_r = h_\sigma \cdot S_5 + \sum_{i=1}^{4} h_i \cdot S_i - h_v \cdot S_1 \tag{2.10}$$

where the heat of vaporization, h_v, is subtracted because the water enthalpy, h_1, is for the water vapour, as ΔH is defined on the basis of liquid water being formed. The definition of the heat of reaction, equation (2.8), is used in equation (2.9), thus

$$\varepsilon_\sigma \rho_\sigma \frac{\partial H_\sigma}{\partial t} + \left\{W\left[h_1^0 + c_1\left(T - T^0\right)\right] + H_W\right\} \cdot S_5$$
$$+ \sum_{i=1}^{4}\left(\varepsilon_\gamma \rho_i \frac{\partial h_i}{\partial t} + \varepsilon_\gamma \rho_i \mathbf{v}_i \cdot \nabla h_i\right) - \frac{\partial(\varepsilon_\sigma \rho_\sigma W)}{\partial t} \cdot h_1 \tag{2.11}$$
$$= k_{eff} \nabla^2 T + Q_r - h_v \cdot S_1$$

Now the enthalpy of moist grain is a function of temperature, T, and moisture content, W. By the chain rule of differentiation we can therefore write

$$\frac{\partial H_\sigma}{\partial t} = \frac{\partial H_\sigma}{\partial W}\frac{\partial W}{\partial t} + \frac{\partial H_\sigma}{\partial T}\frac{\partial T}{\partial t} \tag{2.12}$$

$$\frac{\partial H_\sigma}{\partial t} = \left\{h_1^0 + c_1\left(T - T^0\right) + h_w\right\}\frac{\partial W}{\partial t} + \left(c_\sigma + c_1 W + \frac{\partial H_W}{\partial T}\right)\frac{\partial T}{\partial t} \tag{2.13}$$

$$\frac{\partial(\varepsilon_\sigma \rho_\sigma W)}{\partial t} = \varepsilon_\sigma \rho_\sigma \frac{\partial(W)}{\partial t} + W\frac{\partial(\varepsilon_\sigma \rho_\sigma)}{\partial t} \tag{2.14}$$

Making use of equations (2.6), (2.13) and (2.14), equation (2.11) becomes

$$\varepsilon_\sigma \rho_\sigma \left\{h_1^0 + c_1\left(T - T^0\right) + h_w\right\}\frac{\partial W}{\partial t} + \varepsilon_\sigma \rho_\sigma \left(c_\sigma + c_1 W + \frac{\partial H_w}{\partial T}\right)\frac{\partial T}{\partial t}$$
$$+ \sum_{i=1}^{4}\left\{\varepsilon_\gamma \rho_i \frac{\partial h_i}{\partial t} + \varepsilon_\gamma \rho_i \mathbf{v}_i \cdot \nabla h_i\right\}$$
$$+ \left\{W\left[h_1^0 + c_1\left(T - T^0\right)\right] + H_W\right\}\frac{\partial(\varepsilon_\sigma \rho_\sigma)}{\partial t} \tag{2.15}$$
$$- \left\{\varepsilon_\sigma \rho_\sigma \frac{\partial W}{\partial t} + W\frac{\partial(\varepsilon_\sigma \rho_\sigma)}{\partial t}\right\} \cdot h_1$$
$$= k_{eff} \nabla^2 T + Q_r - h_v \cdot S_1$$

The enthalpy of free water vapour, h_1, is given by

$$h_1 = h_1^0 + c_1\left(T - T^0\right) + h_v \tag{2.16}$$

Simplifying equation (2.15) leads to

$$\begin{aligned}
&\varepsilon_\sigma \rho_\sigma \left(c_\sigma + c_1 W + \frac{\partial H_w}{\partial T} \right) \frac{\partial T}{\partial t} - \varepsilon_\sigma \rho_\sigma h_s \frac{\partial W}{\partial t} \\
&+ \sum_{i=1}^{4} \left\{ \varepsilon_\gamma \rho_i \frac{\partial h_i}{\partial t} + \varepsilon_\gamma \rho_i \mathbf{v}_i \cdot \nabla h_i \right\} - \frac{\partial (\varepsilon_\sigma \rho_\sigma)}{\partial t} \int_0^W h_s dW \\
&= k_{eff} \nabla^2 T + Q_r - h_v \cdot S_1
\end{aligned} \tag{2.17}$$

In arriving at the above equation we have used the identity for the differential heat of sorption,

$$h_s = h_v - h_w \tag{2.18}$$

and used the identity

$$H_W - h_v W = \int_0^W h_w dW - h_v \int_0^W dW \tag{2.19}$$

Now from the definition of enthalpy in the absence of phase change we can write

$$\frac{\partial h_i}{\partial t} = c_i \frac{\partial T}{\partial t} \qquad i = 2,\ 3,\ 4 \tag{2.20}$$

and from (2.16)

$$\frac{\partial h_1}{\partial t} = c_1 \frac{\partial T}{\partial t} + \frac{\partial h_v}{\partial T} \cdot \frac{\partial T}{\partial t} \tag{2.21}$$

Similarly

$$\varepsilon_\gamma \rho_i \mathbf{v}_i \cdot \nabla h_i = \varepsilon_\gamma \rho_i \mathbf{v}_i c_i \cdot \nabla T \qquad i = 2,\ 3,\ 4 \tag{2.22}$$

and

$$\varepsilon_\gamma \rho_1 \mathbf{v}_1 \cdot \nabla h_1 = \varepsilon_\gamma \rho_1 \mathbf{v}_1 c_1 \cdot \nabla T + \varepsilon_\gamma \rho_l \mathbf{v}_l \frac{\partial h_v}{\partial T} \cdot \nabla T \tag{2.23}$$

The density of dry air, ρ_a, is the sum of the individual gas densities of the components of dry air, thus

$$\rho_a = \sum_{i=2}^{4} \rho_i \tag{2.24}$$

The mass fraction of dry air dominates other components, hence it is quite reasonable to write

$$c_i \cong c_a \qquad i = 2,\ 3,\ 4 \tag{2.25}$$

The mass average velocity vector, $\mathbf{v}_\gamma$, of the composition gases is defined as follows (Bird *et al.*, 1960)

$$\rho_\gamma \mathbf{v}_\gamma = \sum_{i=1}^{4} \rho_i \mathbf{v}_\gamma \tag{2.26}$$

Since the composition of the intergranular flow, $\rho_\gamma \mathbf{v}_\gamma$, is dominated by air, we have

$$\rho_\gamma \mathbf{v}_\gamma \cong \rho_a \mathbf{v}_a \tag{2.27}$$

The velocity of water vapour through the intergranular air is given by

$$\mathbf{v}_1 = \mathbf{v}_a + \mathbf{u}_1 \tag{2.28}$$

where $\mathbf{u}_1$ is the diffusion velocity vector of water vapour, which is several orders of magnitude less than $\mathbf{v}_a$ when stored grains are aerated by forced air, thus

$$\mathbf{v}_1 \cong \mathbf{v}_a \tag{2.29}$$

The enthalpy balance (2.17) is then written as

$$\begin{aligned}
&\varepsilon_\sigma \rho_\sigma \left(c_\sigma + c_1 W + \frac{\partial H_W}{\partial T} \right) \frac{\partial T}{\partial t} - \varepsilon_\sigma \rho_\sigma h_s \frac{\partial W}{\partial t} \\
&+ \varepsilon_\gamma \rho_a \left(c_a + c_1 w + \frac{\partial h_v}{\partial T} \right) \frac{\partial T}{\partial t} + \varepsilon_\gamma \rho_a \mathbf{v}_a \left\{ c_a + w \left(c_1 + \frac{\partial h_v}{\partial T} \right) \right\} \cdot \nabla T \\
&= k_{eff} \nabla^2 T + Q_r + S_5 \int_0^W h_s dW - h_v \cdot S_1
\end{aligned} \tag{2.30}$$

Now the moisture balance equation (2.2) is expanded as follows

$$\begin{aligned}
&W \frac{\partial(\varepsilon_\sigma \rho_\sigma)}{\partial t} + \varepsilon_\sigma \rho_\sigma \frac{\partial W}{\partial t} + w \frac{\partial(\varepsilon_\gamma \rho_a)}{\partial t} + \varepsilon_\gamma \rho_a \frac{\partial w}{\partial t} \\
&+ w \nabla(\varepsilon_\gamma \rho_a \mathbf{v}_a) + \varepsilon_\gamma \rho_a \mathbf{v}_a \nabla w = S_1
\end{aligned} \tag{2.31}$$

where w is the humidity ratio of the intergranular air, which is defined as

$$w = \rho_1 / \rho_a \tag{2.32}$$

Simplifying leads to

$$\begin{aligned}
&\varepsilon_\sigma \rho_\sigma \frac{\partial W}{\partial t} + \varepsilon_\gamma \rho_a \frac{\partial w}{\partial t} + \varepsilon_\gamma \rho_a \mathbf{v}_a \nabla w \\
&= S_1 - w(S_2 + S_3 + S_4) - W \cdot S_5
\end{aligned} \tag{2.33}$$

where we have used the identity and equations (2.3), (2.4), (2.5), (2.25), and (2.28)

2.1.3 Boundary conditions

An aerated grain silo is normally composed of several different structural components, the wall, the hopper base, the grain peak, the head space, and the ducts, all of which impact on the conditions within the bulk of stored grains. These components define the boundaries on which the boundary conditions are imposed. The key features of the system are shown in figure 2.1.

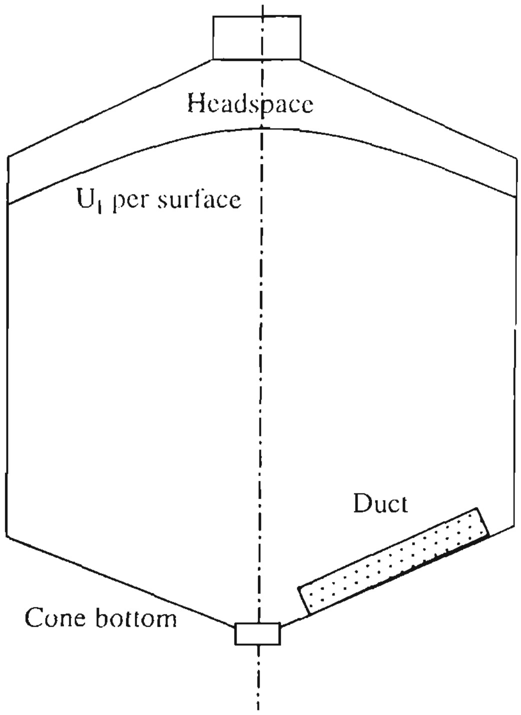

Figure 2.1 Boundary conditions of an aerated silo

In Thorpe's work (1995a) the temperatures of the grains at the wall and hopper base are functions of the incident solar radiation and ambient temperature. In general terms this can be expressed as

$$T_{\sigma} = f_{sur}(T_{amb}, R_s) \tag{2.34}$$

where T_{amb} is the ambient dry-bulb temperature, and R_s is the total solar radiation on the surface.

Both the wall and hopper base are impermeable so the moisture contents of air at the boundary of the wall and hopper are expressed mathematically as

$$\mathbf{n} \cdot \nabla w = 0 \tag{2.35}$$

where $\mathbf{n}$ indicates the normal direction to the surface.

The conditions of grain upper surface are considered as two different situations; aeration is on or off. When aeration system is on the grain temperature can be described as

$$\mathbf{n} \cdot \nabla T = 0 \tag{2.36}$$

On the other hand, when the aeration is off it becomes

$$T_{\sigma} = f_{peak}\left(T_{amb}, R_{s}\right) \tag{2.37}$$

At both conditions of the aeration on or off the air moisture contents at upper surface is given as

$$\mathbf{n} \cdot \nabla w = 0 \tag{2.38}$$

When the aeration system is operating, the grains at the ducts are equilibrium with aerated air both in temperature and moisture content, hence

$$T_{\sigma} = T_{duct} \tag{2.39}$$

$$w = w_{duct} \tag{2.40}$$

where T_{duct} and w_{duct} refer to the temperature and humidity ratio of aeration air in the outlet of the duct.

When the aeration system is off, the grains at the ducts have same condition for the temperatures as the hope base and moisture contents remain unchanged and equations, (2.34) and (2.35), were used.

For a silo, the floor of which is on the ground, it may be considered that the floor is adiabatic , *i.e.*

$$\mathbf{n}\cdot\nabla T = 0 \tag{2.41}$$

and

$$\mathbf{n}\cdot\nabla w = 0 \tag{2.42}$$

2.1.4 Simplifications

In equation (2.1), if the molecular weight of the grain substrate is taken to be 180, and the molecular weight of carbon dioxide, for example, is 44 then for every kilogram of substrate that is oxidized heat is liberated together with

$$\left(\frac{6\times 44}{180}\right) = 1.47 \quad \text{kg of carbon dioxide} \tag{2.43}$$

$$\left(\frac{6\times 18}{180}\right) = 0.6 \quad \text{kg of water} \tag{2.44}$$

as well as consuming

$$\left(\frac{6\times 32}{180}\right) = 1.07 \quad \text{kg of oxygen} \tag{2.45}$$

Now the source terms have the relationships as below

$$S_1 = -0.60 S_5 \tag{2.46}$$

$$S_2 = -1.47 S_5 \tag{2.47}$$

$$S_3 = 1.07 S_5 \tag{2.48}$$

The source term, S_4, related the non-reacting gases is zero, *i.e.*

$$S_4 = 0 \tag{2.49}$$

Therefore, the heat of oxidation of 1 kg of the grain substrate, Δh, is

$$\Delta h = 1.47h_2 + 0.6(h_1 - h_v) - 1.07h_3 - h_\sigma \tag{2.50}$$

Following equation (2.10), the rate of liberation heat per unit volume, Q_r, becomes

$$-Q_r = h_\sigma S_5 - 0.6S_5(h_1 - h_v) - 1.47S_5h_2 + 1.07S_5h_3 \tag{2.51}$$

Hence, we obtain

$$Q_r = S_5\Delta h \tag{2.52}$$

Equation (2.30) and (2.33) may be manipulated into the simple form

$$\begin{aligned}
&\varepsilon_\sigma\rho_\sigma\left(c_\sigma + c_1 W + \frac{\partial H_W}{\partial T}\right)\frac{\partial T}{\partial t} - \varepsilon_\sigma\rho_\sigma h_s \frac{\partial W}{\partial t} \\
&+\varepsilon_\gamma\rho_a\left(c_a + c_1 w + \frac{\partial h_v}{\partial T}\right)\frac{\partial T}{\partial t} + \varepsilon_\gamma\rho_a \mathbf{v}_a\left\{c_a + w\left(c_1 + \frac{\partial h_v}{\partial T}\right)\right\}\cdot\nabla T \\
&= k_{eff}\nabla^2 T + S_5\left(\Delta h + \int_0^W h_s dW + 0.6h_v\right)
\end{aligned} \tag{2.53}$$

$$\begin{aligned}
&\varepsilon_\sigma\rho_\sigma\frac{\partial W}{\partial t} + \varepsilon_\gamma\rho_a\frac{\partial w}{\partial t} + \varepsilon_\gamma\rho_a\mathbf{v}_a\nabla w \\
&= -S_5(0.6 - 0.4w + W)
\end{aligned} \tag{2.54}$$

When there is no biological activity in the grain bulk that neither insects nor fungi are consuming the grains, the source term, S_5, is identically zero. As a result the source terms in equations (2.53) and (2.54) are those that are pre multiplied by S_5 and they are also zero. Thus, the enthalpy and moisture balances can be written as

$$\varepsilon_\sigma \rho_\sigma \left(c_\sigma + c_1 W + \frac{\partial H_W}{\partial T} \right) \frac{\partial T}{\partial t} - \varepsilon_\sigma \rho_\sigma h_v \frac{\partial W}{\partial t}$$
$$+ \varepsilon_\gamma \rho_a \left(c_a + c_1 w + \frac{\partial h_v}{\partial T} \right) \frac{\partial T}{\partial t} + \varepsilon_\gamma \rho_a \mathbf{v}_a \left\{ c_a + w \left(c_1 + \frac{\partial h_v}{\partial T} \right) \right\} \cdot \nabla T \qquad (2.55)$$
$$= k_{eff} \nabla^2 T$$

$$\varepsilon_\sigma \rho_\sigma \frac{\partial W}{\partial t} + \varepsilon_\gamma \rho_a \frac{\partial w}{\partial t} + \varepsilon_\gamma \rho_a \mathbf{v}_a \nabla w = 0 \qquad (2.56)$$

In the enthalpy balance (2.55) since the bulk density of Australian wheat (Wilson, 1993)

$$\varepsilon_\sigma \rho_\sigma = 779 \qquad \text{kg/m}^3 \qquad (2.57)$$

$$\varepsilon_\sigma \rho_\sigma = \mathbf{0}(10^3) \qquad (2.58)$$

The specific heat of Australian wheat is

$$c_\sigma = 1.30 \times 10^3 \qquad \text{J/kg K} \qquad (2.59)$$

and

$$\left(c_\sigma + c_1 W + \frac{\partial H_W}{\partial T} \right) = \mathbf{0}\left(10^3\right) \qquad (2.60)$$

so that

$$\varepsilon_\sigma \rho_\sigma \left(c_\sigma + c_1 W + \frac{\partial H_W}{\partial T} \right) = \mathbf{0}\left(10^5\right) \qquad (2.61)$$

For the water vapour the properties were taken as

$$\rho_a = 1.2 \qquad \text{kg/m}^3 \qquad (2.62)$$

$$c_a = 1 \qquad \text{J/kg K} \tag{2.63}$$

$$w = 0\left(10^{-3}\right) \tag{2.64}$$

$$W = 0\left(10^{-1}\right) \tag{2.65}$$

and the typical value of for porosity, ε_γ, is 0.41 for Australian wheat (Wilson, 1993), hence

$$\varepsilon_\gamma \rho_a \left(c_a + c_1 w + \frac{\partial h_v}{\partial T} \right) = 0\left(10^2\right) \tag{2.66}$$

Thus

$$\varepsilon_\gamma \rho_a \left(c_a + c_1 w + \frac{\partial h_v}{\partial T} \right) << \varepsilon_\sigma \rho_\sigma \left(c_\sigma + c_1 W + \frac{\partial H_W}{\partial T} \right) \tag{2.67}$$

With this result, the enthalpy balance becomes

$$\begin{aligned} &\varepsilon_\sigma \rho_\sigma \left(c_\sigma + c_1 W + \frac{\partial H_W}{\partial T} \right) \frac{\partial T}{\partial t} - \varepsilon_\sigma \rho_\sigma h_s \frac{\partial W}{\partial t} \\ &+ \varepsilon_\gamma \rho_a \mathbf{v}_a \left\{ c_a + w \left(c_1 + \frac{\partial h_v}{\partial T} \right) \right\} \cdot \nabla T \\ &= k_{eff} \nabla^2 T \end{aligned} \tag{2.68}$$

Similarly, for moisture balance with definitions of (2.58), (2.62), (2.63), (2.64) and (2.65) it appears

$$\varepsilon_\gamma \rho_a \frac{\partial w}{\partial t} << \varepsilon_\sigma \rho_\sigma \frac{\partial W}{\partial t} \tag{2.69}$$

Thus, equation (2.55) becomes

$$\varepsilon_\sigma \rho_\sigma \frac{\partial W}{\partial t} + \varepsilon_\gamma \rho_a \mathbf{v}_a \nabla w = 0 \tag{2.70}$$

2.2 Calculation of the velocity field in aerated grains

In the previous section, we saw that the velocity field within the grain bulk must be determined before the thermal energy and moisture conservation equations can be solved. Thorpe (1997) has given a brief history of agricultural engineers' attempts to relate pressure drops through uniformly ventilated beds of the grains. The works of Shedd (1953) and Hukill *et al.* (1955) provided useful compilations of data and expressions for the relationship between the pressure drop and velocity of air flowing through bulks of grains. It was pointed out by Thorpe (1997) that the expressions of Shedd (1953) and Hukill *et al.* (1955) not only have little physical basis, but they are difficult to manipulate mathematically.

Generic studies of flow through porous media perhaps had their genesis with the work of Darcy (1856), who studied the flow of water through sand. This latter work was extended by Kozeny (1927) and Forschheimer (1901) who attempted to provide some physical basis to Darcy's equation, and extend it to account for inertial effects. Ergun (1952) provided a useful expression for the relationship between pressure gradient and velocity of a fluid flowing through a porous medium.

2.2.1 General equations

Hunter (1983) used Shedd's data (1953) and Ergun's equation (1952) to relate the pressure gradient, $\frac{\partial p}{\partial x}$, to the velocity, v_x, of air in the x-direction

$$\frac{\partial p}{\partial x} = -R_p v_x - S_p v_x^2 \tag{2.71}$$

in which R_p and S_p are grain specific empirical constants.

More contemporary analyses of flow through porous media are based on the axioms of continuum mechanics and the spatial averaging theorems.

Brooker (1961) has shown that pressure fields computed in beds of grain are very similar whether or not inertial terms are included in the equations. When inertial terms are neglected, Darcy's law prevails in which case the resistance to air flow is

$$\frac{\partial p}{\partial x} = -R_p v_x \tag{2.72}$$

$$\frac{\partial p}{\partial y} = -R_p u_y \tag{2.73}$$

$$\frac{\partial p}{\partial z} = -R_p w_z \tag{2.74}$$

where u_y and w_z are the velocities of the air in the y-direction and z-direction and which may be expressed more compactly in vector notation as

$$\nabla p = -R_p \mathbf{v} \tag{2.75}$$

where $\mathbf{v}$ is the velocity vector in the fixed-volume element.

At the velocities encountered in a bed of grains, the air flow may be taken as being incompressible in which case

$$\frac{\partial v_x}{\partial x} + \frac{\partial u_y}{\partial y} + \frac{\partial w_z}{\partial x} = 0 \tag{2.76}$$

or in vector notation

$$\nabla \cdot \mathbf{v} = 0 \tag{2.77}$$

Forming the dot product of ∇ and equation (2.75) results in

$$\nabla^2 p = -R_p \nabla \cdot \mathbf{v} = 0 \tag{2.78}$$

i.e. when inertial terms are neglected the pressure field in the grain is governed by Laplace's equation

2.2.2 Boundary conditions of velocity field

At the upper surface of the grain the pressure is set to zero, i.e.

$$p = 0 \tag{2.79}$$

In the duct the pressure is set to p_{duct}, *i.e.*

$$p = p_{duct} \tag{2.80}$$

As the hopper bottom and walls of the silo are impermeable to air the pressure gradients normal to those surfaces are zero, or

$$\mathbf{n} \cdot \nabla p = 0 \tag{2.81}$$

where $\mathbf{n}$ is normal to the impermeable boundaries.

In this study the equation (2.81) does not need to be used explicitly because the impermeability of the walls is ensured by increasing the value of R_p by seven orders of magnitude compared with the value assigned to the grain.

2.2.3 Calculation of the pressure drop across the grain bulk

The pressure gradients in the region of the aeration ducts are steep, and they change rapidly with position. If the pressure drop across the grain is to be determined accurately using a finite difference approximation of Laplace's equation a very fine mesh would be required in the vicinity of the duct. As the position of the aeration ducts is quite arbitrary some suitable and generalized finite differential gridding scheme would have to be implemented. This is quite an onerous task, and in this thesis the pressure drop across the grain bulk is calculated using the methods developed by Hunter (1983). The methods were originally derived to apply to grain storage sheds fitted with longitudinal ducts, but they can be used to estimate the approximate pressure across grain bulk of other shapes.

At a height, y, th pressure, $p(y)$, resulting from the Darcian flow through the grain is given by Hunter (1983) when a round duct is used for aeration as

$$p(y) = -\frac{R_p Q_f}{4\pi L}\left(\ln A_p + \ln B_p\right) \tag{2.82}$$

in which

$$\begin{aligned} A_p &= \sin^2 \frac{\pi b_p}{A_{silo}} \left[\cosh \frac{\pi y}{A_{silo}} - \cosh \frac{\pi x}{A_{silo}\sqrt{2}} \right]^2 \\ &+ \cos^2 \frac{\pi b_p}{A_{silo}} \left[\sinh \frac{\pi y}{A_{silo}} - \sinh \frac{\pi x}{A_{silo}\sqrt{2}} \right]^2 \end{aligned} \tag{2.83}$$

$$\begin{aligned} B_p &= \sin^2 \frac{\pi b_p}{A_{silo}} \left[\cosh \frac{\pi y}{A_{silo}} - \cosh \frac{\pi x}{A_{silo}\sqrt{2}} \right]^2 \\ &+ \cos^2 \frac{\pi b_p}{A_{silo}} \left[\sinh \frac{\pi y}{A_{silo}} + \sinh \frac{\pi x}{A_{silo}\sqrt{2}} \right]^2 \end{aligned} \tag{2.84}$$

where R_p is a grain specific empirical constant, Q_f is the volume flow rate of air through the silo, m^3/s, L_{duct} is a total length of the ducts, m, b_p is a constant, d_{duct} is the diameter of the duct, m, A_{silo} is the area of silo, $\pi \cdot R_{silo}$, m^2, R_{silo} is the radius of silo, m.

The pressure drop, Δp_{linear}, Darcian term is given by

$$\Delta p_{linear} = p_{duct} - p(h_{bulk}) \tag{2.85}$$

where h_{bulk} is the height of the grain bulk above the aeration duct, m.

Close to the duct the velocity is high and the inertial term that involves, S, in Hunter's equation may make a significant contribution to the overall pressure drop. This contribution, Δp_{ic}, is given by the expression

$$\Delta p_{ic} = S_p Q_f^{\ 2} / \left(\pi L_{duct}^{\ 2} \rho_p\right) \tag{2.86}$$

in which R_p is specific empirical constant, Q_f is the volume flow rate of air through the silo, m^3/s, L_{duct} is a total length of the ducts, m, and the wetted perimeter ρ_p in per unit length of duct is given by

$$\rho_p = \pi d_{duct} \tag{2.87}$$

2.2.4 Pressure drop in a bulk of grain with an annular duct

The pressure drop across a bulk of grain fitted with an annular duct is estimated using the method presented by Thorpe *et al.* (1977). It is shown that the pressure distribution, $p(r,y)$, is a circular silo fitted with annular ducts is given by

$$p(r,y) = -2a\left[y - \sum_{n=1}^{\infty} \frac{J_0(\lambda) J_0(\lambda_n r)^{-\lambda_n y}}{\lambda_n J_0^2(\lambda_n)}\right] \tag{2.88}$$

where J_0 is the Bessel function of zeroth order, given as follows

$$J_0(x) = \sum_{n=0}^{\infty} \frac{(-1)^n}{(n!)^2}\left(\frac{x}{2}\right)^{2n} \tag{2.89}$$

and the constant, r, is calculated as follows

$$r = {}^{r_{ad}}\!/_{r_{adius}} \tag{2.90}$$

in which r_{ad} is the radial distance from the center of the silo, m, and r_{adius} is the radius of the silo, m,

$$y = Y/r_{adius} \tag{2.91}$$

in which Y is the height above flow of silo, m, and

$$a = r_{duct}/r_{adius} \tag{2.92}$$

in which r_{duct} is the distance of annular duct from center of silo, m, and λ_n are the roots of $J(x)=0$ in ascending order.

The roots λ_n are calculated as follows

$$\lambda_1 = 3.882 \tag{2.93}$$

$$\lambda_2 = 7.015 \tag{2.94}$$

For higher values of n such as $n = 3$ to 50, successive roots are calculated as follows

$$kk = 9 \tag{2.95}$$

then

$$kk = kk + 4$$

$$\lambda_n = \pi \frac{kk}{4} \tag{2.96}$$

2.3 Conclusions

In this chapter we have presented

- The partial differential equations that govern the heat and mass transfer in bulks of the stored grain.
- The governing equations are rigorously derived from first principles, and they included explicitly the transport both of water vapour and air. An order of magnitude analysis has been carried out to simplify the governing equations.
- Described the relevant boundary conditions.
- Outlined the methods used to calculate the pressure and flow fields.
- Presented an established method for calculating the pressure drop across aerated grain stores.

The heat and mass equations we derived here are coupled and non-linear and they cannot be solved analytically. They must therefore be solved numerically and the processes adopted for this is outlined in Chapter 3.

CHAPTER 3

NUMERICAL SOLUTION

In previous works Thorpe (1992a, 1992b, 1994b) and Singh *et al.* (1993 b) solved the equations (2.68) and (2.70) using finite difference methods. In the some cases the algebra became tedious and problem-specific. In this thesis we shall adopt the control volume method often associated with the work of Patankar (1980). This method has the advantages of having a fairly well established and generic nomenclature, and it is widely used in commercial computational fluid dynamics packages. Processes for solving the partial differential equations are also well established.

The coupled heat and mass (moisture) equations in the Chapter 2 are solved separately here, *e.g.* the temperature, say, that occurs at the start of an integration time step is deemed to stay constant throughout the time step in both thermal energy and mass conservation equations. This also implies that an explicit method is used to solve the equations. This is indeed the case and this represents a point of departure from Patankar's (1980) standard method.

3.1 Control volume method

The control volume approach uses the integral form of the conservation equations as its starting point. The solution domain is subdivided into a finite number of contiguous control volumes, and the conservation equations are applied to each control volume. At the centroid of each control volume there is a computational node at which the values of variables are to be calculated. Interpolation is used to express values of variables at the control volume surface in terms of the nodal values. Surface and volume integrals are approximated using suitable quadrature formulae. As a result, linearized algebraic equations are obtained for each control volume in which a number of neighbor nodal values appear.

3.2 Control volume and grid

The basis of the numerical method here is to focus our attention on the values at the discrete nodal points, instead of the continuous distribution contained in the exact solution of the continuous partial differential equations. Therefore, a grid of the discrete

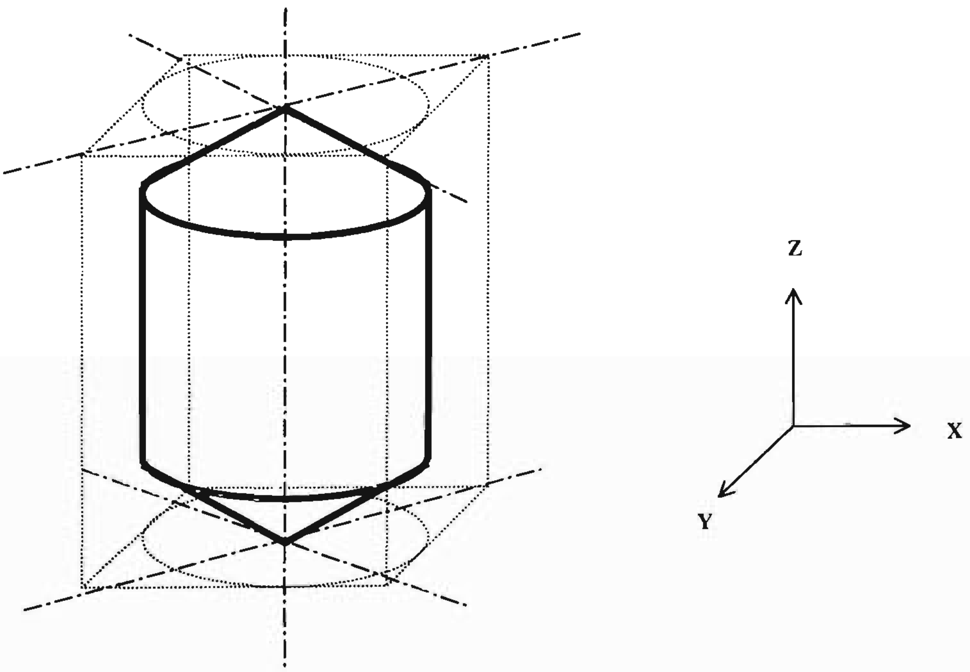

Figure 3.1 Coordinate system used in the numerical solution

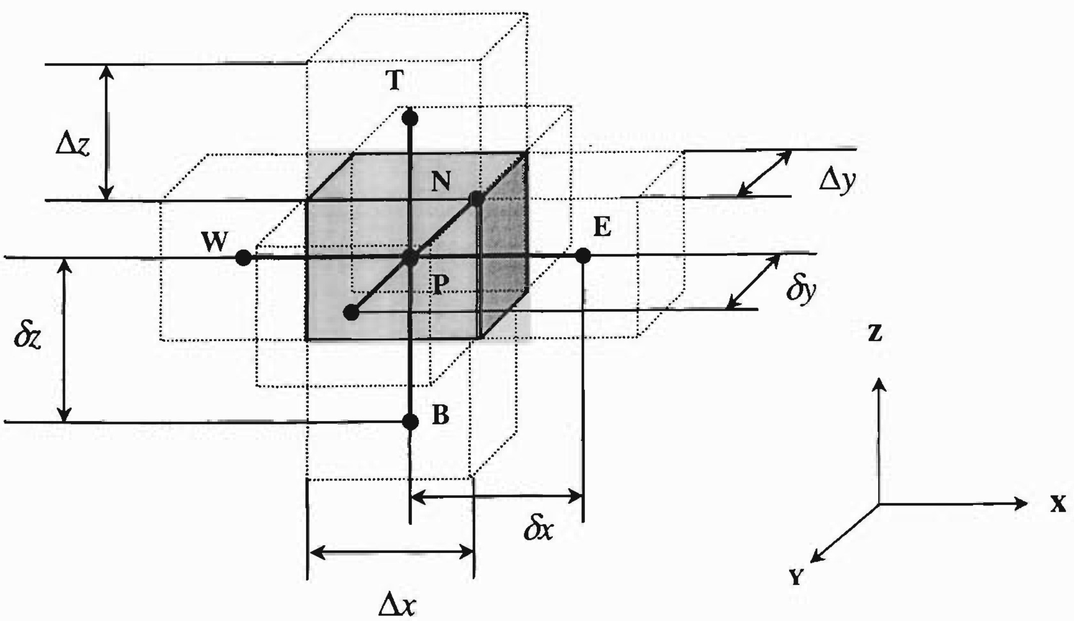

Figure 3.2 Three-dimensional control volume grid mesh

points that fill the domain of interest must be established. In this study a rectangular Cartesian reference system is used to define the grid shown in figure 3.1.

A general meshed section of the three dimensional molecules is shown in figure 3.2. Each control volume has a standard size with dimensions $\Delta x \times \Delta y \times \Delta z$ and a nodal point, *e.g.* **P**, placed at its center, namely the grid point. The lines joining the grid points, δx, δy, and δz, are called grid lines, or mesh lengths. Here x, y, and z are referred to the coordinate directions **x, y, z,** respectively.

We '*carve out*' a circular silo from a parallelepiped as shown in figures 3.3, and 3.4. Figure 3.3 illustrates how the cylindrical portion of a silo is generated, and figure 3.4 shows how the hopper base and the natural peaked surface are also divided into control volumes.

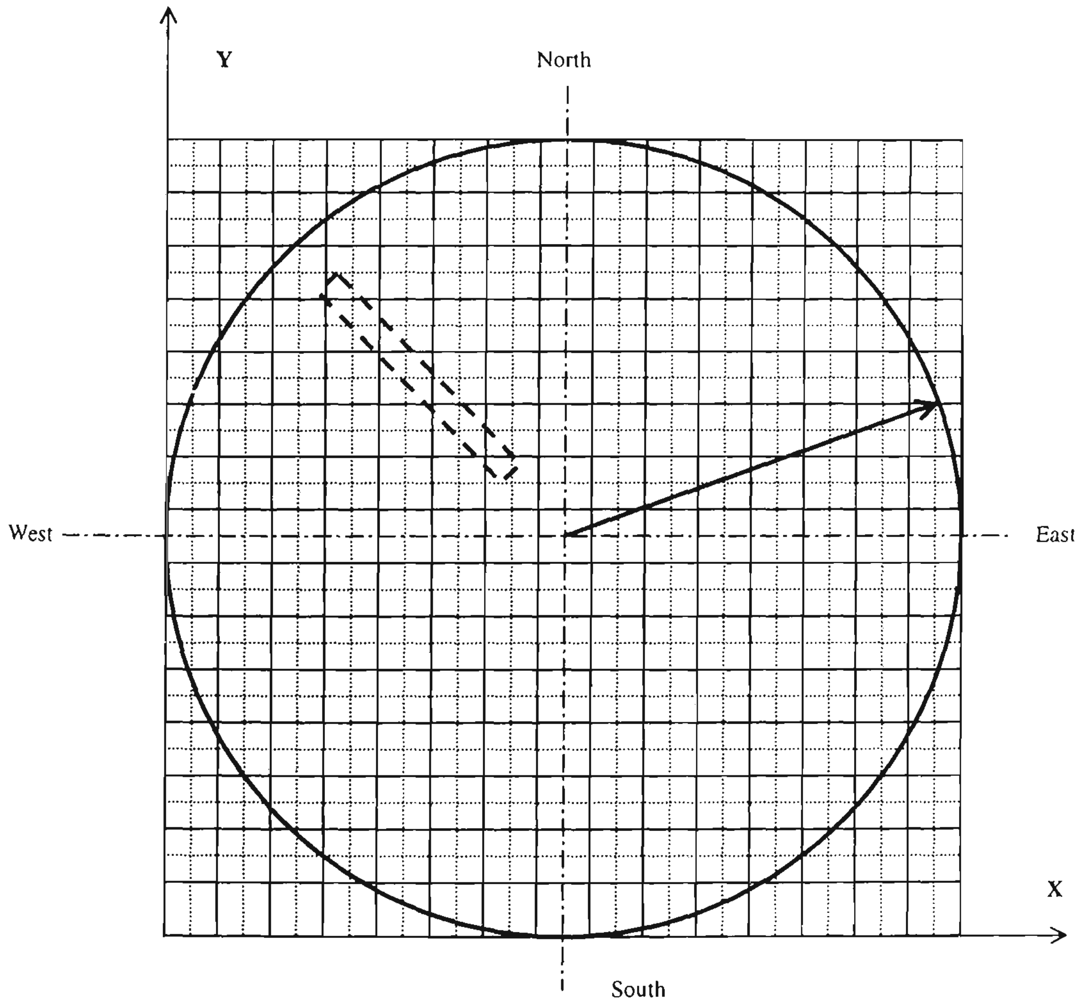

Figure 3.3 Schematic vertical grid layout of the silo

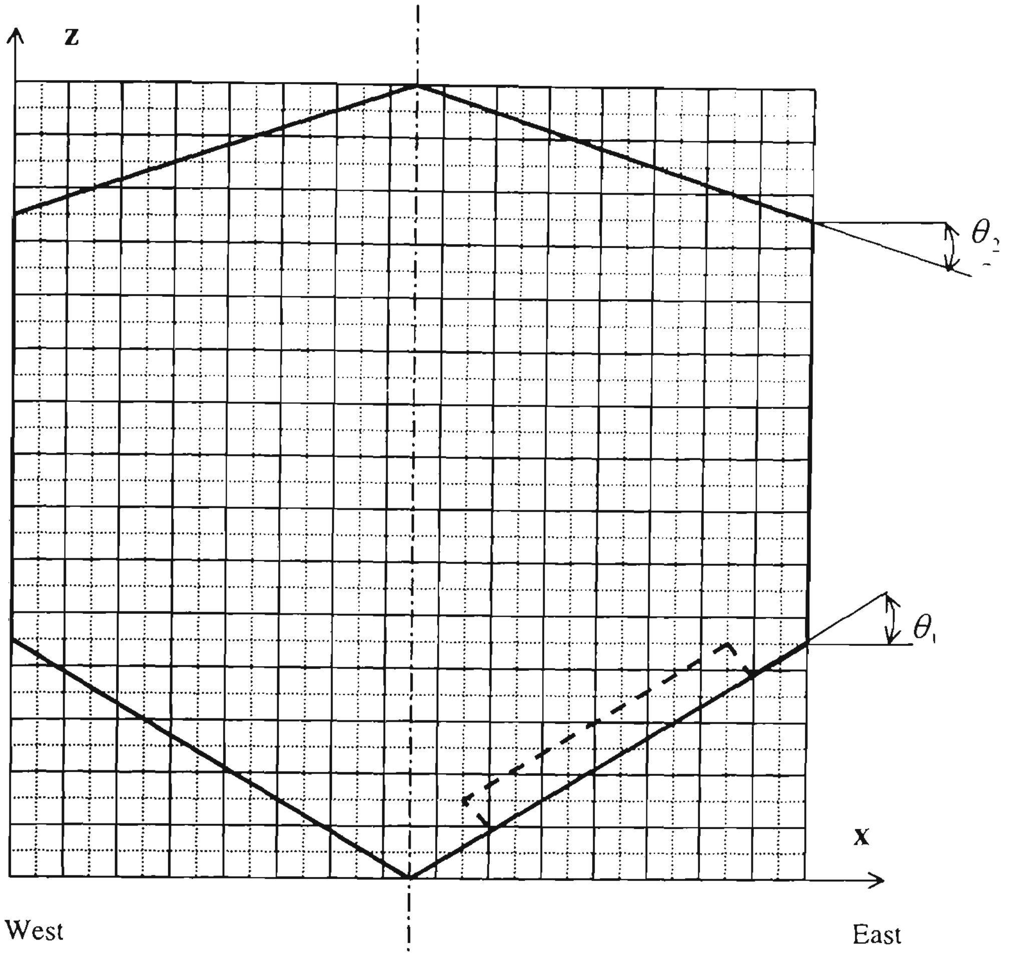

Figure 3.4 Schematic elevation grid layout of the silo

The accuracy of the solutions generally increases as the number of nodes increases. It also preferable to refine the grid in those regions in which the gradients are the greatest. With this approach however, the size of the matrix of coefficients increases rapidly and becomes too large for storage in the immediate access store of personal computers. The Cartesian system makes refining the mesh in the peripheries of the grain bulk somewhat complicated as well. It is found that a uniform mesh is accurate and results in converged solutions both in time and variation of the number of nodes.

3.3 Calculation of the velocity field in aerated grains

As noted in chapter 2, the velocity field of the air in the grain can be calculated from equations (2.75) and (2.78). This implies that we must calculate the pressure field. Thorpe (1998a) calculated the pressure field in the silo with a hopper bottom by means of a mesh transformation and solving the resulting finite difference equations using the Andreyev-Samarskii Alternating Direction Implicit method (Samarskii *et al.*, 1963).

It has been noted that mesh transformation is algebraically intensive, and individual geometries require a unique mathematical formulation. The control volume method does not suffer these limitations, and to be consistent with the approach described by Patankar (1980), the finite volume approach is adapted to calculate the velocity field. One of the key features of calculating the velocity field is to implement a staggered grid. Its use is illustrated by the one dimension case, *e.g.* **x**-direction, showing in figure 3.5.

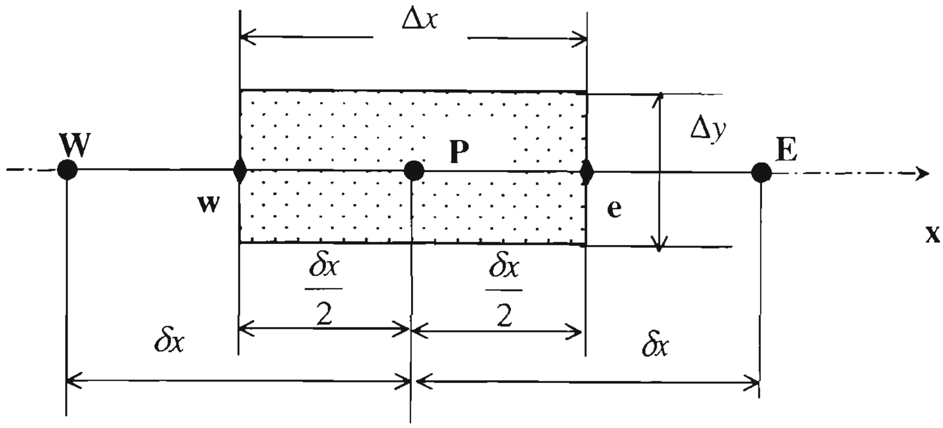

Figure 3.5 Grid-point cluster for node **P** in the one-dimensional problem

Patankar (1980) pointed out that if this configuration of finite volumes is used to calculate the pressure field misleading results of using the momentum equation might arise. The reason for this is that when the pressure gradient in the x-direction (figure 3.5) is computed the pressure, p_P, does not appear in the discretization equation, its value at this point, **P,** could therefore be arbitrary.

One method of obviating this problem is to calculate the velocity on a separate staggered grid as portrayed in figure 3.5. We can very conveniently demonstrate the implementation of staggered grid by considering its application to Darcy's law that governs flow through porous media and it can be expressed as

$$v_e = a_{pr}\left(p_P - p_E\right) \tag{3.1}$$

in which a_{pr} is a constant that depends on the permeability of the grain, the viscosity of air and the distance between **P** and **E,** v_e is the velocity at face **e**.

When the flow in the x-direction is uniform, steady and incompressible the mass balance reduces to

$$v_w = v_e \tag{3.2}$$

where v_w is the velocity at surface **w**.

Equations (3.1) and (3.2) form a set that is particularly easy to solve using a version of the SIMPLE algorithm (Patankar, 1980). First the pressure field in the x-direction is guessed and they are assigned the values p_P^* and p_E^*, and this enables a tentative velocity, v_e^*, to be calculated as follows

$$v_e^* = a_{pr}\left(p_P^* - p_E^*\right) \tag{3.3}$$

Let the true value of the pressure be p which can be written as the following decomposition

$$p = p^* + p' \tag{3.4}$$

where p' is a correction that has to be made to the guessed pressure.

The correct velocity, v, can also be decomposed into the guessed velocity, v^*, calculated from the guessed pressure, p^*, and a velocity correction, v', *i.e.*

$$v = v^* + p' \tag{3.5}$$

Now

$$v_e = a_{pr}\left(p_P^* + p_P' - p_E^* - p_E'\right) \tag{3.6}$$

$$v_e^* + v_e' = a_{pr}\left(p_P^* + p_P' - p_E^* - p_E'\right) \tag{3.7}$$

$$v'_e = a_{pr}(p'_P - p'_E) \tag{3.8}$$

The above expressions and their analogues can be substituted into the continuity equations with the result

$$v^*_w + a_{pr}(p'_W - p'_P) - v^*_e - a_{pr}(p'_P - p'_E) = 0 \tag{3.9}$$

The pressure field can be calculated using the following steps

- Guess the pressure field, p^*.
- Calculate the velocity field, v^*, from the guessed pressure field.
- Solve the equations for the pressure correction terms.
- Add the pressure correction terms to the initial guess and this results in the pressure field.

It is important to note that the solution to the pressure field is completed without any need for iteration. Solutions of system of linear equations that govern the pressure field could also be obtained directly in two and three-dimensional systems, but it would be necessary to invert large matrices, typically $10{,}000 \times 10{,}000$.

An alternative approach is to decompose the problem into a series of one-dimensional systems, analogous to the one we have just solved. In this way it is also possible to exploit the tri-diagonal form of the coefficient matrix of p'. Ferziger *et al.*

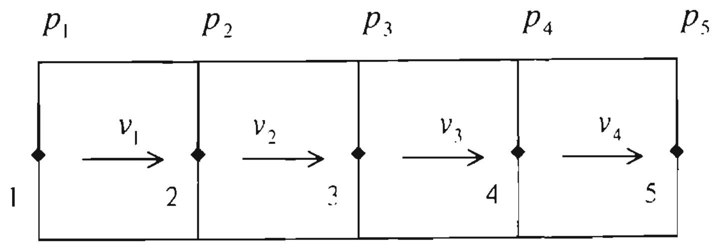

Figure 3.6 Schematic layout of one-dimension grid

(1996) provided several algorithms for solving the equations such as (3.8) and (3.9). After modifying some of details the method presented by Patankar (1980) has been implemented in this study.

Here we use a simple example to demonstrate how we calculate the velocity field in one-dimensional grid (figure 3.6).

We simply set

$$a_{pr} = 1 \tag{3.10}$$

$$p_1 = 1 \tag{3.11}$$

$$p_5 = 0 \tag{3.12}$$

Now, we guess

$$p_2^* = 4 \tag{3.13}$$

$$p_3^* = 4 \tag{3.14}$$

$$p_4^* = 4 \tag{3.15}$$

From equation (3.43), we have guessed values

$$v_1^* = 0 \tag{3.16}$$

$$v_2^* = 0 \tag{3.17}$$

$$v_3^* = 0 \tag{3.18}$$

$$v_4^* = 4 \tag{3.19}$$

Hence, the corrections of p_1' and p_5'

$$p_1' = 0 \tag{3.20}$$

$$p_5' = 0 \tag{3.21}$$

in which equation (3.4) is used.

When equation (3.9) is applied to the grid points 2 to 4 in figure 3.6, we have

$$0 + 1 \cdot (0 - p_2') - 0 - 1 \cdot (p_2' - p_3') = 0 \tag{3.22}$$

$$0 + 1 \cdot (p_2' + p_3') - 0 - 1 \cdot (p_3' + p_4') = 0 \tag{3.23}$$

$$0 + 1 \cdot (p_3' - p_4') - 0 - 1 \cdot (p_4' - 0) = 0 \tag{3.24}$$

In this case there are three equations and three variables, which when solved yield the following solutions

$$p_2' = -1 \tag{3.25}$$

$$p_3' = -2 \tag{3.26}$$

$$p_4' = -3 \tag{3.27}$$

It is therefore found that the corrected pressures are

$$p_2 = 3 \tag{3.28}$$

$$p_3 = 2 \tag{3.29}$$

$$p_4 = 1 \tag{3.30}$$

in which equation (3.4) is used.

Hence, the velocities are

$$v_1 = v_2 = v_3 = v_4 = 1 \tag{3.31}$$

where equation (3.1) is used.

This example highlights that when Darcy's law applies the velocity and pressure distributions can be obtained directly without the need for an iterative solution.

3.4 Discretization of heat and mass conservation equations

The equation that governs the transport of a quantity, Φ, through a fluid or porous medium, say, may be expressed as

$$\rho\frac{\partial\Phi}{\partial t} + \rho\mathbf{v}\cdot\nabla\Phi = \Gamma\nabla^2\Phi + S \tag{3.32}$$

in which $\rho\frac{\partial\Phi}{\partial t}$ is governs the transient behavior of Φ, $\rho\mathbf{v}\cdot\nabla\Phi$ is a convection term, $\Gamma\nabla^2\Phi$ is a diffusion term, and S is a source term.

This is the general equation presented by Patankar (1980), and in the context of this research Φ could represent the temperature, T, in the enthalpy balance Equation (2.68) and the moisture content, W, in the mass balance Equation (2.70).

3.4.1 Principle of discretization in a one-dimensional system

We start our discretization in a one-dimensional system because it not only illustrates most of the principles of the solution process, but also ensures that the algebra is kept as simple as possible.

Considering control-volume element with a standard size $\Delta x \times 1 \times 1$ shown in figure 3.5 for the node **P**, we discretise the convection term, $\rho \mathbf{v} \cdot \nabla\Phi$, in **x**-direction as follows

$$\rho \mathrm{v} \cdot \nabla\Phi = \frac{\rho v_e \Phi_e - \rho v_w \Phi_w}{\Delta x} \tag{3.33}$$

where v_e and v_w are the velocities at the faces **e** and **w** in **x**-direction.

The diffusion term, $\Gamma\nabla^2\Phi$, is discretized as

$$\Gamma\nabla^2\Phi = \frac{\left(\Gamma\dfrac{d\Phi}{dx}\right)_e - \left(\Gamma\dfrac{d\Phi}{dx}\right)_w}{\Delta x} \tag{3.34}$$

In the control-volume scheme, the value of Φ at a grid point, *e.g.* **W**, **P** or **E,** is assumed to prevail over the control volume surrounding it, hence, the diffusion term becomes

$$\Gamma\nabla^2\Phi = \frac{\left(\Gamma_e \dfrac{\Phi_E - \Phi_P}{\delta x}\right) - \left(\Gamma_w \dfrac{\Phi_P - \Phi_W}{\delta x}\right)}{\Delta x} \tag{3.35}$$

When we setup the domain with the same values for Δx and δx, and the general diffusion coefficient Γ is a constant, then this reduces to

$$\Gamma\nabla^2\Phi = \Gamma\frac{\Phi_E + \Phi_W - 2\Phi_P}{\Delta x^2} \tag{3.36}$$

which is recognized as an oft used discretization term in finite difference analysis.

For the unsteady term, $\rho\dfrac{\partial\Phi}{\partial t}$, we obtain the solution by marching in time from a given initial value of Φ^0. In this study, we set up the time step, Δt, and the discretization equation is now derived by integrating Equation (3.32) over the control volume shown in figure 3.5 and over the time interval form t to $t+\Delta t$. Thus, we have the result as

$$\int_w^e \int_t^{t+\Delta t} \left(\rho \frac{\partial \Phi}{\partial t} \right) dt dx = \int_w^e \int_t^{t+\Delta t} \left(\Gamma \nabla^2 \Phi - \rho v \Delta \Phi + S \right) dt dx \tag{3.37}$$

Note that we assume that the grid-point value of Φ prevails throughout the control volume, we have

$$\int_w^e \int_t^{t+\Delta t} \rho \Phi dx dt = \rho \left(\Phi_P - \Phi_P^0 \right) \Delta x \tag{3.38}$$

where Φ_P^0, the old value, represents the value of variable Φ at the node **P** at the time, t, and Φ_P , the new value, is the value the time step, $t+\Delta t$.

We also introduce a weighting factor, f, between 0 and 1, to assume how the left side Equation (3.37), $\left(\Gamma \nabla^2 \Phi - \rho v \Delta \Phi + S \right)$, varies with time from t to $t+\Delta t$, *e.g.*

$$\begin{aligned} \int_t^{t+\Delta t} \left(\Gamma \nabla^2 \Phi - \rho v \Delta \Phi + S \right) dt = \Big[f \left(\Gamma \nabla^2 \Phi - \rho v \Delta \Phi + S \right) \\ - (1-f) \left(\Gamma \nabla^2 \Phi - \rho v \Delta \Phi + S \right)^0 \Big] \Delta t \end{aligned} \tag{3.39}$$

where $\left(\Gamma \nabla^2 \Phi - \rho v \Delta \Phi + S \right)^0$ is the old value at the time, t, and $\left(\Gamma \nabla^2 \Phi - \rho v \Delta \Phi + S \right)$ is the new value at the time $t+\Delta t$.

Now, Equation (3.37) becomes

$$\begin{aligned} &\int_w^x \int_t^{t+\Delta t} \left(\Gamma \nabla^2 \Phi - \rho v \cdot \Delta \Phi + S \right) dt dx \\ &= \left\{ f \left[\Gamma \frac{\Phi_E + \Phi_W - 2\Phi_P}{\Delta x} - \rho v_e \Phi_e + \rho v_w \Phi_w + S \Delta x \right] \right. \\ &\left. - (1-f) \left[\Gamma \frac{\Phi_E + \Phi_W - 2\Phi_P}{\Delta x} - \rho v_e \Phi_e + \rho v_w \Phi_w + S \Delta x \right]^0 \right\} \Delta t \end{aligned} \tag{3.40}$$

in which Equation (3.33) and Equation (3.36) are used.

For certain specific values of the weighting factor, f, the discretization equation (3.39) reduces to one of the well-known schemes for parabolic differential equations.

3.4.2 Explicit scheme

Thorpe (1992b) recommended the explicit scheme, $f = 0$, for obtaining numerical solutions of the mathematical models of grain temperatures and moisture contents. The reason for this preference is that in the explicit scheme the old value Φ^0 essentially is assumed to prevail throughout the entire time step except at time $t + \Delta t$ and it is easy to formulate the equations with the given initial conditions. We note that the condition for the explicit scheme to be stable is expressed as (Patankar, 1980),

$$\Delta t < \frac{\rho(\Delta x)^2}{\Gamma} \tag{3.41}$$

in which the time step has to be small enough to ensure that the results are realistic.

In fact, this condition is very easily satisfied when modeling the stored grains systems because the bulk density of the grains is much larger than the density of air.

When the explicit scheme, $f = 0$, is applied for Equation (3.39) and (3.40), the discretization Equation (3.37) becomes

$$\begin{aligned} &\rho\left(\Phi_P - \Phi_P^0\right)\Delta x \\ &= \left(\Gamma \frac{\Phi_E + \Phi_W - 2\Phi_P}{\Delta x} - \rho v_e \Phi_e + \rho v_w \Phi_w + S\Delta x\right)^0 \Delta t \end{aligned} \tag{3.42}$$

Thus, the final discretization equation is written as

$$\begin{aligned} &\frac{\rho \Delta x \Phi_P}{\Delta t} = \frac{\Gamma}{\Delta x}\Phi_E^0 + \frac{\Gamma}{\Delta x}\Phi_W^0 - \rho v_e^0 \Phi_e^0 + \rho v_w^0 \Phi_w^0 + S^0 \Delta x \\ &+ \left(\frac{\rho \Delta x}{\Delta t} - 2\frac{\Gamma}{\Delta x}\right)\Phi_P^0 \end{aligned} \tag{3.43}$$

3.4.3 Upwind-difference scheme

When convective flows are simulated numerically care must be taken to ensure that the resulting solution is stable. One way of ensuring this is to make use of the upwind-difference scheme (Patankar, 1980).

According to the upwind-difference scheme the value of Φ at an interface is equal to the value of Φ at the grid point on the *upwind* side of the face. According to figure 3.5, we get

$$\Phi_e = \Phi_P \qquad \text{if} \quad v_e > 0 \tag{3.44}$$

and

$$\Phi_e = \Phi_E \qquad \text{if} \quad v_e < 0 \tag{3.45}$$

The value of Φ_w can be defined similarly

$$\Phi_w = \Phi_W \qquad \text{if} \quad v_w > 0 \tag{3.46}$$

and

$$\Phi_w = \Phi_P \qquad \text{if} \quad v_w < 0 \tag{3.47}$$

The conditional statements (3.44) to (3.47) can be more compactly written when a new operator is defined, such that $[[A, B]]$ donates the greater of A and B. Then the upwind-difference scheme implies

$$\rho v_e \Phi_e = F_e \Phi_e = \Phi_P [[F_e, 0]] - \Phi_E [[-F_e, 0]] \tag{3.48}$$

where symbol F_e indicates the strength of the convection defined as

$$F_e = \rho v_e \tag{3.49}$$

and

$$(\rho v)_w \Phi_w = F_w \Phi_w = \Phi_W [[F_w,0]] - \Phi_P [[-F_w,0]] \tag{3.50}$$

where F_w is

$$F_w = \rho v_w \tag{3.51}$$

Hence, the discretization equation for the grid point, **P,** becomes

$$\begin{aligned}\frac{\rho\Delta x}{\Delta t}\Phi_P &= \left(\frac{\Gamma}{\Delta x}\right)\Phi_E^0 + \left(\frac{\Gamma}{\Delta x}\right)\Phi_W^0 - \left(\Phi_P^0[[F_e,0]] - \Phi_E^0[[-F_e,0]]\right) \\ &+ \left(\Phi_W^0[[F_w,0]] - \Phi_P^0[[-F_w,0]]\right) + S^0\Delta x + \left(\frac{\rho\Delta x}{\Delta t} - 2\frac{\Gamma}{\Delta x}\right)\Phi_P^0\end{aligned} \tag{3.52}$$

and it can be re-written as

$$\begin{aligned}\frac{\rho\Delta x}{\Delta t}\Phi_P &= \left(\frac{\Gamma}{\Delta x} + [[-F_e,0]]\right)\Phi_E^0 + \left(\frac{\Gamma}{\Delta x} + \Phi_W[[F_w,0]]\right)\Phi_W^0 \\ &+ S^0\Delta x + \left(\frac{\rho\Delta x}{\Delta t} - 2\frac{\Gamma}{\Delta x} - [[F_e,0]] - \Phi_W[[-F_w,0]]\right)\Phi_P^0\end{aligned} \tag{3.53}$$

In equation (3.2), when the flow in the x-direction is uniform, steady and incompressible the continuity equation is

$$v_w = v_e \tag{3.2}$$

Since the given flow field must satisfy the continuity equation (3.2), hence in the one-dimensional system that we are discussing, it reduces to

$$[[F_w,0]] = [[F_e,0]] \tag{3.54}$$

and

$$[[-F_e,0]] = [[-F_w,0]]$$

in which Equation (3.49) for F_e and equation (3.51) for F_w are used.

To arrange the equation more compactly, we define a new symbol D that represents the diffusion conductance, as follows

$$D_e = \frac{\Gamma}{\delta x} \tag{3.55}$$

$$D_w = \frac{\Gamma}{\delta x} \tag{3.56}$$

The discretization equation (3.52) becomes

$$\alpha_P \Phi_P = \alpha_E \Phi_E^0 + \alpha_W \Phi_W^0 + b_P + \alpha_P^0 \Phi_P^0 \tag{3.57}$$

where

$$\alpha_E = D_e + [[-F_e, 0]] \tag{3.58}$$

$$\alpha_W = D_w + [[F_w, 0]] \tag{3.59}$$

$$\alpha_P = \frac{\rho \Delta x}{\Delta t} \tag{3.60}$$

$$b_P = S\Delta x \tag{3.61}$$

$$\alpha_P^0 = \alpha_P - \alpha_E - \alpha_W \tag{3.62}$$

where the result of equation (3.54) is used.

3.4.4 The exact results in one-dimensional system

In the previous section we made use of the upwind-difference scheme to calculate the variable at the faces of control-volume, *e.g.* Φ_e and Φ_w. In practical cases, the situation of the upwind-difference scheme only happens when the convection is much stronger than the diffusion activity in the control-volume (Patankar, 1980).

To define the actual $\Phi \sim x$ profile we introduce a convection-diffusion coefficient, A, and it is a function of the Peclet number, P. The Peclet number is the ratio of the strengths of convection and diffusion defined by

$$P = \frac{\rho v}{\frac{\Gamma}{\Delta x}} = \frac{\rho v \Delta x}{\Gamma} \tag{3.63}$$

From the definitions of the strength of the convection, F, and the diffusion conductance, D, the Peclet number can be written as

$$P = \frac{F}{D} \tag{3.64}$$

In Patankar's work (1980), the Power-Law scheme was recommended to calculate the convection-diffusion coefficient, A

$$A(|P|) = [[0, (1 - 0.1|P|)^5]] \tag{3.65}$$

The approach to the exact results is to modify the diffusion conductance, D, by multiplying the convection-diffusion coefficient, A, and then we have

$$\alpha_E = D_e A(|P_e|) + [[-F_e, 0]] \tag{3.66}$$

$$\alpha_W = D_w A(|P_w|) + [[-F_w, 0]] \tag{3.67}$$

where

$$P_e = \frac{F_e}{D_e} \tag{3.68}$$

$$P_w = \frac{F_w}{D_w} \tag{3.69}$$

3.4.5 Discretization equation in three-dimensional system

Now we have all the ideas needed for writing the discretization equation corresponding to the general differential equation (3.32) and the control-volume element, $\Delta x \times \Delta y \times \Delta z$, in figure 3.2. It is given as

$$\begin{aligned}\alpha_P \Phi_P &= \alpha_E \Phi_E^0 + \alpha_W \Phi_W^0 + \alpha_N \Phi_N^0 + \alpha_S \Phi_S^0 + \alpha_T \Phi_T^0 + \alpha_B \Phi_B^0 \\ &+ b_P + \alpha_P^0 \Phi_P^0\end{aligned} \tag{3.70}$$

where

$$\alpha_E = D_e A(|P_e|) + [[-F_e, 0]] \tag{3.71}$$

$$\alpha_W = D_w A(|P_w|) + [[-F_w, 0]] \tag{3.72}$$

$$\alpha_N = D_n A(|P_n|) + [[-F_n, 0]] \tag{3.73}$$

$$\alpha_S = D_s A(|P_s|) + [[-F_s, 0]] \tag{3.74}$$

$$\alpha_T = D_t A(|P_t|) + [[-F_t, 0]] \tag{3.75}$$

$$\alpha_B = D_b A(|P_b|) + [[-F_b, 0]] \tag{3.76}$$

$$\alpha_P = \frac{\rho \Delta x \Delta y \Delta z}{\Delta t} \tag{3.77}$$

$$b_P = S \Delta x \Delta y \Delta z \tag{3.78}$$

$$\alpha_P^0 = \alpha_P - \alpha_E - \alpha_W - \alpha_N - \alpha_S - \alpha_T - \alpha_B \tag{3.79}$$

$$F_e = \rho v_e \Delta y \Delta z \tag{3.80}$$

$$D_e = \frac{\Gamma \Delta y \Delta z}{\Delta x} \tag{3.81}$$

$$P_e = \frac{F_e}{D_e} \tag{3.82}$$

$$F_w = \rho v_w \Delta y \Delta z \tag{3.83}$$

$$D_w = \frac{\Gamma \Delta y \Delta z}{\Delta x} \tag{3.84}$$

$$P_w = \frac{F_w}{D_w} \tag{3.85}$$

$$F_n = \rho u_n \Delta z \Delta x \tag{3.86}$$

$$D_n = \frac{\Gamma \Delta z \Delta x}{\Delta y} \tag{3.87}$$

$$P_n = \frac{F_n}{D_n} \tag{3.88}$$

$$F_s = \rho u_s \Delta z \Delta x \tag{3.89}$$

$$D_s = \frac{\Gamma \Delta z \Delta x}{\Delta y} \tag{3.90}$$

$$P_s = \frac{F_s}{D_s} \tag{3.91}$$

$$F_t = \rho w_t \Delta x \Delta y \tag{3.92}$$

$$D_t = \frac{\Gamma \Delta x \Delta y}{\Delta z} \tag{3.93}$$

$$P_t = \frac{F_t}{D_t} \tag{3.94}$$

$$F_b = \rho w_b \Delta x \Delta y \tag{3.95}$$

$$D_b = \frac{\Gamma \Delta x \Delta y}{\Delta z} \tag{3.96}$$

$$P_b = \frac{F_b}{D_b} \tag{3.97}$$

where the form $[[A, B]]$ denotes the greater of A and B, the subscript coefficients, b, e, n, s, t, and w refer to the control-volume faces (figure 3.2) and we choose the distance Δx same as δx, Δy same as δy, and Δz same as δz.

Finally, we set out the solution to the general differential equation (3.32), which is

$$\begin{aligned}\Phi_P = &(\alpha_E \Phi_E^0 + \alpha_W \Phi_W^0 + \alpha_N \Phi_N^0 + \alpha_S \Phi_S^0 + \alpha_T \Phi_T^0 + \alpha_B \Phi_B^0 \\ &+ b_P + \alpha_P^0 \Phi_P^0) / \alpha_P\end{aligned} \tag{3.98}$$

3.5 Calculation of heat and mass transfer

In this thesis the discretization equations of heat and mass transfer are based on the forms of equations (2.68) and (2.70)

$$\begin{aligned}&\varepsilon_\sigma \rho_\sigma \left(c_\sigma + c_1 W + \frac{\partial H_W}{\partial T} \right) \frac{\partial T}{\partial t} - \varepsilon_\sigma \rho_\sigma h_s \frac{\partial W}{\partial t} \\ &+ \varepsilon_\gamma \rho_a \mathbf{v}_a \left\{ c_a + w\left(c_1 + \frac{\partial h_v}{\partial T} \right) \right\} \cdot \nabla T \\ &= k_{eff} \nabla^2 T\end{aligned} \tag{2.68}$$

$$\varepsilon_\sigma \rho_\sigma \frac{\partial W}{\partial t} + \varepsilon_\gamma \rho_a \mathbf{v}_a \nabla w = 0 \tag{2.70}$$

Thorpe (1998b) recommended that in equation (3.94) the moisture term, $\varepsilon_\sigma \rho_\sigma h_s \frac{\partial W}{\partial t}$, is treated as a source term, *i.e.*

$$\begin{aligned} &\varepsilon_\sigma \rho_\sigma \left(c_\sigma + c_1 W + \frac{\partial H_W}{\partial T} \right) \frac{\partial T}{\partial t} \\ &+ \varepsilon_\gamma \rho_a \mathbf{v}_a \left[c_a + w \left(c_1 + \frac{\partial H_W}{\partial T} \right) \right] \nabla T \\ &= k_{eff} \nabla^2 T + \varepsilon_\sigma \rho_\sigma h_s \frac{\partial W}{\partial t} \end{aligned} \tag{3.99}$$

Comparing with the general differential equation (3.32) with equation (3.98) the general dependent variable, Φ, is the temperature, T. The strength of convection, F, and the diffusion conductance, D, for the discretization equation of equation (3.98) are calculated as follows

$$F_e = \varepsilon_\gamma \rho_a \left[c_a + w \left(c_1 + \frac{\partial H_W}{\partial T} \right) \right] v_e \Delta y \Delta z \tag{3.100}$$

$$D_e = \frac{k_{eff}}{\Delta x} \tag{3.101}$$

and the same treatments as F_e and D_e for F_w and D_w, F_n and D_n, F_s and D_s, F_t and D_t, F_b and D_b in equation (3.80) to (3.89). For the coefficient α_P in equation (3.75), it becomes

$$\alpha_P = \frac{\varepsilon_\gamma \rho_a \left[c_a + w \left(c_1 + \frac{\partial H_W}{\partial T} \right) \right]}{\Delta t} \Delta x \Delta y \Delta z \tag{3.102}$$

The term related to the differential heat of wetting, $\frac{\partial H_w}{\partial T}$, is very hard to calculate accurately. It has been claimed by Close *et al.* (1972) that its value is negligible, hence α_P becomes

$$\alpha_P = \frac{\varepsilon_\gamma \rho_a (c_a + wc_1)}{\Delta t} \Delta x \Delta y \Delta z \tag{3.103}$$

The source term, b_P, in equation (3.76) is written as

$$b_P = \varepsilon_\sigma \rho_\sigma h_s \frac{\partial W}{\partial t} \Delta x \Delta y \Delta z \tag{3.104}$$

and the coefficient α_P^0 can be obtained with equation (3.79).

In the moisture balance equation (2.70) the dependent variable in unsteady term, W, is different from the one in the convection team, w. However, making the use of the discretization process in section 3.3.1, in the one-dimensional system (figure 3.5) we write

$$\int_w^e \int_t^{t+\Delta t} \left(\varepsilon_\sigma \rho_\sigma \frac{\partial W}{\partial t} \right) dt dx = \int_w^e \int_t^{t+\Delta t} (\varepsilon_\gamma \rho_\gamma v \Delta w) dt dx \tag{3.105}$$

where we find that the variable related to the convection terms is only w and W is associated with unsteady state terms. Hence we have the discretization equation for moisture balance (2.70) as

$$\begin{aligned} W_P = (&\alpha_E w_E^0 + \alpha_W w_W^0 + \alpha_N w_N^0 + \alpha_S w_S^0 + \alpha_T w_T^0 + \alpha_B w_B^0 \\ &+ b_P + \alpha_P^0 W_P^0) / \alpha_P \end{aligned} \tag{3.106}$$

and the corresponding coefficients for the discretization equation (3.105) are

$$F_e = \varepsilon_\gamma \rho_a v_e \Delta y \Delta z \tag{3.107}$$

$$D_e = 0 \tag{3.108}$$

The similar processes are used for F_w and D_w, F_n and D_n, F_s and D_s, F_t and D_t, F_b and D_b in equations (3.80) to (3.89). The coefficient α_P and the source term b_P now become

$$\alpha_P = \frac{\varepsilon_\sigma \rho_\sigma}{\Delta t} \Delta x \Delta y \Delta z \tag{3.109}$$

$$b_P = 0 \tag{3.110}$$

Similarly, the coefficient α_P^0 can be obtained with equation (3.79).

Note that the variables are normally stored in computers in three dimensional arrays. The conversion between the grid notation and storage location in computer is indicated in table 3.1.

Table 3.1 Conversion betweent the grid notation and storage location

Grid notation	Storage location
P	*i, j, k*
W	*i-1, j, k*
E	*i+1, j, k*
S	*i, j-1, k*
N	*i, j+1, k*
T	*i, j, k+1*
B	*i, j, k-1*

We have obtained the numerical expression for the enthalpy balance (3.99) as follows

$$\begin{aligned} T_{i,j,k} = \big(&\alpha_{i+1,j,k} T^0_{i+1,j,k} + \alpha_{i-1,j,k} T^0_{i-1,k,j} + \alpha_{i,j+1,k} T^0_{i,j+1,k} + \alpha_{i,j-1,k} T^0_{i,j-1,k} \\ &+ \alpha_{i,j,k+1} T^0_{i,j,k+1} + \alpha_{i,j,k-1} T^0_{i,j,k-1} + b_{i,j,k} + \alpha^0_{i,j,k} T^0_{i,j,k}\big) / \alpha_{i,j,k} \end{aligned} \tag{3.111}$$

and the relevant coefficients are obtained from equation (3.100) ~ (3.104) are given by the following

$$\alpha_{i,j,k} = \alpha_P \tag{3.112}$$

$$\alpha^0_{i,j,k} = \alpha^0_P \tag{3.113}$$

$$\alpha_{i+1,j,k} = \alpha_E \tag{3.114}$$

$$\alpha_{i-1,j,k} = \alpha_W \tag{3.115}$$

$$\alpha_{i,j+1,k} = \alpha_N \tag{3.116}$$

$$\alpha_{i,j-1,k} = \alpha_S \tag{3.117}$$

$$\alpha_{i,j,k+1} = \alpha_T \tag{3.118}$$

$$\alpha_{i,j,k-1} = \alpha_B \tag{3.119}$$

$$b_{i,j,k} = b_P \tag{3.120}$$

The moisture balance equation (2.70) becomes

$$\begin{aligned} W_{i,j,k} = \big(&\alpha_{i+1,j,k} w^0_{i+1,j,k} + \alpha_{i-1,j,k} w^0_{i-1,j,k} + \alpha_{i,j+1,k} w^0_{i,j+1,k} \\ &+ \alpha_{i,j-1,k} w^0_{i,j-1,k} + \alpha_{i,j,k+1} w^0_{i,j,k+1} + \alpha_{i,j,k-1} w^0_{i,j,k-1} + \alpha^0_{i,j,k} W^0_{i,j,k}\big) / \alpha_{i,j,k} \end{aligned} \tag{3.121}$$

3.6 Numerical implementation of boundary conditions in an aerated silo

As mentioned in section 3.2 the silo is 'carved out' of a rectangular parallelepiped. When all nodes labeled as 1, *e.g.* $k_{ind} = 1$, the first assignation of the labels is achieved by identifying those grain nodes, *e.g.* $k_{ind} = 3$, that lay within a right cylinder surface which coincides with the silo wall, shown in figures 3.3 and 3.4.

One of the most definitive characteristics of those kind of nodes, grain and non-grain, is that the resistance to air flow corresponds to the resistance to air flow through grains. Outside of the grain domain the resistance to air flow is set seven orders of magnitude higher. This is one of the methods that Patankar (1980) recommended for delineating the region of fluid flow. An alternative would be to set the viscosity of the fluid at comparatively high values in the zones that coincide with the impermeable region such as the wall, *e.g.* $k_{ind} = 2$, and base, *e.g.* $k_{ind} = 6$, of the silo.

It is possible to set the temperatures of those nodes that are immediately external to the grain bulk to those temperatures that prevail on the external surface of the silo. If the thermal conductivity of the external nodes is set to a high value it is equivalent to the grain being adjacent to the wall of a typical thin walled silo.

The pressure and flow fields in the aerated grain domain can be established by specifying pressure in those nodes that correspond to the region of aeration ducts, *e.g.* $k_{ind} = 7$.

Table 3.2 The labels of nodes according to its type

Label assigned to node (k_{ind})	Description with corresponding to grain
1	All cells initially labeled as '1"
2	Silo wall
3	Grain bulk
4	Headspace above the grain
5	Upper surface of the grain
6	Hopper bottom of the silo
7	Region of the aeration duct

The above process was accomplished by labeling each node according to its type as shown in table 3.2.

3.6.1 Designation of silo wall

The first assignation of the labels is achieved by identifying those that lay within a right cylindrical surface which coincides with the silo wall using prescriptions described above. The effect of this step is to 'bore' a cylinder in the right parallelepiped. Hence the second step we had is to assign those nodes immediately adjacent to, but external to the cylinder, *e.g.* $k_{ind} = 2$, which signifies that they are silo walls showing in figures 3.7 and 3.8.

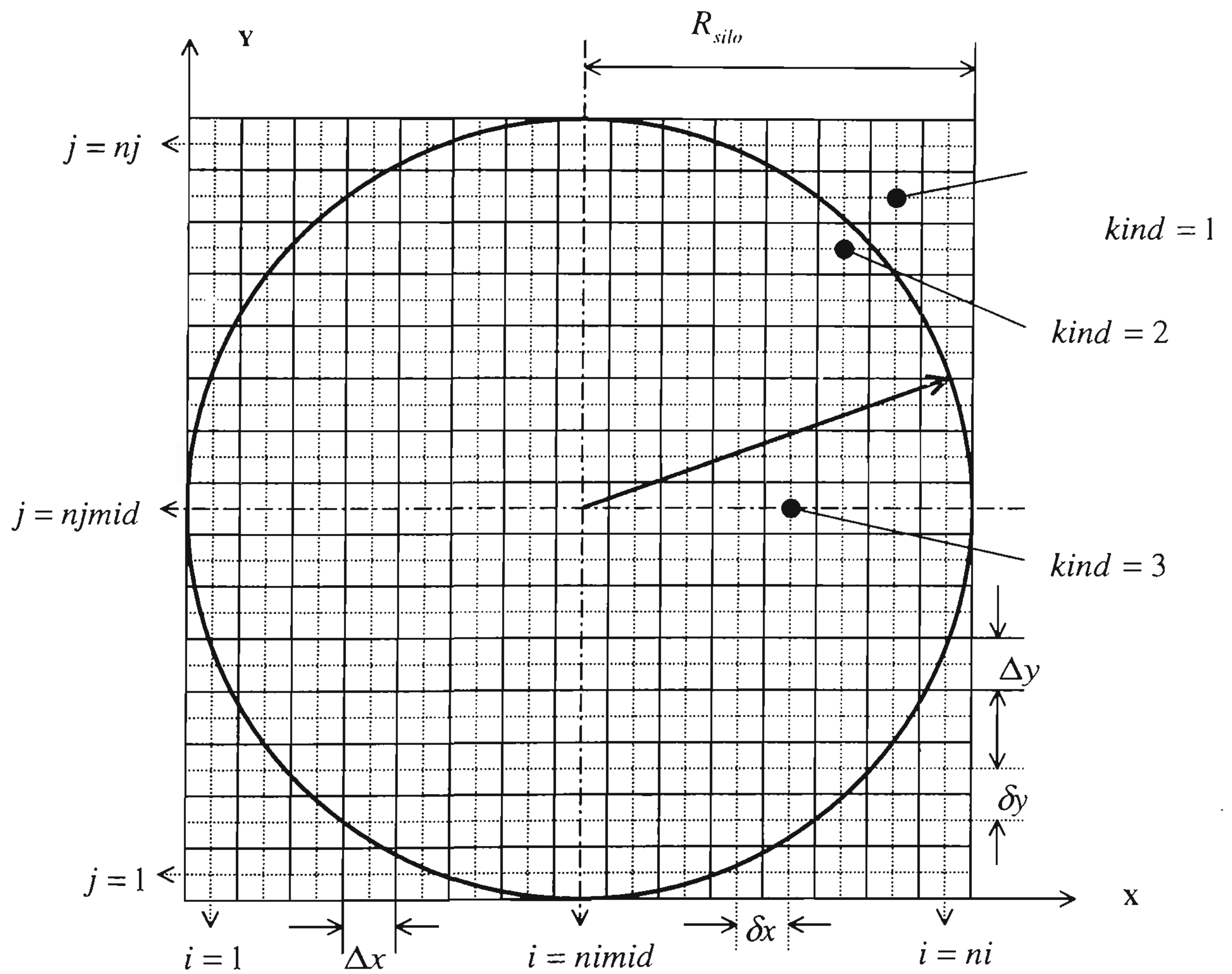

Figure 3.7 The labels of nodes according its type, vertical layout

This is achieved by sweeping the x-y plane firstly in x-direction and then y-direction. The idea is this: when carrying out a sweep in x-direction and the sweep is still to the left of the diameter, *i.e.*

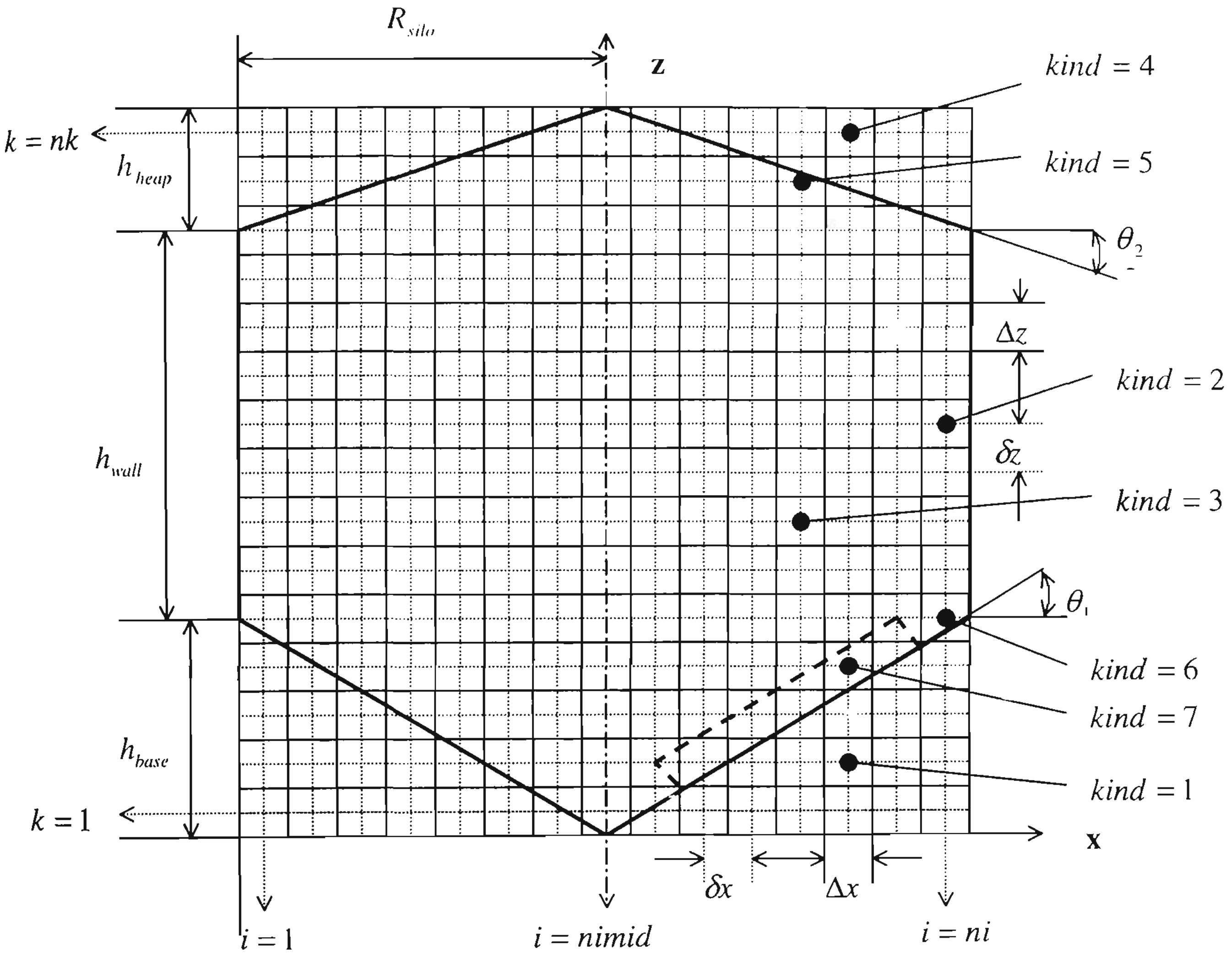

Figure 3.8 The labels of nodes according its type, elevation layout

$$i < n_{imid} \tag{3.122}$$

where $n_{imid} = (ni + 1)/2$

where n_{imid} signifies the value of i that is the mid-point between 1 and ni.

It follows that for given values of j and k there are two successive nodes such that

if $k_{ind}(i, j, k) = 1$ (non-grain)

and $k_{ind}(i+1, j, k) = 3$ (grain) then

$k_{ind}(i, j, k) = 2$ 3.123)

in which $k_{ind}(i, j, k)$ is assigned the value 2 that indicates a wall node.

In the cases when

$$i < n_{imid} \tag{3.124}$$

the wall nodes determined as follows

$$\begin{aligned} &\text{if} \quad k_{ind}(i-1, j, k) = 3 \\ &\text{and} \quad k_{ind}(i, j, k) = 1 \quad \text{then} \\ &k_{ind}(i, j, k) = 2 \end{aligned} \tag{3.125}$$

i.e. the node (i, j, k) has been assigned as a wall node.

An analogous method is used to determine the wall nodes during the sweep in the y-direction. When $k_{ind}(i, j, k) = 2$, the calculation of temperature and moisture content used the equations (2.33) and (2.34) as follows

$$T(i, j, k) = f_{sur}(T_{amb}, R_s) \tag{3.126}$$

$$\begin{aligned} &w(i, j, k) = w(i, j+1, k) \qquad \text{when} \quad j < n_{jmid} \\ &\text{or} \\ &w(i, j, k) = w(i, j-1, k) \qquad \text{when} \quad j > n_{jmid} \end{aligned} \tag{3.127}$$

in which we used the y-direction instead of the normal direction to surface of silo.

3.6.2 Designate the cell type coincident with hopper bottom

The hopper bottom is impermeable to air, and it is assigned a temperature that depends on the temperature of ambient air and solar radiation. The locations of the nodes that coincide with the hopper bottom are formed by calculating their height above the lowest point of the silo.

The base geometry is embodied in the following algorithmic representation

$$d_{ist} = \sqrt{(x(i) - xl/2)^2 + (y(j) - yl/2)^2} \tag{3.128}$$

$$h_{igh} = d_{ist} \times \tan(\theta_1) \tag{3.129}$$

in which d_{ist} represents the radial distance of the node (i, j, k) from the vertical center-line of the silo, xl and yl are the diameter of the silo, and θ_1 is the angle of the hopper bottom to the horizontal (figure 3.8).

The process of 'carving out' the silo continues by testing whether or not the distance $z(k)$ for each i and j is longer than the height of the grain. If it is then $k_{ind}(i, j, k)$ is assigned a value 1, which indicates that node (i, j, k) is not in the grain bulk.

Nodes that correspond to the hopper bottom are assigned a value of 6 and they are assigned by implementing the following logic

If $k_{ind}(i, j, k) = 3$,

$k_{ind}(i, j, k-1) = 1$

and $z(k) < h_{base}$ then

$$k_{ind}(i, j, k) = 6 \tag{3.130}$$

Hence, the temperature and moisture content of the nodes at the hopper bottom can be calculated similarly with the nodes of wall by using equations (3.126) and (3.127).

3.6.3 Designate the cell types coincident with the headspace and the grain peak

The process for designating the types of cells that are located in the headspace and at the peak of the grain bulk is similar to that used for locating the hopper bottom. One difference is that the nodes in these regions remain permeable to air. Another, minor, difference to the algorithm is that the height is measured downwards from the highest point of the grain bulk. Those nodes that are greater than or equal to this height are delineated as

$$\begin{aligned}
&\text{If} \quad k_{ind}(i,j,k)=3, \\
&\qquad k_{ind}(i,j,k-1)=1 \\
&\text{and} \quad z(k)\geq h_{base}+h_{wall}+h_{heap} \qquad \text{then} \\
&k_{ind}(i,j,k)=4
\end{aligned} \tag{3.131}$$

where

$$\begin{aligned}
&d_{ist}=\sqrt{(x(i)-xl/2)^2+(y(j)-yl/2)^2} \\
&\text{and} \\
&h_{heap}=d_{ist}\times\tan(\theta_2)
\end{aligned} \tag{3.132}$$

in which θ_2 is the angle of the repose of the commodity being stored (figure 3.8) and xl and yl are the diameter of the silo.

Nodes that coincide with the upper surface of the grain may then be determined as follows

$$\begin{aligned}
&\text{if} \quad k_{ind}(i,j,k)=4 \\
&\text{and} \\
&\qquad k_{ind}(i,j,k-1)=3 \ \text{then} \\
&k_{ind}(i,j,k-1)=5
\end{aligned} \tag{3.133}$$

When $k_{ind}(i,j,k)=5$, the calculation of temperature and moisture content used the equations (2.35) when the fan is on

$$T(i,j,k)=T(i,j,k-1) \tag{3.134}$$

and when the fan is off the following equations are used

$$T(i,j,k)=f_{peak}(T_{amb},R_s) \tag{3.135}$$

in which equation (2.36) is used, where T_{amb} is ambient temperature.

According to Equation (2.37) the moisture content of grain at the nodes of hopper bottom can be processed as

$$w(i, j, k) = w(i, j, k-1) \tag{3.136}$$

3.6.4 Location of nodes coincide with aeration ducts

Conventional aeration ducts in aerated hopper bottomed silos consist of straight lengths of perforated tubes that are placed radially. Traditionally, aerated silos are fitted with a single radial duct, but there is a trend towards using multiple ducts which results in lower pressure drops and more uniform air flow. These features are particularly important when grains are to be dried in-store. The computer program accommodates up to eight redial ducts placed along north (N), northeast (NE), east (E), southeast (SE), south (S), southwest (SW), west (W), and northwest (NW) radii directions.

There is an increasing trend towards the use of annular ducts (Thorpe *et al.*, 1998), and indeed the silo that is the focus of this study has an annular duct, although it is built into structure of the silo. Annular ducts have the features of providing a more uniform air flow than a single radial duct. In addition they may be formed using a plenum so

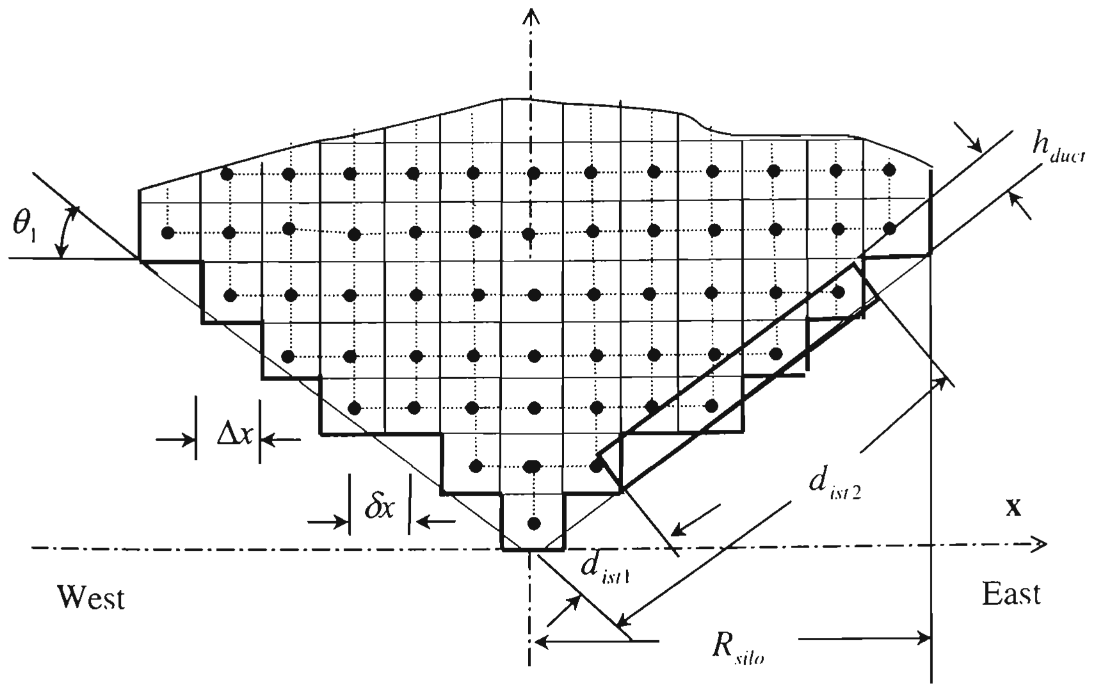

Figure 3.9 Schematic layout of a East duct outlet in a silo

that they interlace a large surface of grain through which air enters the silo. The effect of this is to reduce the velocity of the air as it enters the grain, and this in turn reduces the pressure drop in this region. Using the terminology of Hunter (1983), annular ducts help to reduce the constriction pressure drop caused by aeration duct.

The lengths of the eight possible linear aeration ducts are set by specifying d_{ist1} and d_{ist2} which are the shorter and longer distances of each duct along the hopper base from the center of the silo (figure 3.9). Corresponding to each distance, d_{ist1} or d_{ist2}, the nodes that the end point of d_{ist1} or d_{ist2} locates in are named n_{r1} or n_{r2} respectively. Considering a linear duct that lies east of center shown in figure 6.9, we have

$$r_{e1} = d_{ist1} \tag{3.137}$$

$$r_{e2} = d_{ist2} \tag{3.138}$$

where the distance, n_{r1}, from the center of the coordinate which corresponds to the end of the duct near to the centre of the silo is given by

$$n_{r1} = R_{silo} + r_{e1} / \cos\theta_2 - \delta x / 2 \tag{3.139}$$

and the distance, n_{r2}, further away from the center of the silo is expressed by

$$n_{r1} = R_{silo} + r_{e2} / \cos\theta_2 + \delta x / 2 \tag{3.140}$$

then for the node (i, j, k) we have

$$\begin{aligned} &\text{If } k_{ind}(i, j, k) = 6 \\ &\text{and } n_{r1} \le x(i) \le n_{r2} \text{ then} \\ &k_{ind}(i, j, k) = 7 \end{aligned} \tag{3.141}$$

If we consider a linear duct that lies in the north-west direction (figure 3.3)

$$n_{r1} = \sqrt{\begin{aligned}&\left(R_{silo} - r_{e1}\cos\theta_2 / \cos 45^\circ + \delta x / 2\right)^2 \\ &+ \left(R_{silo} + r_{e1}\cos\theta_2 / \sin 45^\circ - \delta y / 2\right)^2\end{aligned}} \tag{3.142}$$

$$n_{r1} = \sqrt{\begin{aligned}&\left(R_{silo} - r_{e2}\cos\theta_2 / \cos 45^\circ - \delta x / 2\right)^2 \\ &+ \left(R_{silo} + r_{e2}\cos\theta_2 / \sin 45^\circ + \delta y / 2\right)^2\end{aligned}} \tag{3.143}$$

we have

If $k_{ind}(i, j, k) = 6$

$R_{silo} - x(i) = y(j) - R_{silo}$

and $n_{r1\le}\sqrt{x(i)^2 + y(j)^2} \le n_{r2}$ then

$$k_{ind}(i, j, k) = 7 \tag{3.144}$$

The similar processes can be carried out when the ducts are placed along N, NE, SE, S, SW, W and NW radii.

When $k_{ind}(i, j, k) = 7$, the temperature and moisture content of the node are

$$T(i, j, k) = T_{duct} \tag{3.145}$$

$$w(i, j, k) = w_{duct} \tag{3.144}$$

where T_{duct} and w_{duct} refer the temperature and moisture content of aeration air in the outlet of the duct and equations (2.38) and (2.39) are used.

3.7 Conclusions

The results of this chapter can be summarized as follows

- A mesh of finite discrete nodes has been set up using a control volume method to represent a silo.

- The discretization equations have been derived from the partial differential equations that govern heat and mass transfer in the bulk grain for every grid node in the domain of interest in.
- The grid nodes at the boundaries are found. The relevant boundary conditions are expressed in a simple linearized algebraic form.
- All variables are converted to arrays that are easy to store in a computer.

CHAPTER 4

VALIDATION OF THE MATHEMATICAL MODEL

Equations that encapsulate the physics of aerated grains have been formulated, and numerical schemes have been devised for their solution. However, the phenomena that occur both within and external to an aerated silo are quite complicated. We shall examine how the mathematical models capture the details of the conditions that occur in an aerated on-farm silo containing canola oil seeds.

To achieve this goal, results generated by the mathematical model were compared against experimental data obtained independently by CSIRO Entomology.

4.1 Field trial

The experiments were conducted at Wongan Hills, Western Australia, where the climate is characterized by being hot and arid during the summer months. As well as providing data for validating the mathematical model, the experiments were designed to be intrinsically valuable in providing data on aeration. The motivation behind the experiments was not only to cool grain for long term storage, but also to dry them within the first ten or so days after they had been placed in storage. For this reason the air flow rate during the drying phase was 13.8 L/s/t, and during the long-term storage phase was reduced to1.6 L/s/t.

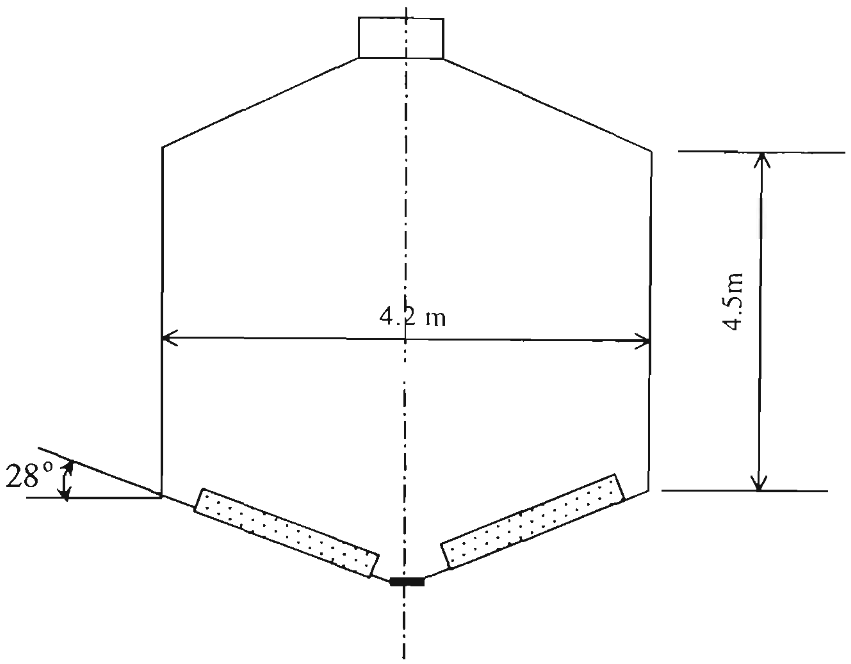

Figure 4.1 Schematic diagram of the silo used in the field experiment conducted at Wongan Hills, Western Australia

4.1.1 Experimental set up

Figure 4.1 shows the diagram of the silo used in the field at Wongan Hills. The wall of the silo is 4.5m high and the diameter is 4.2m. 47.5 tonnes of canola (an oil seed) was loaded in the silo at 30th November 1998. The grain initially had an average temperature of 40°C, an average moisture content of 6.5% wet basis, and an oil content

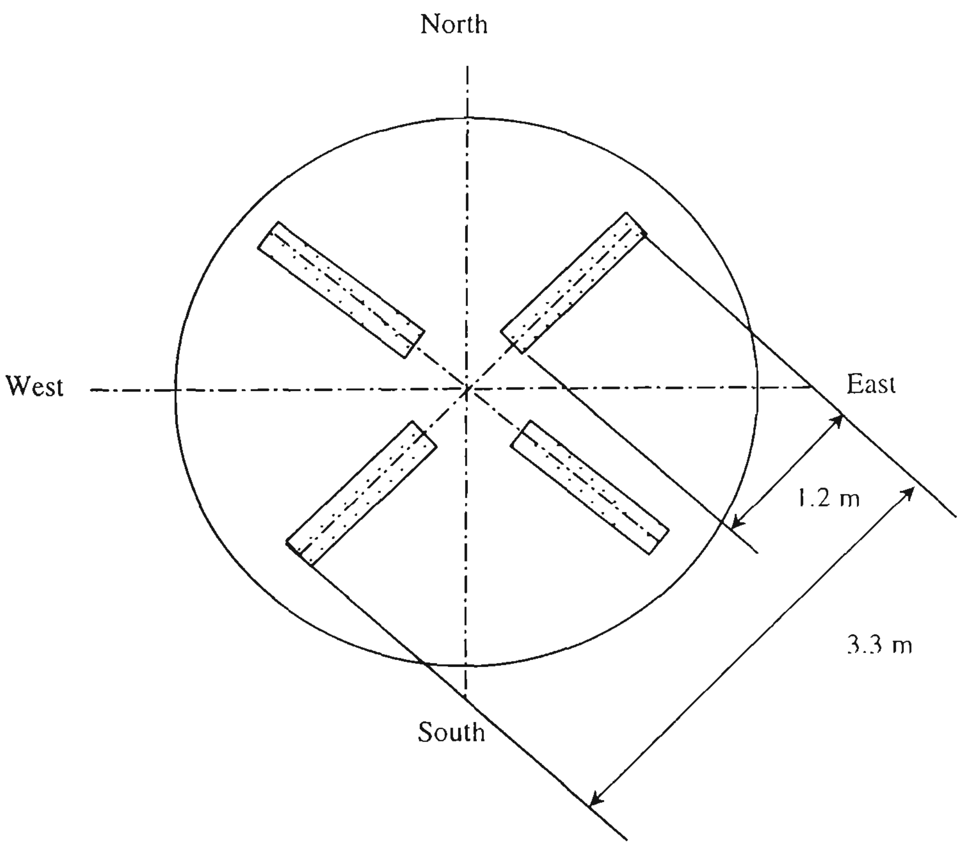

Figure 4.2 Aeration ducts placed in a cruciform pattern on the silo base, Wongan Hills

of 42% dry basis. Figure 4.2 shows the layout of four linear ducts in the silo. The ducts had a length of 1.2m and were laid in a cruciform manner on the sloping base of the silo.

During the first nine testing days from 4pm 9th November 1998 to 4pm 18th November 1998, an aeration fan was run at an airflow rate of 13.8 L/s/t and the air emanated from four ducts (Figure 4.2). The purpose of this aeration process was to cool the grain quickly. After nine days a smaller aeration fan provided airflow to one duct, the southeast duct, at a flow rate of 1.6 L/s/t, in order to cool and maintain the grain during long term storage.

Table 4.1 Aeration system activity schedule at Wongan Hill, Western Australia

Date	Time	Fan size	Fan status	Set Point		
				RH	Dry-bulb temperature, ^{o}C	Wet-bulb temperature, oC
09/11/98	14:00	Large	Manul on			
10/11/98	9:00	Large	Manul off			
10/11/98	11:00	Large	Auto on	>20%	<40	
11/11/98	8:00	Large	Auto on	95%~40%	<40	
13/11/98	9:00	Large	Manul off			
13/11/98	12:00	Large	Auto on	95%~40%	<40	
13/11/98	18:00	Large	Auto on	90%~40%	<40	
14/11/98	10:00	Large	Auto on	80%~40%	<40	
16/11/98	8:00	Large	Auto on	85%~35%	<40	
18/11/98	18:00	Small	Manul on			
19/11/98	9:30	Small	Manul off			
19/11/98	10:30	Small	Auto on	>0%		
23/11/98	12:30	Small	Auto on	>0%		<18
27/11/98	6:00	Small	Auto on	>0%		<15
03/12/98	6:00	Small	Auto on	>0%		<12

In both aeration processes, the fans were operated according to a schedule derived by selecting suitable ambient conditions and displayed in Table 4.1.

4.1.2. Measurement

The main features of the measurements included:

- ambient conditions such as dry-bulb temperature, wet-bulb temperature, relative humidity, wind speed, wind direction, and solar radiation;
- surface temperatures on the outside of wall, roof and hopper cone;
- grain conditions such as temperatures and moisture contents at various locations, *e.g.* along the centerline of the silo, the boundaries such as the wall, hopper cone, upper surface and ducts;
- air temperatures and relative humidity in the head space.

The sensors were mainly placed along southeast (SE), northeast (NE), northwest (NW) and southwest (SW) radii directions and data were recorded at 207 locations or points inside or nearby to the silo. The time interval at which the measurement sensors were scanned was 31 minutes.

4.2 Simulation conditions

4.2.1 Simulation conditions - outputs

The mathematical model provides three-dimensional profiles of grain temperature and moisture contents. Although not germane to the validation study, the model also provides information on the biological potential of insect populations to increase, and seed viability. For validating the mathematical model with the experimental data, the simulation outputs in this thesis are expressed based on the locations or points that corresponded to the experimental measurement points.

Figure 4.3 shows the locations of some of the measured values against which the modelled values were compared. Three typical variables were selected; namely the grain temperatures along the centerline of the silo at heights 1.5 m, 3.0 m and 4.5 m from the floor of silo, as representative of the grain temperatures in the lower level (1.5

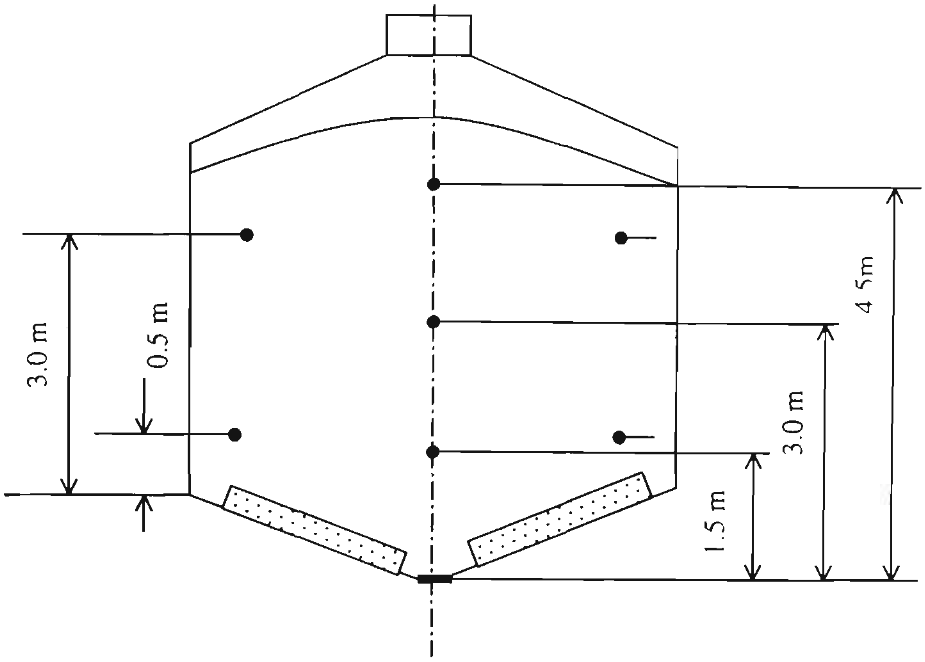

Figure 4.3 Temperature cables, SE-NW cross-section

m), middle level (3.0 m), and upper level (4.5 m). The reason of this selection is that the sensors placed on the central line of the silo help to capture some of the non-uniformly distributed phenomena associated with aeration with linear ducts.

Note that there may be inappropriate storage conditions occurring at the boundaries, due to unsatisfactory ambient conditions such as intense solar radiation, or high ambient temperatures. In practice, the stored grains can reduce in value and even become completely ruined by a small spoilage arising from localised mould growth or insect development. Hence, the second consideration of our simulation is the measurement of

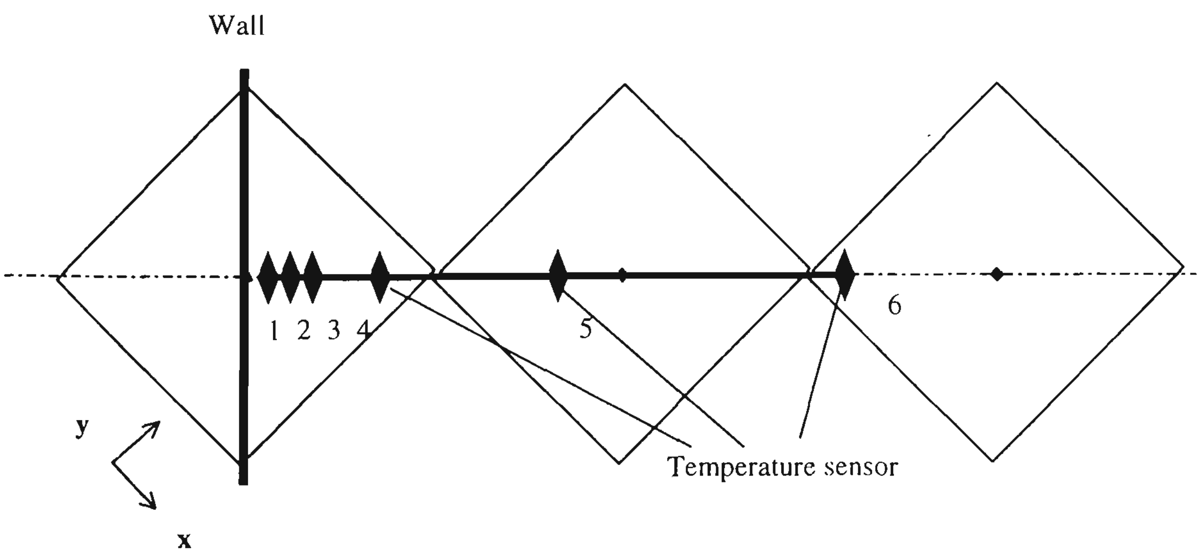

Figure 4.4 Schematic layout of grid and NW temperature sensors, Wongan Hills

temperatures near the periphery of the grain store.

In the program, the grid was chosen as $19\times19\times19$ initially and a convergence check is carrying out in section 4.3.1. Figure 4.4 shows the positions of measured temperature points in the grid at northwest side of wall boundary. It can be seen that sensors 1 to 4 are located adjacent to the wall boundary, assumed to be as ambient conditions in the program. We chose sensor 6 as the simulation point since sensor 5 in NWA failed to function during the experiment.

Table 4.2 The temperatures to be simulated, Wongan Hills

Label assigned to experiment	Description of the variables
Centre drop cable 450 cm	At a height of 450cm along the centreline from the lowest point of silo
Centre drop cable 300 cm	At a height of 300cm along the centreline from the lowest point of silo
Centre drop cable 150cm	At a height of 150cm along the centreline from the lowest point of silo
SWB6	Located at southwest side of silo with a height of 3.0m from the lowest point of silo and a distance of 52cm from the silo wall
SWA6	Located at southwest side of silo with a height of 1.5m from the lowest point of silo and a distance of 52cm from the silo wall
SEB6	Located at southeast side of silo with a height of 3,0m from the lowest point of silo and a distance of 52cm from the silo wall
SEA6	Located at southeast side of silo with a height of 1.5m from the lowest point of silo and a distance of 52cm from the silo wall
NEB6	Located at northeast side of silo with a height of 3.0m from the lowest point of silo and a distance of 52cm from the silo wall
NEA6	Located at northeast side of silo with a height of 1.5m from the lowest point of silo and a distance of 52cm from the silo wall
NWB6	Located at northwest side of silo with a height of 3.0m from the lowest point of silo and a distance of 52cm from the silo wall
NWA6	Located at northwest side of silo with a height of 1.5m from the lowest point of silo and a distance of 52cm from the silo wall

There are two groups of temperature sensors each side of wall boundary shown in figure 4.3. Altogether, three temperatures along the centerline and eight temperatures in proximity to the wall boundary of the silo were simulated (Table 4.2).

4.2.2 Simulation input

The computational program estimated the ambient conditions using meteorological data including the mean daily maximum dry-bulb temperature, mean daily minimum dry-bulb temperature, humidity ratio, and solar radiation for a range of geographic locations in Australia (BOM, 2000). To predict the dynamic characteristics of the ambient conditions, a periodic sine-function was used to capture the daily trend of dry-bulb temperature as follows (Hunter, 1981)

$$T_{amb}(t_h) = T_{mean} + \sin(\frac{t_h - 9}{12} \times \pi) \tag{4.1}$$

where T_{amb} is the ambient temperature, t_h is the time of day and T_{mean} is the daily average ambient temperature calculated as follows

$$T_{mean} = (T_{\max} + T_{\min})/2 \tag{4.2}$$

and $T_{\max}$ is the mean daily maximum dry-bulb temperature, $T_{\min}$ is mean daily minimum dry-bulb temperature.

Table 4.3 The meteorological data at Wongan Hill, Western Australia

	November	December
Mean daily maximum dry-bulb temperature, °C	28.7	32.5
Mean daily minimum dry-bulb temperature, °C	13.0	15.9
Mean 9:00am relative humidity, %	47	44
Mean 3:00pm relative humidity, %	28	24

Source: BOM, 2000

The principles of the solar radiation calculation are based on Duffie *et al.*'s work (1980). At Wongan Hills, the meteorological data (BOM, 2000) of November and December are shown in Table 4.3.

The operating schedule in the program is processed to accord to the hours per day that the users want the aeration system on. A default schedule was also setup to turn on the fans 0:00am to 6:00am.

In figure 4.5 both recorded and the ambient temperatures calculated from average climatic data are plotted, as well as the experimental fan status. We see clearly that the experimental schedule of fan operation caught the lowest periods of recorded ambient temperatures well that is significantly different from the default schedule in the program such as operating between 0:00am and 6:00am. We make use of the experimental fan status for the operating schedule and recorded ambient conditions including the temperatures and relative humidity in the simulation processes.

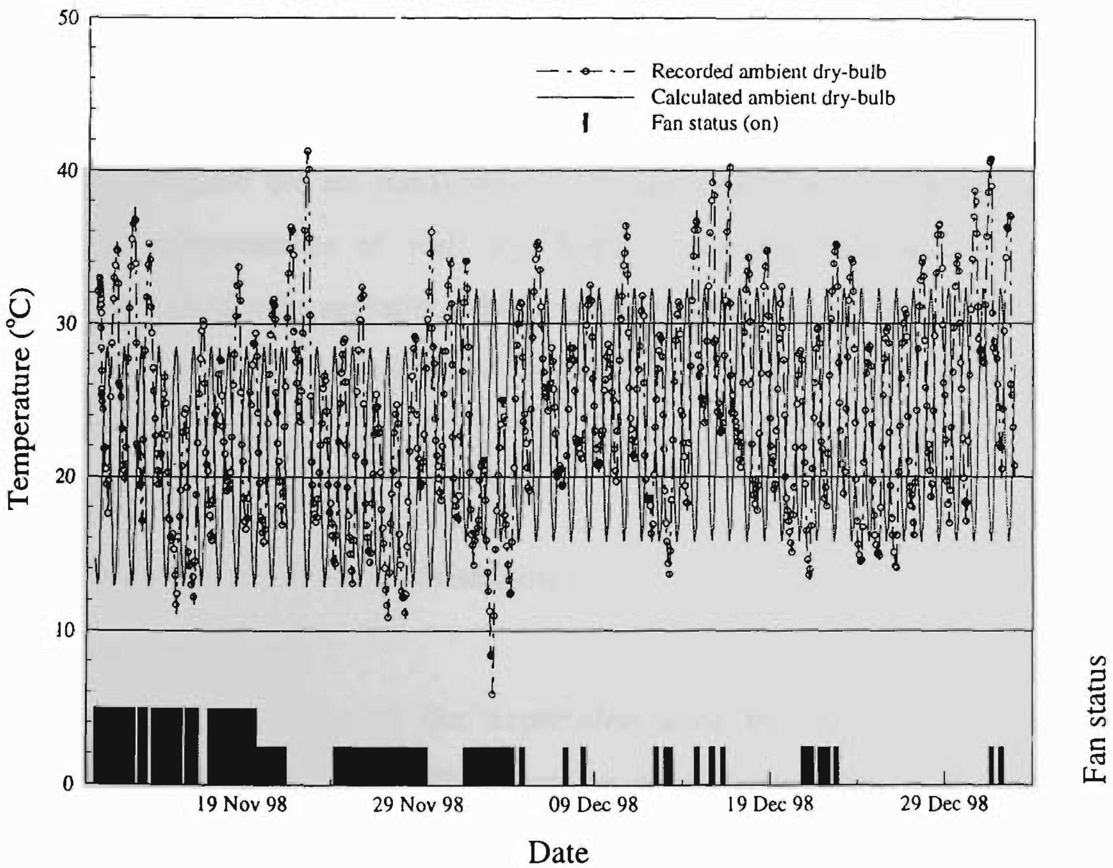

Figure 4.5 The comparison of recorded ambient temperatures and calculated ambient temperatures, and experimental fan status (on) Wongan Hills

Since the solarimeter used in the trial for solar radiation had an incorrect calibration, we utilised the meteorological data of Perth, Western Australia, which is the nearest station recording solar radiation (BOM, 1998), for solar radiation calculations.

The experimental data were recorded at the experimental time interval, 31 minutes, so the time step of the program simply used a quarter of this time interval, 7.75 minutes, started at 15:27:59 06/11/1998 and finished at 23:36:42, 31/12/1998. Furthermore, we assumed any fan status such as on or off, started at a half time between the previous record and the current record and finished at a half time between the current record and the next record. The convergence study confirming suitability of the choice of the time step is in section 4.3.1.

The program incorporates structural and physical parameters of commonly used silos and ducts. The physical model of the silo was setup in the program with actual geometric data. In this thesis, we simply make use the physical parameters of the program combining with structural parameters of the experimental silo to set up physical features of the silo.

4.2.3 Simulation boundary conditions

In the program the air conditions in the headspace are considered these of ambient air. The temperatures of wall and hopper base are calculated from the ambient temperatures and solar radiation. The experimental processes introduced the ambient air as the aeration air so in this study the conditions of aeration air are same as the measured ambient conditions.

4.3 Simulation results and discussion

4.3.1 Convergence study

Convergence criterion is the expression used to indicate that the approximate computed solution of partial differential equations approaches to the exact solution of the finite difference problem as the grid spacing in time and distance tend to zero (Carnahan *et al.* 1969). In previous section, we setup a time step as 7.75 minutes and a grid $19 \times 19 \times 19$ in the program.

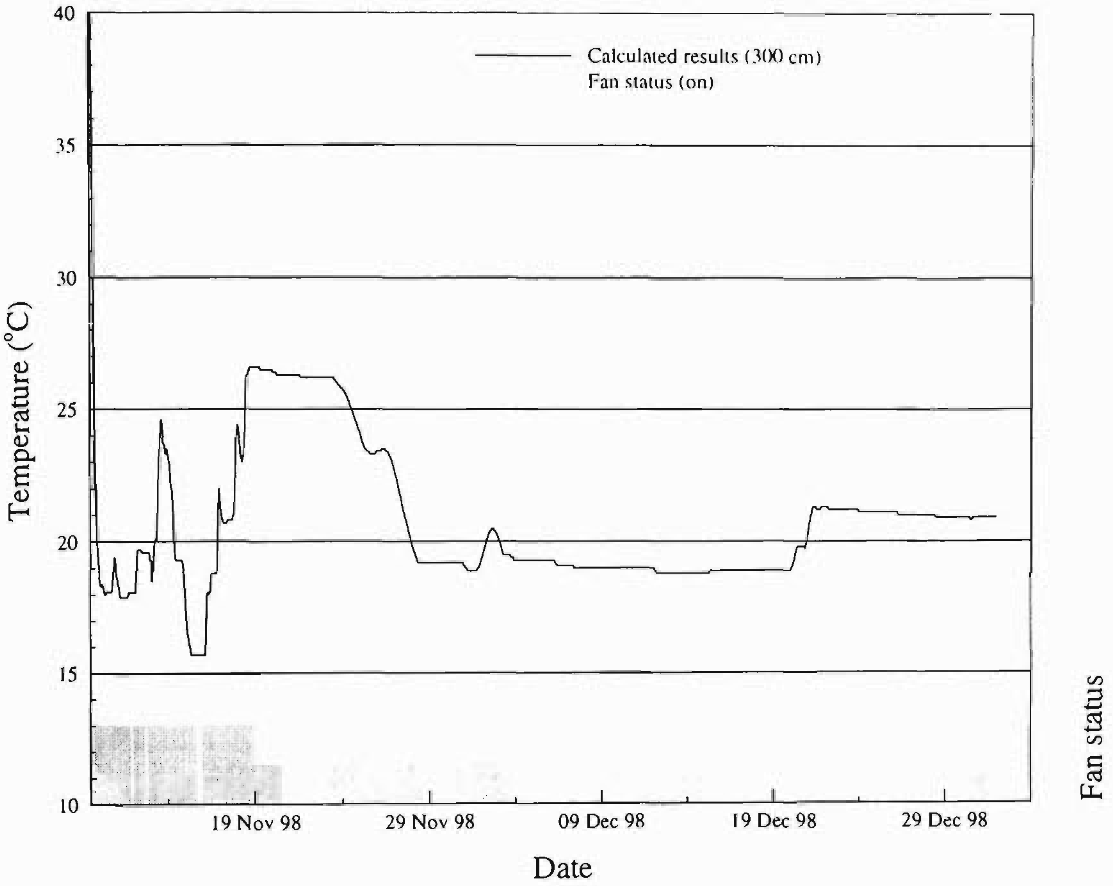

Figure 4.6 Calculated results for the centre drop cable 300 cm, Wongan Hills, and the grid is setup as 19x19x19 and the time step is 7.75 minutes in the program

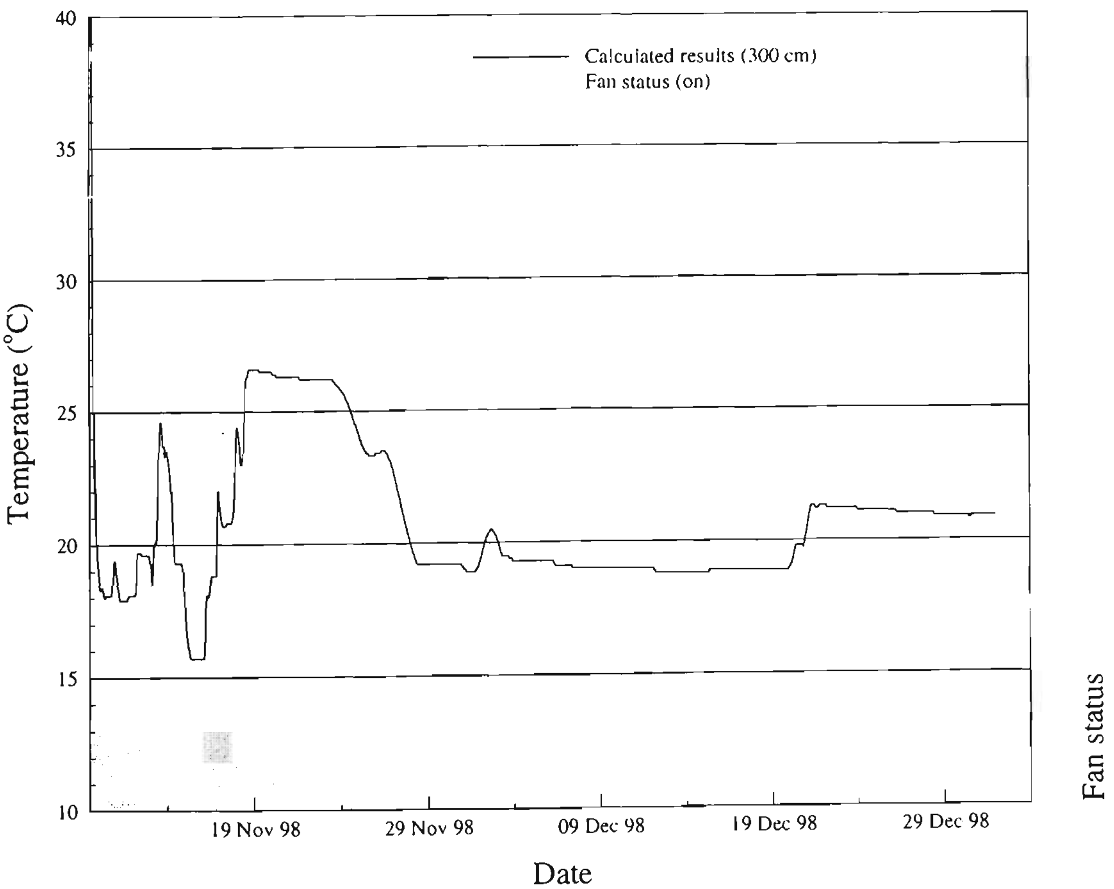

Figure 4.7 Calculated results for the centre drop cable 300 cm, Wongan Hills, and the grid is setup as 39x39x39 and the time step is 7.75 minutes in the program

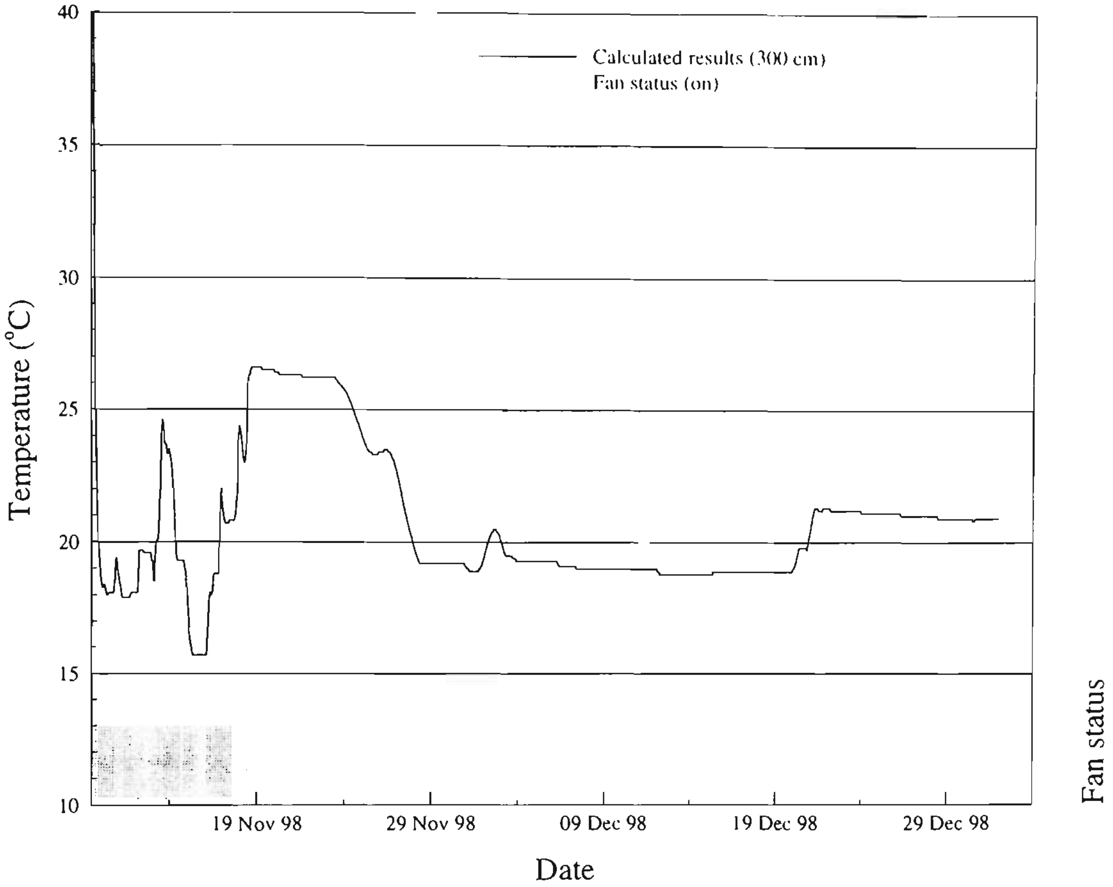

Figure 4.8 Calculated results for the centre drop cable 300 cm, Wongan Hills, and the grid is setup as 79x79x79 and the time step is 7.75 minutes in the program

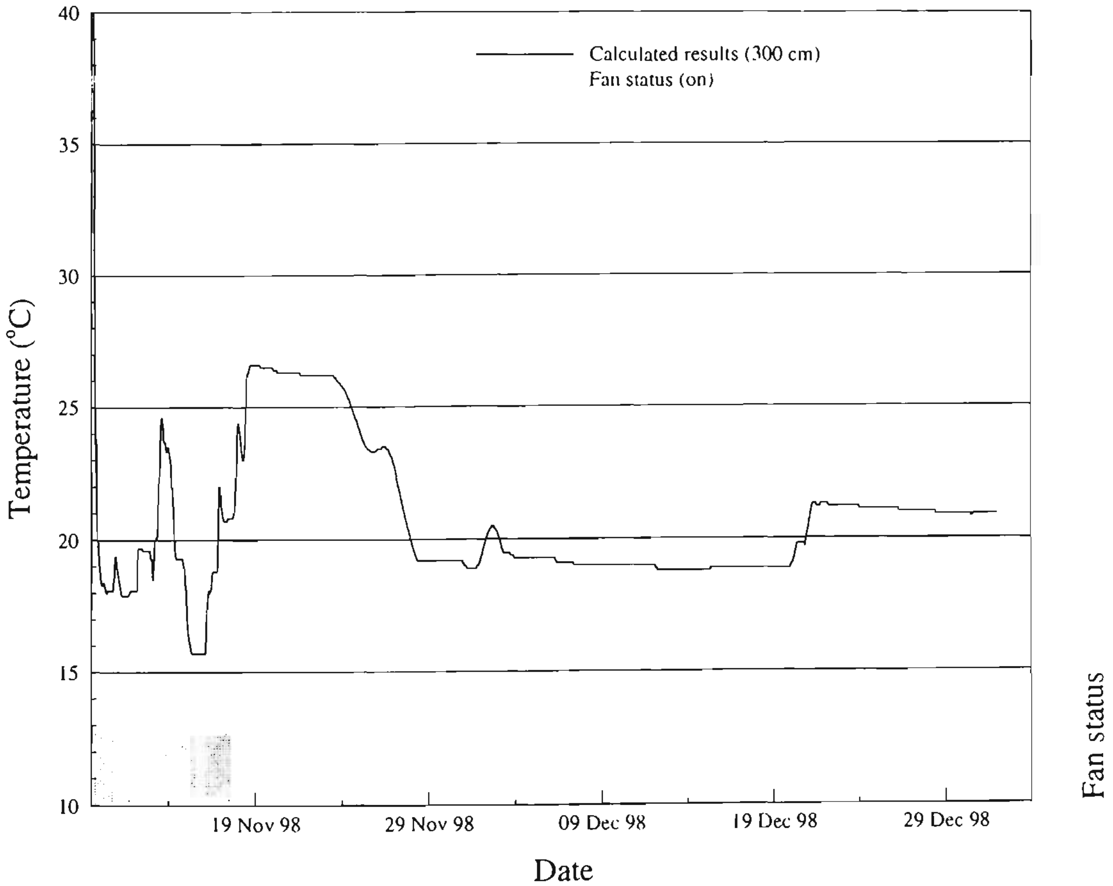

Figure 4.9 Calculated results for the centre drop cable 300 cm, Wongan Hills, and the grid is setup as 19x19x19 and the time step is 3.875 minutes in the program

We also made use of grids of $39\times39\times39$ and $79\times79\times79$ with the time step, 7.75 minutes and a smaller time step 3.875 minutes with the grid $19\times19\times19$. A typical grain temperature, the centre drop cable 300 cm, was selected to show the calculated result of the program and the calculated results are shown in figures 6.6 to 6.9. We found that in spite of the longer running time of the program the calculated results are same in those four setups in the program.

Hence, we conclude that the calculated solution of the program with the grid $19\times19\times19$ and the time step of 7.75 minutes is convergent.

4.3.2 Simulation results

In the figures 4.10 to 4.13, simulation results and recorded data are plotted against experimental time for the selected three centre locations in the silo.

In all the three cases, the plots indicate that the temperature distribution calculated by the program clearly follows the recorded plots. This indicates that the mathematical model is able to capture the general trend of the recorded data such as sharp increase or decrease in the grain temperatures. We noted that at the upper level, figure 4.8, there are some discrepancies in the measured and modeled temperatures when the small fan was operating. It is suspected that the model underestimated the temperature of the upper surface of the grains.

Figures 4.13 to 4.20 show the simulation results of variables adjacent to the wall. It can be seen that the simulated plots at of the variables at wall boundaries are in good agreement with the actual data when the large fan was on. When the small fan was on (at 18^{th} November, 1998), there are poor agreements between the plots of simulation and experimental record points.

There are temperature discrepancies existing in the simulated results of all eight variables. Simulated plots are mostly below the actual data and, in particular, the simulated plots do not capture the increasing trend showed in experimental plots when the small fan was operating.

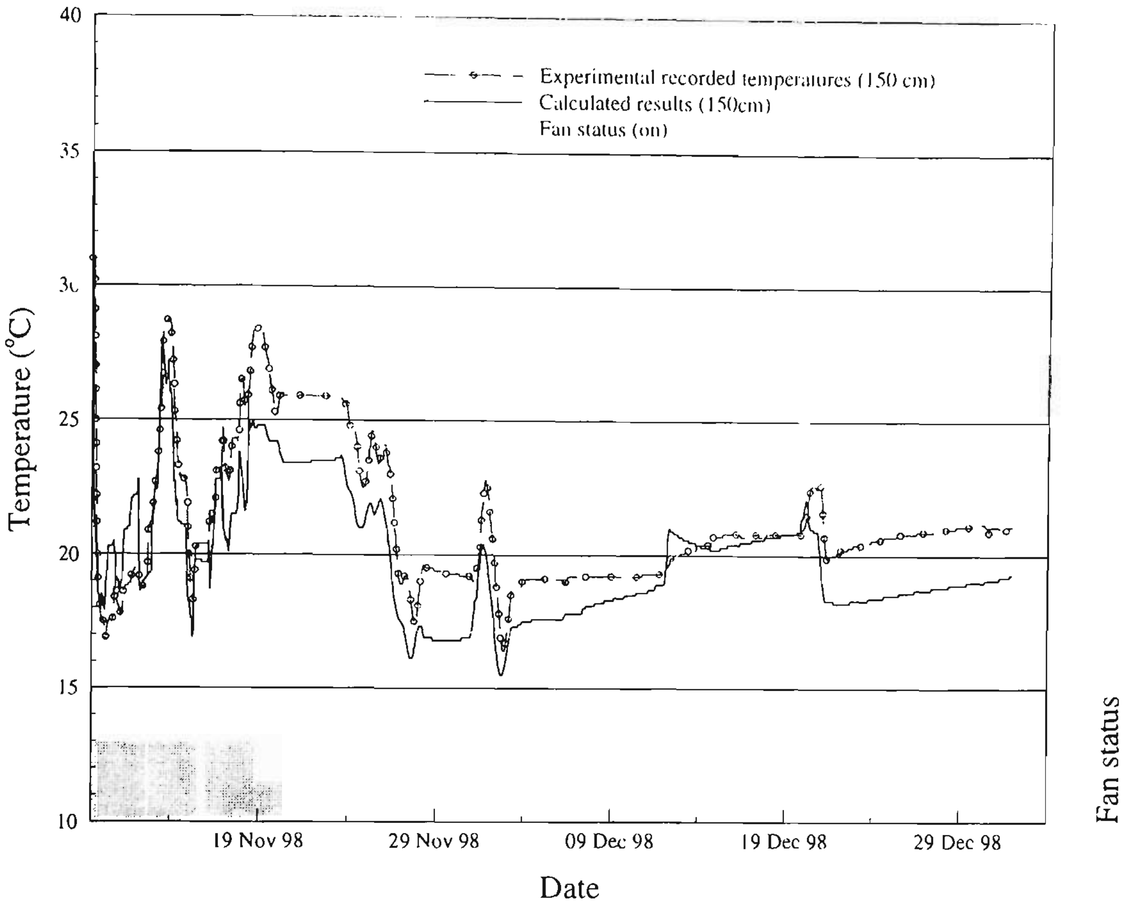

Figure 4.10 Comparison of experimental recorded temperatures and simulated results for the centre drop cable 150 cm, Wongan Hills

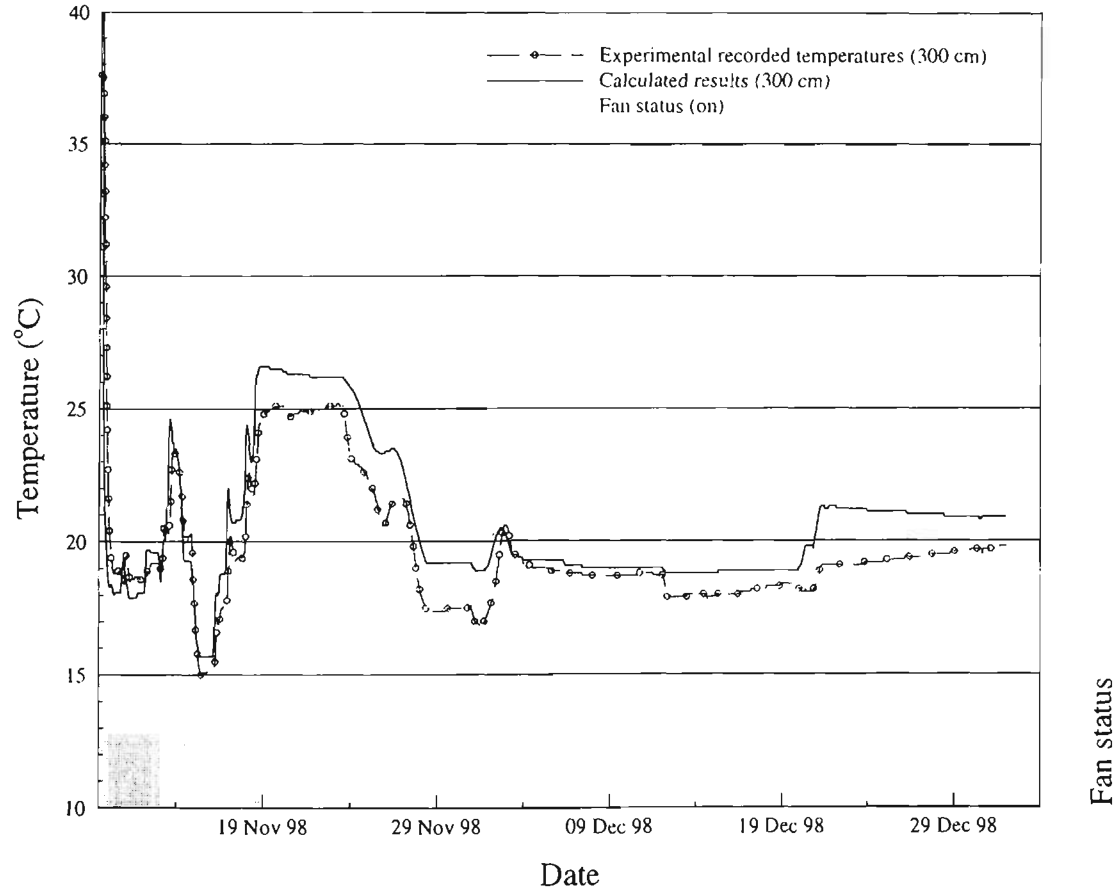

Figure 4.11 Comparison of experimental recorded temperatures and simulated results for the centre drop cable 300 cm, Wongan Hills

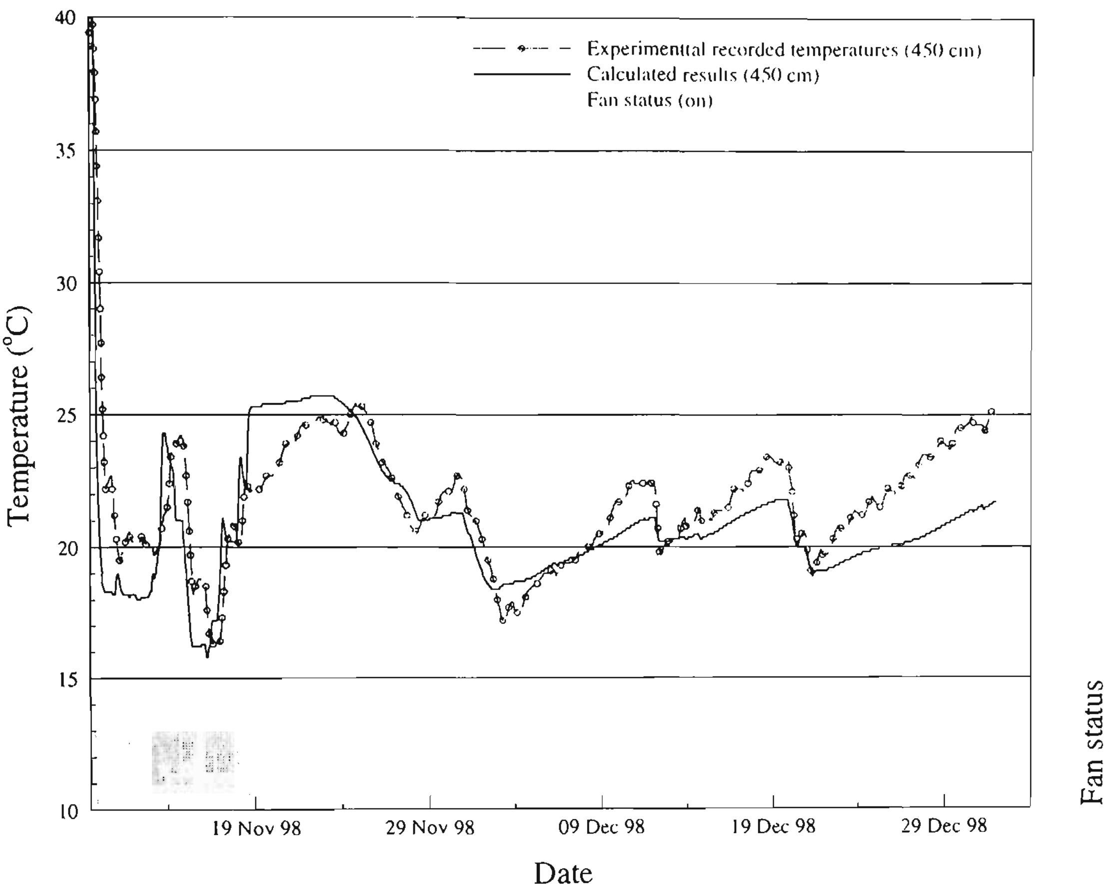

Figure 4.12 Comparison of experimental recorded temperatures and simulated results for the centre drop cable 450 cm, Wongan Hills

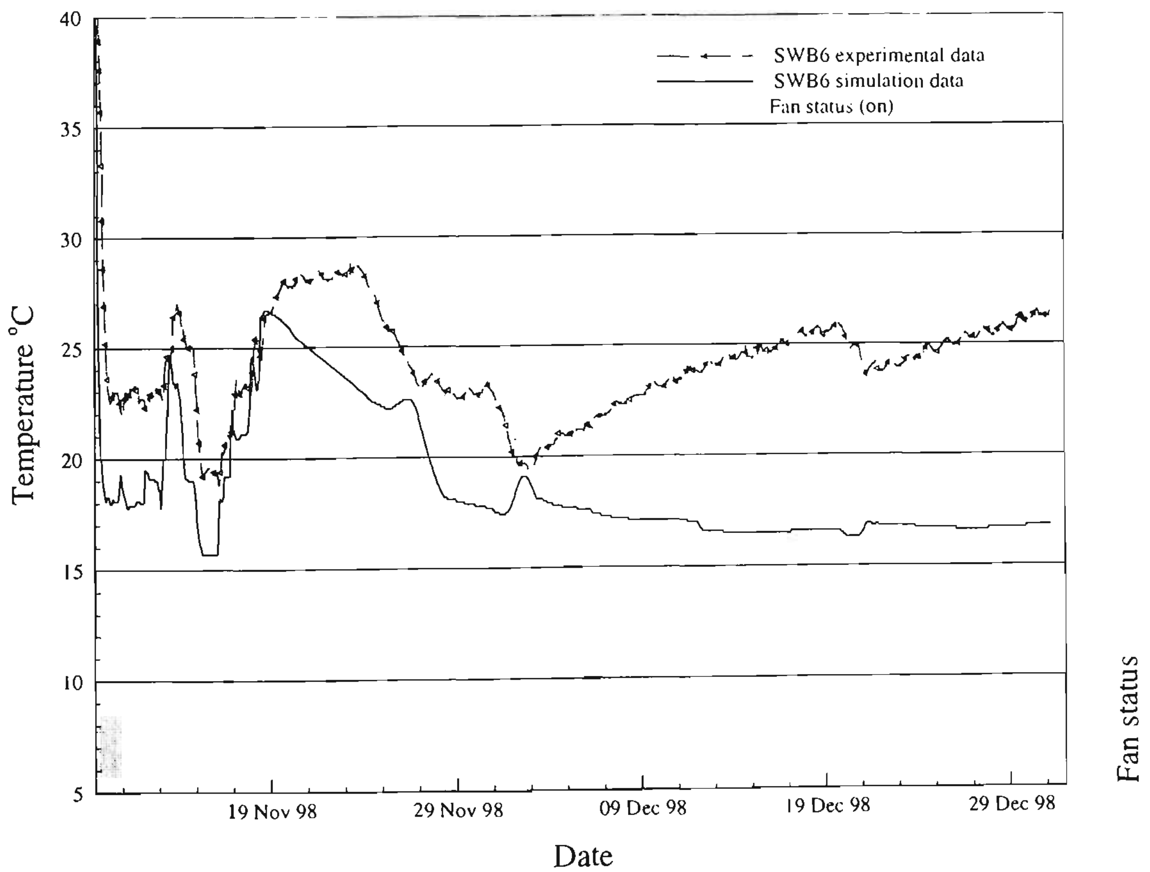

Figure 4.13 Comparison of experimental recorded temperatures and simulated results for the SW upper sensor SWB6, Wongan Hills

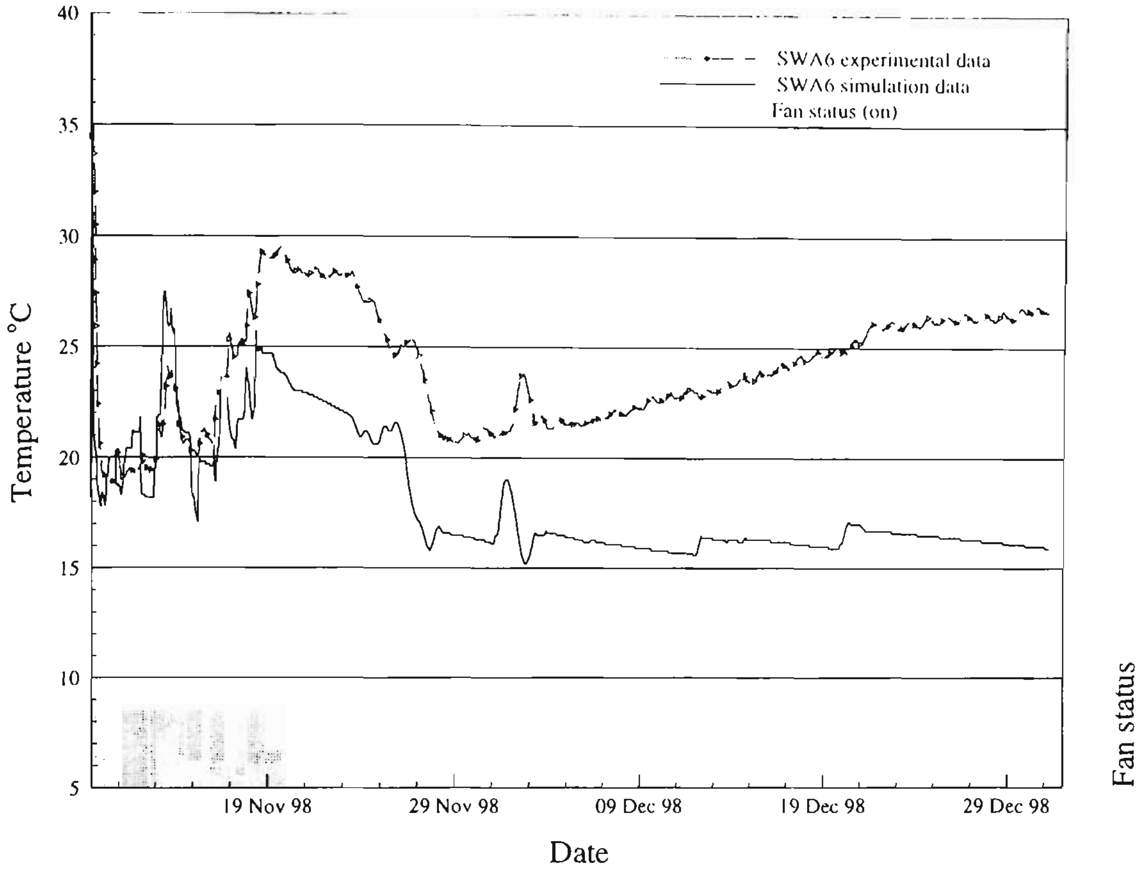

Figure 4.14 Comparison of experimental recorded temperatures and simulated results for the SW lower sensor SWA6, Wongan Hills

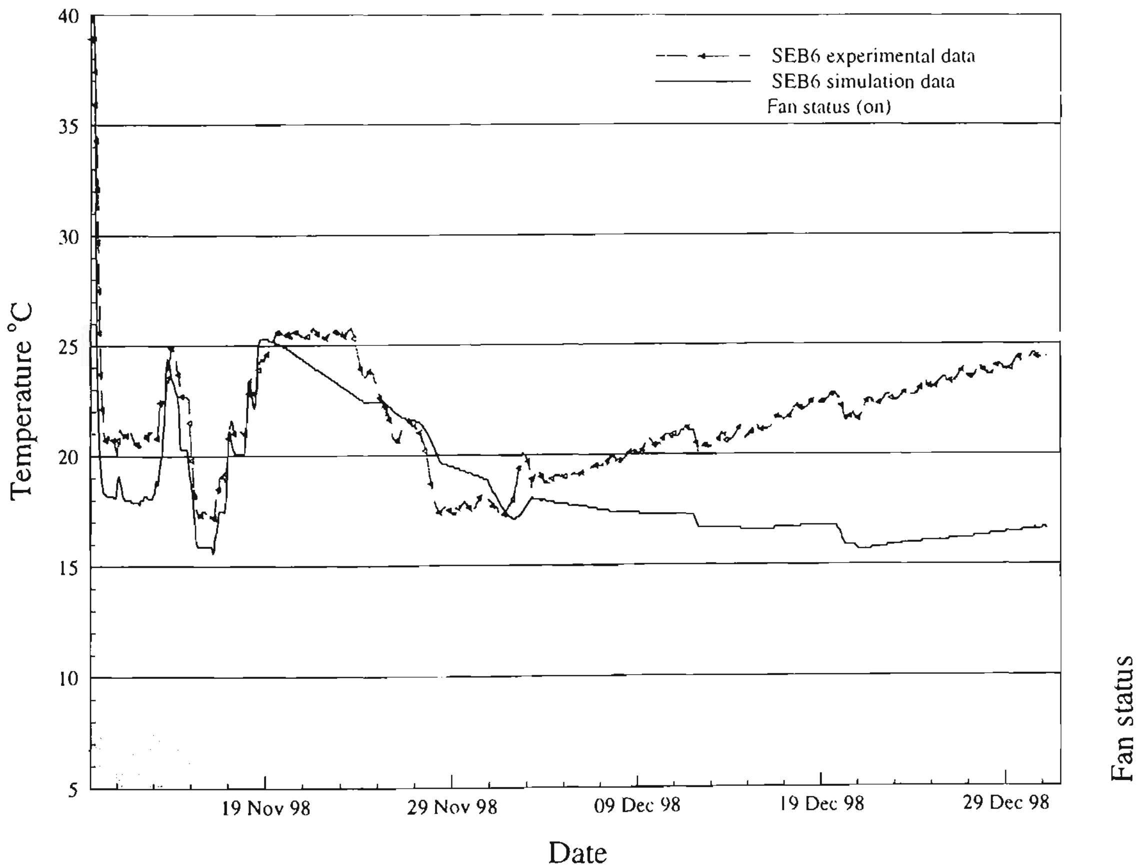

Figure 4.15 Comparison of experimental recorded temperatures and simulated results for the SE upper sensor SEB6, Wongan Hills

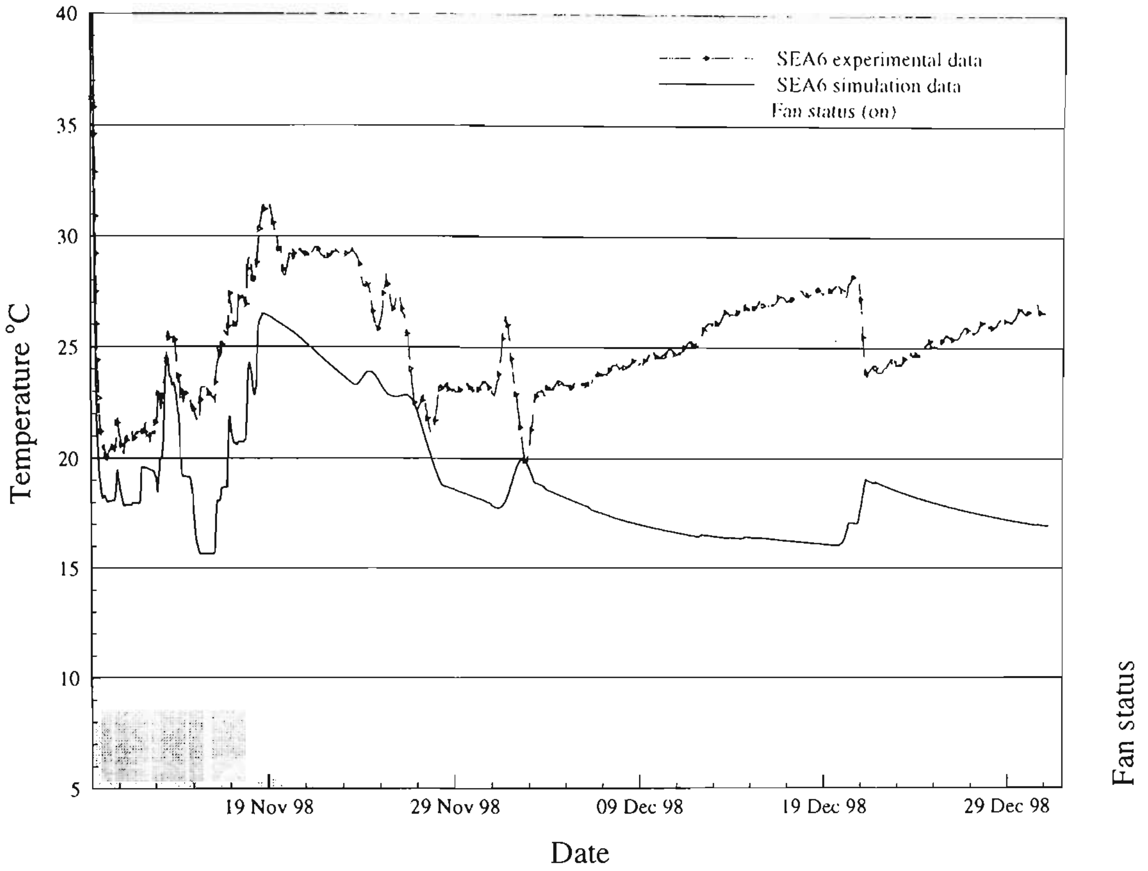

Figure 4.16 Comparison of experimental recorded temperatures and simulated results for the SE lower sensor SEA6, Wongan Hills

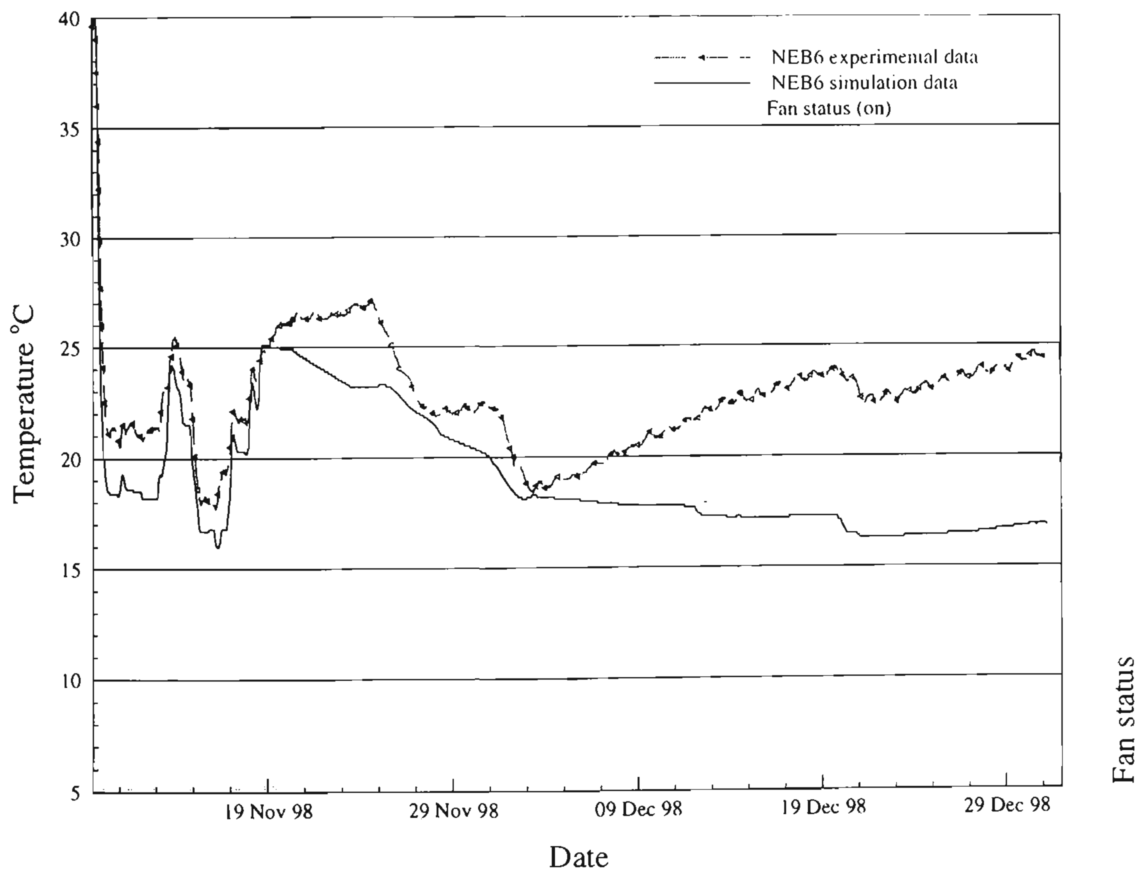

Figure 4.17 Comparison of experimental recorded temperatures and simulated results for the NE upper sensor NEB6, Wongan Hills

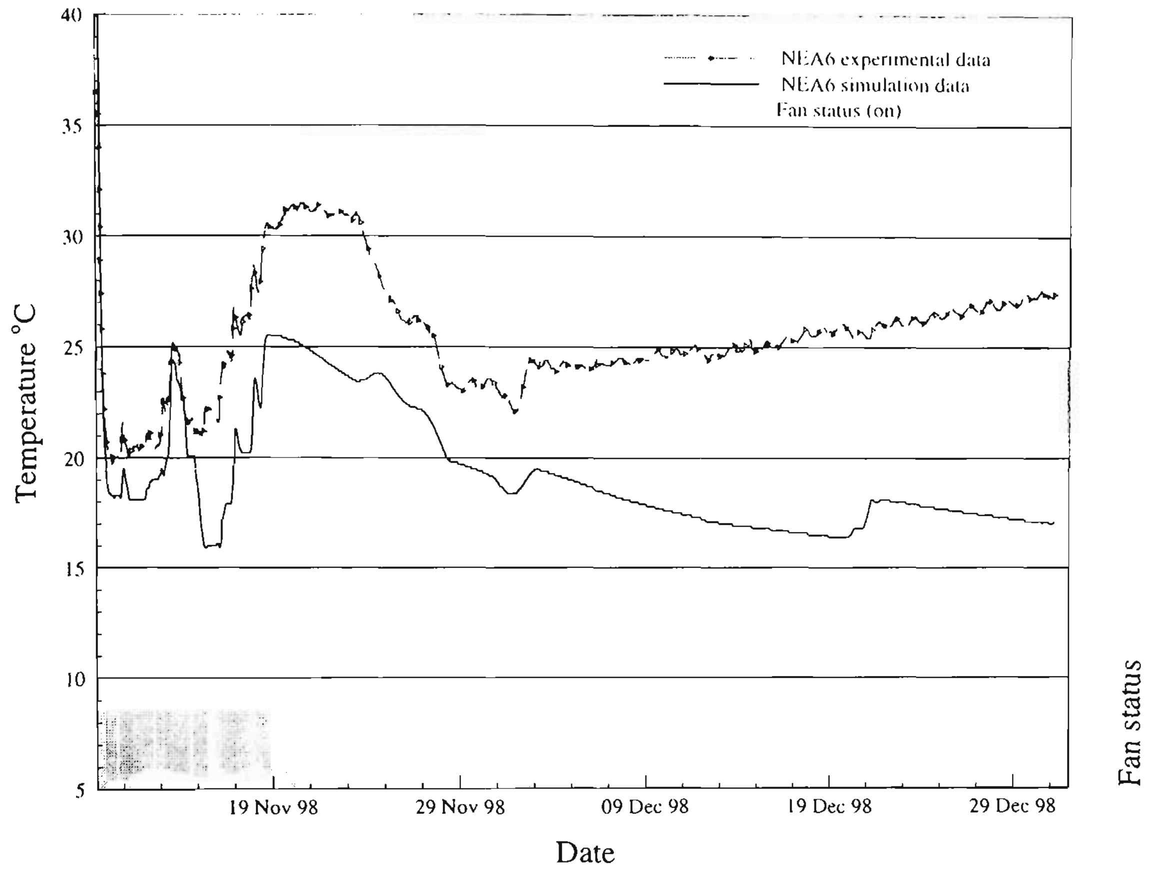

Figure 4.18 Comparison of experimental recorded temperatures and simulated results for the NE lower sensor NEA6, Wongan Hills

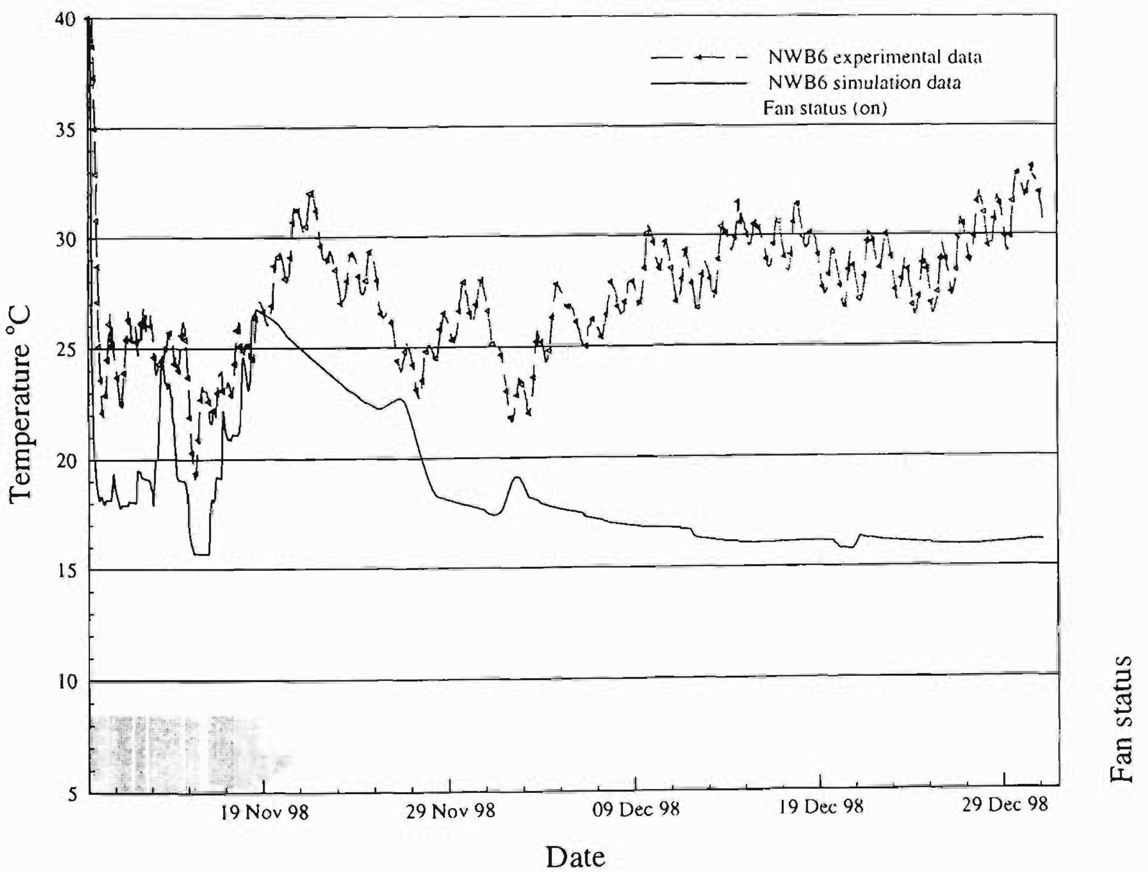

Figure 4.19 Comparison of experimental recorded temperatures and simulated results for the NW upper sensor NWB6, Wongan Hills

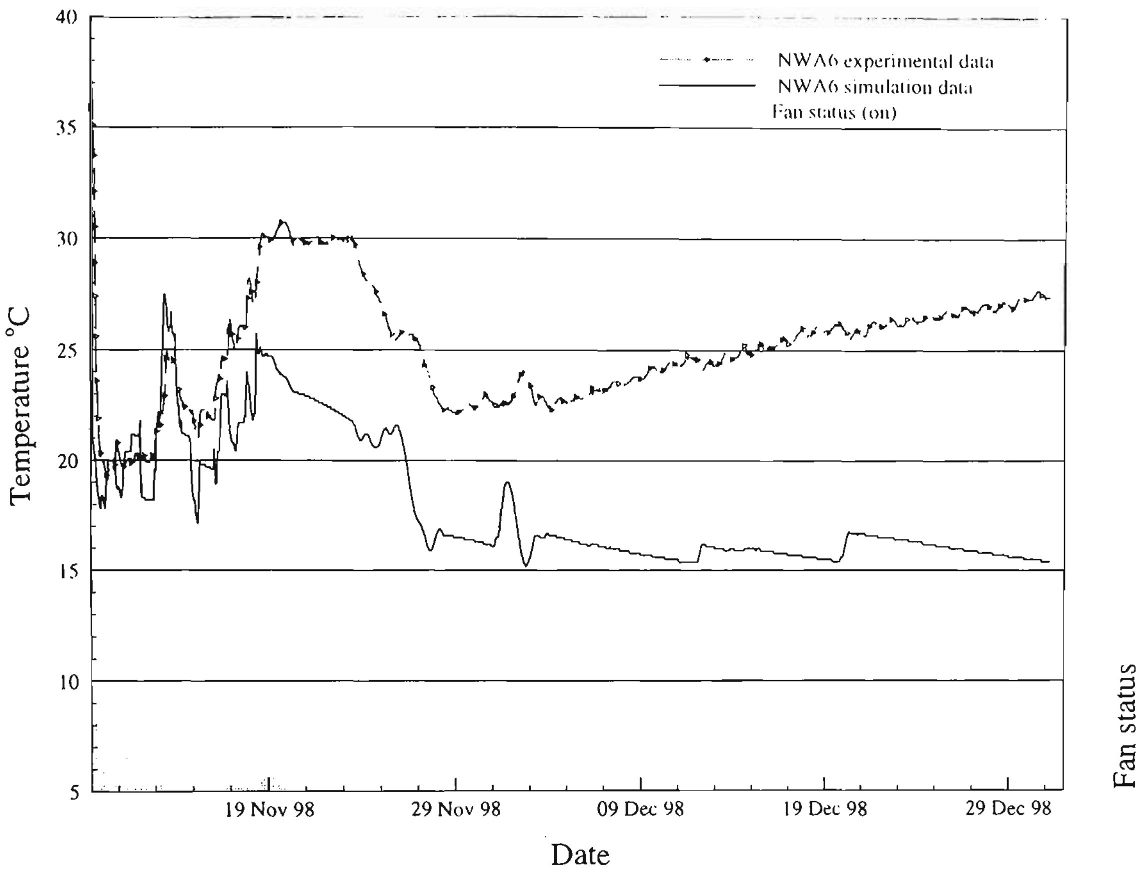

Figure 4.20 Comparison of experimental recorded temperatures and simulated results for the NW lower sensor NWA6, Wongan Hills

Since at internal boundary adjacent to the wall of the silo convection mainly dominates the heat and mass transfer when aeration air has a high flow rate with the large fan on and conduction mainly dominates heat and mass transfer between the aeration air and the grains when aeration air has a low flow rate with the small fan on, the results showing in figure 4.13 to 4.20 may be caused by the model of conduction for the wall boundary or the approximation of thermal conditions of the wall surface of silo in the program.

Because the simulation results are in poor agreement with experimental data, especially in the upper level along the centreline and all locations of wall boundary, three modified simulation processes were carried out in this thesis for studying the reasons for the poor agreement.

4.3.2 Modified simulation 1

In figure 4.21, the recorded temperatures in headspace and ambient air are plotted. It was found that the recorded air temperatures in the headspace were significantly higher than the ambient temperatures that we used for the air conditions in the headspace in the

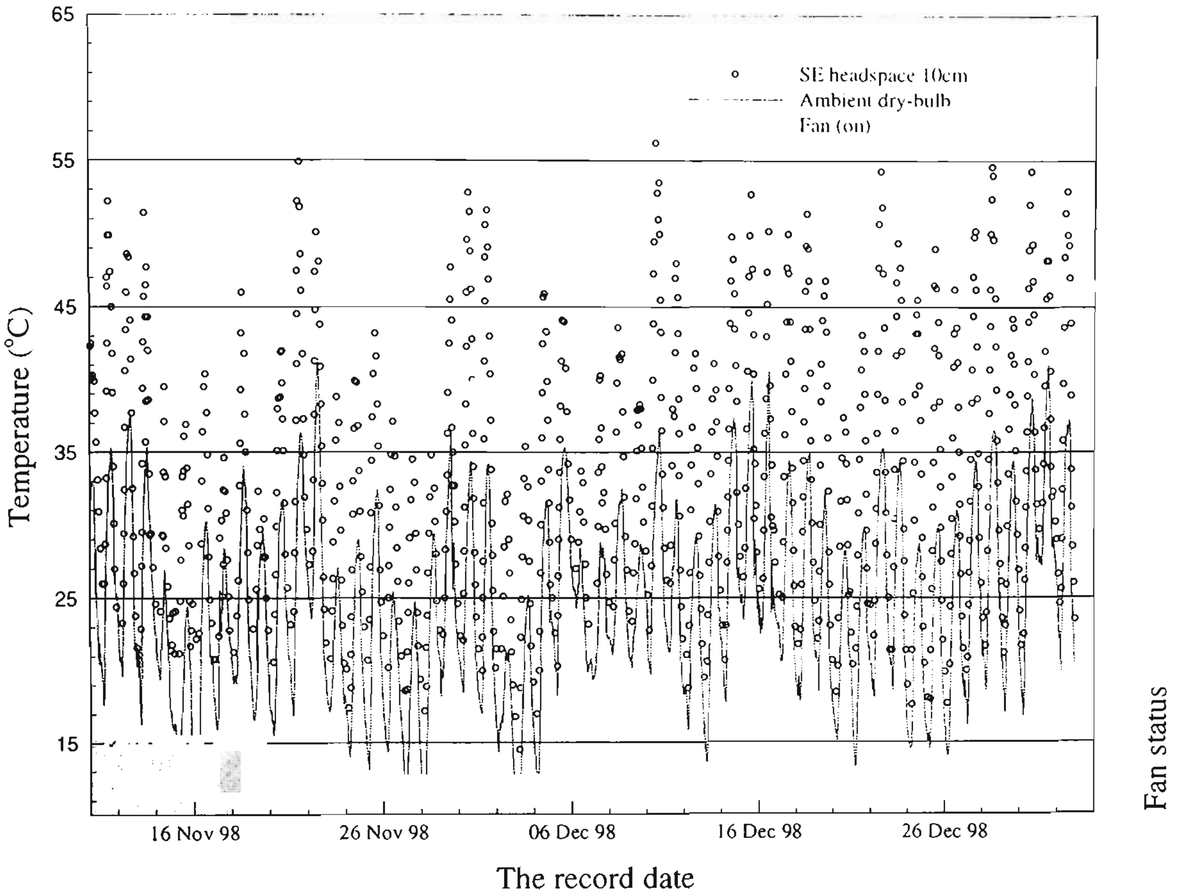

Figure 4.21 The recorded temperatures in the headspace (distance from grain surface, 10 cm) and recorded ambient temperatures

program. This situation may affect the simulated temperature values against the recorded data. Hence, the recorded headspace temperatures were introduced into the process of modified simulation 1.

The simulation results of centerline temperatures are shown in figures 4.22 to 4.24. Note that the simulated plots in upper level capture the recorded data extremely well and the temperature differences shown in the figure 4.12 did not appear. In the lower level, figure 4.22, and middle level, figure 4.23, the results of the modified simulation 1 are similar to the results of the simulation showing in figures 4.10 and 4.11. We believed that the forced convection caused by the aeration air mainly influence the variables at lower and middle levels along the centerline of silo.

When the aeration air had a high flow rate, the center variable at the upper level was affected mainly by convection of aeration air flow when the aeration fan was operated with a high flow rate. Both the conduction from the headspace and convection of aeration air flow affected this variable when the aeration was operated with a low air flow rate.

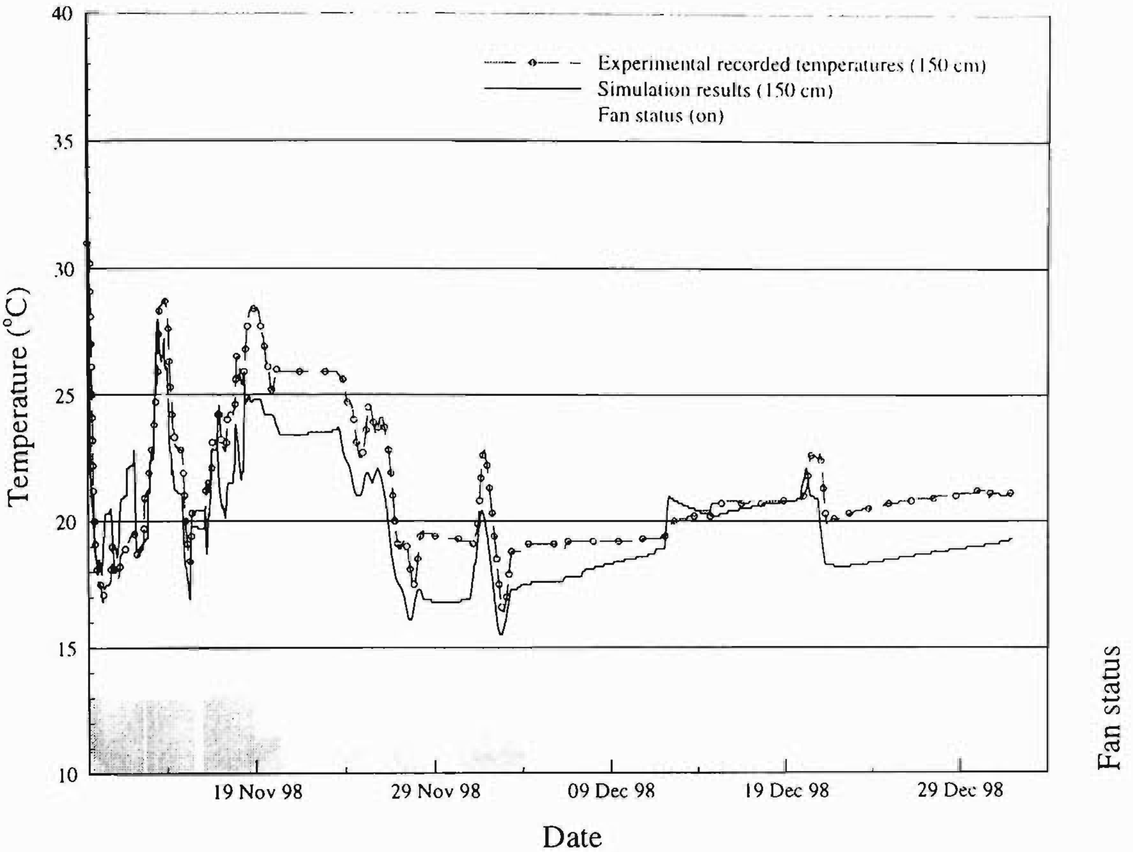

Figure 4.22 Comparison of experimental recorded temperatures and calculated results for the centre drop cable 150 cm - modified simulation 1 (recorded data used for the temperatures of headspace)

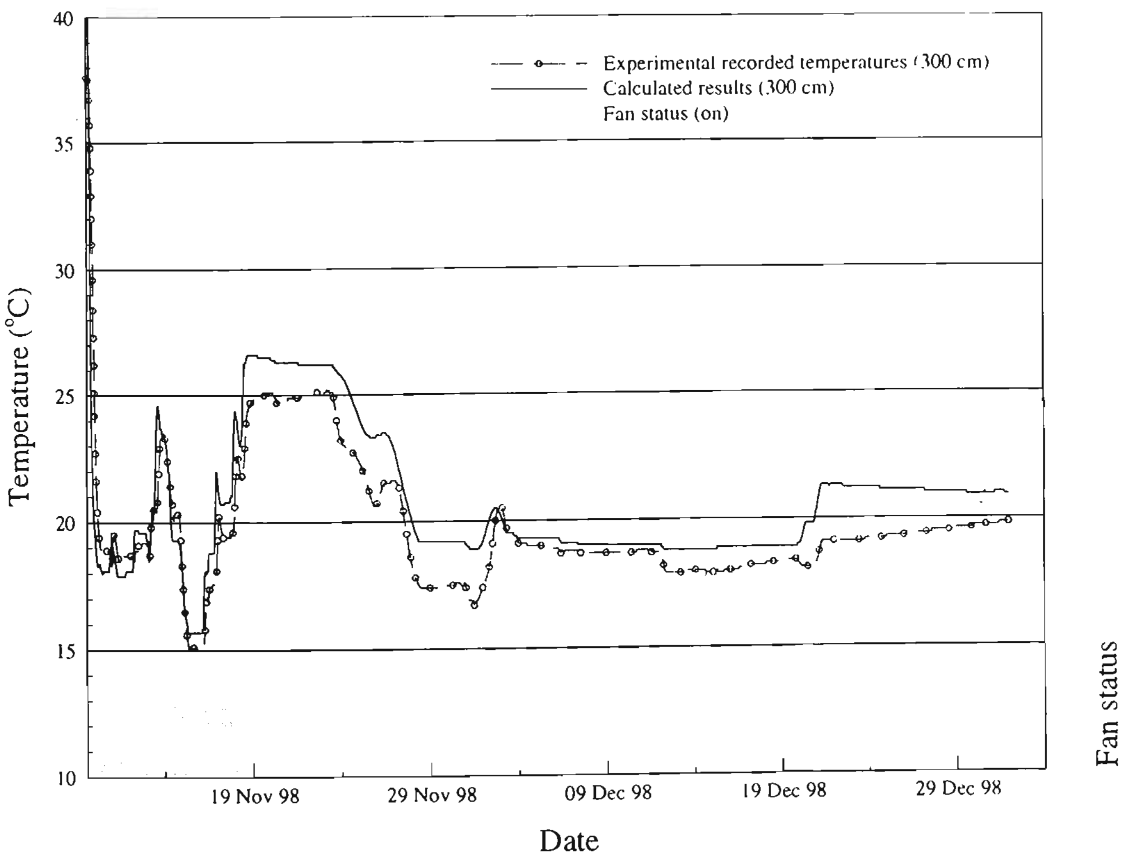

Figure 4.23 Comparison of experimental recorded temperatures and calculated results for the centre drop cable 3050 cm - modified simulation 1 (recorded data used for the temperatures of headspace)

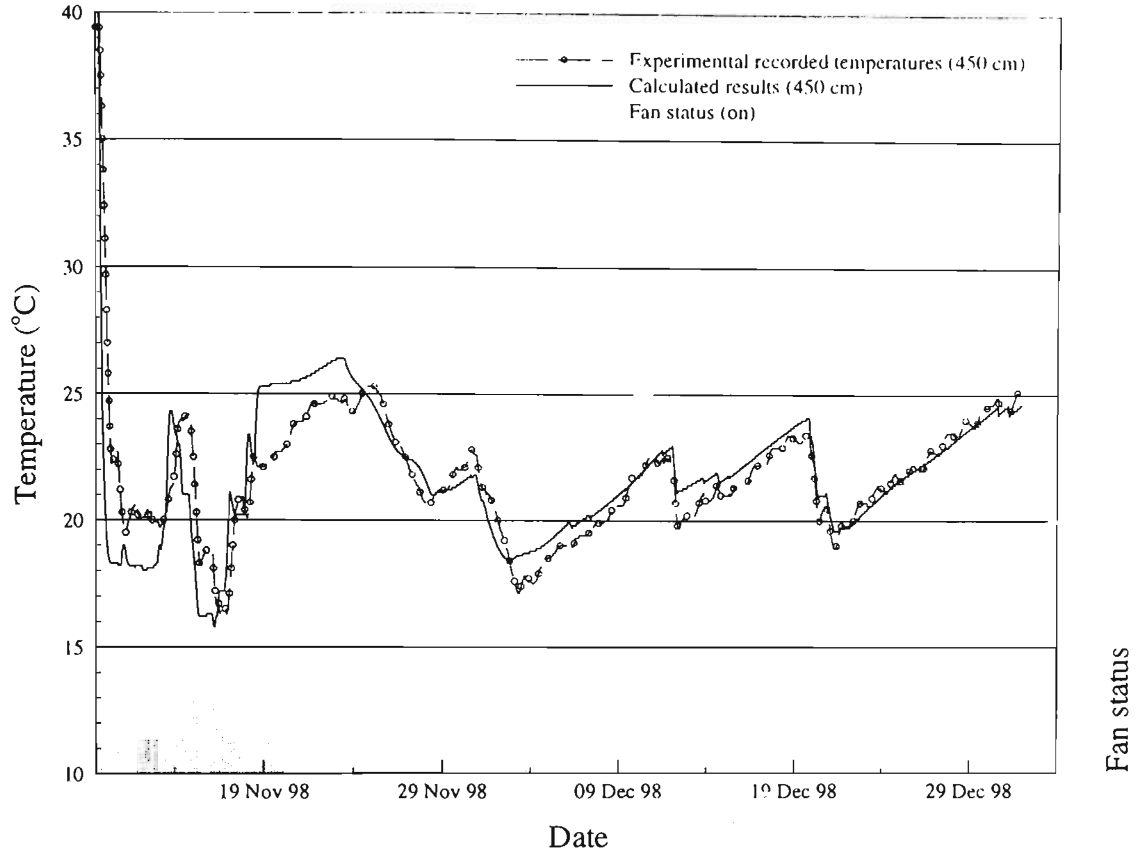

Figure 4.24 Comparison of experimental recorded temperatures and calculated results for the centre drop cable 450 cm - modified simulation 1 (recorded data used for the temperatures of headspace)

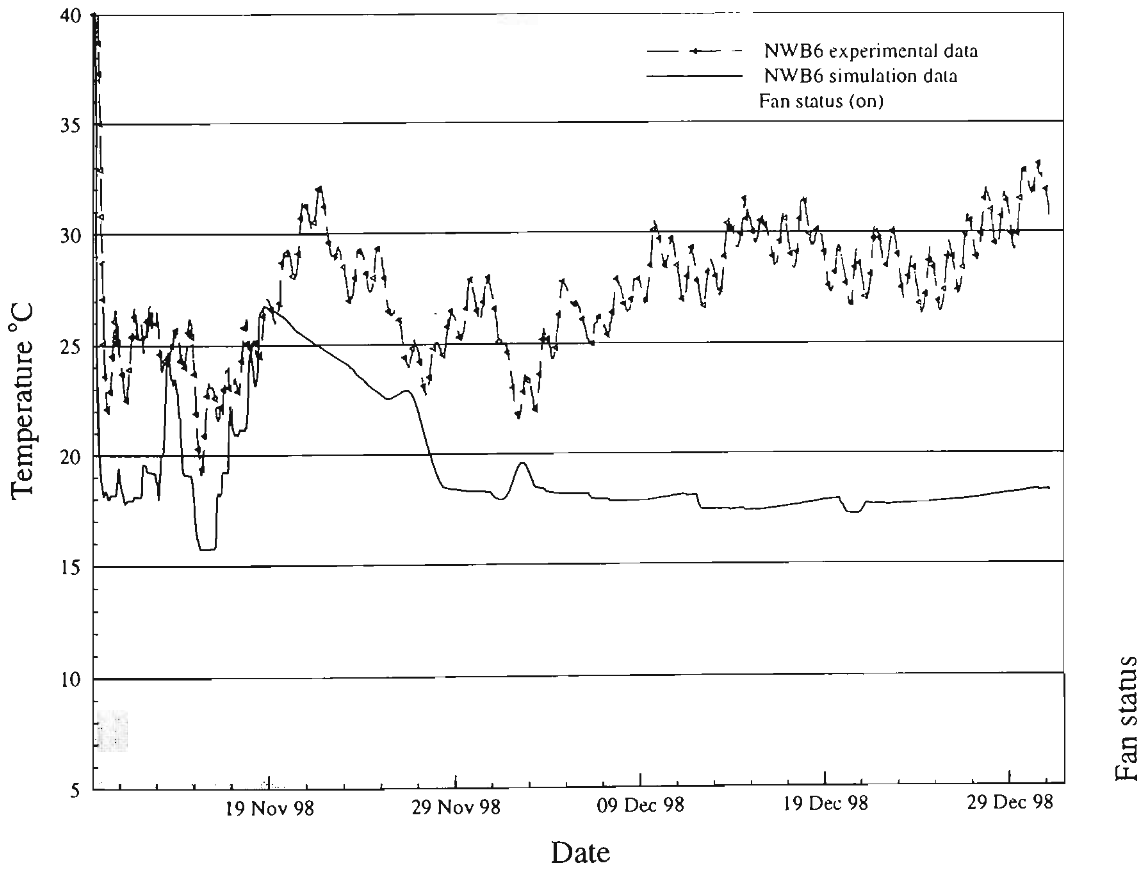

Figure 4.25 Comparison of experimental recorded temperatures and simulated results for the NW upper sensor NWB6 - modified simulation 1 (recorded data used for the headspace temperatures)

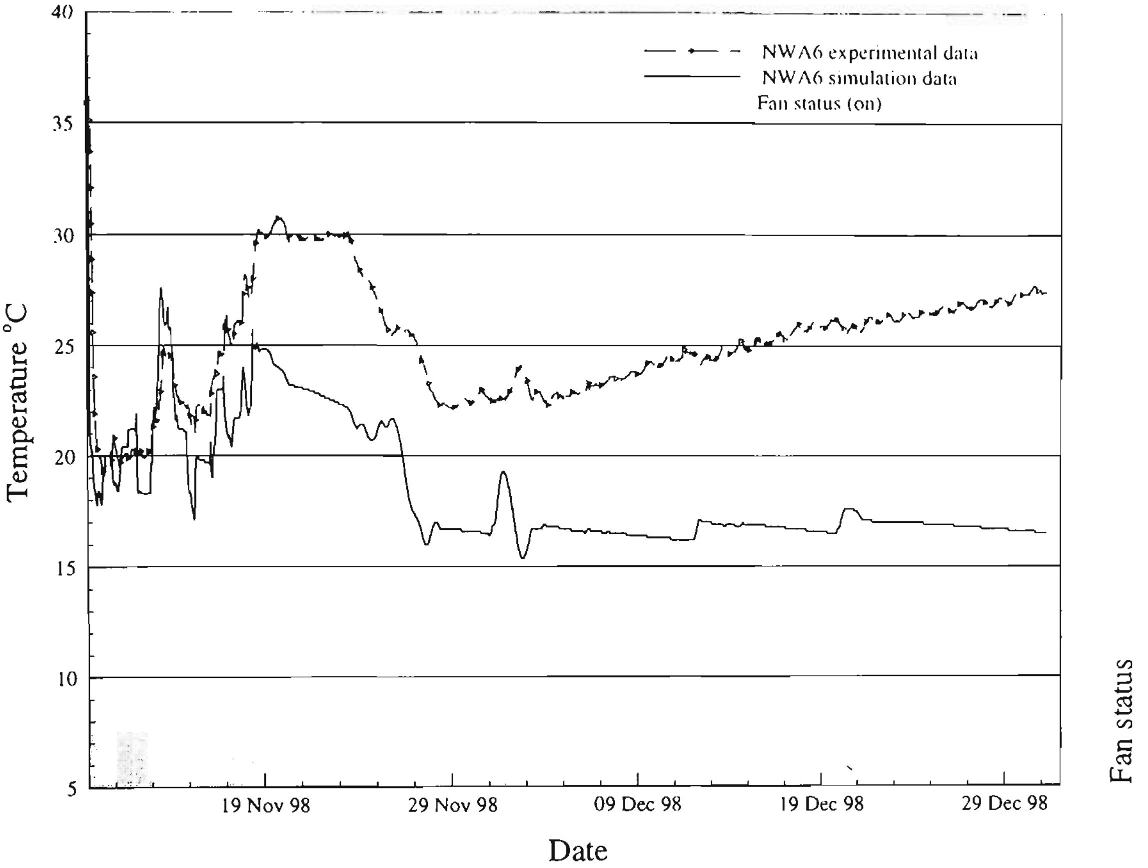

Figure 4.26 Comparison of experimental recorded temperatures and simulated results for the NW lower sensor NWA6 - modified simulation 1 (recorded data used for the headspace temperatures)

It indicates that the consideration of headspace condition in the initial program do not agree with reality very well.

The results of the eight variables of wall boundary from modified simulation 1 do not show any improvement. In figures 4.25 and 4.26 the simulation results for two typical variables, NWB6 and NWA6, and the corresponding experimental data are plotted.

Comparing with the plots in figure 4.19 and 4.20, we found that the air condition in the headspace did not influence the conditions at those locations of the wall boundary.

4.3.3 Modified simulation 2

In the modified simulation 1, the poor agreements between the calculated temperatures and recorded data in wall boundary do not improve. It is noted that those poor agreements only happened when the small fan was operating. As we mentioned in Chapter 2, the conduction may be the main cause for the heat transfer when the aeration flow rate is low. It is necessary to check the considerations of the model of conduction for the wall boundary or the approximation of thermal conditions of wall of silo in the program. In the process of modified simulation 2 we introduced the recorded temperatures of wall into the calculation for wall boundary condition.

Those simulation results of three variables along the centerline are plotted in figures 4.27 to 4.29. Comparing the calculated results at the lower level plotted in figures 4.10 and 4.27, the results at middle level in figures 4.11 and 4.28 and the results at upper level in figure 4.12 and 4.29, we found out that there are no clear differences in all plots of the three variables along the centerline of the silo. It is found that the conditions at the wall have little effect on grain temperatures along the centerline of silo in the program.

The results of the eight variables at wall boundary from modified simulation 2 show in figures 4.30 to 4.37.

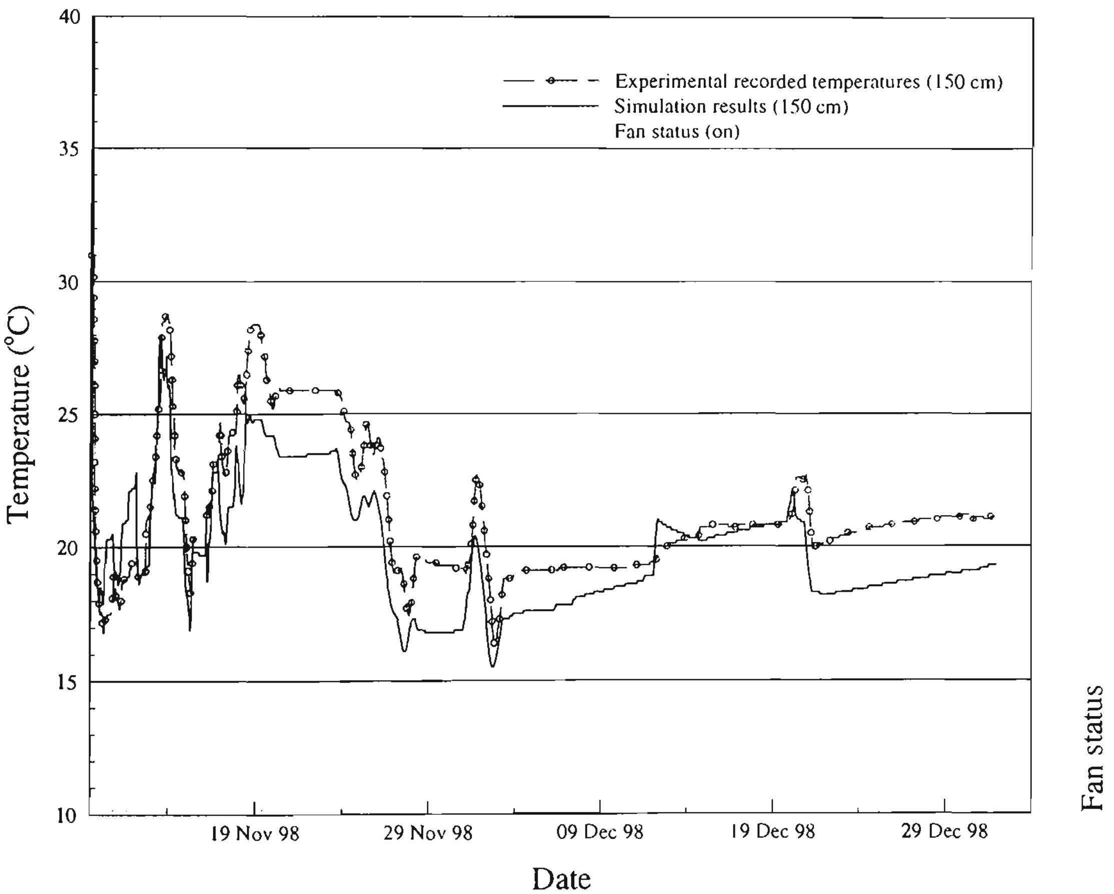

Figure 4.27 Comparison of experimental recorded temperatures and calculated results for the centre drop cable 150 cm - modified simulation 2 (recorded data used for the temperatures of the wall)

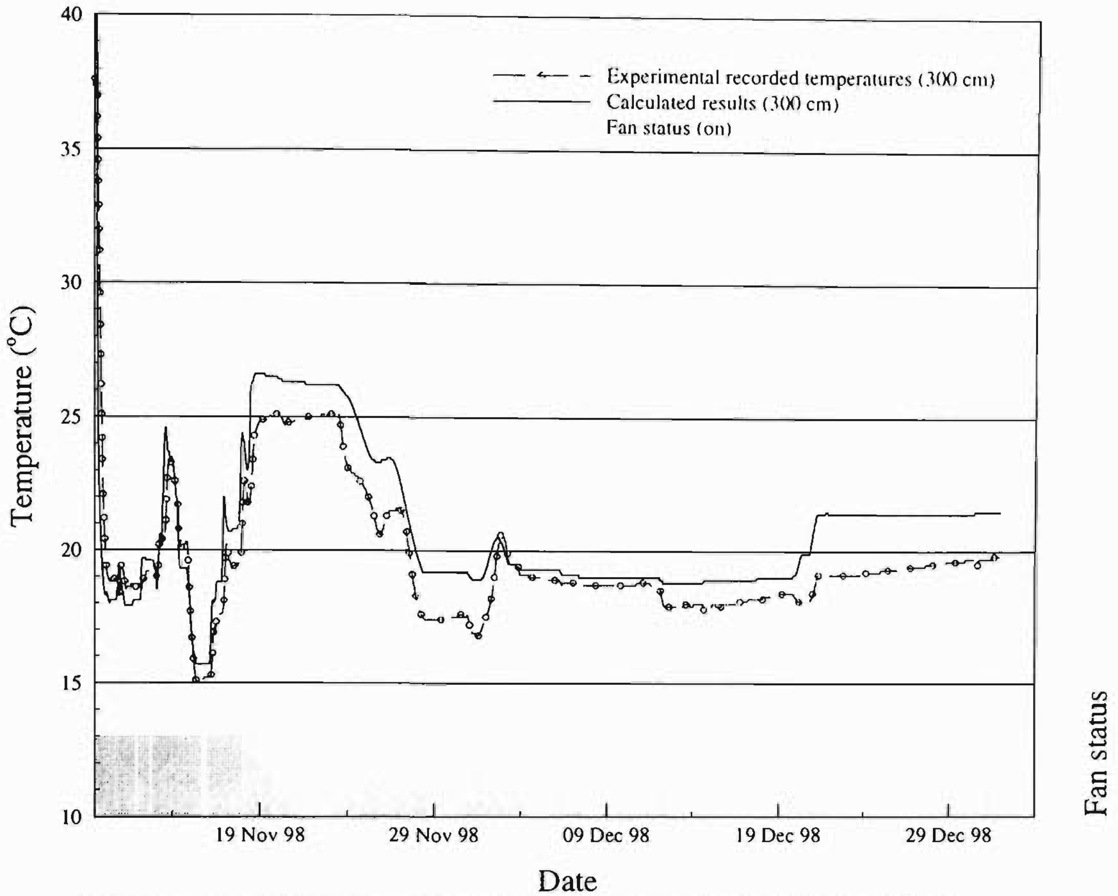

Figure 4.28 Comparison of experimental recorded temperatures and calculated results for the centre drop cable 300 cm - modified simulation 2 (recorded data used for the temperatures of the wall)

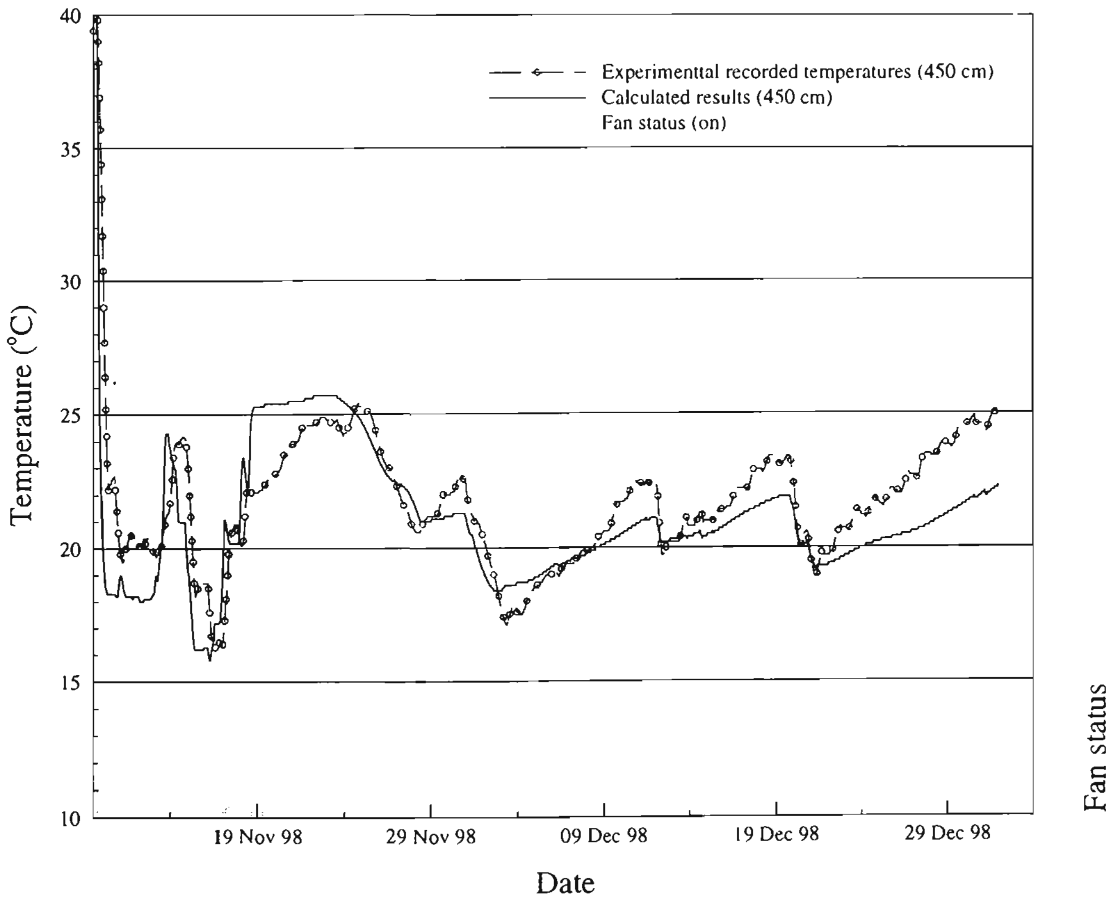

Figure 4.29 Comparison of experimental recorded temperatures and calculated results for the centre drop cable 450 cm - modified simulation 2 (recorded data used for the temperatures of the wall)

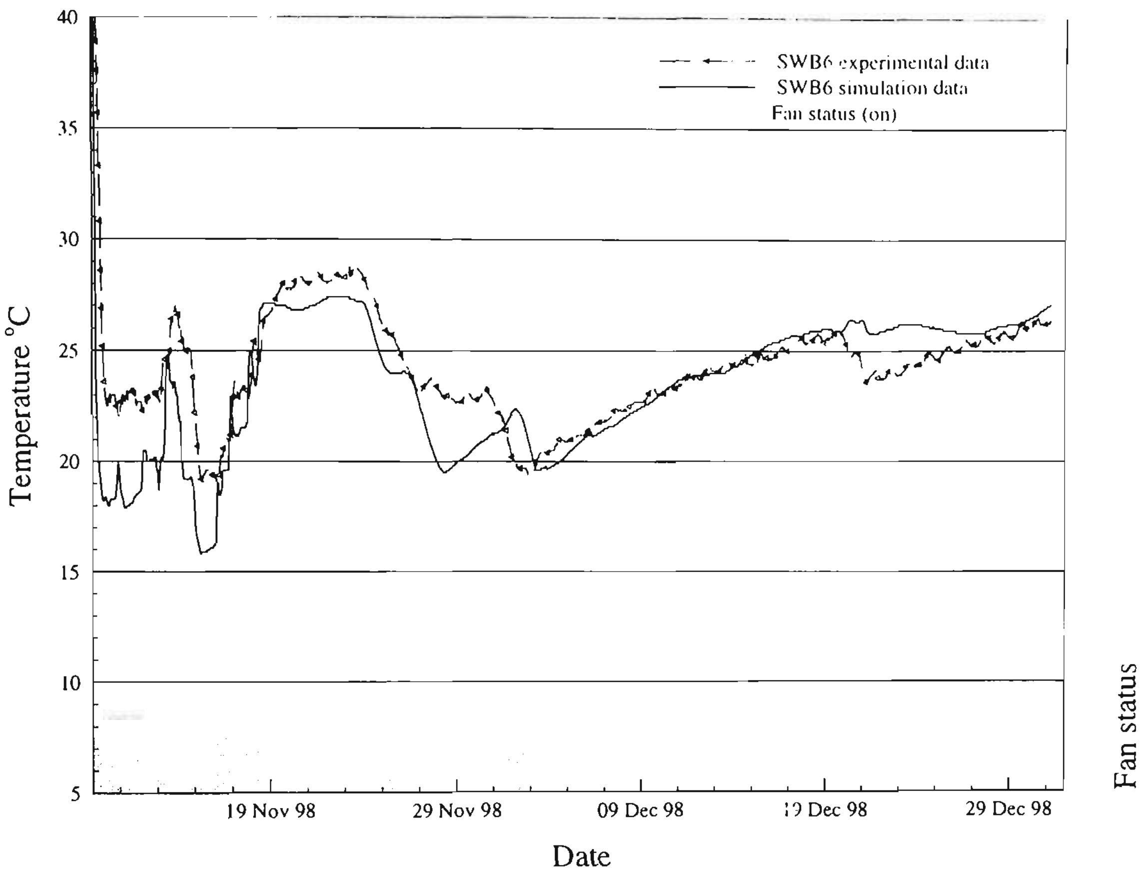

Figure 4.30 Comparison of experimental recorded temperatures and simulated results for the SW upper sensor SWB6 - modified simulation 2 (recorded data used for the wall)

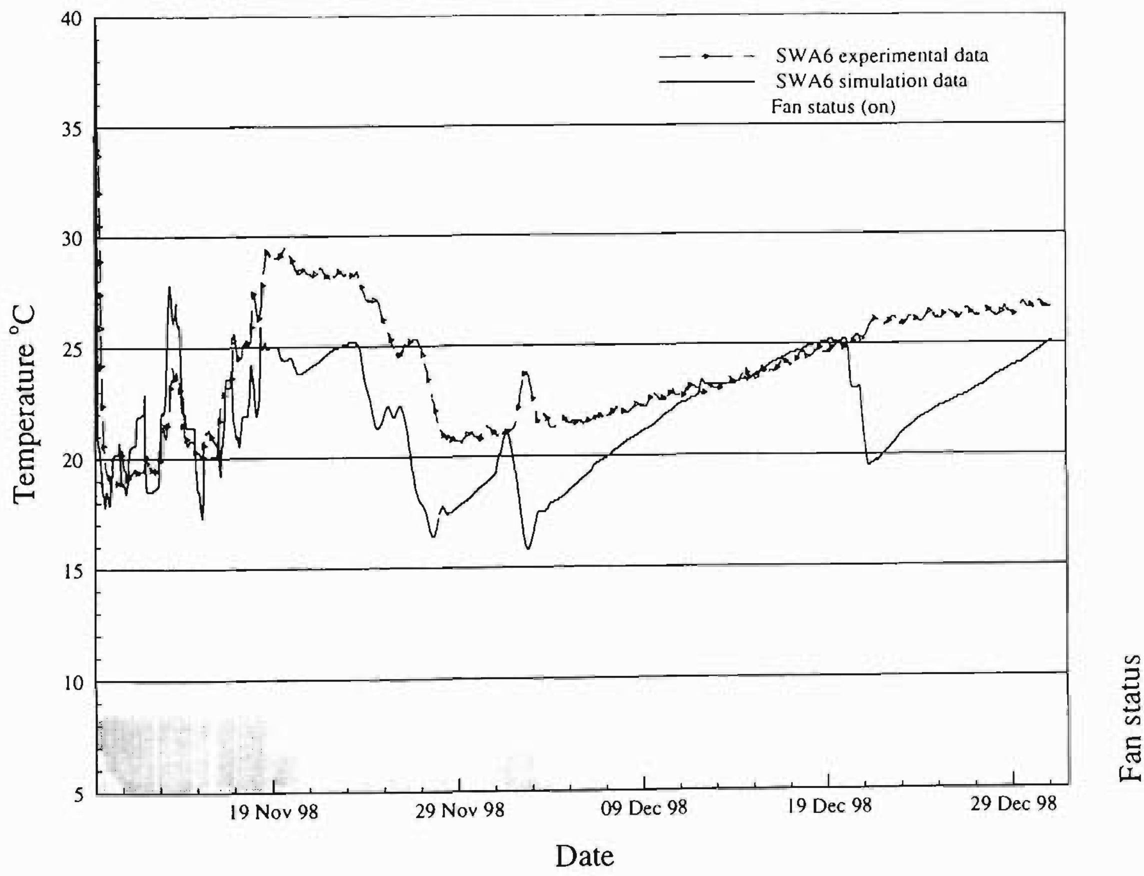

Figure 4.31 Comparison of experimental recorded temperatures and simulated results for the SW lower sensor SWA6 - modified simulation 2 (recorded data used for the wall)

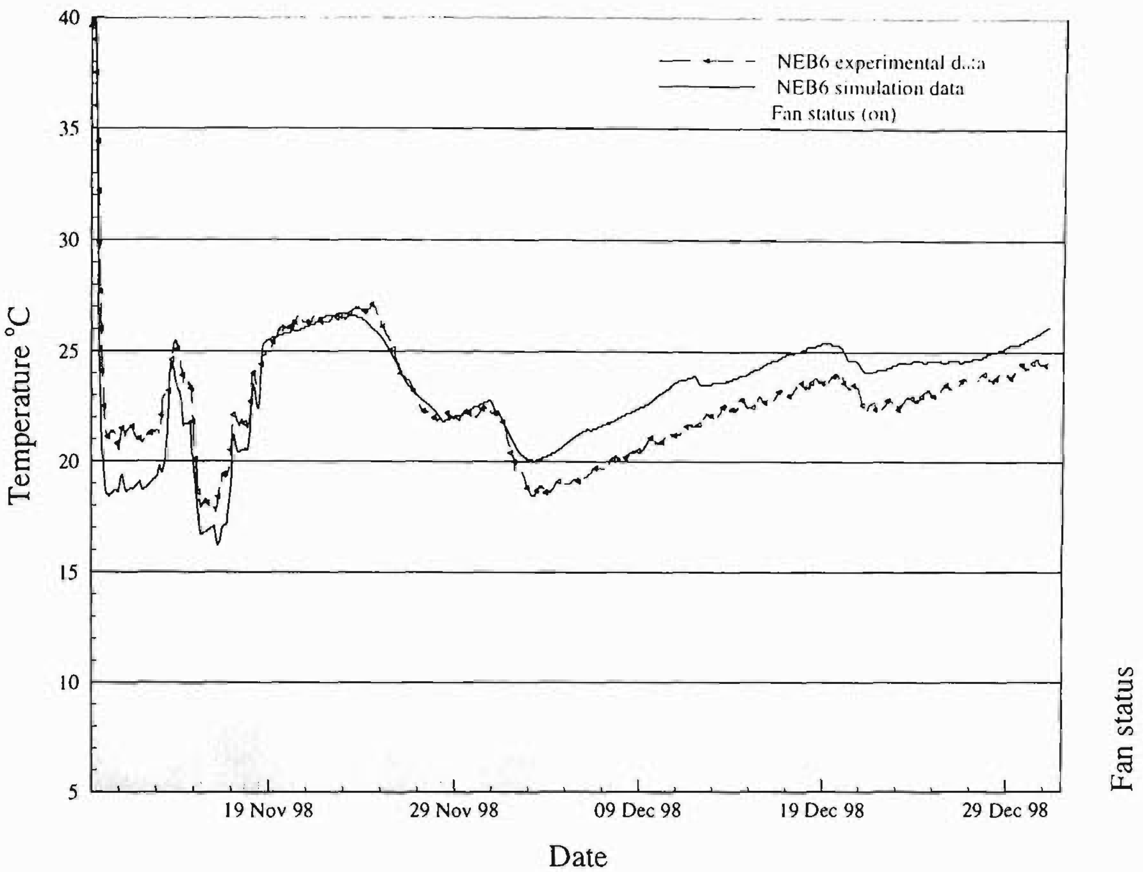

Figure 4.34 Comparison of experimental recorded temperatures and simulated results for the NE upper sensor NEB6 - modified simulation 2 (recorded data used for the wall)

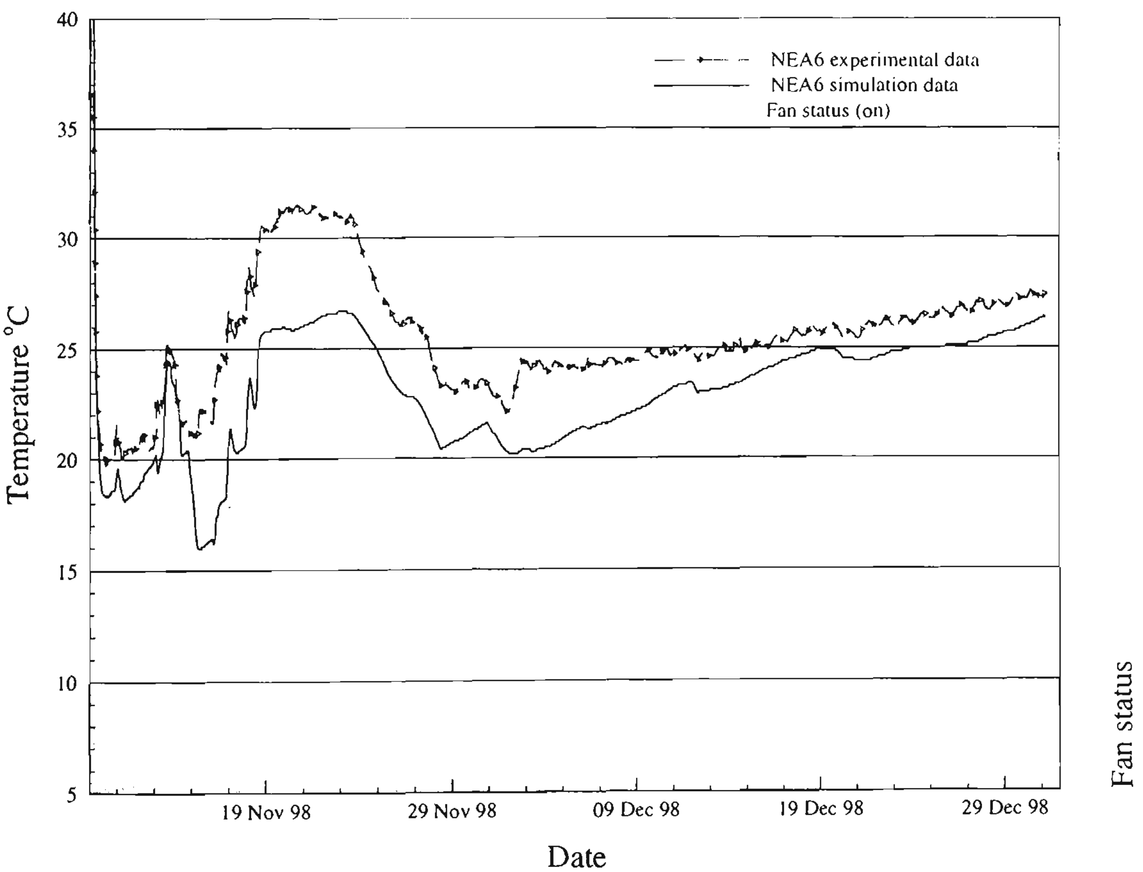

Figure 4.35 Comparison of experimental recorded temperatures and simulated results for the NE lower sensor NEA6 - modified simulation 2 (recorded data used for the wall)

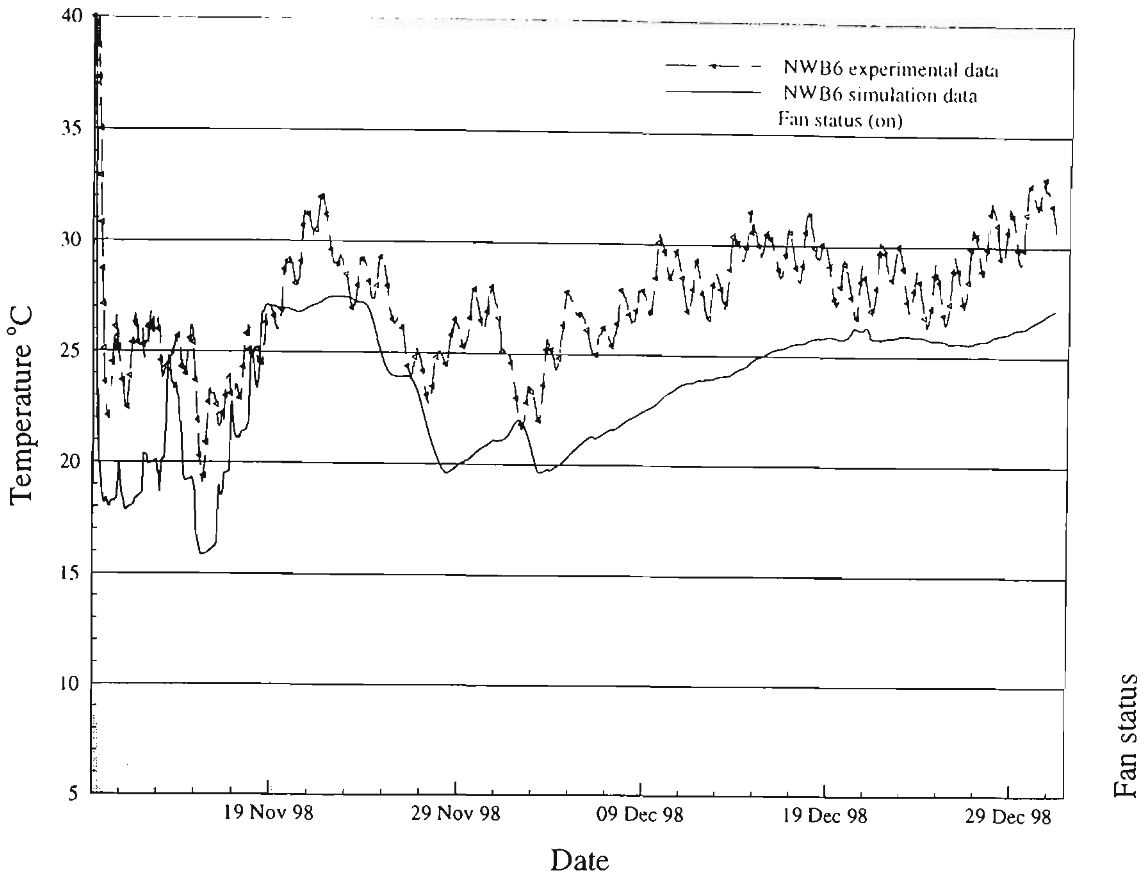

Figure 4.36 Comparison of experimental recorded temperatures and simulated results for the NW upper sensor NWB6 - modified simulation 2 (recorded data used for the wall)

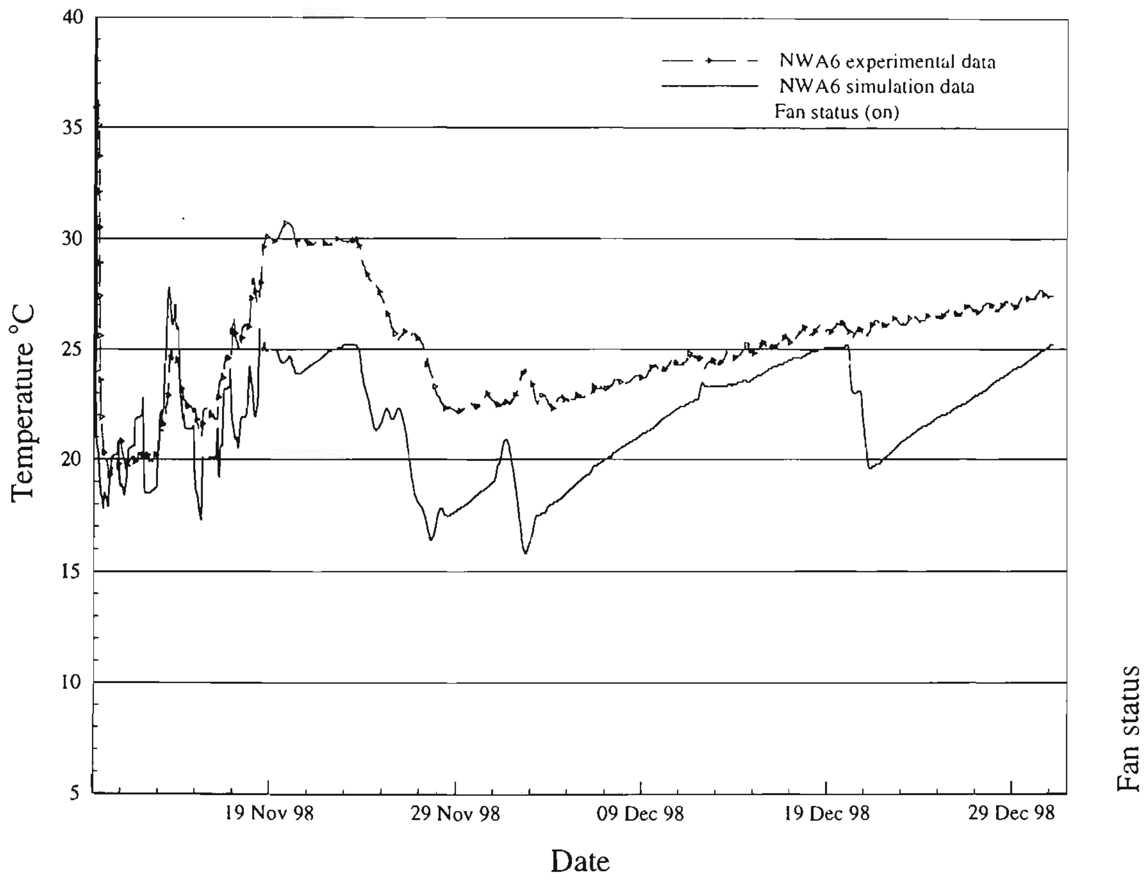

Figure 4.37 Comparison of experimental recorded temperatures and simulated results for the NW lower sensor NWA6 - modified simulation 2 (recorded data used for the wall)

It shows that using recorded data at the wall boundary in the validation improved agreement with the experimental temperature. This indicates that the assumption of wall boundaries in the program do not represent the practical conditions very well.

4.3.4 Modified simulation 3

Note that the simulation results at the upper level along the centerline were improved but those simulation results at the wall did not show these improvements when the recorded data were used for the headspace in modified simulation 1. On the other hand, the simulation results of variables at the wall boundary were improved but those simulation results at the upper level along the centerline did not show those improvements when the recorded temperatures were used for the wall of silo modified simulation 2. In simulation 3 we used the recorded temperatures in the headspace and the wall. The aim of this simulation was to asssess the conduction from the wall and headspace air and convection or aeration air flow at the same time.

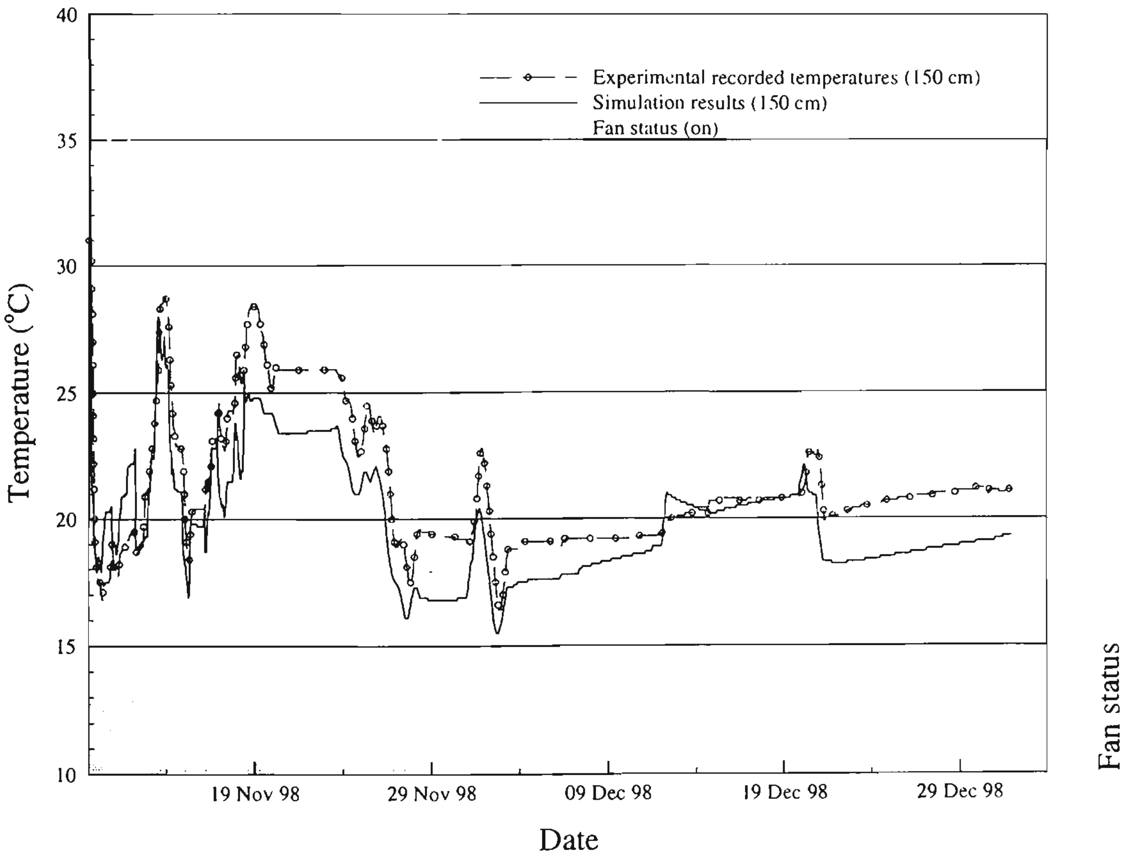

Figure 4.38 Comparison of experimental recorded temperatures and calculated results for the centre drop cable 150 cm - modified simulation 3 (recorded data used for the headspace and wall)

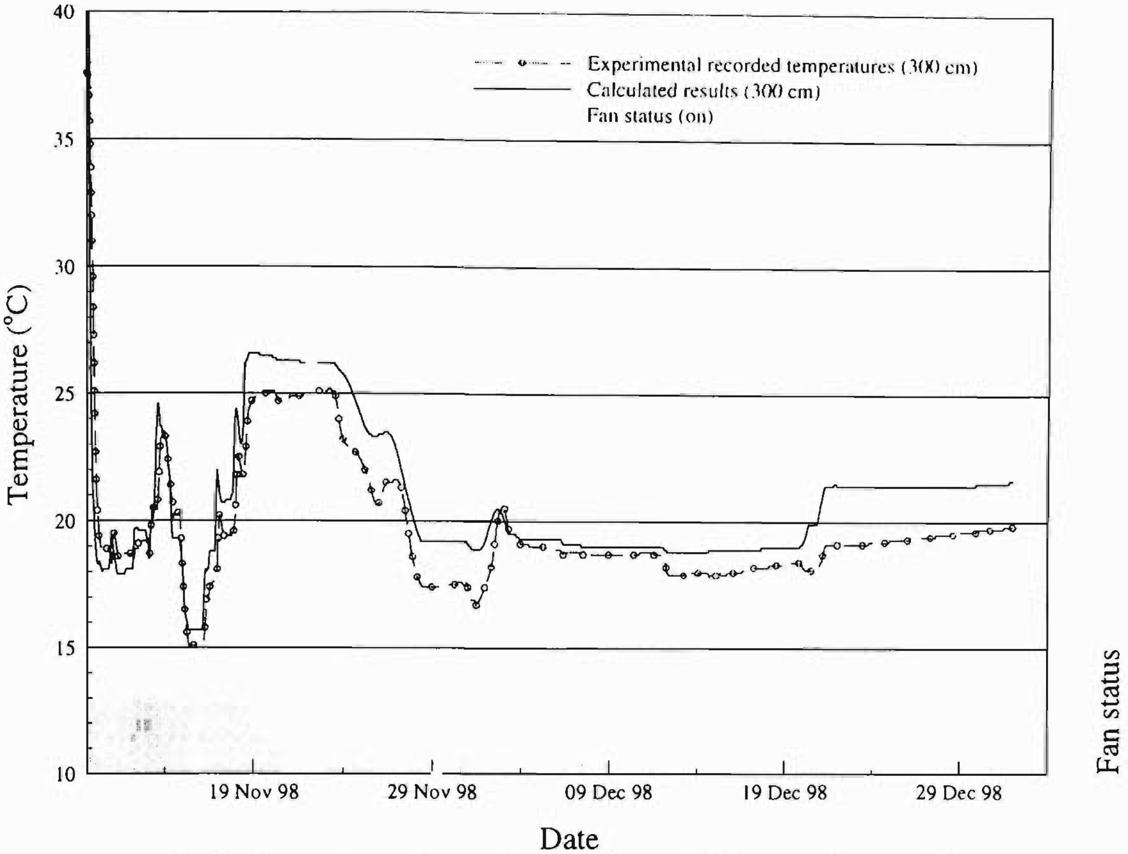

Figure 4.39 Comparison of experimental recorded temperatures and caiculated results for the centre drop cable 300 cm - modified simulation 3 (recorded data used for the headspace and wall)

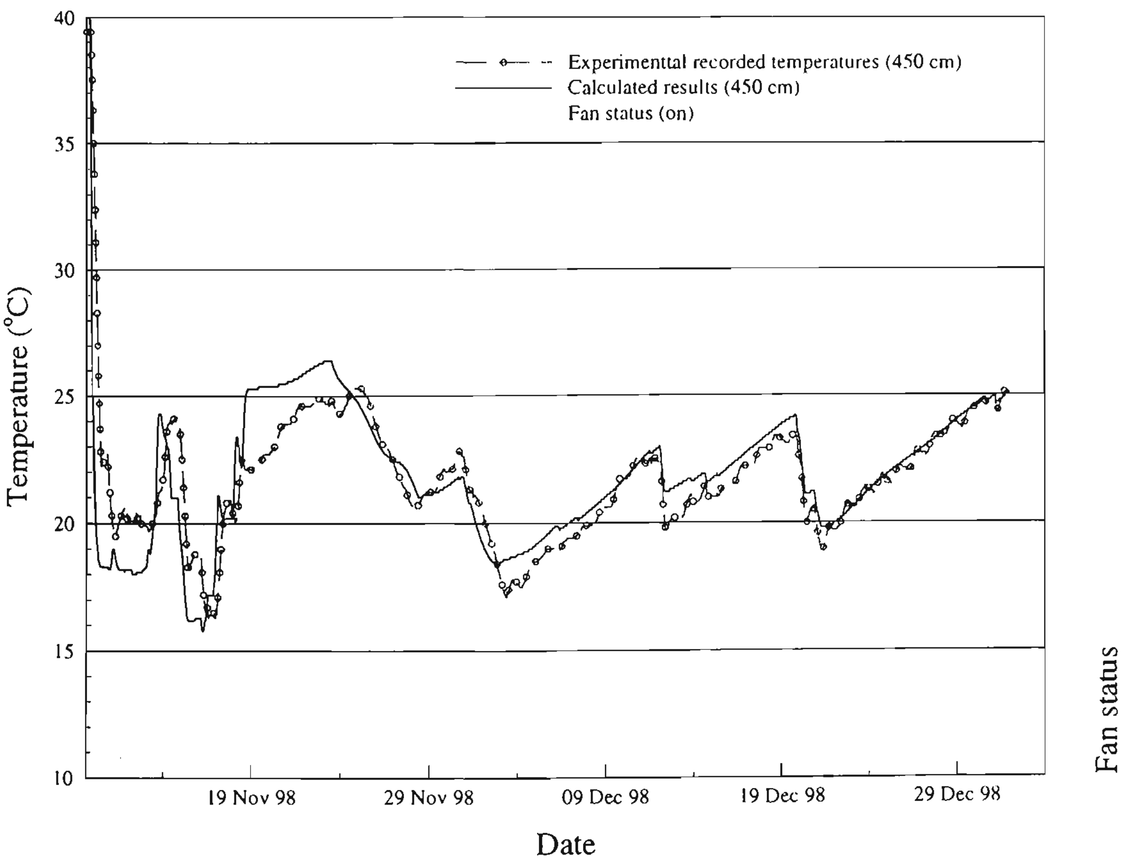

Figure 4.40 Comparison of experimental recorded temperatures and calculated results for the centre drop cable 450 cm - modified simulation 3 (recorded data used for the headspace and wall)

The calculated results for the temperatures of along the centerline are shown in figures 4.38 to 4.340. Note that there are no clear differences between the temperatures plots of modified simulation 1 and modified simulation 3 for the three variables along the centerline of silo after comparing figures 4.17 and 4.33, figures 4.18 and 4.34, and figures 4.19 and 4.35. We also concluded that the conduction from wall boundary did not reach the three variables along the centerline of the silo.

For the variables at wall boundary, the results of modified simulation 3 are similar with those of modified simulation 1. Figures 4.36 and 4.37 are shown the typical plots of modified simulation 3 for the variables at northwest wall boundary of silo. Comparing with figures 4.31 and 4.32 of modified simulation 2, there are no changes in figures 4.36 and 4.37 of modified simulation 3. Hence, the eight variable points at the wall boundary are mainly influenced by the conduction from wall surface when the aeration air flow rate was low.

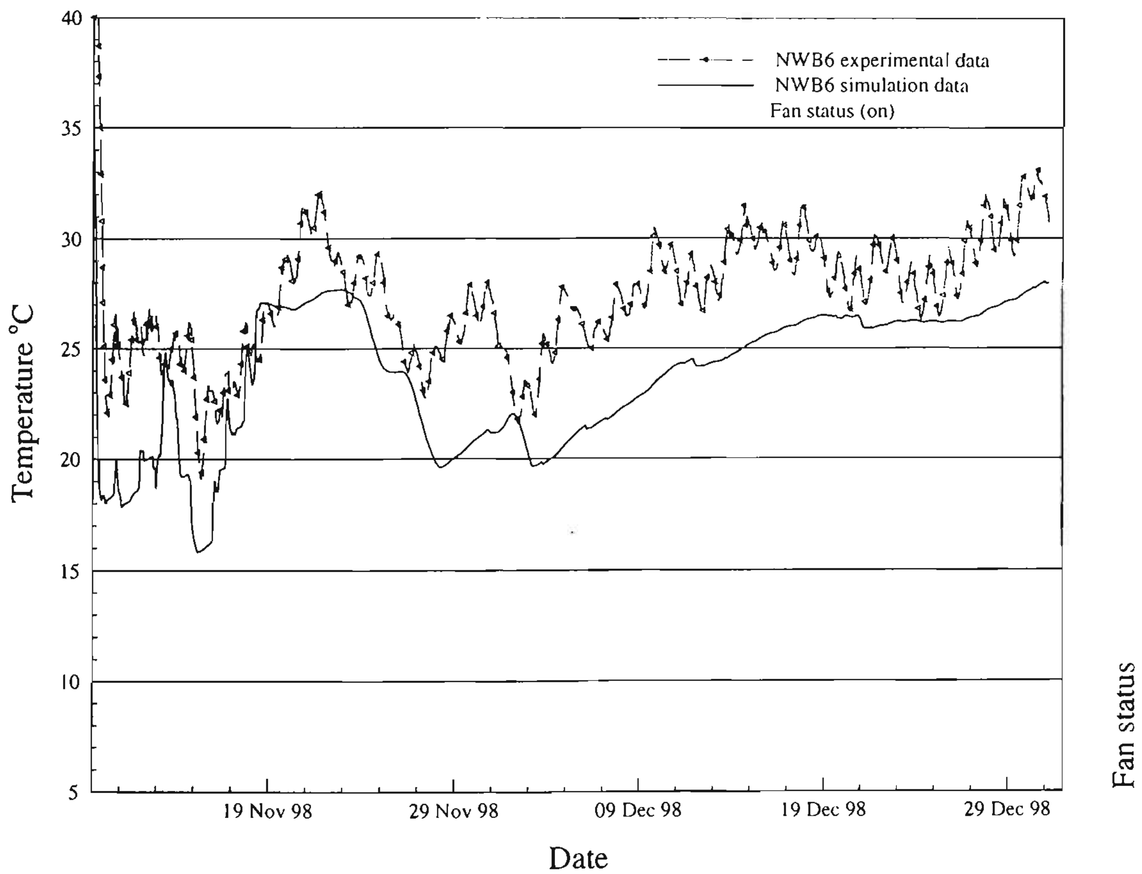

Figure 4.41 Comparison of experimental recorded temperatures and simulated results for the NW uppersensor NWB6 - modified simulation3 (recorded data used for the headspace and wall)

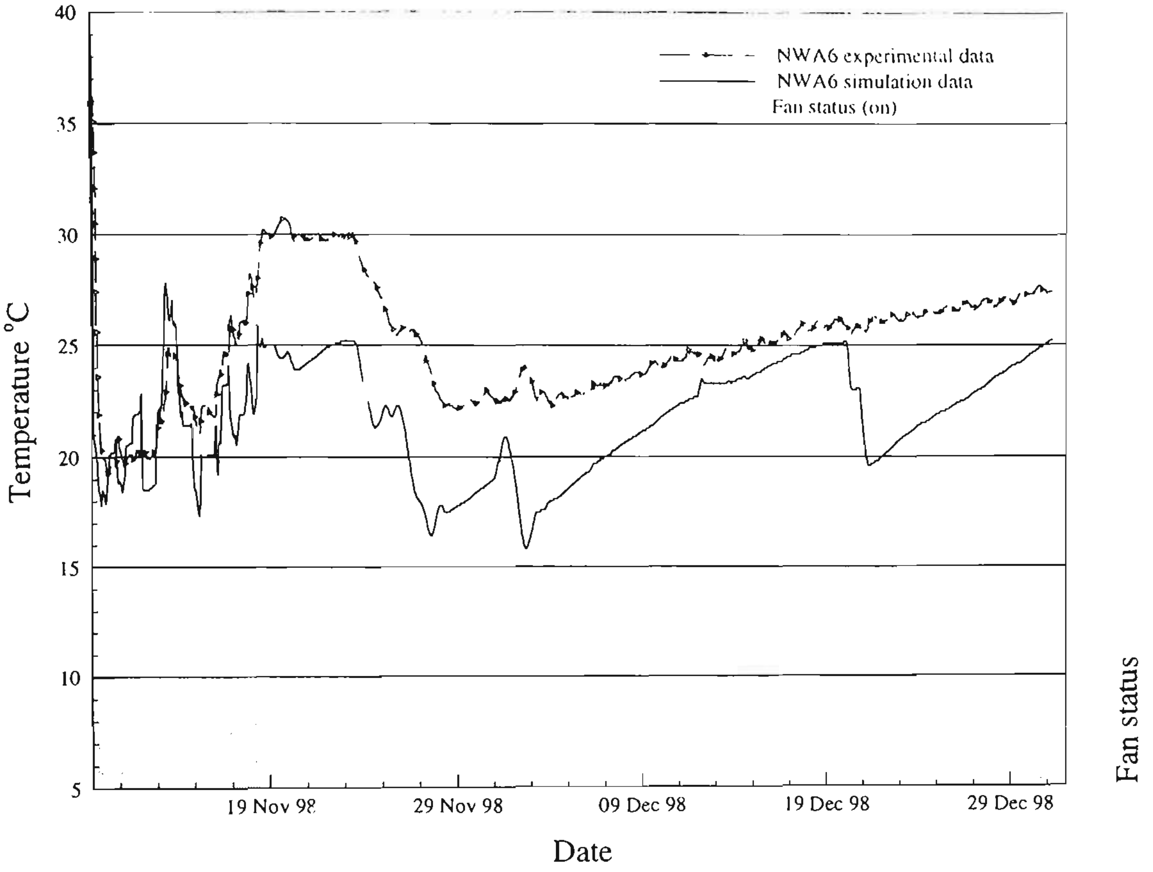

Figure 4.42 Comparison of experimental recorded temperatures and simulated results for the NW lower sensor NWA6 - modified simulation3 (recorded data used for the headspace and wall)

4.4 Conclusions

In this chapter the mathematical model was compared with experimental data. Four simulation versions calculated three points along the centerline of the silo representing the grain temperature variation at the lower, middle and upper levels; and eight points at the wall boundary which indicate the grain temperature variation near the wall of the silo. The four simulations used different boundary conditions based on the degree of use experimental recorded data. The following results were obtained.

- The default operating schedule, intended to match the hours per day that the users require for aeration, system did not match the coolest time during the testing periods.
- The program showed promising simulation results in predicting grain temperature along the centerline of the silo. However, there was a slower increase in simulated results of the grain temperature at upper levels in the silo than recorded data points when the boundary consideration of program was used the headspace.

- When the recorded temperatures of headspace air were used instead of the boundary conditions in the program, the simulated plots of the program at upper levels captured the experimental data very well. It is believed that the headspace boundary condition in the initial program does not fit the real situations very well.
- When we were changing the simulation data of wall boundary conditions such as using boundary conditions based on the averaged data or using experimental data, the simulated temperature plots along the centerline did not show the difference but the simulated plots of the grain temperatures at wall boundary responded strongly. We can say that the grain temperatures along the centerline are affected mainly by aeration air and weakly by the wall surface conditions.
- When the experimental temperature data of the wall surface were used rather than the averaged conditions used in the program, the simulated temperature plots showed the significant improvement in prediction. This shows that the wall boundary conditions in the program might agree with the practical conditions poorly because the initial program used only average conditions.
- The better results did not appear in the simulated grain temperatures at the wall boundary when we changed the headspace condition with the recorded data. We may say that the conditions of the wall surface affected the grain temperatures mainly at wall boundary and rarely reached the centerline of the silo.

We concluded that the simulation temperature results of the computer program developed from the mathematical model have good agreement with experimental data for the three variables along the centerline when the recorded ambient air condition was used in the process. Since the eight variables at wall boundary showed the unsatisfactory agreement with the experimental data when the boundary considerations of the program are applied, we suggested the simulation and prediction studies with the program are most effective along the centerline. It is essential that more accurate methods of simulating the temperatures of the silo and headspace be implemented.

CHAPTER 5

EXPERIMENTAL STUDY

A key feature of the desiccant unit is its overall performance. For example, we need to know by how much it can reduce the wet-bulb temperature of ambient air and how long it takes to regenerate the desiccant. To measure its performance, a field study of on-farm grain storage cooling was conducted during the 2000 ~ 2001 summer harvest season in Ararat, Victoria. The experimental study had the following objectives:

- To explore the outlet behaviour of the air during both cooling and regeneration processes of the novel desiccant device.
- To develop empirical formulae both of the cooling and regeneration processes for practical application.
- To discuss the degree of cooling in grain silos.

Preliminary results on the performance of the unit were determined under the relatively well-controlled environment of a laboratory. The thermodynamic performance of the cooling unit was then determined under field conditions. The ultimate test of the performance of the unit was evaluation of its ability to cool two types of grain, namely wheat and canola. Two grain silos were aerated, a 50 tonne silo filled with canola oil seeds and a 100 tonne silo filled with wheat. A total of 62 sensors were located inside and around the unit and in the silos, and they provided more than 700,000 data points. The principal findings were

- Compared with ambient condition, the wet-bulb temperature of air can be reduced by 5 ~ 7 degrees during the cooling process, and a set of regression formulae for evaluating the outlet conditions including wet-bulb temperature reduction has been obtained.

- The desiccant device can be regenerated completely in six hours with a regeneration temperature of 65 °C.
- The average grain temperatures were reduced by 11°C in both wheat and canola silos.

Since experimental results must be interpreted within an intellectual framework, before the discussion of the experiments we highlight the principles of heat and mass transfer that occur in the beds of desiccant, as these determine the overall performance of the unit. The instrumentation used to collect the data is described in detail in this chapter.

5.1 Desiccant cooling unit

5.1.1 Desiccant

One of most widely available sorption materials, silica gel, was used in this research. The desiccant cooling unit can work isothermally drying ambient air as described in Chapter 1. The sorption of water by silica gel depends on the relative humidity of

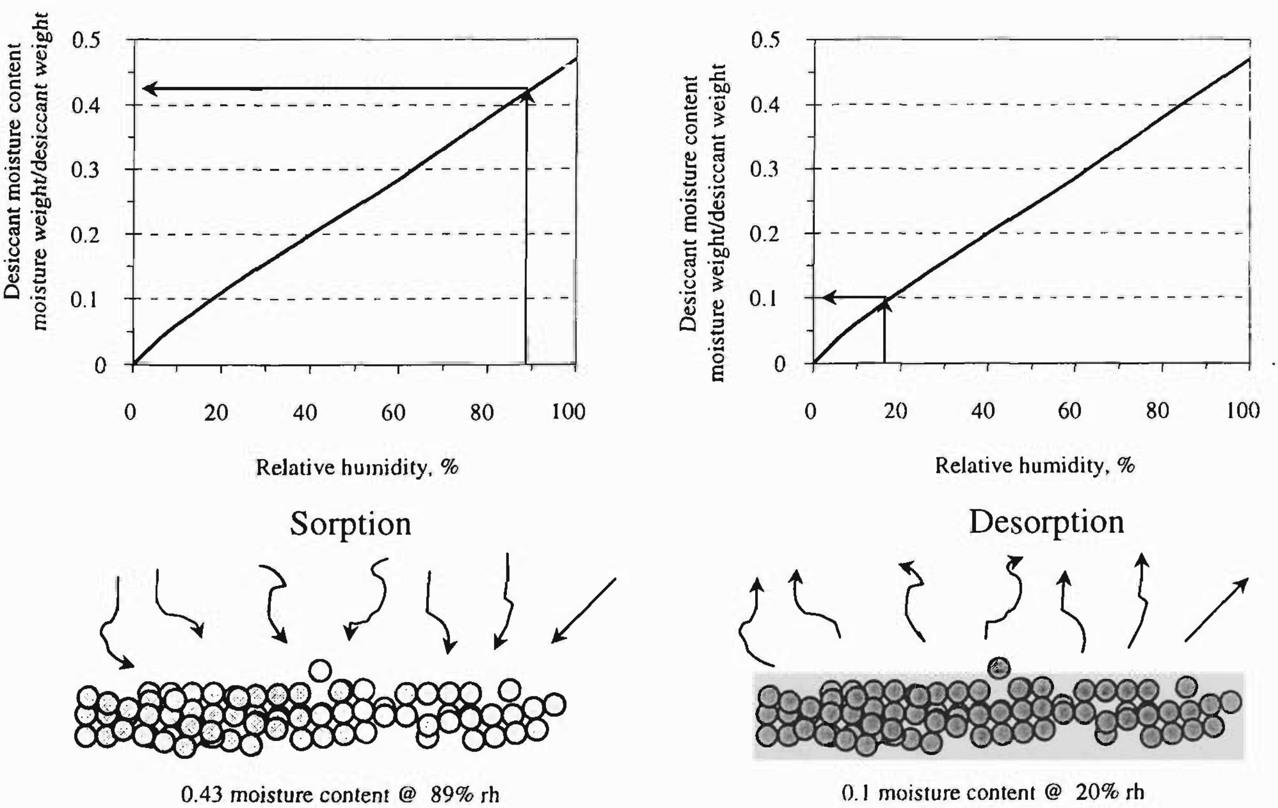

Figure 5.1 Principle of the silica gel desiccant cycle

surrounding, or intergranular air (GRI, 2000a). Silica gel can adsorb approximately 0.40 of its weight of moisture (dry basis) when the relative humidity of surrounding air is 90%, as shown in figure 5.1. The corresponding value of the moisture content in desiccants can be reduced to less than 0.1 when the air relative humidity is less than 15%.

In figure 5.1 the moisture content of silica gel, W_{silica}, is linearly related to the relative humidity, ϕ, of the surrounding air.

$$W_{silica} = 0.046\phi \tag{5.1}$$

We are interested in situations when the air and desiccant are not in moisture equilibrium when sorption or desorption occur until this equilibrium is approached. We also note that the heat of sorption is released during the sorption or gained during desorption.

5.1.2 Principles of the desiccant device

The open cycle desiccant system consists of a sorption process, in which ambient air is dried isothermally, and a regeneration process when the desiccant is dried. Due to the air-conditioning purposes, the sorption process usually is called a cooling process.

Ambient air increases in relative humidity and cools at night. When this humid and cool air is blown into the device filled with dry desiccant, the desiccant absorbs the moisture of the air, and the dry and cool conditioned air is produced for cooling stored grain. Because it is undesirable for the dry air to be heated by the heat of sorption, secondary air must be introduced to enable the heat of sorption to be removed.

Naturally, the desiccant becomes moist after a sorption process. The warm and dry ambient air that occurs during day is heated to obtain a very low relative humidity, about 10%. This heated air is able to regenerate, or dry, the moist desiccant when it is forced through it. After the regeneration process during the day, the desiccant is ready for the next night process.

Because of the low flow rate, the process air is in thermal equilibrium with the desiccant at all time and at any location in the device, but moisture equilibrium may not be attained (Thorpe *et al*, 1992a, b).

The underlying principles of the two desiccant processes are illustrated by figure 5.2 on a psychrometric chart.

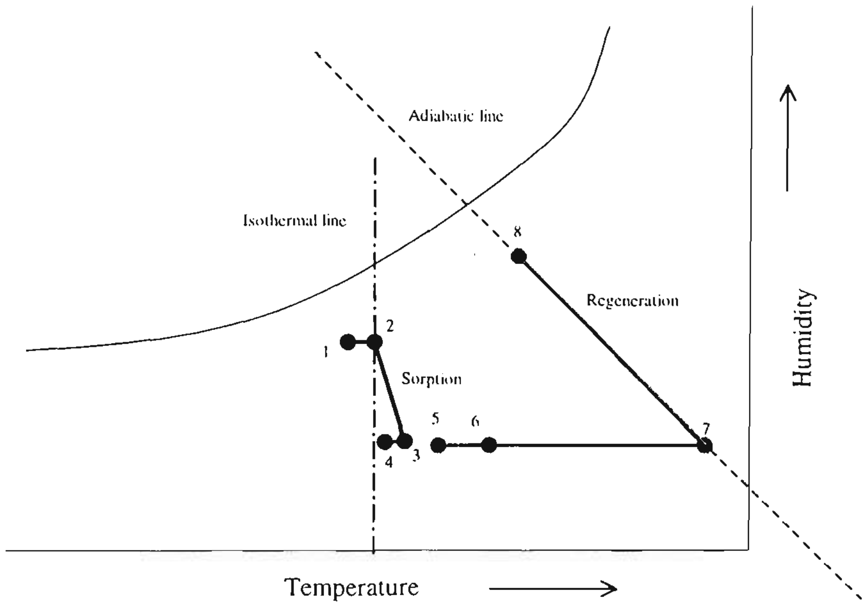

Figure 5.2 Thermodynamic states of ambient air passing through the desiccant cooling system during sorption and regeneration processes

During the sorption process at night, the ambient air, which is cool and humid at state 1, is compressed by the centrifugal fan to state 2 and then conditioned from state 2 to 3 by passing it through the desiccant device. At the beginning of the operation, the outlet air at state 3 has a relative humidity that is in moisture equilibrium with the initial desiccant condition. Because of heat of sorption released, the process from state 2 to 3 could not be completely isothermal even though secondary air is used to cool down the primary air. The air at state 3 has a temperature higher than the initial temperature of desiccant. In practice, the outlet air cools down further to state 4 through ducts on the way to silos.

As the process time increases more moisture is adsorbed from the process air and the desiccant becomes increasing wet such that the desiccant absorbs less amount of moisture from the process air. Consequently, the relative humidity of the outlet air increases as the desiccant bed becomes wetter. As the time of operation increases, the state of the outlet air is located along a process path somewhere between sates 2 and 3.

During a regeneration process during the day, ambient air at state 5 is first warmed by the centrifugal fan to state 6. Then the air is heated to state 7 by a gas heater or other kind of heat source and obtains a very low relative humidity and gains in temperature. When this heated air passes through the wetted desiccant, it absorbs moisture from the desiccant and loses temperature as it supplies the heat of sorption. This desorption process continues until the air and desiccant are in moisture equilibrium.

According to psychrometrics, this regeneration process is close to a typical adiabatic process in which the regeneration air scarcely changes in enthalpy and its wet-bulb temperature will be approximately constant during the process. Hence, the outlet air at state 8 achieves a condition that is close to the wet-bulb temperature of the regeneration air and a relative humidity in moisture equilibrium with desiccant.

During the initial stage of regeneration, the relative humidity of the outlet air is in moisture equilibrium with the desiccant at its initial condition. As time increases, the desiccant becomes drier so the relative humidity of the outlet air reduces along the wet-bulb temperature line that passes through states 7 and 8. The regeneration process is completed when the outlet condition approaches to the inlet condition of the regeneration air, state 7. Furthermore, the air with a high temperature, state 7, produces the high outlet humidity at state 8. As a result, the higher regeneration temperature, state 7, the faster the regeneration process.

We should note here that the processes depicted in figure 5.2 are idealized. In practice, the inlet conditions to the desiccant bed change with time.

5.1.3 Outlet conditions during a cooling process

The theory of heat and moisture transfer in desiccant beds that operate adiabaticaly is well established (Close *et al*, 1972). In such systems, five zones form when the bed is ventilated with air and they are shown in figure 5.3. These zones are clearly observed in beds of grain that are cooled using that air that has a low relative humidity (Thorpe, 1982). The same phenomena occur in beds of ventilated silica gel, but in the cooling

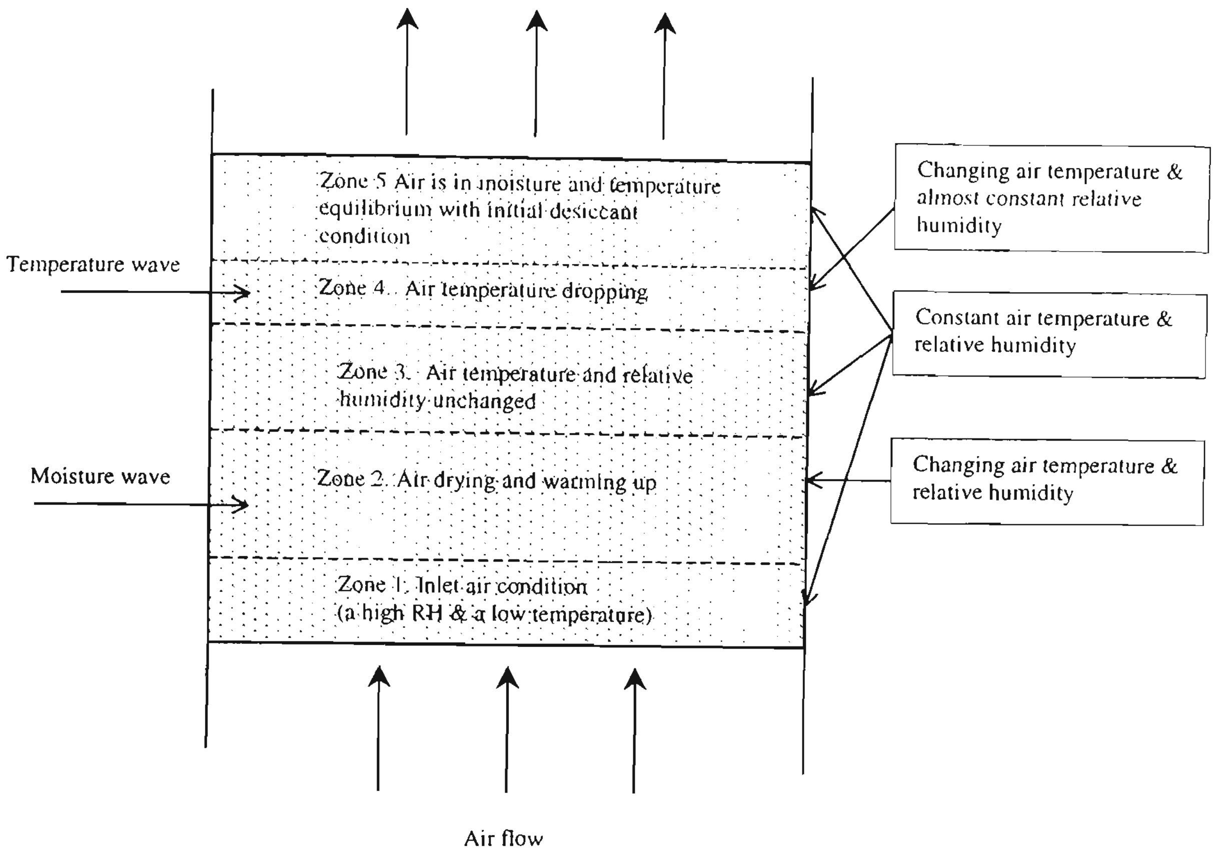

Figure 5.3 The formation of temperature and moisture waves in a processing desiccant device at time t - night

region, the system operates almost isothermally and the five zones are less distinct.

Firstly, after the system has been operating for some time, the desiccant closest to the air inlet is in moisture and thermal equilibrium with the inlet air. This forms Zone 1 where desiccant is cool and moist. On the other hand, the process air does not reach the region near the outlet in the early stage of operating. This is the region of Zone 5 where the desiccant retains its initial condition, normally dry and cool.

We have noted that when moisture of the air is adsorbed by the silica gel, heat is released. This causes the temperature of the desiccant to increase and forms Zone 2, which is known as moisture wave because it is the region that the moisture content of the silica gel changes most markedly. Beyond Zone 2, the temperature and moisture plateaus and this region is Zone 3 that is traditionally known as the dwell state. Zone 4 is known as a temperature wave because in a cooling process this is the region in which the temperature changes the most. The states of five zones are also displayed on a psychrometric chart shown in figure 5. 4.

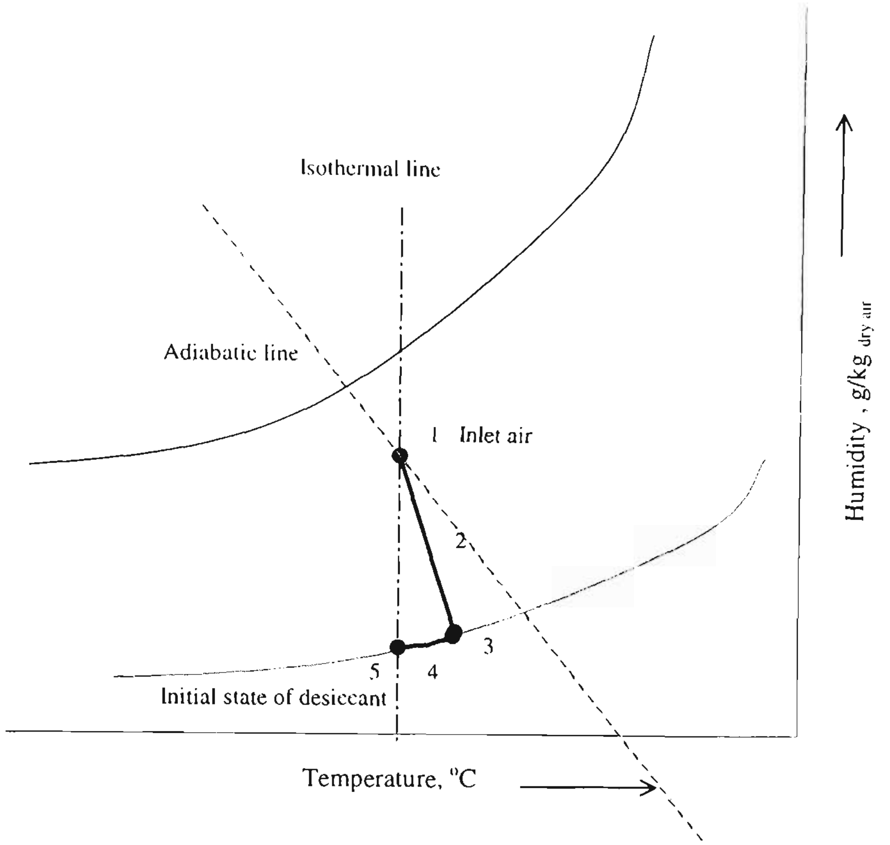

Figure 5.4 Thermodynamic states of five zones formed when process air passing through the desiccant bed during cooling processing

As the process continues the desiccant becomes spent. The relative humidity of the air leaving the desiccant device begins to increase as the zones traverse the desiccant bed. Therefore, the outlet temperature and relative humidity trajectories appear as showing as in figure 5.5 when they are plotted against the process time.

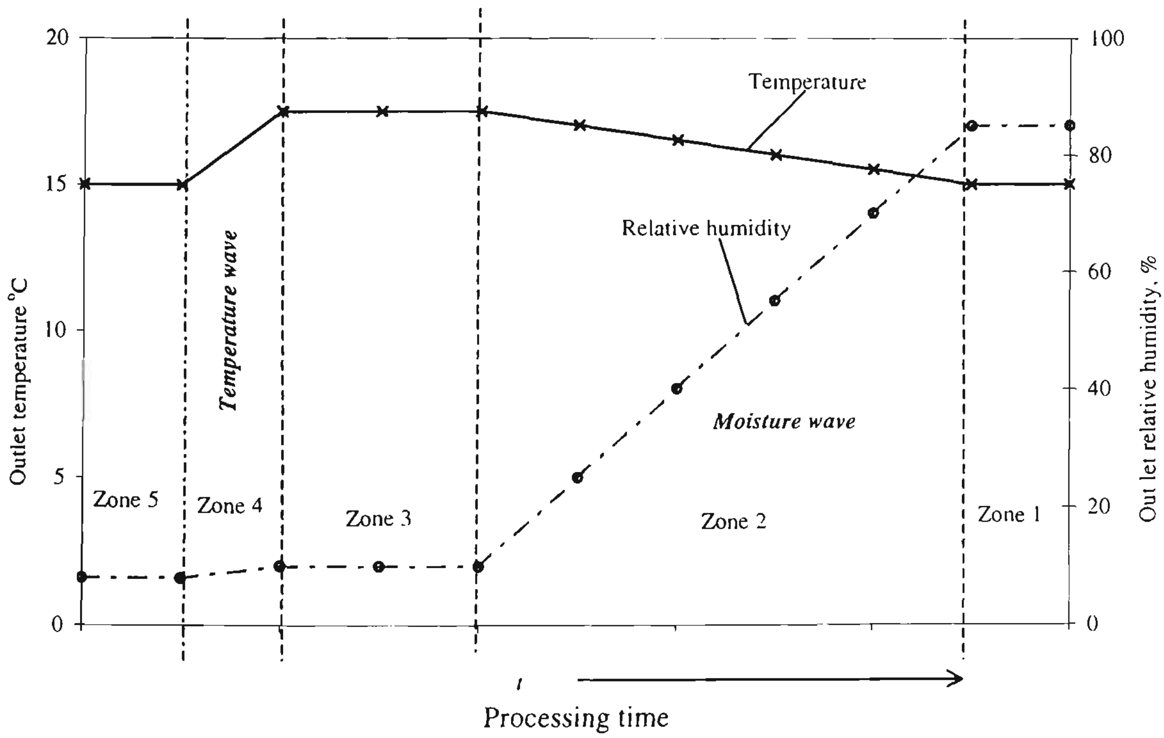

Figure 5.5 Outlet prediction in a desiccant bed during a cooling process

5.1.4 Outlet conditions during a regeneration process

When the desiccant has become spent it must be regenerated using the air with a low relative humidity. The rate of regeneration is strongly dependent on the temperature of the regeneration air.

In figure 5.6 we plot the states of a regeneration process on a psychrometric chart. Similarly, there are five zones formed when the hot and dry regeneration air is blown through the desiccant device.

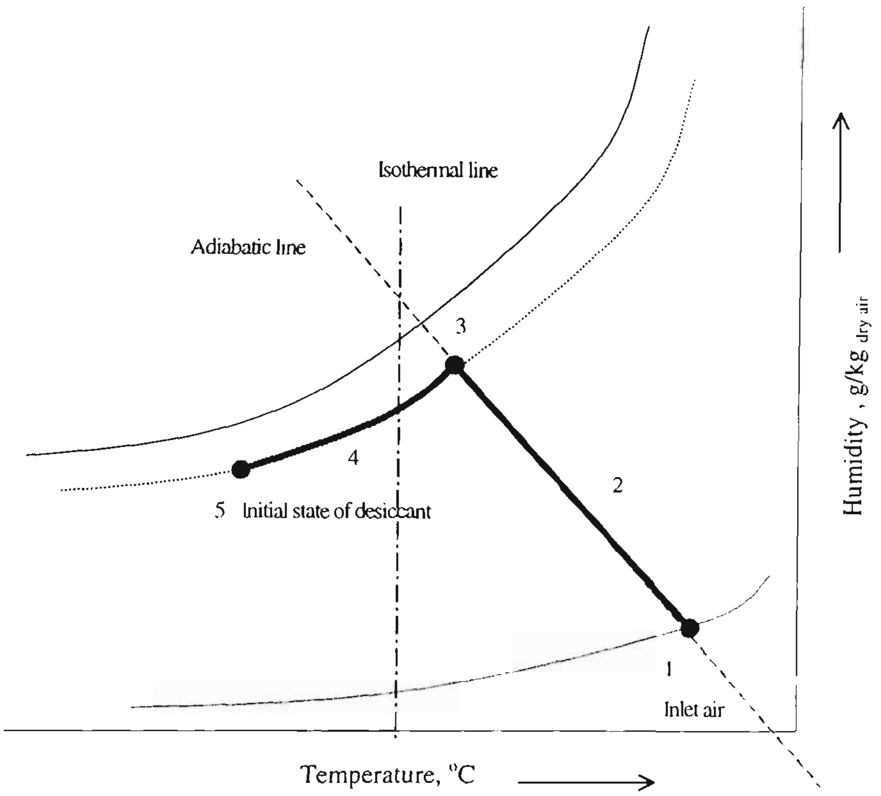

Figure 5.6 Thermodynamic states of five zones formed when regeneration air passes through the desiccant bed during regeneration processing

Zone 1 is at the inlet air condition which is hot and dry. In Zone 5 the air is in moisture and temperature equilibrium with the initial condition of desiccant that shows a cool and moist condition. In Zone 2, there is a moisture wave in which the moisture content of the desiccant changes sharply. The temperature wave is in Zone 4 that the temperature of desiccant decreases speedily. In Zone 3, the temperature and moisture content are in a relatively stable state.

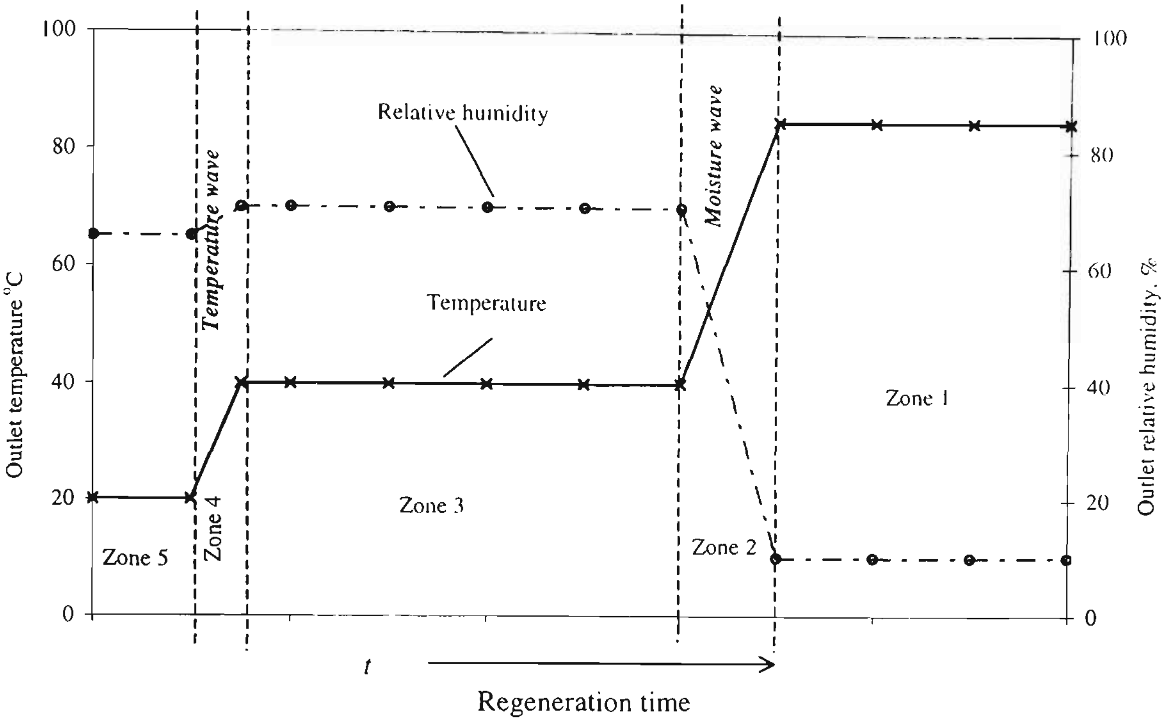

Figure 5.7 Prediction of the outlet state of air leaving in a desiccant bed during a regeneration process

In the same way as predicting the outlet conditions as the cooling process, the outlet conditions of a regeneration process can be shown as in figure 5.7 when the air temperature and relative humidity are plotted versus the regeneration time.

5.1.5 Desiccant device

We designed a desiccant system that is based on the previously described principles. One of the most important variables is the quantity of silica gel required to cool grain. This amount also affects the rate at which it is regenerated. In this thesis, the following are considered:

- Darwin in the Northern Territory and Ararat in Victoria have contrasting climates. Darwin has a hot and humid tropical climate, which demands a large amount of desiccant. Ararat has a temperate warm and dry climate, which requires less desiccant.
- Aeration cooling for stored grains needs a low specific air flow rate, 0.5 ~ 2.5 L/s/t. Considering the on-farm silo with the capacity of 50 ~ 200 tonnes, 0.15 m^3/s is chosen as the design air flow rate for the system.
- A capacity of moisture sorption of silica gel, 0.25 kg/kg dry basis, is used.
- The average relative humidity of the system outlet during the cooling process

is approximated as 25% in both locations.

- After passing through the desiccant, the dry-bulb temperatures of ambient air are estimated to be about 2°C higher than the inlet during cooling processes, which are 30.5°C for Darwin, and 18.5°C for Ararat, respectively.

Table 5.1 Selection of desiccant amount in the system

Location	Darwin, NT	Ararat, Vic
Month	January	January
Mean 9am dry-bulb temperature °C	27.9*	16.3*
Mean 9am wet-bulb temperature °C	25.4*	12.8*
Mean 9am humidity ratio g/kg $_{dry\ air}$	19.5	7.8
Air flow rate m^3/s	0.15	0.15
Operation hour per day	6	6
Air flow m^3	2160	2160
Predicted outlet dry-bulb temperature °C	30.0	18.5
Predicted outlet relative humidity %	25	25
Predicted outlet humidity ratio g/kg $_{dry\ air}$	6.5	3.5
Moisture sorption capacity of silica gel kg/kg dry basis	0.25	0.25
Predicted moisture sorption kg	34	17
Silica gel kg	136	68

*BOM, 2000

The specifications are presented in table 5.1 which indicates that 136 kg desiccant of silica gel are needed in Darwin and 68 kg in Ararat.

The second consideration here is to facilitate the dissipation of heat of sorption during cooling process. Therefore, the typical form of cubic container with some small channels is used that enables the secondary air passing through the channels and removing the heat of sorption from desiccants. The container is shown in figure 5.8.

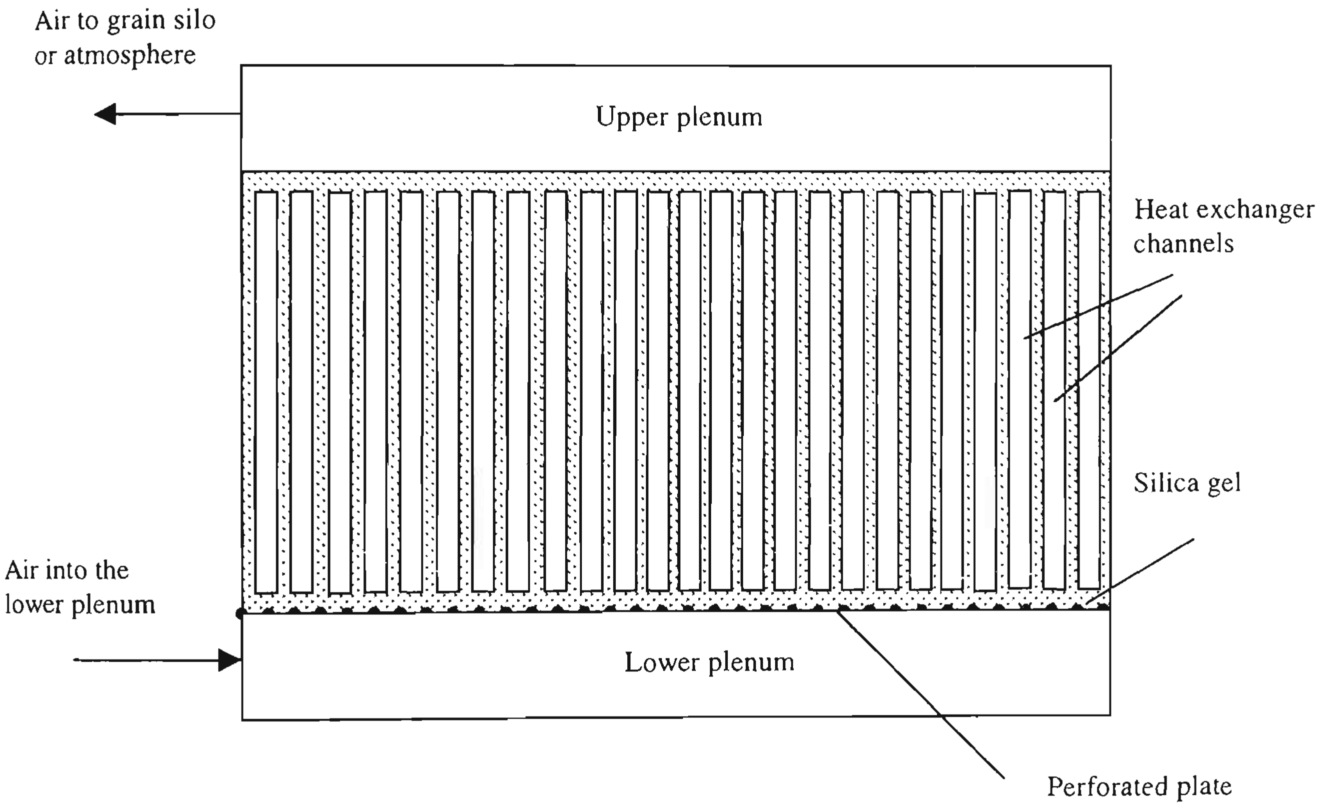

Figure 5.8 A schematic diagram of the desiccant bed grain cooling device

The third consideration of the device is to reduce the average wet-bulb temperature of ambient air sufficiently to be useful from the point of view preserving grains. This means reducing the wet-bulb temperature by 6°C or more. The average degree of temperature reduction is a function of the air flow rate of the secondary air flowing through the empty heat transfer channels so this air flow rate must be specified.

For the regeneration processes, the moisture wave can be moved out as soon as possible so the desiccant can be regenerated in a reasonable time. Hence, the fourth consideration is to specify the air flow rate and temperature of the air used for regeneration. As a starting point, the air flow rate of regeneration is chosen as same as the cooling process, 0.15 m^3/s.

Adjusting the amount of desiccants is also one of the main considerations because although the more desiccants can adsorb the more moisture from the process air it takes longer time to regenerate the desiccants and consumes more energy. The device designed in this thesis is constructed so that desiccant can be easily added or removed from the channels and the amount of desiccant can be optimized simply.

5.1.6 Novel desiccant cooling system

The novel desiccant cooling system is shown in figure 5.9. The system consists of desiccant beds contained in a heat exchanger, a back-up heater and one centrifugal fan.

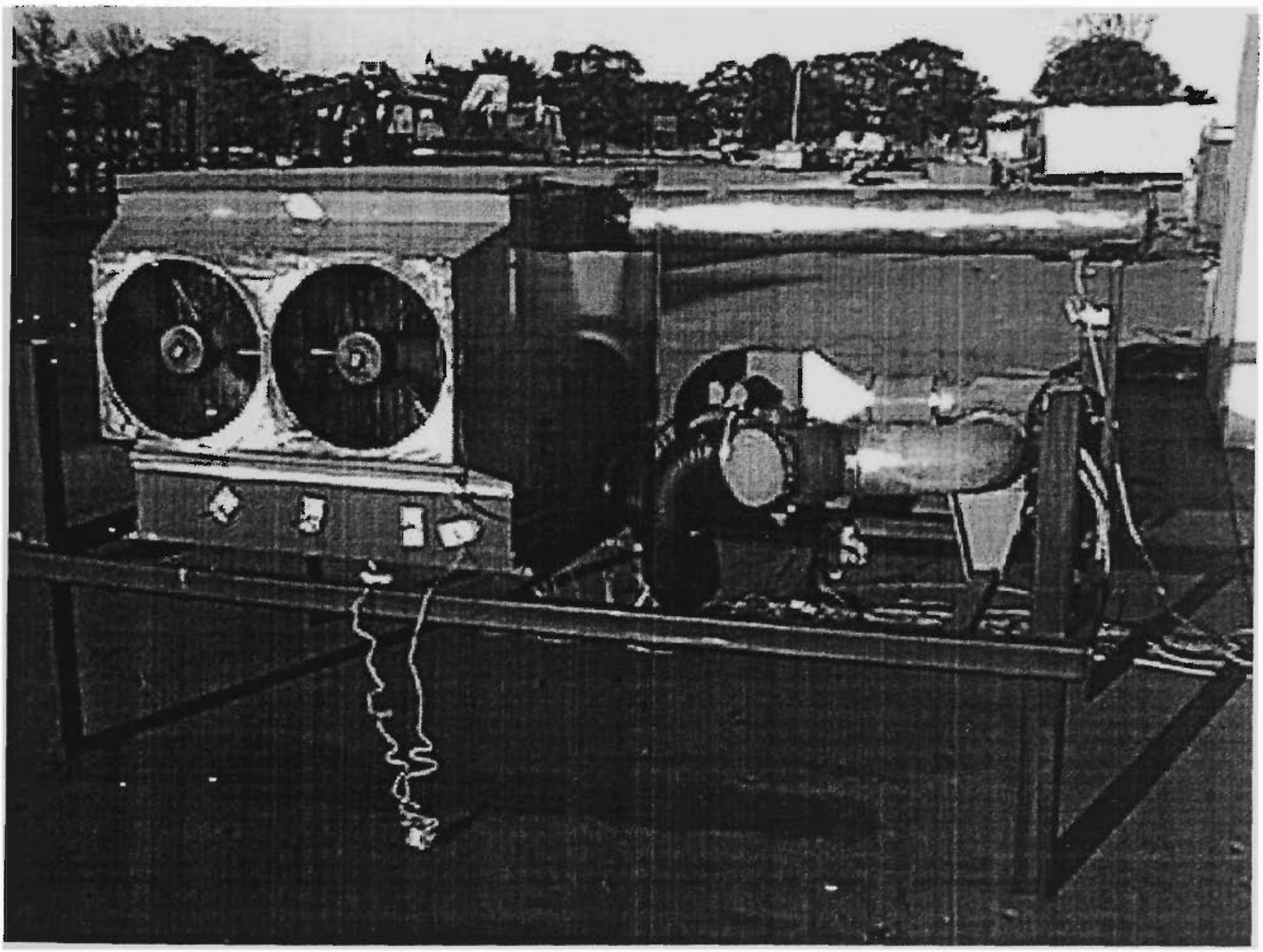

Figure 5.9 Typical view of the desiccant cooling system – first prototype

Table 5.2 Specification of the first prototype of the novel desiccant cooling system

1	Desiccant dehumidifier	
	Weight (kg)	125
	Height (mm)	800
	Width (mm)	1000
	Length (mm)	1000
	Number of the channels	30
	Height of each channel (mm)	600
	Width of each channel (mm)	5
	Distance between the channel (mm)	5
	Height of silica gel with in each channel (mm)	580
	Height headspace (mm)	15
	Height of bottom space (mm)	15
2	Centrifugal fan	
	Air flow capacity (m^3/s)	0.15
3	Axial fans	
	Air flow capacity (m^3/s)	1.0
4	Gas heater	
	LPG consumption (kg/h)	1.2

The first prototype that we tested had two axial fans to draw the secondary air flow through the heat exchanger channels; the second prototype had three axial fans. A back-up gas heater can be used to enhance the regeneration performance during the day. The centrifugal fan forces the ambient air through the desiccant material both of cooling and regeneration processes.

In the initial state, 150 kg of silica gel was filled in the channels that had a capacity of 40 kg moisture absorption during one cooling process. The specification of the system is indicated in table 5.2.

5.2 Instrumentation and measurement

5.2.1 Instrumentation

The scheme of experimental data acquisition is sketched in figure 5.10 consisting of a set of probes, a data logger and a PC.

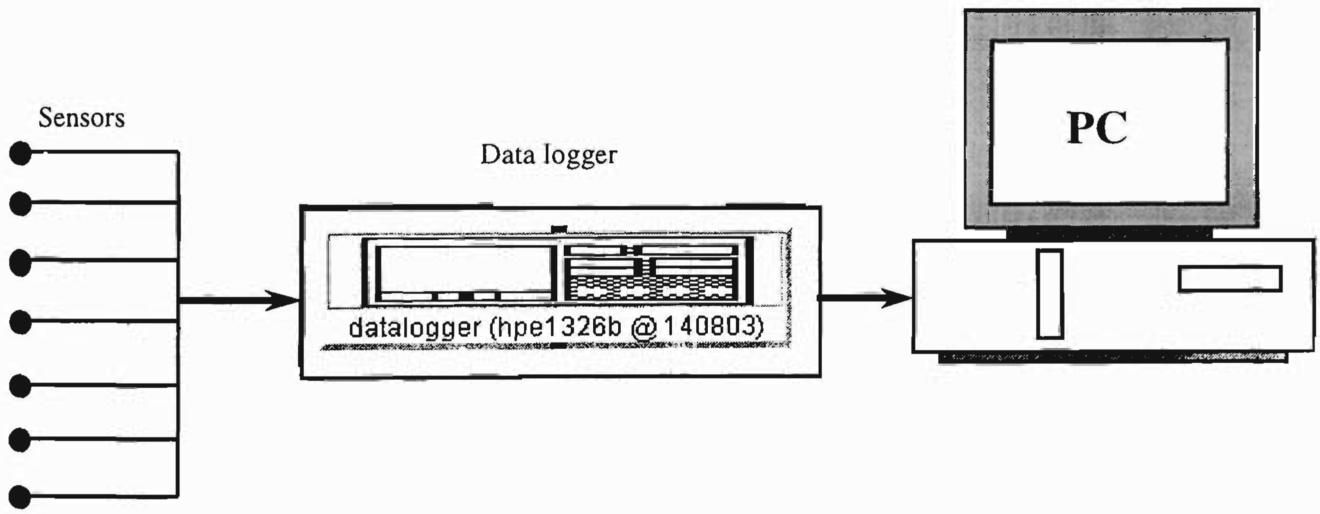

Figure 5.10 Scheme of the process of experimental data recording, Ararat

To realize the objectives mentioned at the start of the chapter, the key parameters to measure are:

- The reduction in wet-bulb temperature of the air passing though the desiccant device during the cooling process.
- The regeneration air temperature of the regeneration process.
- The operating time of the regeneration process.
- The energy consumption during both of cooling and regeneration processes.

- The variation and distribution of stored grain temperature and moisture content during the field trials.

It is noted in Chapter 1 that two properties, dry-bulb temperature and relative humidity, determine the air condition and properties of the air that wet-bulb temperature, enthalpy and humidity ratio can be found easily on a psychrometric chart with the two known properties. The sensor, namely humidity and temperature transmitter, is used in the places where the we-bulb temperatures need to be measured. The main instrumentation used in the thesis is listed table 5.3. Details of HP Vee program are given in Appendix A

Table 5.3 Instrumentation applied in Ararat experiments

Instrument	Type	Purpose
Data logger	HP E 1326B 5 1/2 Digit Multimeter	Transfer the measurement signals from sensors to PC
PC		Recording and saving the data
Thermocouples	Type - T, heavy gauge	Measuring temperature
Humidity & Temperature transmitter	Vaisala HMP45A V0520014	Measuring the relative humidity and temperature
Pitot tube		Measuring air flow rates

5.2.2 Placement of instrumentation in the desiccant cooling system

The key measurements of the desiccant system are shown in figure 5.11 that are the air conditions entering and exiting the desiccant cooling system, which include the dry-bulb temperatures, T_2 and T_3, and relative humidity, RH_2 and RH_3, the air temperatures before the desiccant device, T_4 in the lower plenum chamber, and after desiccant device are also measured, T_5 in the lower plenum chamber. The ambient air conditions are also recorded with T_1 and RH_1. Characteristics of the fans are measured by airflow rate, F_1 of the process air, and F_2 of the secondary air, and pressure for the secondary air flow.

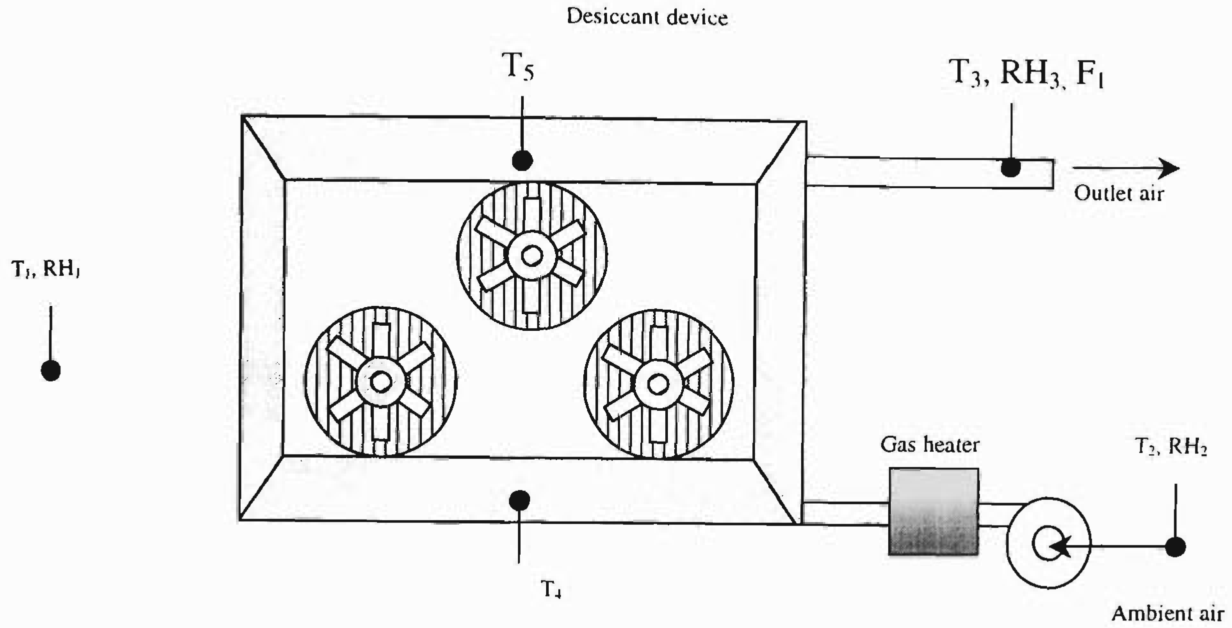

Figure 5.11 Measurement of the desiccant cooling unit – second prototype

5.2.3 Placement of measuring sensors in the silos

Two silos with capacities of 50 tonnes and 100 tonnes were involved in the field trials. It is not necessary to record the grain condition at every location in the silos when we can describe the entire grain condition clearly with several recording values in the silos. Considering the conclusions in Chapter 4, we need to find the following values

- The grain temperatures along the centerline of the silo that represent the influence of the aeration air.
- The grain temperatures at wall boundaries that indicate the storage conditions affected by ambient conditions such as intense solar radiation, or high ambient temperatures.
- The air temperatures in the headspace that provide the useful information not only for the solar energy application in future, but also for improving the headspace boundary consideration in the mathematical modeling process.
- The air temperatures in the recycling duct that show the air condition exiting the headspace and it can give us the valuable information for recycling air in the system in future study.

Therefore, in the 100 tonne capacity silo shown in figure 5.12, the readings to be taken are

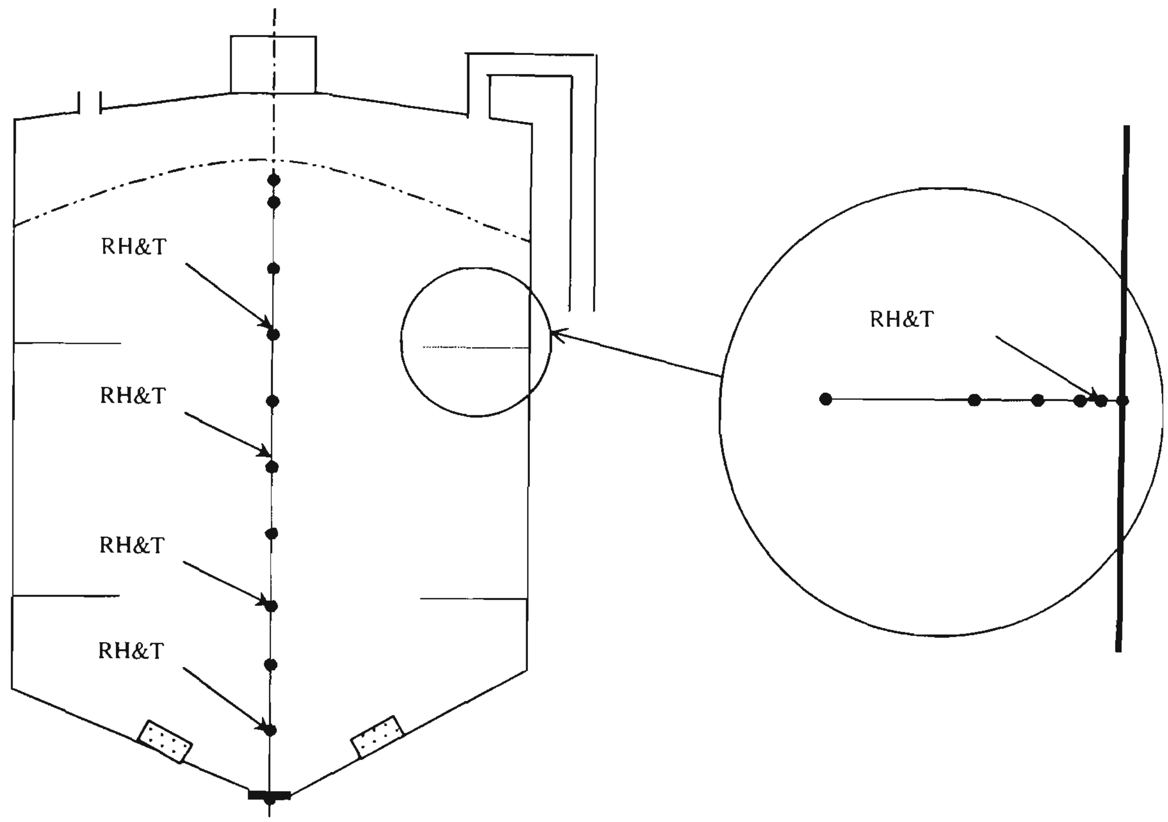

Figure 5.12 Locations of the grain temperatures and moisture contents measured in 100 tonne silo, SE-NW cross-section

- Eleven thermocouple sensors placed along the centerline at heights of 0m 1m, 2m, 3m, 4m, 5m, 6m, 7m, 8m, 9m and 9.25m from the bottom of the silo.
- Four humidity and temperature transmitters along the centerline at heights of 1m, 3m, 5m and 7m from the bottom of the silo.
- Twenty-four thermocouple sensors placed along radii adjacent wall to north-west and south-east at heights of 8m and 4m, and each radial line located six thermocouple sensors at the distances of 0m, 0.05m, 0.1m, 0.2m, 0.5m and 1m from the wall.
- Four humidity and temperature transmitters placed along the four radial lines at the distance of 0.05m from the wall.
- One thermocouple sensor placed in the headspace near the air entrance of the roof shown in figure 5.13.
- One thermocouple sensor placed in the exit duct shown in figure 5.13.

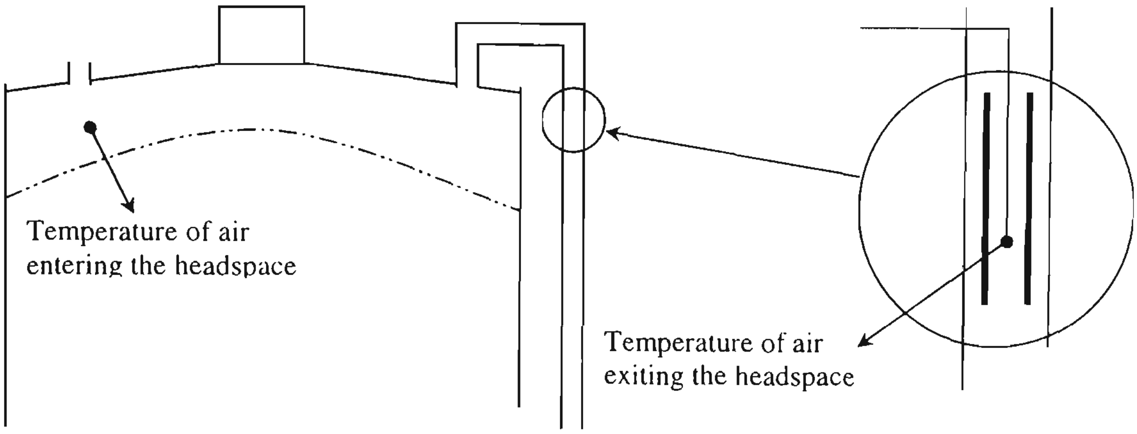

Figure 5.13 Locations of the air temperatures measured in the headspace of 100 tonne silo, SE-NW cross-section

In the 50 tonne silo shown in figure 5.14, the variables measured are:

- 5 thermocouple sensors placed along the centerline at heights of 0m 1m, 2m, 3m, 4m, 5m from the bottom of the silo.

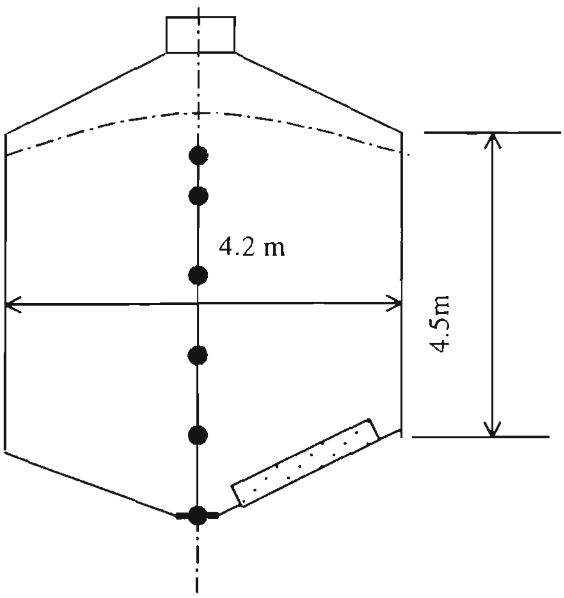

Figure 5.14 Locations at which temperatures and relative humility are to be measured in 50 tonne capacity silo

5.2.3 Measurement of initial grain moisture contents

100 samples of wheat and 50 samples of canola were collected when the silos were being filled. As the silos were filled and samples taken, the moisture contents jars were measured by an oven method. Hence, increasing sample numbers referred to those regions of grain that were furthest from the base of the silo.

5.2.4 Programming the data acquisition system

The schematic of the program used in the data acquisition system is shown in figure 5.15. Temperature and humidity data were measured automatically every five minutes. This was achieved using a HP E 1326B 5 1/2 Digit Multimeter made by Hewlett-Packard fitted with temperature compensation boards that enabled voltages across thermocouples to be converted into temperatures. A power source generated 10V and to which the humidity and temperature transmitter were connected. A PC programmed using HPVee control language controlled the data acquisition system. In order to simplify processing of experimental data, all data are recorded and saved in Excel spreadsheets programmed with VBA.

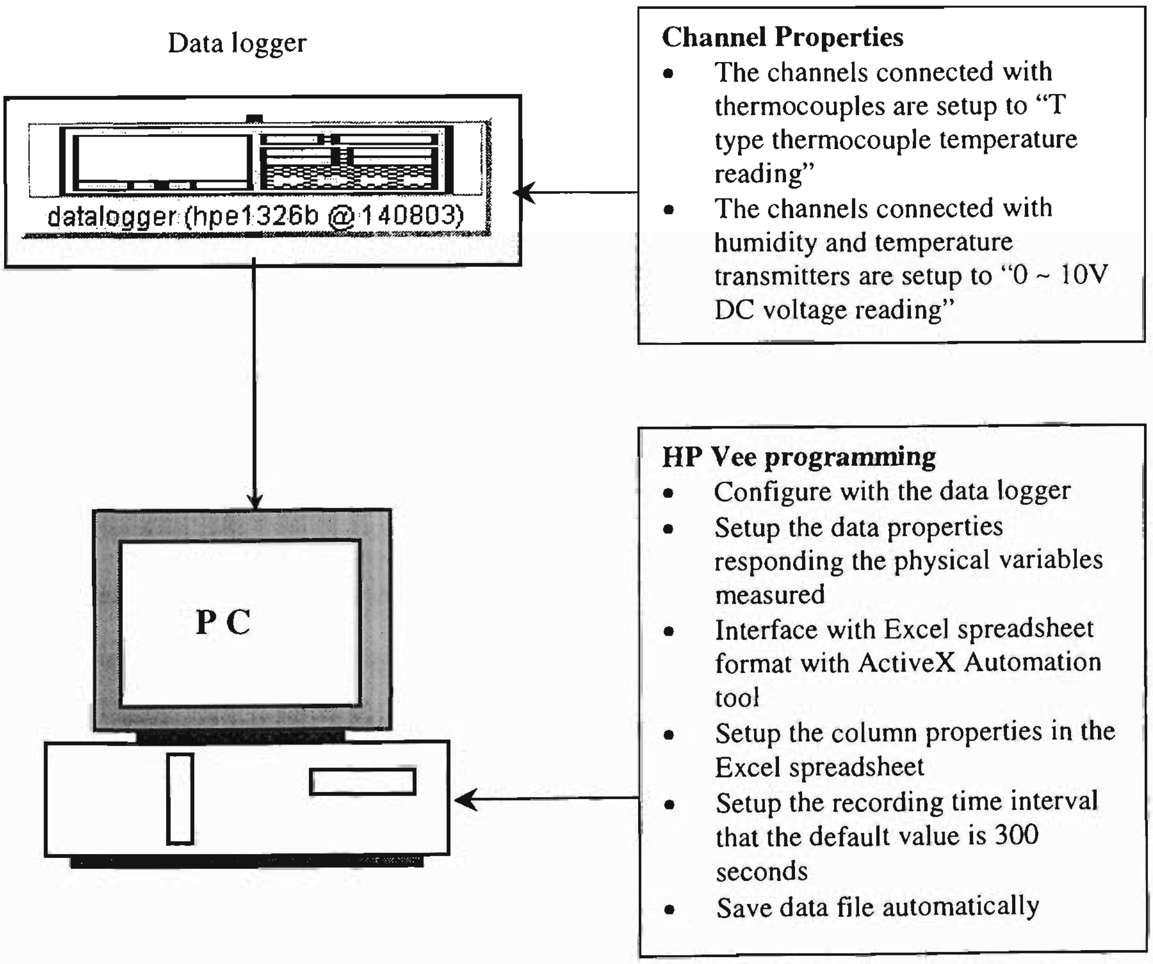

Figure 5.15 Schematic of experimental data recording procedure

5.3 Discussion of laboratory Results

5.3.1 Cooling process in laboratory

Preliminary experiments were conducted on the cooling unit in the laboratory. The principal aims were to gain insights into the overall performance of the unit that included the degree of wet-bulb temperature depression and its trajectory through the time. Another area of interest was the approach to isothermal conditions within the beds of desiccant, as this is an indicator of the rate at which heat of sorption is removed. The results of three cooling processes are shown in table 5.4.

Table 5.4 Laboratory results for first prototype

Process	Time	Condition	Average dry-bulb temperature °C	Average RH %	Average wet-bulb temperature °C	Average humidity ratio g/kg $_{dry\ air}$	Average enthalpy kJ/kg $_{dry\ air}$
Cooling 1	18:03 13 ~ 8:38 14 April, 2000	Ambient	16.2	96.5	15.8	11.1	44.5
		Outlet	19.6	46.5	12.7	6.4	36.2
Cooling 2	21:52 19 ~ 9:18 20 April, 2000	Ambient	8.9	95.0	8.4	6.6	25.6
		Outlet	10.0	46.1	5.1	3.8	20.4
Cooling 3	22:21 11 ~ 8:46 12 May, 2000	Ambient	9.3	87.5	8.2	6.2	25.1
		Outlet	12.5	23.7	4.6	2.1	17.8

Air flow rate: 0.15 m^3/s

There are two key features in table 5.4 that are interesting to us, namely in two of the processes, cooling 1 and cooling 3, the average of the average dry-bulb temperature of the air leaving the unit was over 3°C higher than average ambient temperatures and the average reduction in average wet-bulb temperature was typically 3.5°C. Furthermore, since the system was designed to operate for only six hours per night the inlet and outlet conditions were averaged over this period and listed in table 5.5. It can be seen in table 5.5 that the rise in average ambient temperature was typically 4°C, and the average depression of wet-bulb temperature was 4°C. This situation may be caused by the unsatisfactory removal of sorption heat.

In figures 5.16 to 5.18 the recorded data in of temperatures and relative humidity in these three cooling processes are plotted. We found that the cooling 2 is unsatisfactory clearly so far as the outlet relative humidity, 45.7%, was much higher than the designed value of 25%. Scrutiny of the experimental plots in figure 5.17 shows the beginning value of the outlet relative humidity was already very high at 45%, so the uncompleted regeneration may be the main reason for those results.

Table 5.5 Performance in the first six hours during the cooling processes - first prototype in laboratory

Cycle	Time	Air condition	Average dry-bulb temperature °C	RH %	Average wet-bulb temerature °C	Humidity ratio g/kg $_{dry\ air}$	Enthalpy kJ/kg $_{dry\ air}$
Cooling 1	18:03 14~ 00:03 15 April, 1999	Ambient	16.6	96.1	16.2	11.4	45.5
		Average outlet	20.9	26.9	10.9	4.1	31.4
Cooling 2	21:52 19 ~ 03:52 20 April, 2004	Ambient	8.7	97.8	8.6	6.9	26.0
		Average outlet	10.4	45.7	5.4	3.5	19.3
cooling 3	22:21 11 ~ 04:21 12 May, 2000	Ambient	9.4	88.1	8.4	6.4	25.5
		Average outlet	13.5	15.7	4.3	1.5	17.2

Air flow rate: 0.15 m^3/s

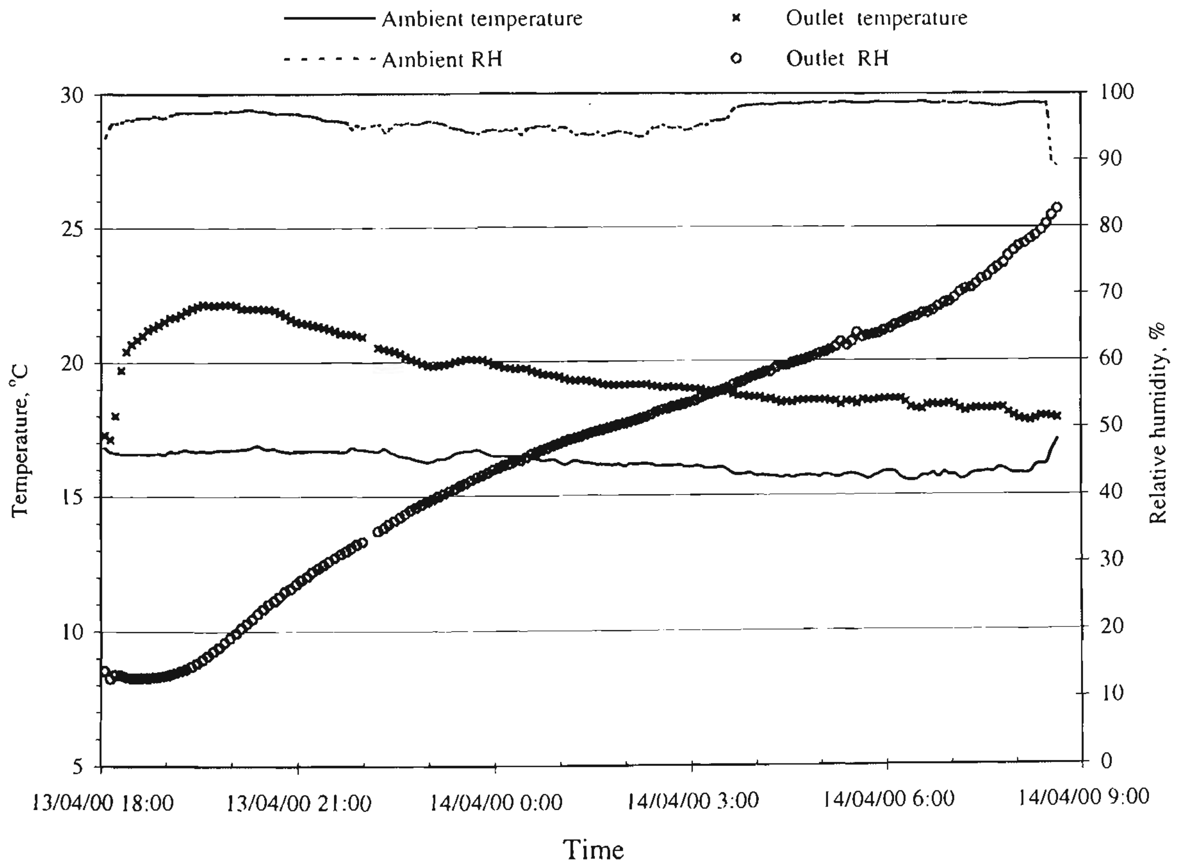

Figure 5.16 Temperatures and relative humidity of ambient and outlet of the cooling process 1 (18:03 13 April ~ 8:38 14 April, 2000)

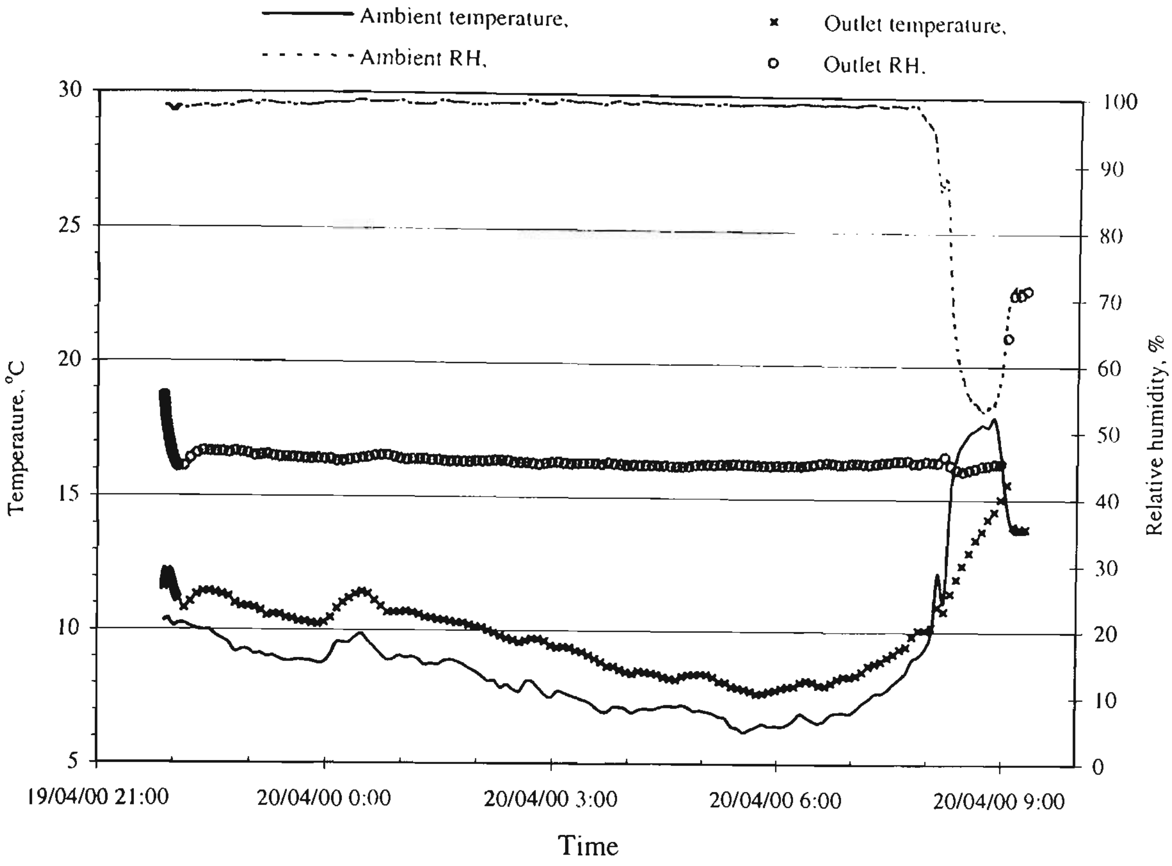

Figure 5.17 Temperatures and relative humidity of ambient and outlet of the cooling process 2 (21:52 19 April ~ 9:18 20 April, 2000)

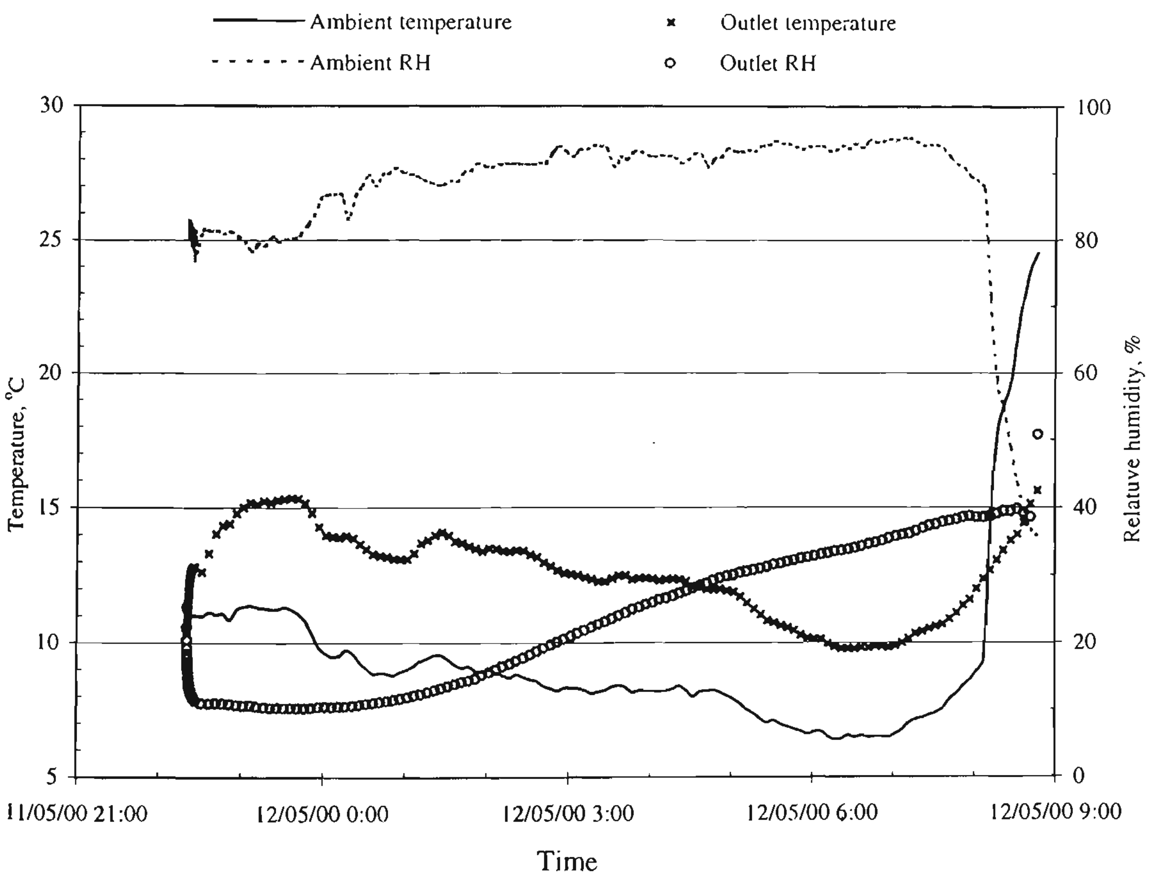

Figure 5.18 Temperatures and relative humidity of ambient and outlet air in cooling process 3 (22:21 11 May ~ 8:46 12 May, 2000)

Comparing the figure 5.16 and 5.18 with figure 5.5, especially the plots of the outlet temperature and relative humidity, the following conclusions are reached:

- The plots of the outlet conditions agreed with the general pattern portrayed in figure 5.5.
- The initial desiccant temperature changed quickly in minutes, as outlet air temperatures increased soon after the process started.
- The outlet air never reached the temperature of the inlet air during operation, *i.e.* Zone 1 did not completely traverse the bed before shutdown.
- The temperatures of the outlet air reached its maximum after 2 hours in the cooling process 1 (figure 5.16), 0.5 hour in the cooling process 2 (figure 5.17), and 1 hour in the cooling process 3 (figure 5.18), which was the time of outlet in the Zone 4, and temperature wave exited the bed
- The temperature difference between inlet (ambient) and outlet air was quite constant in figures 5.16 and 5.17 or changed smoothly in figure 5.18, and outlet temperatures captured the change trend of inlet well.
- The outlet relative humidity started to rise after about one hour of the cooling operation in process 1 (figure 5.16) and 2.5 hours in cooling process 3 (figure 5.18), which was the time that the outlet started the Zone 2 in figure 5.5.
- The outlet relative humidity did not rise in cooling process 2 (figure 5.17).
- It was hard to see if Zone 3 existed in these three cooling processes because the outlet temperature reflected the variable trends of the inlet temperature.

The performance of the system was degraded because the average outlet temperature was 4°C higher than ambient temperature and the design temperature rise was only 2°C (table 5.1), hence the desiccant unit did not operate isothermally. This indicates that the heat of sorption was not removed sufficiently in the first prototype (figure 5.9).

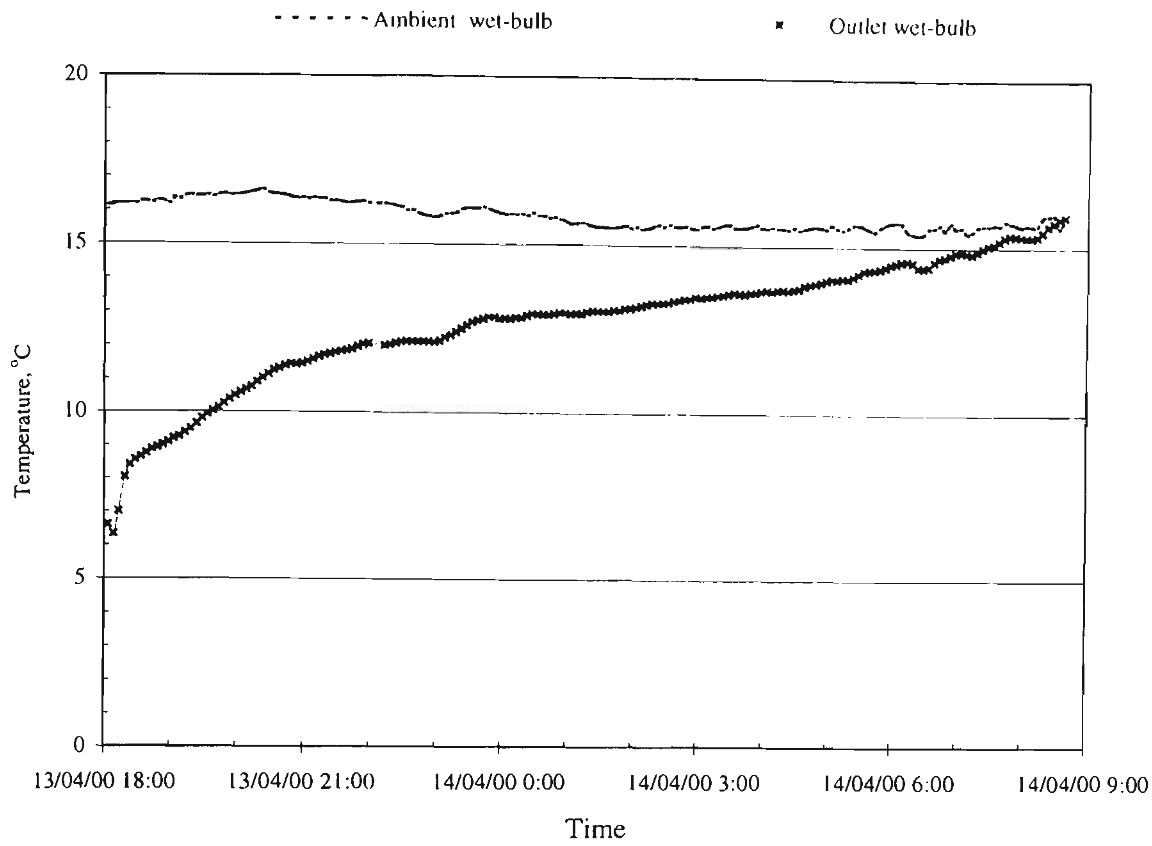

Figure 5.19 Wet-bulb temperature of ambient and outlet of the cooling process 1 (18:03 13 April ~ 8:38 14 April, 2000)

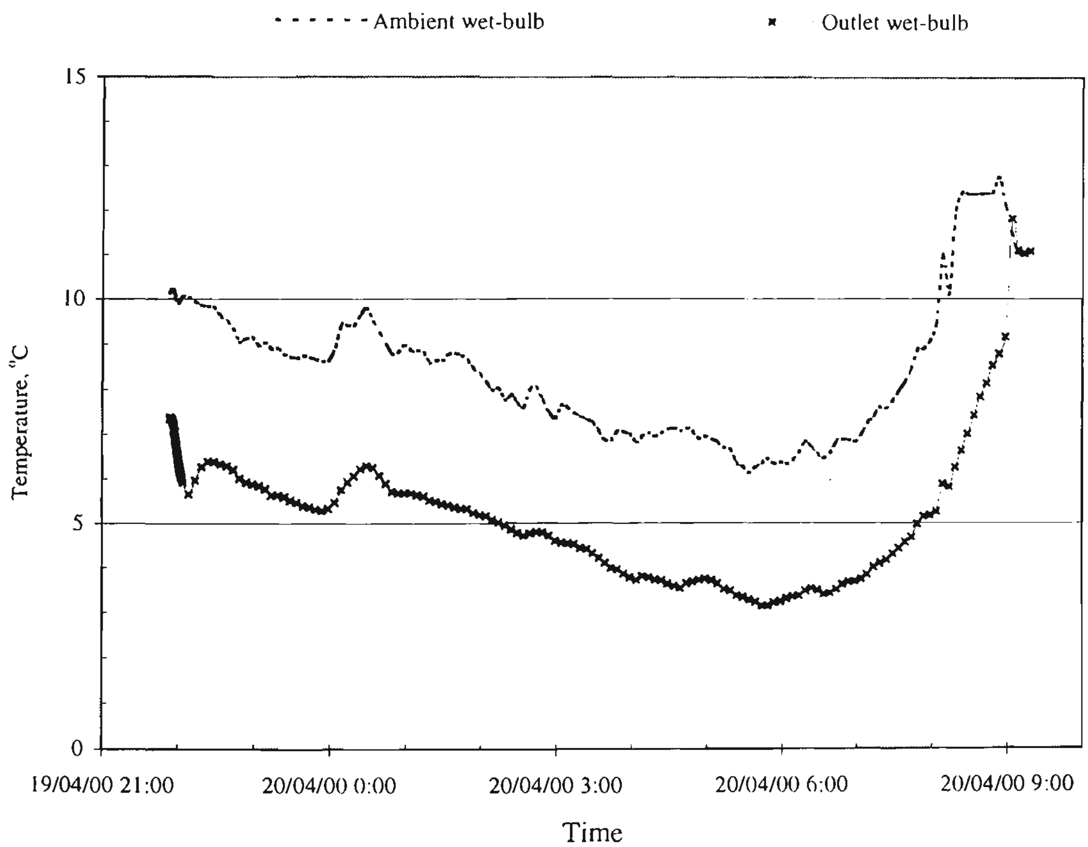

Figure 5.20 Wet-bulb temperature of ambient and outlet of the cooling process 2 (21:52 19 April ~ 9:18 20 April, 2000)

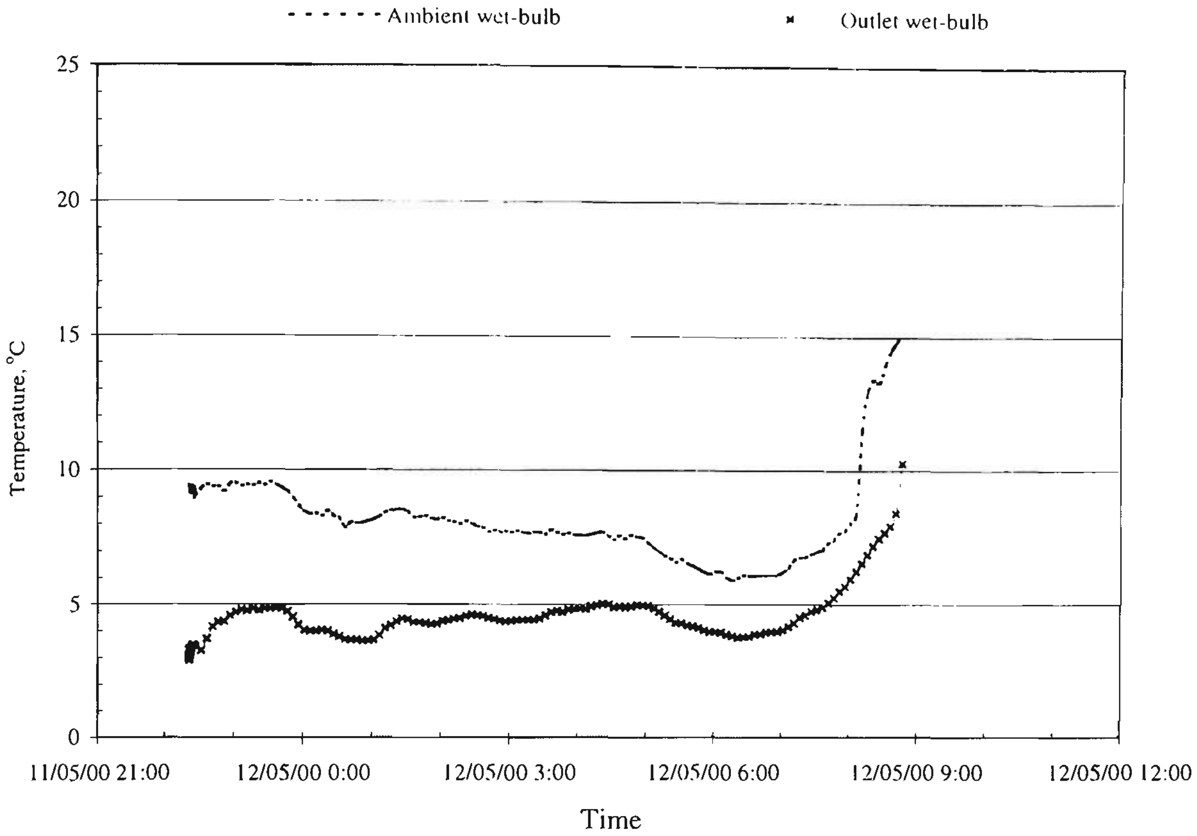

Figure 5.21 Wet-bulb temperatures of ambient and outlet air of the cooling process 3 (22:21 11 May ~ 8:46 12 May, 2000)

When the relative humidity of the outlet air increases, it can be seen in figures 5.19, 5.20 and 5.21 that the wet-bulb temperature differences between the inlet (ambient) and outlet air of the system decreases as the processing time increases. It seems that the inlet variation does not affect the difference between inlet and outlet both in dry-bulb and wet-bulb temperatures. We conclude that the difference between inlet and outlet depends more strongly on the condition of the desiccant.

5.3.2 Regeneration processes in the laboratory

Figures 5.22 and 5.23 show the measured regeneration temperature and conditions of outlet air during the regeneration processes 1 and 3. There were no data recorded for regeneration process 2.

Comparing the figures 5.22 and 5.23 with figure 5.7, we observe the following results of the regeneration processes.

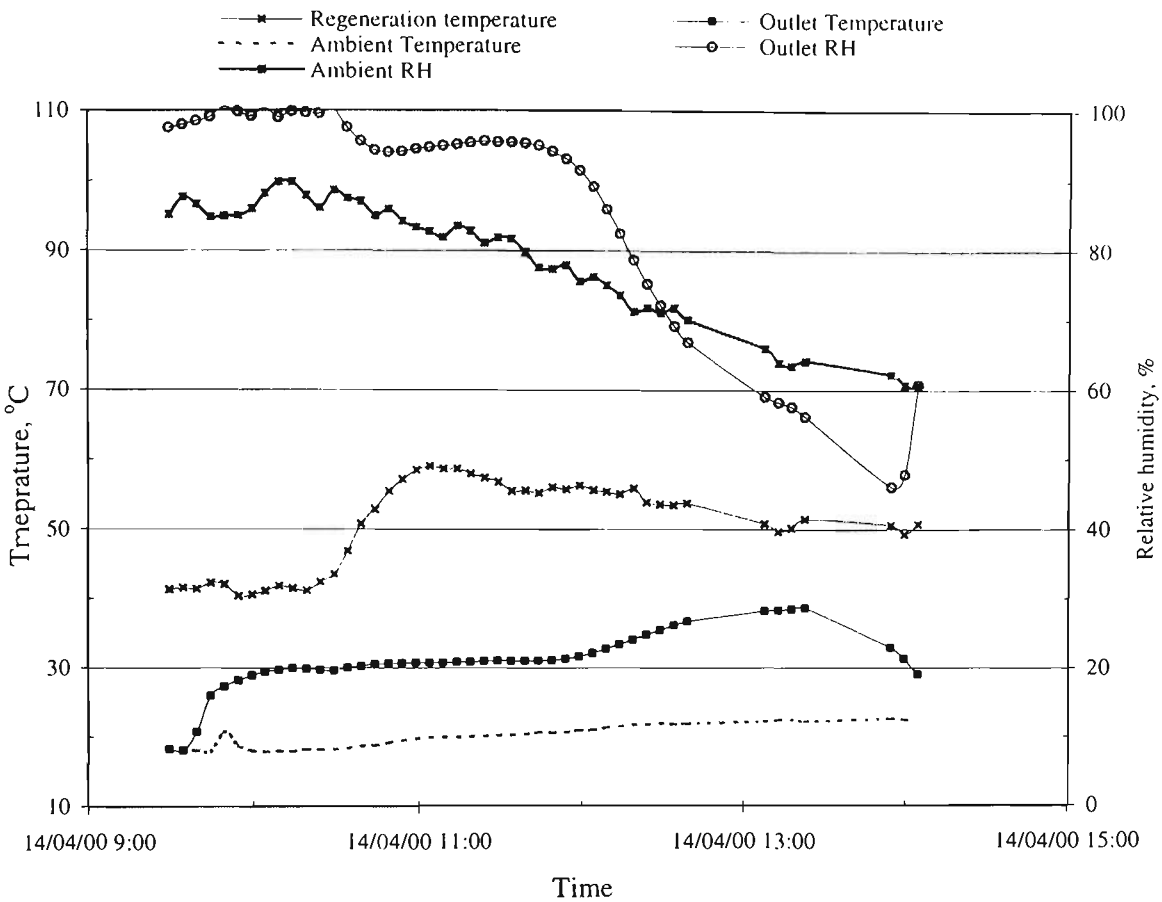

Figure 5.22 Regeneration temperature and outlet conditions during the regeneration process 1 (09:29 ~ 14:05 12 April, 2000)

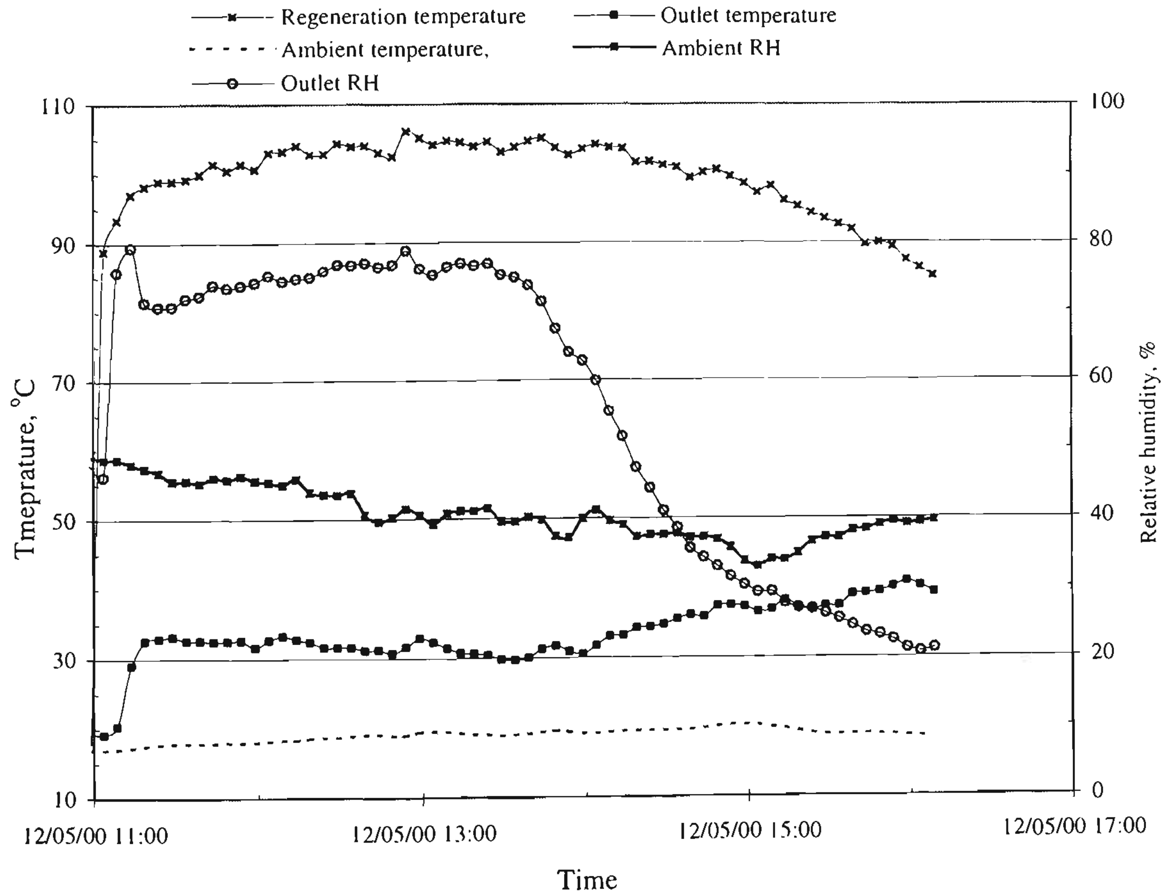

Figure 5.23 Regeneration temperature and outlet conditions during the regeneration process 3 (09:23 ~ 16:08 12 May, 2000)

- The experimental plots in figures 5.22 and 5.23 exhibit the features of the plots shown in figure 5.7.
- The outlet relative humidity reached its maximum value immediately in both regeneration processes 1 and 3 at the start of operation, in which the relative humidity was in equilibrium with the initial desiccant condition that means the outlet reached Zone 4.
- The state of the relative humidity of the outlet air in equilibrium with initial desiccant condition lasted for a very short time, about 10 minutes after the regeneration operation started.
- The outlet temperature remained constant at 30°C in the regeneration process 1 for about 2 hours in figure 5.22, and 32°C in regeneration process 3 in figure 5.23 for nearly 3 hours that was the time of Zone 3 existing in figure 5.7.
- In the regeneration process, figure 5.22, the outlet temperature increased a relatively small amount when the regeneration temperature rose from 40°C to 55°C and this reflects the physics of desorption; air wet-bulb temperature was constant.
- In figure 5.22, when the regeneration temperature was raised the outlet relative humidity dropped slightly and the reason for this feature was not clear at this stage.
- The outlet relative humidity started dropping after 2 hours in regeneration process 1 in figure 5.22, about 2.5 hours in process 3 in figure 5.23, and meanwhile the outlet temperature was increasing, which is a feature of Zone 2 described in figure 5.7.
- In both processes 1 and 3, the outlet relative humidity was depressed with a sharp slope at the beginning stage, and the slope then decreased.
- These processes were terminated before the system had reached a steady state, hence, the air corresponding to that in Zone 1 was not observed in totality.

The summary of the regeneration processes is shown in table 5.6. The performance of the second cooling process was, from a practical point of view, unsatisfactory. This is because the first regeneration process was not taken to finality, and an additional time would be needed for satisfactory regeneration.

Table 5.6 Experimental results of regeneration processes - first prototype

Cycle	Time	Average ambient dry-bulb °C	Average ambient RH %	Beginning outlet air RH %	Average regeneration temperature °C	Regeneration time hour	Final outlet air RH %
Regeneration 1	09:29 ~ 14:04 14 April, 2000	20.1	78.9	97.5	69.7	4.6	46.1
Regeneration 2*							
Regeneration 3	11:03 ~ 16:03 15 May, 2000	19.4	49.6	85.9	99.6	5.0	20.1

* There were no data recorded for regeneration process 2
\# Air flow rate: 0.15 m^3/s

5.3.3 Conclusions drawn from the laboratory studies

The results obtained during the laboratory experiments allow us to draw the following conclusions:

- The cooling and regeneration processes accorded with those anticipated from qualitative analysis given in section 5.2.3.
- The inlet variation in air temperature did not affect the reduction in dry-bulb and wet-bulb temperatures of the process air in the cooling processes.
- In the designed six-hour operation time, it was possible to reduce the wet-bulb temperature of inlet air by more than 5°C.
- The depression of the average wet-bulb temperatures of the air leaving the unit appears to be a strong function of the regeneration rate of desiccant.
- During the cooling processes, the dry-bulb temperature of the air leaving the unit was typically 4°C higher than ambient. This was twice as high as anticipated.
- The initial relative humidity of the inlet air during a cooling process corresponds closely to the relative humidity of the air obtained at the end of the regeneration process.

5.4 Discussion of field results

5.4.1 Modifications to the first prototype

After carrying out the laboratory experiments it became clear that the performance of the desiccant unit could be improved. The principal problem appeared to be that the heat of sorption could not be dissipated sufficiently quickly. The two most likely causes of this are

- The heat could not be transferred quickly enough from desiccant to the secondary air.
- The flow rate of the secondary air was too low, hence, it heated up too much which reduced the temperature driving force between the desiccant and the primary air.

In an attempt to remedy these deficiencies two modifications were made to the design, namely.

- The channels containing the silica gel and those through which the secondary air flow were reduced in width from 15mm to 10mm.
- An additional axial cooling fun was installed to increase the flow rate of secondary air as shown in figure 5.11.

During data processing for the field results, we found that the sensor for the ambient condition measurement, T_3, RH_3 in figure 5.11, did not work after the third day of testing. According to the results in the first two days, the data points of the sensor placed in front of the aeration fan, T_1, RH_1 in figure 5.11, were in close agreement to the ambient condition sensor. Therefore, we applied the data of the sensor, T_1, RH_1, for the ambient condition.

5.4.2 Outlet conditions of the cooling processes

In a total of 31 cooling processes recorded in the field at Ararat, Victoria, the air flow rate was fixed as 0.137 m^3/s. Each cooling process lasted between 6 and12 hours. To make the results comparable with each other, we considered the performance of each process over a six-hour operational period as displayed in table 5.7.

Table 5.7 Average performances of cooling processes in Ararat - six-hour operation

Process	Time	Average ambient temperature	Average ambient RH	Average ambient wet-bulb temperature	Average outlet temperature	Average outlet RH	Average outlet wet-bulb temperature	Wet-bulb temperature reduction
		°C	%	°C	°C	%	°C	°C
1	22:03 23 ~ 04:03 24 Jan 2001	24.2	55.1	18.0	25.8	27.6	14.5	-3.5
2	22:35 24 ~ 04:35 25 Jan 2001	21.4	92.2	20.5	25.4	40.4	16.6	-3.9
3	22:05 25 ~ 04:05 26 Jan 2001	22.5	88.1	21.1	24.0	48.9	16.9	-4.2
4	22:10 27 ~ 04:10 28 Jan 2001	12.2	78.9	10.2	13.5	57.7	9.2	-1.0
5	22:30 28 ~ 04:30 29 Jan 2001	13.3	71.9	10.5	14.0	45.1	8.3	-2.2
6	22:05 29 ~ 04:05 30 Jan 2001	14.5	84.6	12.9	16.8	33.3	8.9	-4.0
7	22:30 30 ~ 04:30 31 Jan 2001	11.5	73.8	9.1	12.0	45.7	6.8	-2.3
8	22:04 31 Jan ~ 04:04 1 Feb 2001	15.4	82.6	13.6	16.5	48.2	10.7	-3.0
9	22:02 2 ~ 04:02 3 Feb 2001	25.8	43.9	17.5	27.2	26.0	15.1	-2.4
10	22:35 3 ~ 04:35 4 Feb 2001	18.4	88.5	17.1	21.1	32.9	12.0	-5.1
11	22:03 5 ~ 04:03 6 Feb 2001	14.4	84.3	12.9	15.3	49.8	9.9	-2.9
12	23:00 6 ~ 05:00 7 Feb 2001	24.8	65.4	20.1	26.0	37.6	16.5	-3.6
13	22:16 7 ~ 04:16 8 Feb 2001	27.0	53.7	20.1	29.5	25.3	16.3	-3.8
14	02:13 ~ 08:13 10 Feb 2001	13.9	80.4	12.0	16.2	16.2	6.2	-5.8
15	22:10 10~ 04:10 11 Feb 2001	12.9	80.4	11.0	15.3	11.4	5.0	-6.0
16	22:00 11 ~ 04:00 12 Feb 2001	17.1	65.9	13.2	19.8	14.2	7.9	-5.3
17	23:11 12 ~ 05:11 13 Feb 2001	18.4	93.2	17.7	21.2	25.7	10.9	-6.8

Table 5.7 Average performances of cooling processes in Ararat - six-hour operation (Continued)

Process	Time	Average ambient temperature	Average ambient RH	Average ambient wet-bulb temperature	Average outlet temperature	Average outlet RH	Average outlet wet-bulb temperature	Wet-bulb temperature reduction
		°C	%	°C	°C	%	°C	°C
18	22:35 13 ~ 04:35 14 Feb 2001	14.5	80.9	12.6	17.0	17.0	6.8	-5.8
19	22:11 14 ~ 04:11 15 Feb 2001	11.8	82.7	10.2	13.4	52.0	8.5	-1.6
20	21:00 17 ~ 03:00 18 Feb 2001	20.0	49.6	13.6	21.8	16.2	9.6	-4.0
21	00:05 ~ 06:05 22 Feb 2001	15.7	81.1	13.8	17.7	25.9	8.6	-5.2
22	00:05 ~ 06:05 27 Feb 2001	15.0	85.8	13.5	17.2	26.7	8.3	-5.2
23	00:05 ~ 06:05 28 Feb 2001	11.4	82.3	9.8	14.0	10.9	4.1	-5.7
24	00:05 ~ 06:05 1 Mar 2001	9.9	74.9	7.8	11.1	16.7	2.9	-4.8
25	00:05 ~ 06:05 2 Mar 2001	12.1	83.0	10.5	14.7	12.2	4.7	-5.8
26	00:05 ~ 06:05 3 Mar 2001	12.4	84.5	11.0	14.8	16.2	5.3	-5.6
27	00:05 ~ 06:05 6 Mar 2001	17.2	66.0	13.4	19.5	18.7	8.6	-4.8
28	00:05 ~ 06:05 7 Mar 2001	16.9	57.6	12.2	18.9	13.6	7.5	-4.7
29	00:05 ~ 06:05 8 Mar 2001	17.6	58.7	12.9	19.7	14.9	8.1	-4.8
30	00:05 ~ 06:05 9 Mar 2001	18.9	47.5	12.4	20.6	15.5	8.7	-3.7
31	00:05 ~ 06:05 11 Mar 2001	13.4	70.0	10.5	14.8	28.1	6.9	-3.6

Air flow rate: 0.137 m^3/s

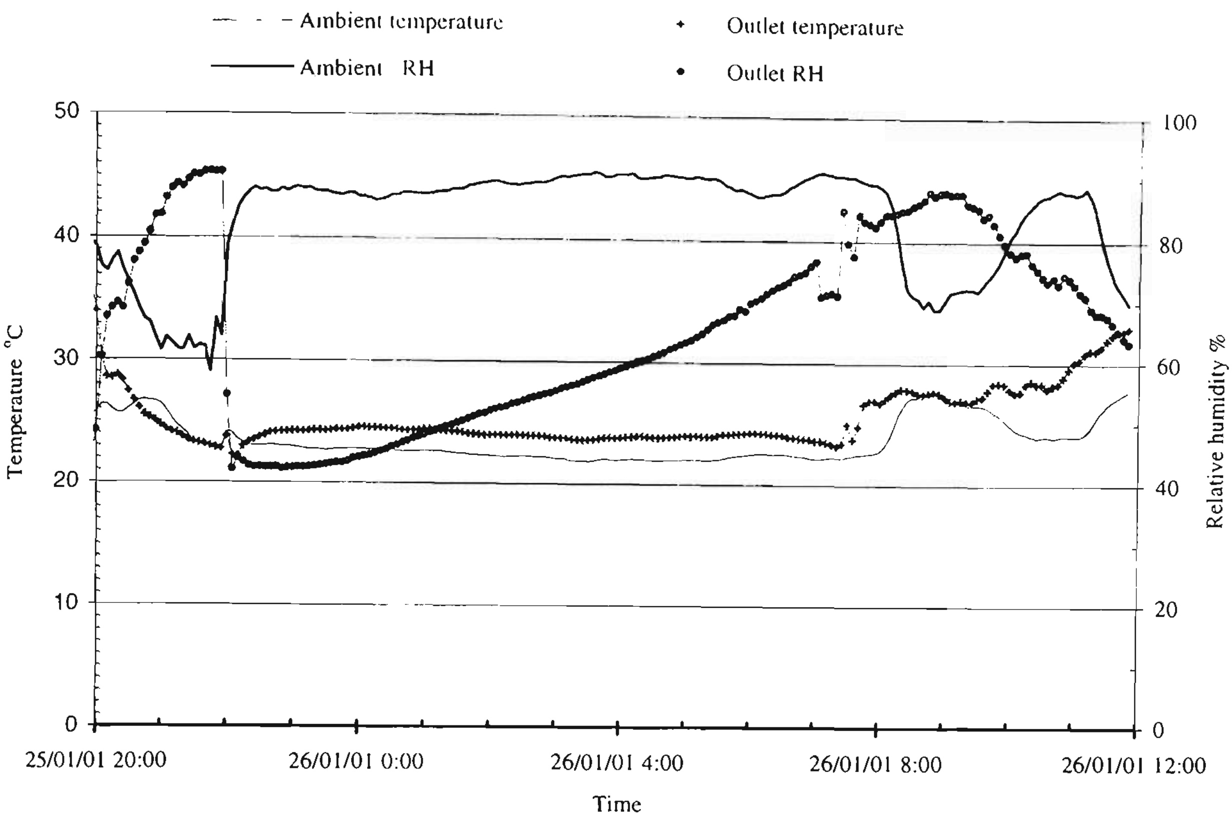

Figure 5.24 Temperature and relative humidity of ambient and outlet air during the cooling process 4 (22:05 25 ~ 04:05 26 Jan 2001)

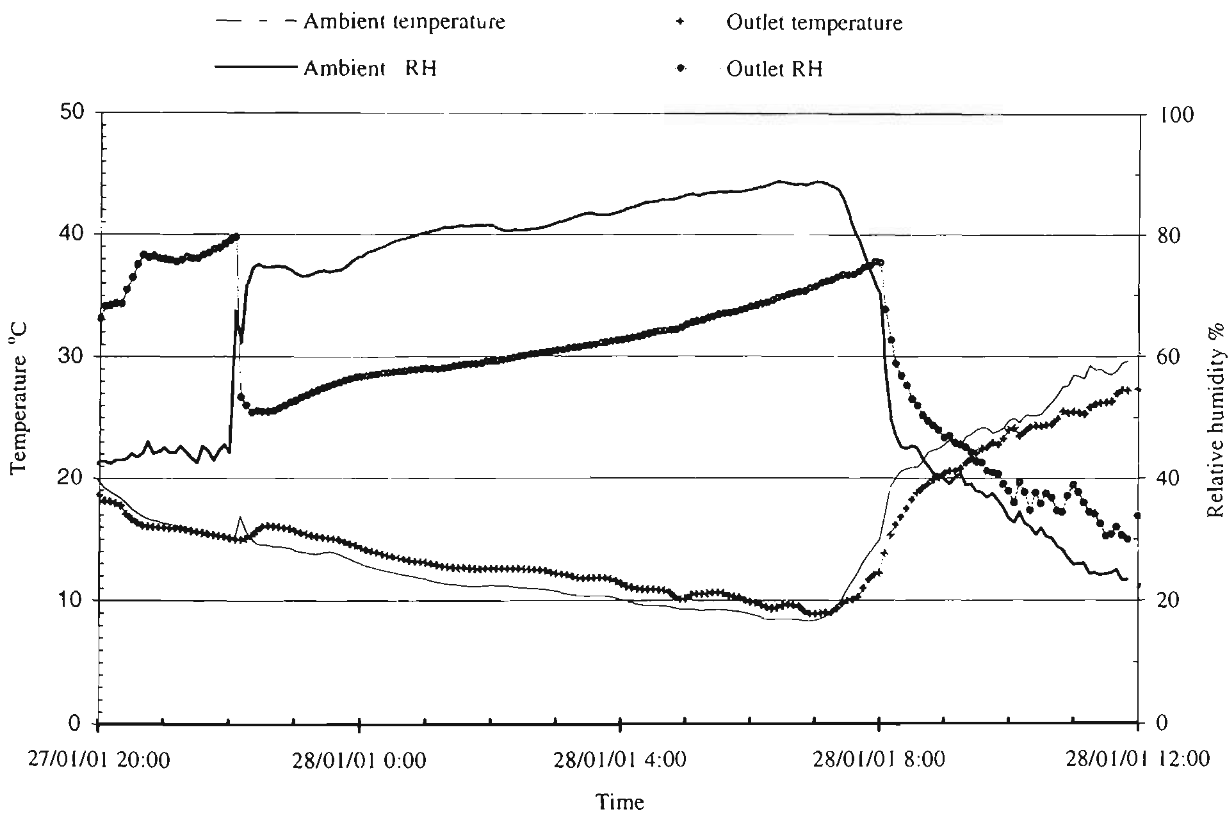

Figure 5.25 Temperature and relative humidity of ambient and outlet air during the cooling process 5 (22:10 27 ~ 04:10 28 Jan 2001)

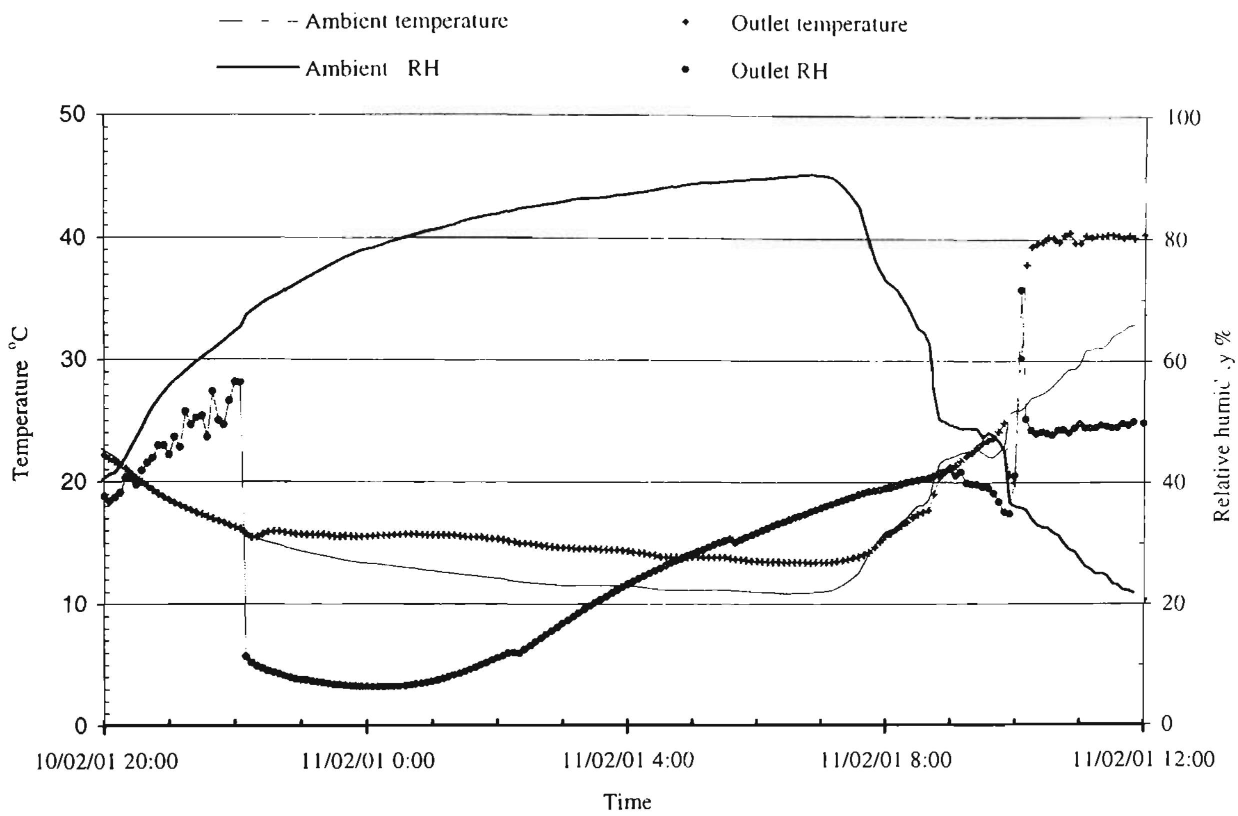

Figure 5.26 Temperature and relative humidity of ambient and outlet air during the cooling process 15 (22:10 10 ~ 04:10 11 Feb 2001)

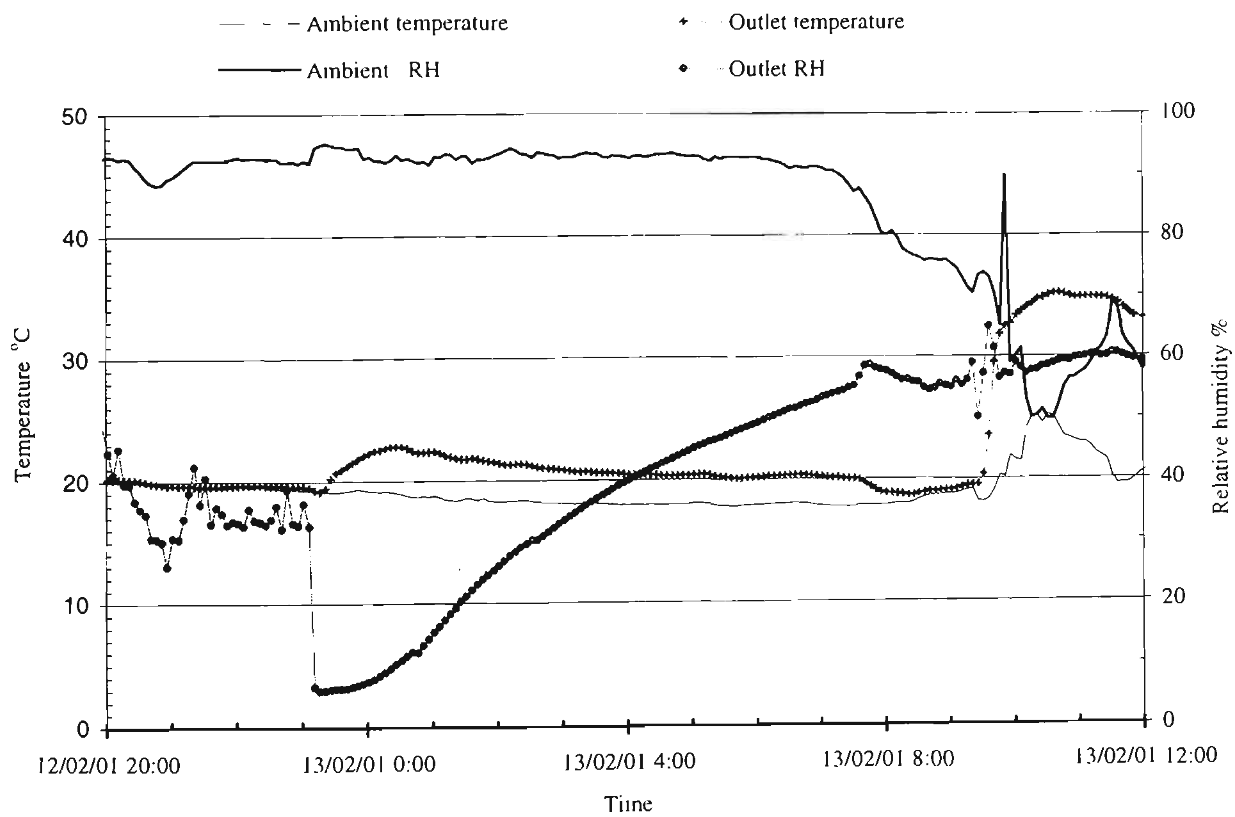

Figure 5.27 Temperature and relative humidity of ambient and outlet air during the cooling process 17 (22:11 12~ 04:11 13 Feb 2001)

In figures 5.24 to 5.27 we plot four typical cooling processes that display a range of performances. It was again observed that the performance of system agreed qualitatively with that anticipated in section 5.2.3 and shown in figure 5.5.

Note that the outlet temperatures were 1~ 2°C higher than ambient air, that is an improvement on the performance in the laboratory study. It is also found that this temperature difference was quite constant throughout the cooling process. We explain this constant temperature rise as follows.

When the silica gel is initially very dry, the rate in which heat of sorption is liberated is high. At this stage, the wetting wave has penetrated only a small distance into silica gel, and as a consequence, there is a large surface area through which the heat of sorption may be removed by the secondary air. As the cooling process progresses, the rate at which heat of sorption liberated is reduced because the total rate at which moisture adsorbed is also reduced. By this time the wetting wave has moved further into the device, the area available for transferring the heat to the secondary air is also less. A consequence of these phenomena is that the temperature difference between outlet and inlet is almost the same.

The relative humidity of the outlet air in the two less effective cooling processes 4, figure 5.24, and 5, figure 5.24, started with a quite high value, above 40%, but the corresponding value was less in than 10% the two better cooling processes 15 and 17 in figure 5.26 and 5.27. Less effective cooling processes generally follow incomplete regeneration processes.

5.4.3 Wet-bulb temperature reduction during the cooling processes

In table 5.7, there are 11 of 31 processes that produced 5°C or more depression in wet-bulb temperature and the largest depression was 6.8°C in cooling process 17. On the other hand, there was only 1°C wet-bulb temperature drop in cooling process 4.

To make the analysis of data points in table 5.7 straightforward, we plotted average reductions in wet-bulb temperatures of the process air against the average ambient temperatures in figure 5.28, the average ambient relative humidity in figure 5.29, and initial relative humidity of desiccant in figure 5.30. Meanwhile, we processed the correlation of the wet-bulb temperature reductions with the ambient conditions and initial relative humidity of desiccant by using the linear regression. The correlation coefficient used here is coefficient of determination, R^2, the proportion of the variability of y accounted for by x.

From the results of coefficient of determination, R^2, we found that in the experimental data region only about 1% of the variability in wet-bulb temperature reductions can be accounted for by the average ambient temperature (figure 5.28), and 8% by the average ambient relative humidity (figure 5.29). With 59% of R^2 in figure 5.30, it means that 59% of the variability in wet-bulb temperature reduction can be accounted for by the initial relative humidity of the desiccant.

From a practical point of view this result indicates that the desiccant must be completely regenerated so that the air leaving the desiccant has a relative humidity less than 10%.

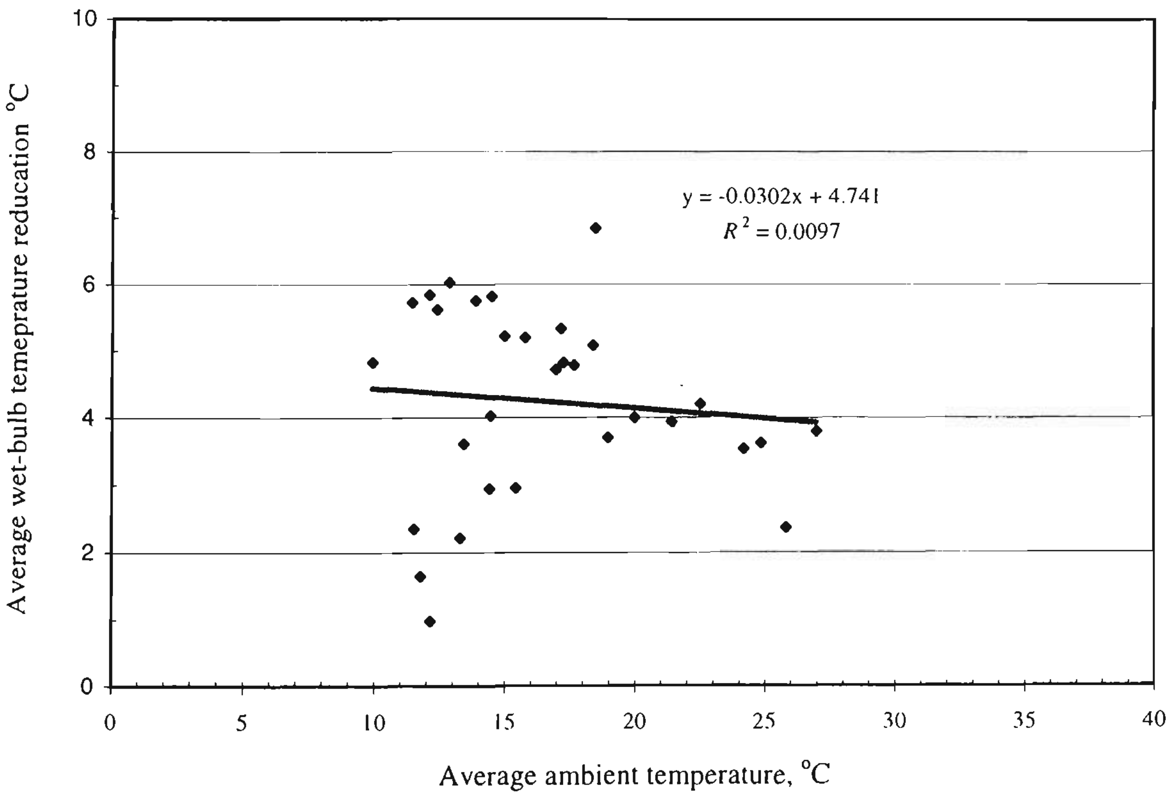

Figure 5.28 Average wet-bulb reduction of outlet versus average ambient temperature inlet - six-hour cooling processes

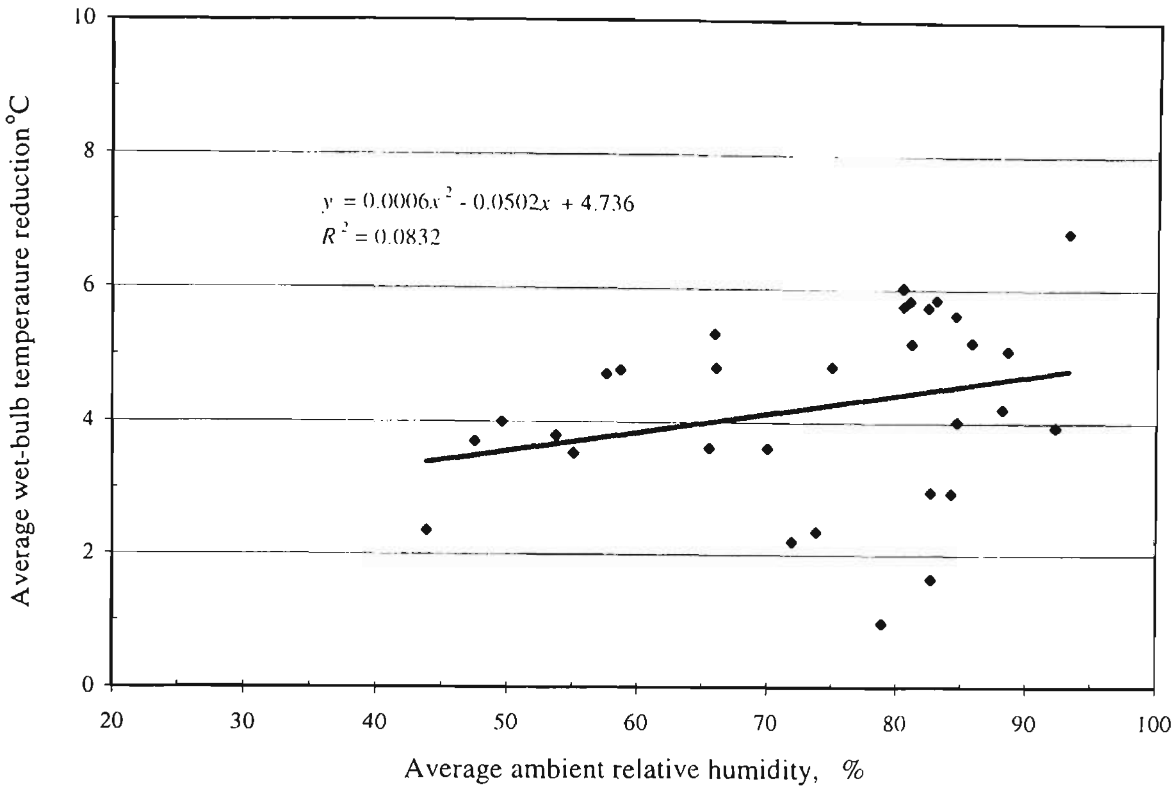

Figure 5.29 Average wet-bulb reduction of processing air versus average ambient relative humidity - six-hour cooling processes

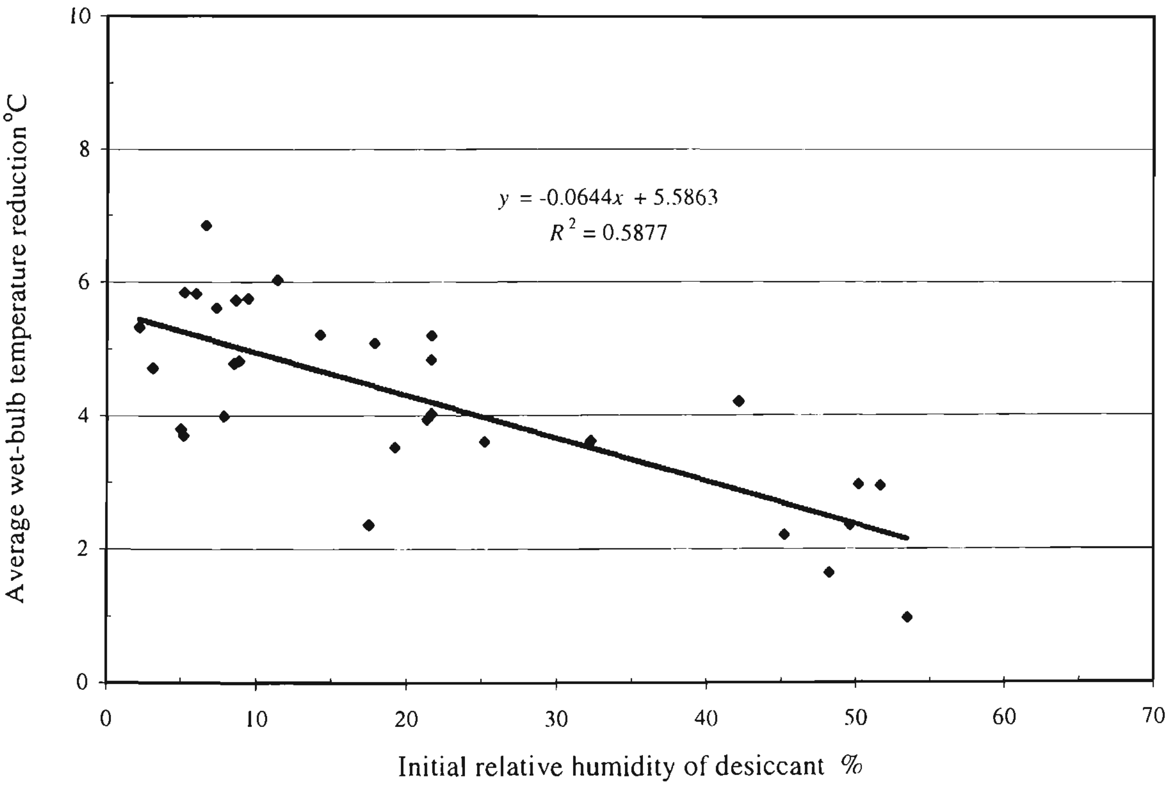

Figure 5.30 Average wet-bulb reduction of processing air versus the initial relative humidity of the desiccant - six-hour cooling processes

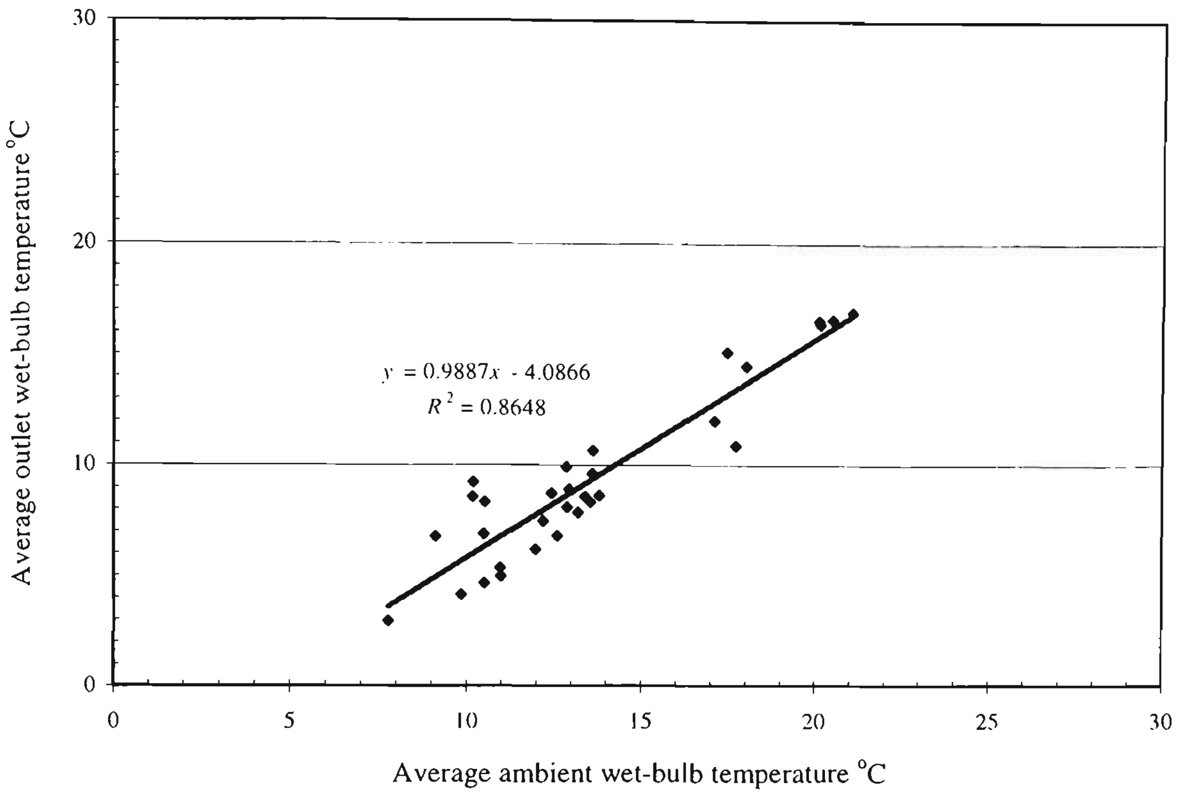

Figure 5.31 Average outlet wet-bulb temperature versus ambient average wet-bulb temperature - six-hour cooling processes

Figure 5.31 shows the average wet-bulb temperatures of the outlet air against average inlet wet-bulb temperatures. The regression relation of these two variables is almost a straight line with a slope value nearly 1 and a y-intercept about -4.1. However, it is not practical to use this regression relation for calculating the outlet conditions of cooling processing since the strongest influence on outlet, desiccant regeneration degree, has not accounted for.

5.4.4 Dry-bulb temperature of the air leaving the unit

Figure 5.32 shows the average outlet temperatures of the process air against the average inlet temperatures. There is a very good regression relation shown in figure 5.23 between these two variables and the average temperature of the process air had a 1.6°C increasing during six-hour processing periods. However, this regression model does not account for the degree of regeneration of the desiccant. Figures 5.33 to 5.35 show the temperature changes of the process air against the average temperatures of inlet air. In figure 5.33, there is only about 2% of the variability in the temperature of the process air can be accounted for by the average ambient temperatures and in figure 5.34 8% by the average ambient relative humidity.

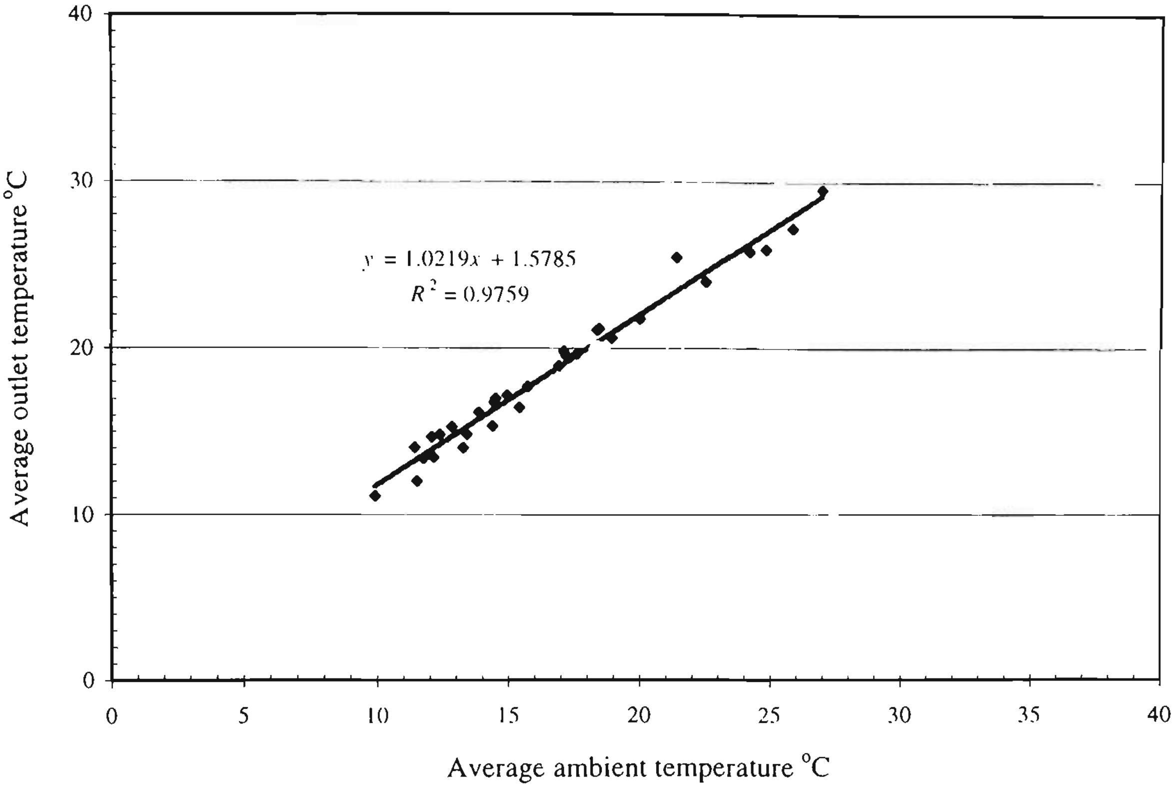

Figure 5.32 Average outlet temperature versus ambient average wet-bulb temperature - six-hour cooling processes

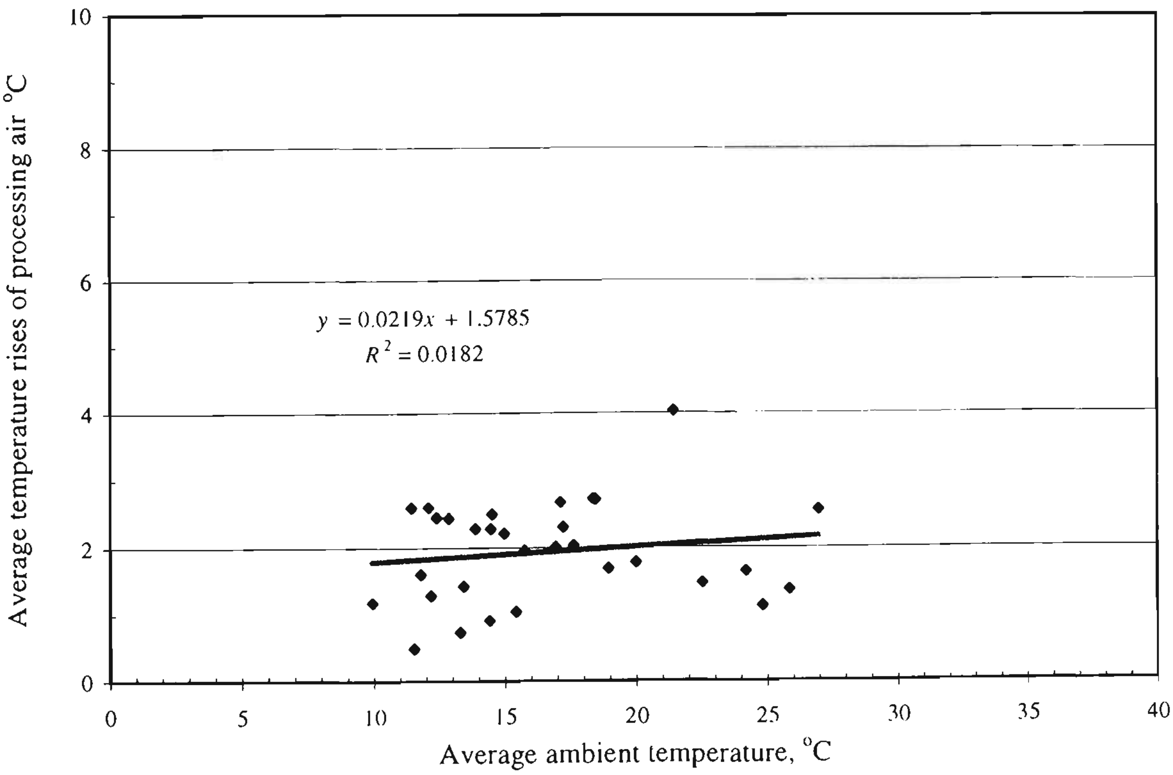

Figure 5.33 Average temperature rises of processing air versus average ambient temperature - six-hour cooling processes

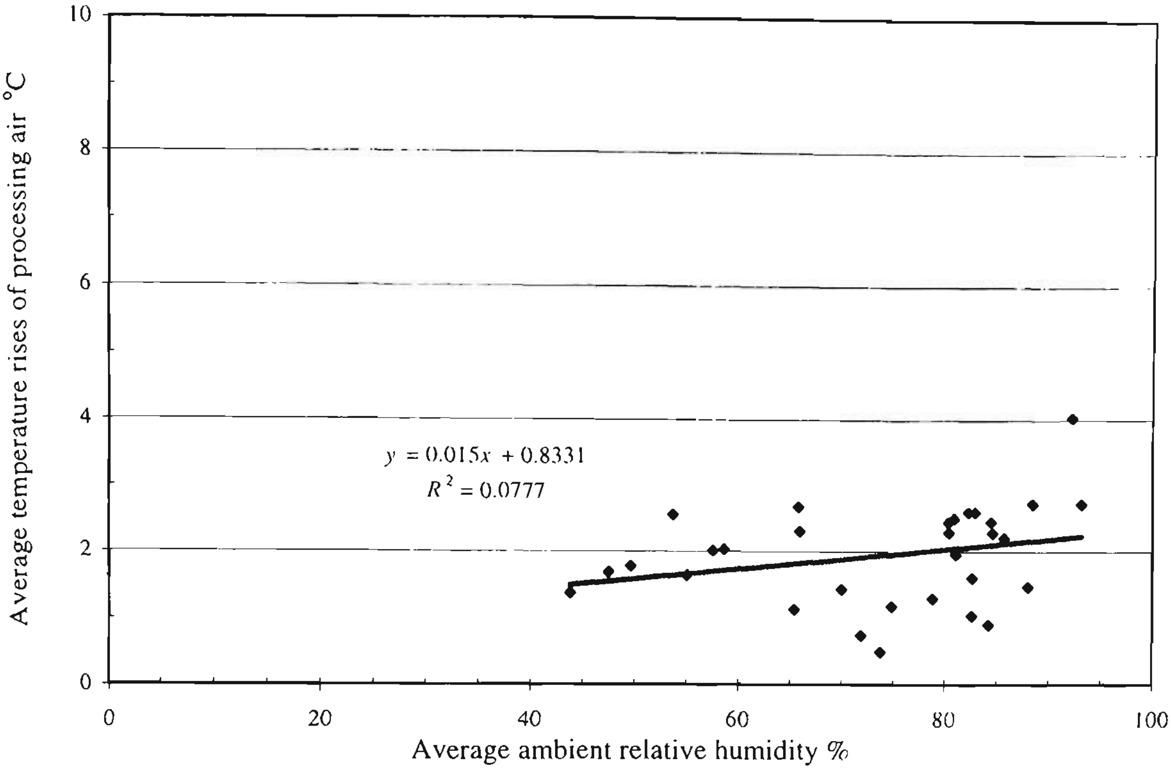

Figure 5.34 Average temperature rises of processing air versus average ambient relative humidity - six-hour cooling processes

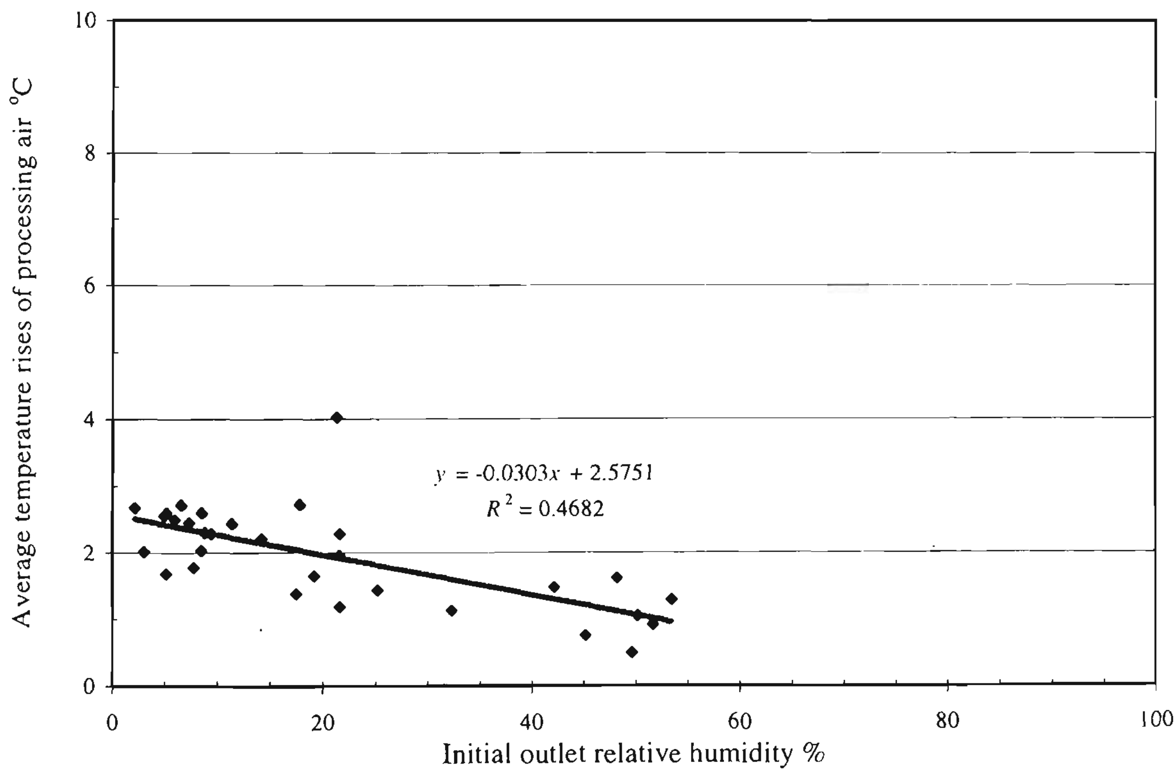

Figure 5.35 Average temperature rises of processing air versus initial outlet relative humidity - six-hour cooling processes

With a value 47% of R^2 in figure 5.35, it means that 47% of the variability in the temperature changes of the process air can be accounted for by the initial relative humidity of desiccant. This indicates that the degree of regeneration is the main reason causing the process air temperature increasing for the cooling unit. The process air temperature increased more when the desiccant was at lower moisture content.

5.4.5 Calculated conditions of the air leaving the unit

Equation (5.2) and (5.3) are the regression formula from the figures 5.30 and 5.35.

$$\Delta T_{WB_{cool}} = 0.0644\phi_{initial} - 5.5863 \tag{5.2}$$

$$\Delta T_{cool} = -0.0303\phi_{initial} + 2.5751 \tag{5.3}$$

where $\Delta T_{WB_{cool}}$ and ΔT_{cool} are the changes of average wet-bulb and dry-bulb temperatures of the process air, and $\phi_{initial}$ is the initial relative humidity of the air leaving the desiccant unit during the cooling processes.

We used equations (5.2) and (5.3) to calculate the depressions in the average wet-bulb temperatures and the rises in the average temperature of the process air during cooling processes. The results are listed in table 5.8.

Considering a example here that an ambient average wet-bulb temperature, 10.5°C, in cooling processes 5, 25, and 31, the calculated depressions of the wet-bulb temperature were 2.7°C, 5.3°C and 4.0°C, on the other hand, the corresponding experimental data points are 2. 2°C, 5.8°C and 3.6°C. We believe the equation (5.2) displayed very well the influence of desiccant regeneration degree on wet-bulb temperature reduction of process air.

The calculated results of equation (5.3) enable us to express the experimental observations that the process air temperature increases more when the desiccant has the lower moisture content.

Table 5.8 Comparison of the calculated results to recorded data for the outlet conditions of cooling processes - six-hour operation

Process	Average ambient temperature	Average ambient RH	Average ambient wet-bulb temperature	Initial outlet RH	Increase in dry-bulb temperature	Calculated increases in dry-bulb temperature	Reduction in wet-bulb temperature	Calculated reduction in wet-bulb temperature
	°C	%	°C	%	°C	°C	°C	°C
1	24.2	55.1	18.0	19.2	1.6	2.0	3.5	4.3
2	21.4	92.2	20.5	21.3	4.0	1.9	3.9	4.2
3	22.5	88.1	21.1	42.1	1.5	1.3	4.2	2.9
4	12.2	78.9	10.2	53.5	1.3	1.0	1.0	2.1
5	13.3	71.9	10.5	45.2	0.7	1.2	2.2	2.7
6	14.5	84.6	12.9	21.6	2.3	1.9	4.0	4.2
7	11.5	73.8	9.1	49.6	0.5	1.1	2.3	2.4
8	15.4	82.6	13.6	50.2	1.0	1.1	3.0	2.4
9	25.8	43.9	17.5	17.5	1.4	2.0	2.4	4.5
10	18.4	88.5	17.1	17.9	2.7	2.0	5.1	4.4
11	14.4	84.3	12.9	51.7	0.9	1.0	2.9	2.3
12	24.8	65.4	20.1	32.3	1.1	1.6	3.6	3.5
13	27.0	53.7	20.1	5.0	2.6	2.4	3.8	5.3
14	13.9	80.4	12.0	9.4	2.3	2.3	5.8	5.0
15	12.9	80.4	11.0	11.4	2.4	2.2	6.0	4.9
16	17.1	65.9	13.2	2.2	2.7	2.5	5.3	5.4
17	18.4	93.2	17.7	6.6	2.7	2.4	6.8	5.2
18	14.5	80.9	12.6	6.0	2.5	2.4	5.8	5.2
19	11.8	82.7	10.2	48.2	1.6	1.1	1.6	2.5
20	20.0	49.6	13.6	7.8	1.8	2.3	4.0	5.1
21	15.7	81.1	13.8	21.6	2.0	1.9	5.2	4.2

Table 5.8 Comparison of the calculation results to recording data for the outlet conditions of cooling processes - six-hour operation (Continued)

Process	Average ambient temperature	Average ambient RH	Average ambient wet-bulb temperature	Initial outlet RH	Increase in dry-bulb temperature	Calculated increases in dry-bulb temperature	Reduction in wet-bulb temperature	Calculated reduction in wet-bulb temperature
	°C	%	°C	%	°C	°C	°C	°C
22	15.0	85.8	13.5	14.2	2.2	2.1	5.2	5.0
23	11.4	82.3	9.8	8.6	2.6	2.3	5.7	4.2
24	9.9	74.9	7.8	21.6	1.2	1.9	4.8	5.3
25	12.1	83.0	10.5	5.2	2.6	2.4	5.8	5.1
26	12.4	84.5	11.0	7.3	2.5	2.4	5.6	5.0
27	17.2	66.0	13.4	8.9	2.3	2.3	4.8	5.4
28	16.9	57.6	12.2	3.1	2.0	2.5	4.7	5.0
29	17.6	58.7	12.9	8.5	2.0	2.3	4.8	5.3
30	18.9	47.5	12.4	5.2	1.7	2.4	3.7	4.0
31	13.4	70.0	10.5	25.2	1.4	1.8	3.6	5.0

We recommend equations (5.2) and (5.3) as the empirical formulae for simulation and prediction applications of cooling processes for the device.

5.4.6 Outlet conditions during the regeneration processes

The data presented in figures 5.36 to 5.39 show principally the conditions that obtained during the regeneration processes. However, they also indicate the conditions that obtained at the end of the cooling processes. From the graphs we can make the following generalizations:

- The relative humidity of outlet air had a pulse at the beginning of regeneration operation, and this may be due to the saturation on the top surface of desiccants or the internal surface of the device. Because the pulse only lasted very short time it would not affect the entire outlet condition much.

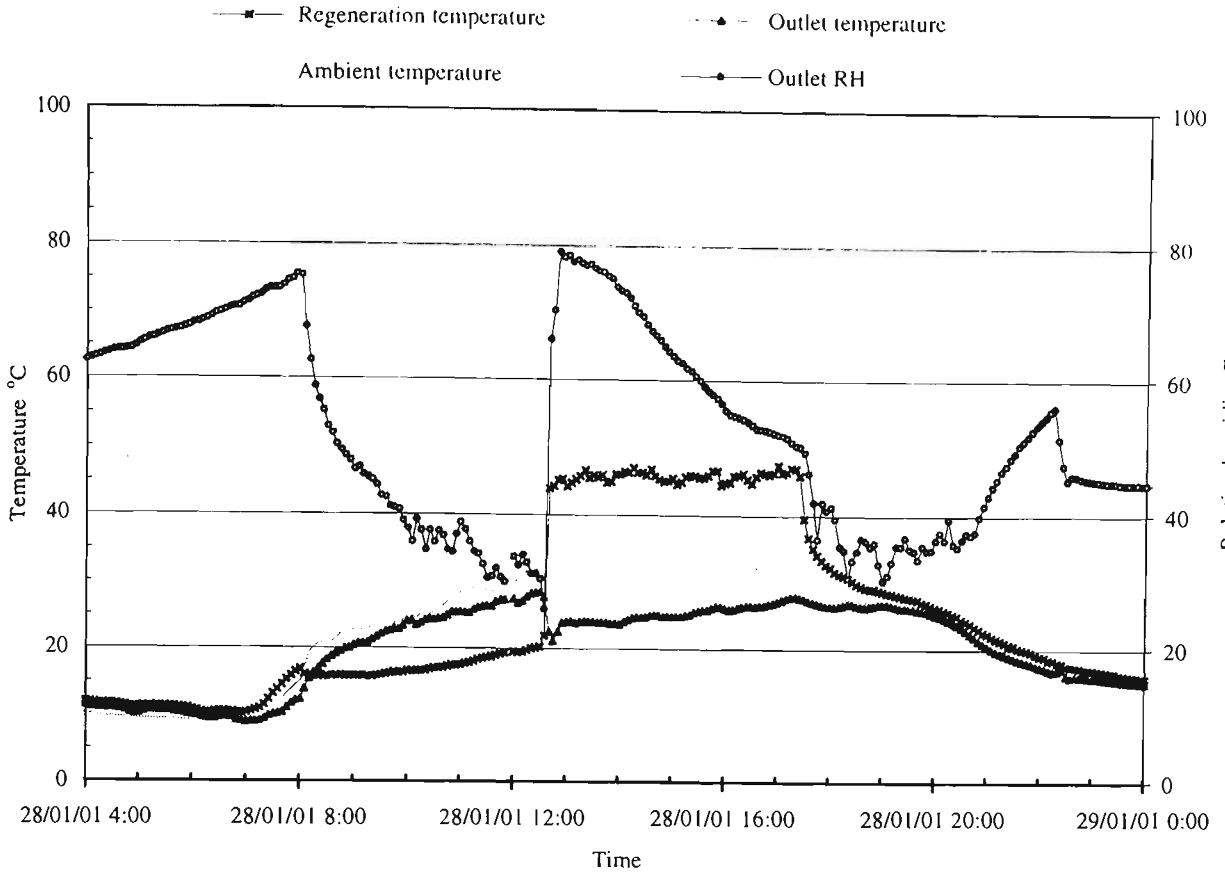

Figure 5.36 Regeneration temperature and outlet relative humidity in the regeneration process 4 (12:40 ~ 17:30 28 Jan 2001)

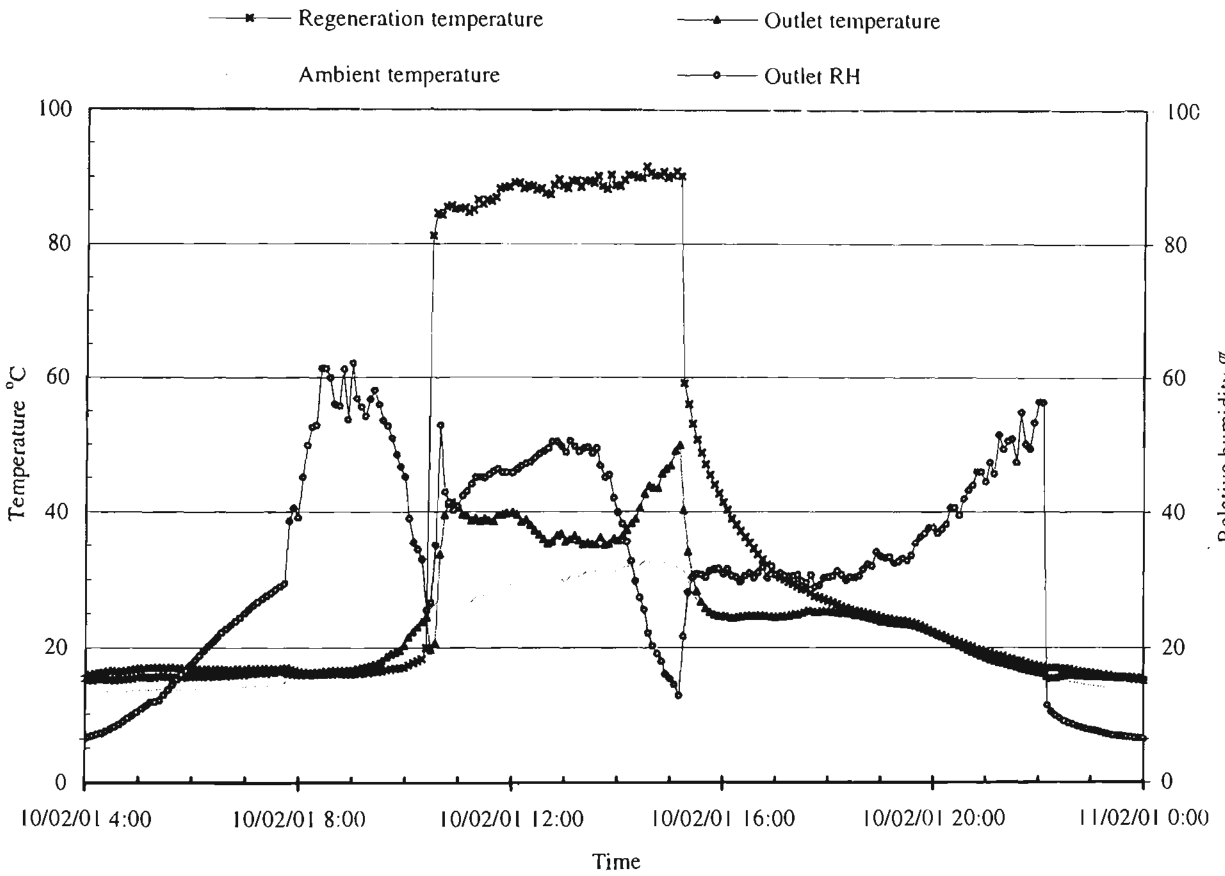

Figure 5.37 Regeneration temperature and outlet relative humidity in the regeneration process 13 (10:28 ~ 15:15 10 Feb 2001)

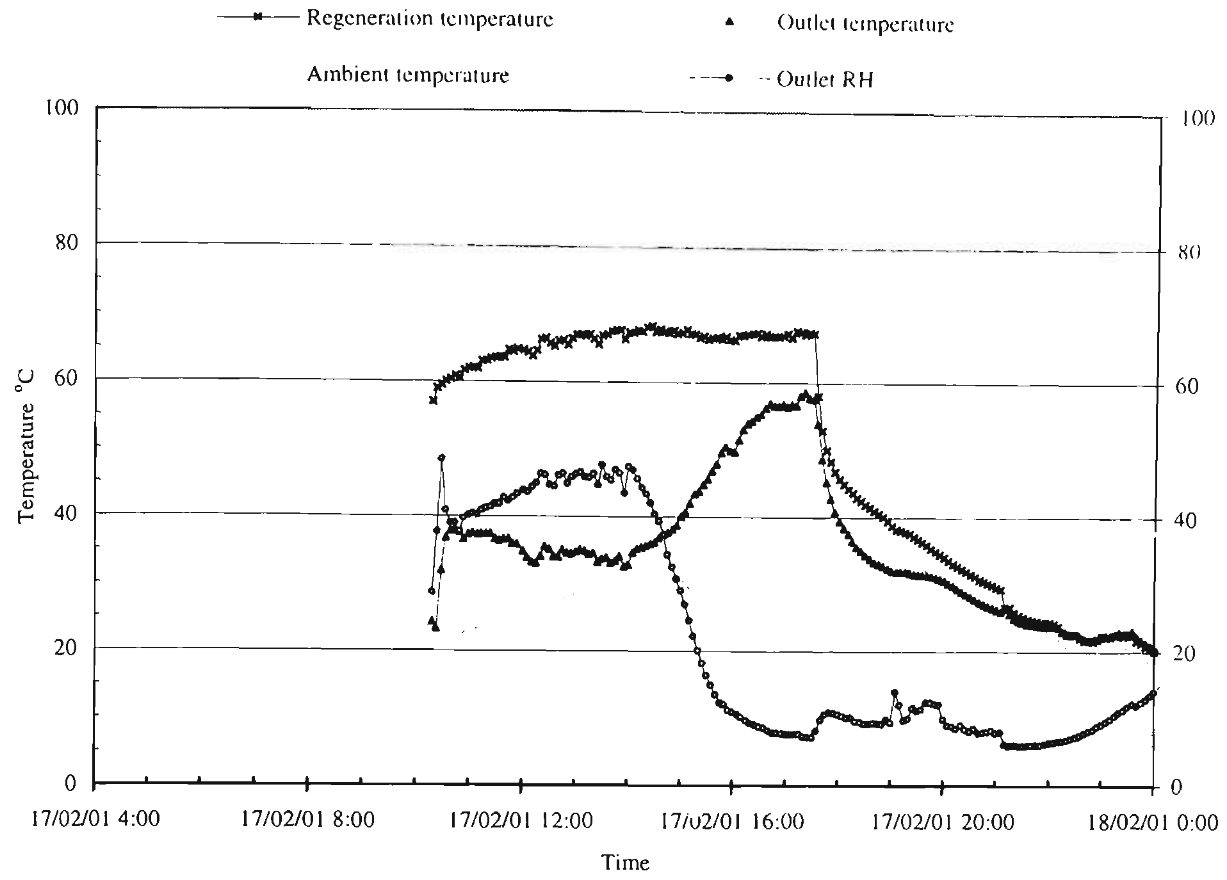

Figure 5.38 Regeneration temperature and outlet relative humidity in the regeneration process 17 (10:18 ~ 19:30 17 Feb 2001)

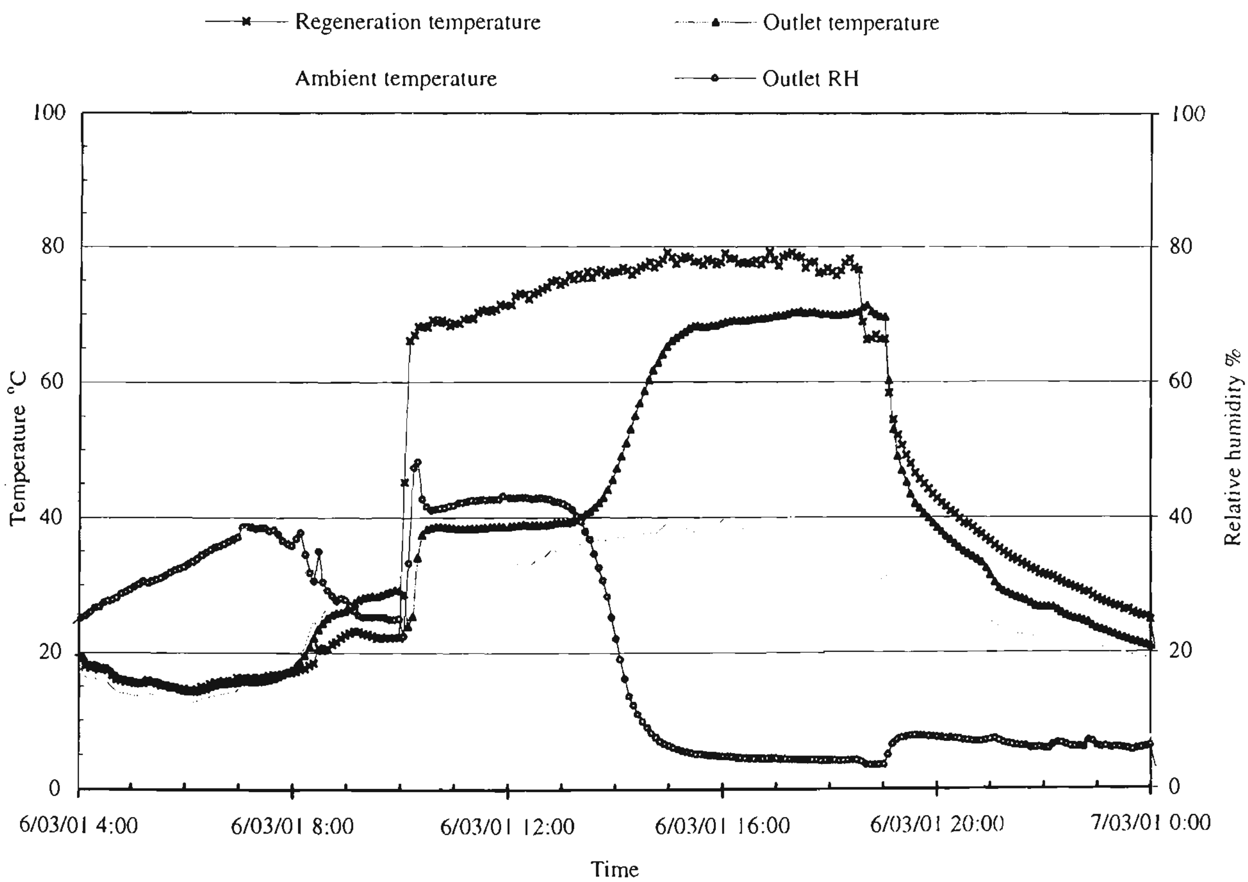

Figure 5.39 Regeneration temperature and outlet relative humidity in the regeneration process 25 (10:00 ~ 19:00 6 Mar 2001)

- The outlet relative humidity started with a higher value than the last relative humidity in the previous cooling process. This is probably because the desiccant in the lower regions of the bed had high moisture contents, but the exact mechanism is worthy of future study.
- It took a very short time, about 10 minutes, for the outlet air temperature to reach a plateau. This indicates that the temperature front (figure 5.7) was expelled at an early stage of the regeneration processes.
- The outlet temperatures remained constant, or the condition of outlet air was in Zone 3, for about 3 ~ 4 hours. This means the initial moisture front of desiccant needed 3 ~ 4 hours to move out of the device.
- Comparing with process 17 in figure 5.38 with process 13 in figure 5.37, the higher regeneration temperature the less time is required to force the initial moisture front, Zone 3, through the desiccant bed.
- When the regeneration temperature was over 60°C, once the relative humidity of outlet air started to reduce it reduced relatively quickly at the beginning and then became slowly when the values were less than 20%. This is consistent with the adiabatic drying of a porous medium.
- It took about 1 hour for the relative humidity of outlet air to reach the value 20% after it started to reduce from 40% ~ 55% when the regeneration temperature was over 60°C. It took another 1 hour for the relative humidity of outlet air to reach its minimum value *e.g.* 5%, from 20%.
- When the relative humidity of outlet air reached 5%, it remained constant and the outlet temperature was constant when the regeneration air was still supplied. It means the regeneration was completed.

5.4.7 The time taken to regenerate the desiccant

Table 5.9 shows a summary of a total 32 regeneration processes and the times taken to regenerate the desiccant. We plot the average regeneration temperatures against the average reduction in relative humidity of regeneration in figure 5.40 and the regeneration time against an average reduction in relative humidity of regeneration air in figure 5.41.

Table 5.9 Performances of regeneration processes in Ararat

Process	Date	Operating time	Regeneration time	Average regeneration temperature	Average ambient temperature	Outlet beginning RH	Outlet final RH	RH drop
			Hour	°C	°C	%	%	%
1	24-Jan-01	10:10 ~ 20:50	10.5	51.3	32.0	41.2	17.8	23.4
2	25-Jan-01	11:39 ~ 19:00	6.3	54.4	31.3	61.7	45.8	15.9
3	26-Jan-01	07:35 ~ 13:40	6.1	40.8	23.7	77.5	56.7	20.8
4	28-Jan-01	12:40 ~ 17:30	4.8	45.6	23.2	66.0	49.4	16.6
5	29-Jan-01	07:40 ~ 16:25	8.8	44.7	21.1	53.8	42.2	11.6
6	30-Jan-01	10:20 ~ 16:55	6.4	42.3	21.5	43.6	54.4	-10.8
7	2-Feb-01	08:12 ~ 19:57	11.8	51.1	30.4	42.7	18.4	24.3
8	3-Feb-01	09:42 ~ 18:10	8.5	53.2	34.1	39.2	17.4	21.8
9	6-Feb-01	08:18 ~ 18:55	10.6	57.9	31.7	60.9	32.4	28.5
10	7-Feb-01	11:40 ~ 22:05	10.4	100.1	33.5	53.6	6.2	47.4
11	8-Feb-01	11:53 ~ 18:35	6.7	82.1	35.0	53.6	23.7	29.9
12	9-Feb-01	13:26 ~ 15:48	2.4	84.8	26.5	40.3	9.6	30.7
13	10-Feb-01	10:28 ~ 15:15	4.8	87.7	22.0	26.6	21.6	5.0
14	11-Feb-01	09:55 ~ 15:26	5.5	89.9	27.9	34.8	2.6	32.2
15	12-Feb-01	09:50 ~ 17:26	7.6	76.5	29.6	39.8	9.5	30.3
16	13-Feb-01	09:31 ~ 18:00	8.5	64.2	21.2	57.2	12.1	45.1
17	17-Feb-01	10:18 ~ 17:30	7.2	65.7	28.8	28.7	7.2	21.5
18	21-Feb-01	10:00 ~ 19:00	9.0	59.2	29.0	17.2	24.2	-7.0
19	26-Feb-01	12:00 ~ 19:00	7.0	55.0	29.2	42.2	16.3	25.9
20	27-Feb-01	10:05 ~ 18:40	8.6	54.8	24.9	36.0	10.3	25.7
21	28-Feb-01	10:40 ~ 18:40	8.0	55.9	21.5	32.5	29.8	2.7
22	1-Mar-01	11:00 ~ 17:00	6.0	60.9	26.3	23.3	5.8	17.5
23	2-Mar-01	10:00 ~ 16:00	5.0	61.4	23.5	26.3	8.6	17.7
24	5-Mar-01	17:17 ~ 22:02	4.8	80.5	27.2	45.4	9.2	36.2
25	6-Mar-01	10:00 ~ 15:30	5.5	74.3	29.6	22.5	3.5	19.0

Table 5.9 Performances of regeneration processes in Ararat (Continued)

Process	Date	Operating time	Regeneration time	Average regeneration temperature	Average ambient temperature	Outlet beginning RH	Outlet final RH	RH drop
			Hour	°C	°C	%	%	%
26	7-Mar-01	10:00 ~ 16:00	6.0	67.7	31.8	29.1	4.7	24.4
27	8-Mar-01	10:00 ~ 15:30	5.5	62.1	33.8	25.5	6.0	19.5
28	9-Mar-01	11:10 ~ 16:00	5.0	55.9	31.6	30.4	12.4	18.0
29	10-Mar-01	10:00 ~ 16:00	6.0	49.0	23.5	30.6	28.4	2.2
30	11-Mar-01	10:00 ~ 17:00	7.0	55.6	21.9	30.1	5.7	24.4
31	12-Mar-01	10:00 ~ 19:00	9.0	52.4	16.5	20.4	23.9	-3.5
32	13-Mar-01	10:00 ~ 14:45	9.0	68.8	17.7	16.0	5.9	10.1

* Air flow rate 1.85 m^3/s

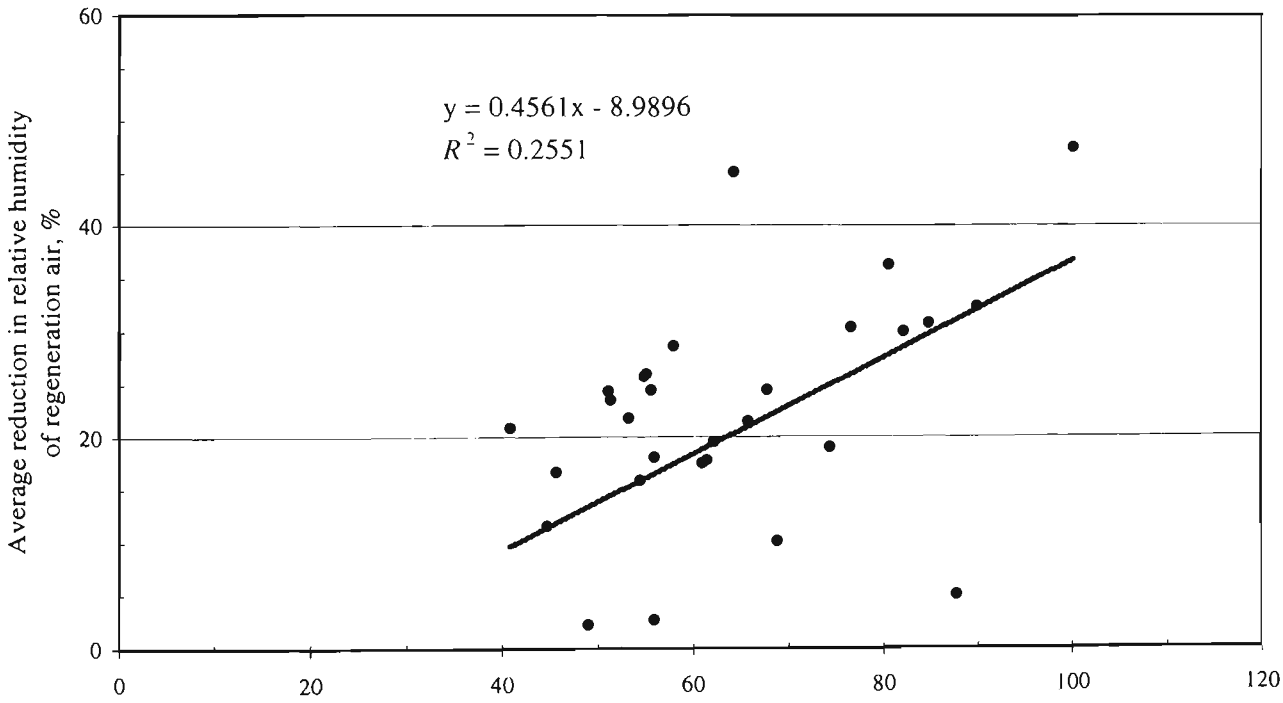

Figure 5.40 Regeneration temperature versus average reduction in relative humidity of regeneration air - regeneration processes

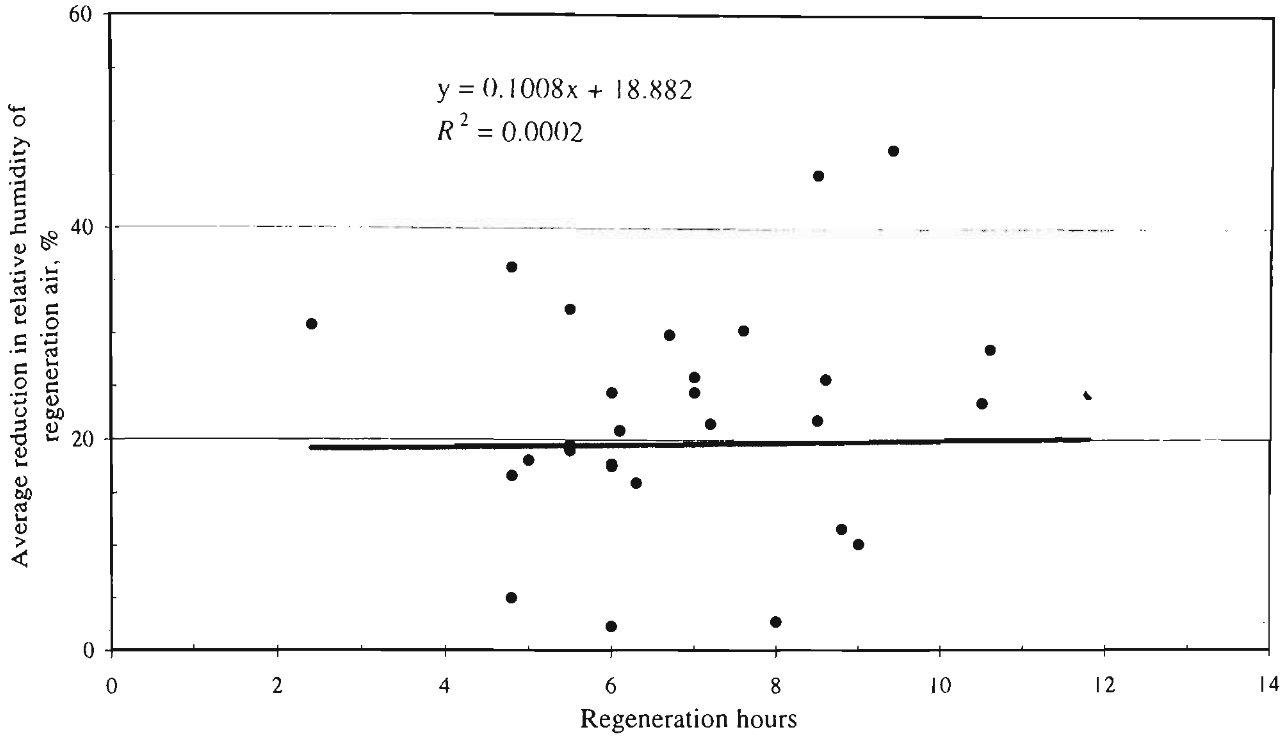

Figure 5.41 Regeneration time versus average reduction in relative humidity of regeneration air - regeneration processes

From the results of coefficient of determination, R^2, in figures 5.40 and 5.41, about 26% of the variability in average reduction in relative humidity of regeneration can be accounted for by average regeneration temperature in the experimental data region, and only 0.02% by the regeneration time.

It seemed that in the experimental data region the correlations between average reduction in relative humidity of regeneration air and regeneration temperatures or regeneration time were not so strong as the correlation results we had in cooling processes and there are no regression formulas formed for regeneration processes. A much more mechanistic on phenomenological approach to the performance of the grain cooling unit is required.

5.4.8 Cooling performance in the silos

The ultimate test of the desiccant grain cooling system is the rate and the degree with which grains can be cooled, hence, experiments were carried on silos containing wheat and canola.

From the principles of grain storage cooling described Chapter 1 and shown in figure 1.3, the process air conditions in the silo are determined principally by the wet-bulb temperature of the air and the moisture content of the grain. The process air and aerated grains should approach the average wet-bulb temperature of the aeration air. The dry-bulb temperature of the grain corresponds to intersection of the lines that govern wet-bulb temperature and the equilibrium moisture content of grain on a psychrometric chart. Basically, the grain with the lower moisture content will attain the higher dry-bulb temperature than the grain with the higher moisture content.

The wheat silo began to be loaded on 19th January 2001 and loading was completed on 20th January 2001. The initial moisture contents of wheat are listed in table 5.10 that 100 samples aggregated in order to the testing result of 10 samples. The average moisture of wheat was 9.86%. We found that the upper and lower levels of wheat with the higher moisture contents than the middle. The cooling experiment started at 22:00 22 January 2001 for the wheat silo. The total operation period lasted 54 days with 31 cooling processes and they resulted a total of 255 hours of cooling.

Table 5.10 The initial wheat moisture contents, Ararat

Sample type	Reference	Oven moisture (%) dry basis
Wheat	W1-W10	11.0
Wheat	W11-W20	10.7
Wheat	W21-W30	10.0
Wheat	W31-W40	9.7
Wheat	W41-W50	9.0
Wheat	W51-W60	8.8
Wheat	W61-W70	8.8
Wheat	W71-W80	9.6
Wheat	W81-W90	10.5
Wheat	W91-W100	10.5

* Agrifood Technology Pth Ltd

The canola silo was loaded with grains over two consecutive days beginning on 31 January 2001. The average temperature of the canola fell to 17.3°C from 28.3°C. The initial moisture contents of canola are listed in table 5.11 that 50 samples aggregated in order to the testing result of 5 samples. The average moisture content of canola was 4.1%. In table 5.11, the moisture content of the canola is highly variable. It varies from the about 5.2% at the lower levels of the silo, down to about 3.1% near the top of the silo. Near the very top, the moisture content was 5.2%.

Table 5.11 The initial canola moisture contents, Ararat

Sample type	Reference	Oven moisture (%) dry basis
Canola	C1-C10	5.2
Canola	C11-C20	4.7
Canola	C21-C30	4.6
Canola	C31-C40	3.1
Canola	C41-C50	5.1

* Agrifood Technology Pth Ltd

The operation period for the canola silo was lasted for 25 days and it was subjected to 25 cooling processes and a total of 202 hours of cooling.

To avoid confusion of the temperature-time trajectories in the silos, plotted sets of separated sets of data are shown in figures 5.42 to 5.47.

Figure 5.48 plotted the average outlet data of wet-bulb temperatures of the desiccant unit during the cooling processes. Noted that there were relatively warm periods during which the outlet of average wet-bulb temperatures in figure 5.48 were over 15°C at 26th and 27th of January 2001 and 3rd, 7th and 8th of February 2001. It is found that the features in figures 5.42 to 5.47 clearly show the passage of the cooling waves through the grains. These temporary periods of high ambient conditions were reflected in the grain temperatures. Qualitatively, and subjective quantitatively, the results reflect the degree of cooling that would be expected.

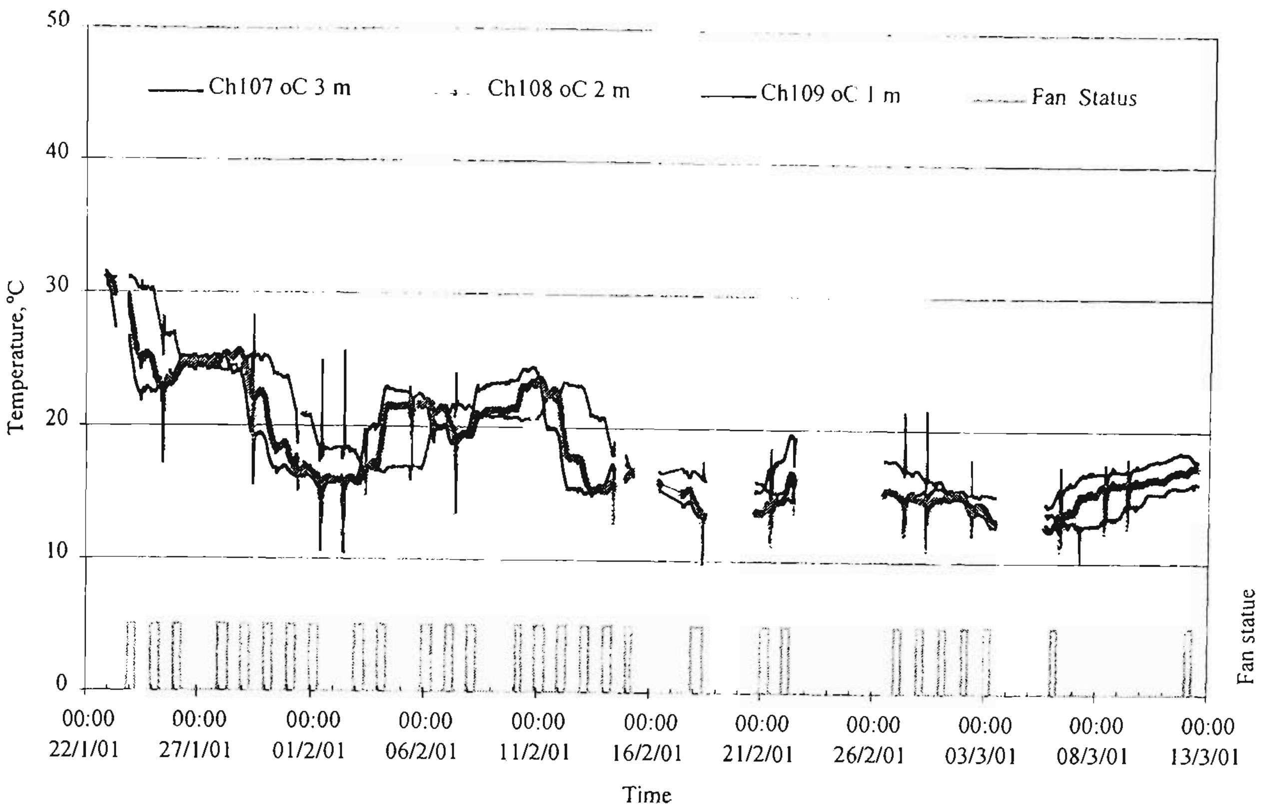

Figure 5.42 Grain temperatures at heights of 1m, 2m and 3m along the centerline of the silo containing wheat

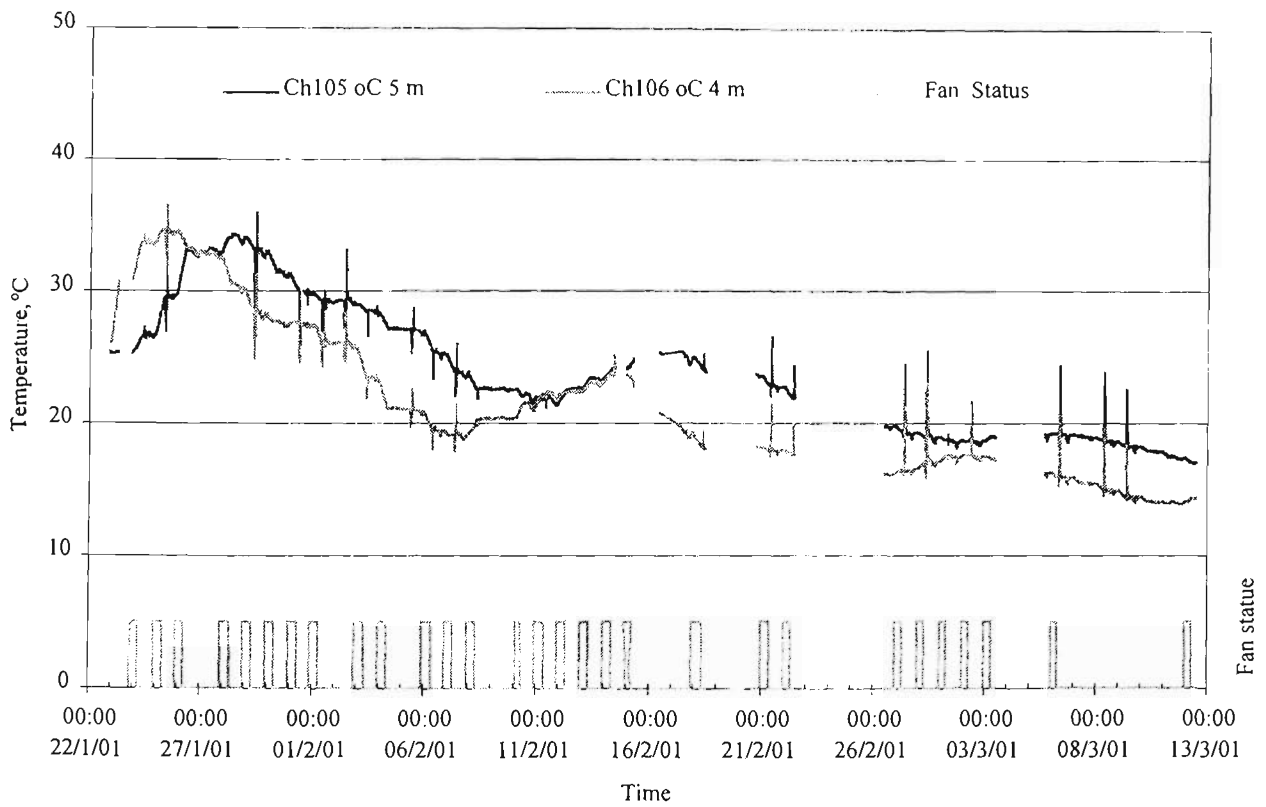

Figure 5.43 Grain temperatures at heights of 4m and 5m along the centerline of the silo containing wheat

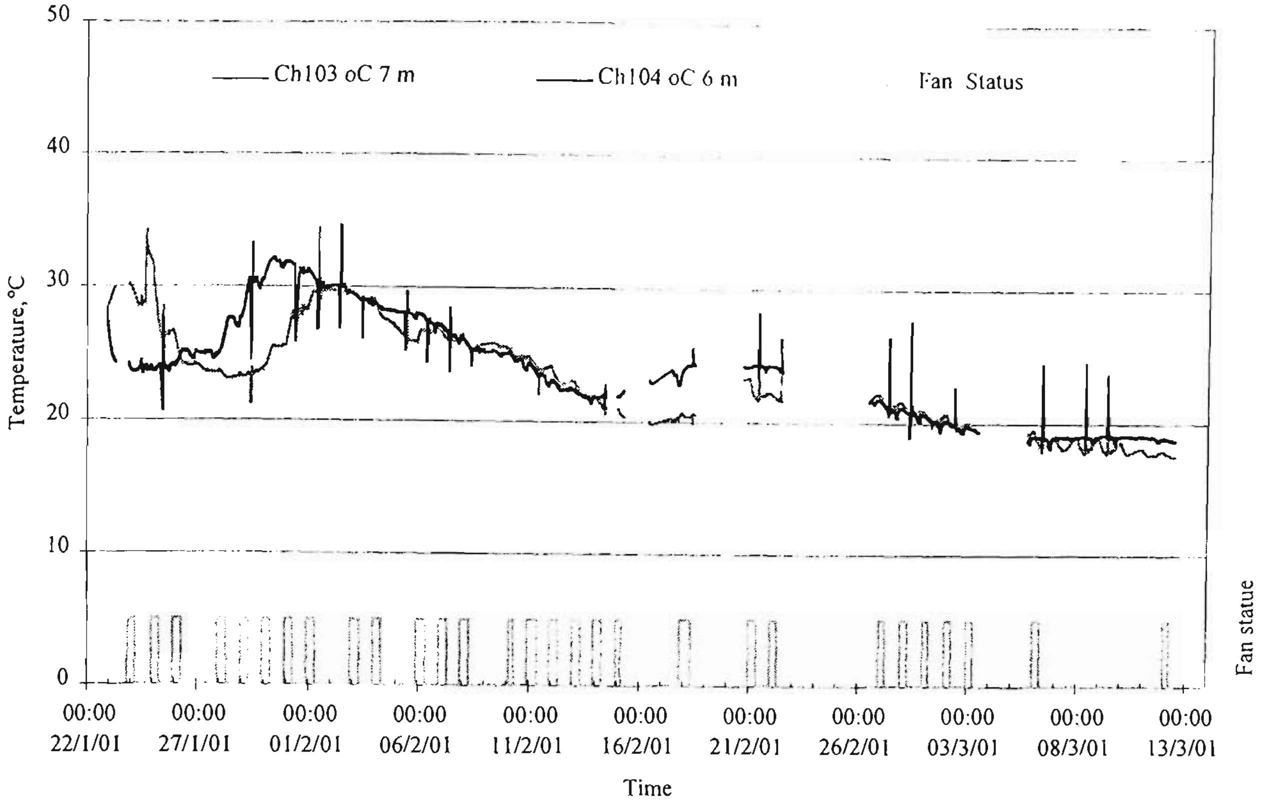

Figure 5.44 Grain temperatures at heights 6m and 7m along the centerline of the silo containing wheat

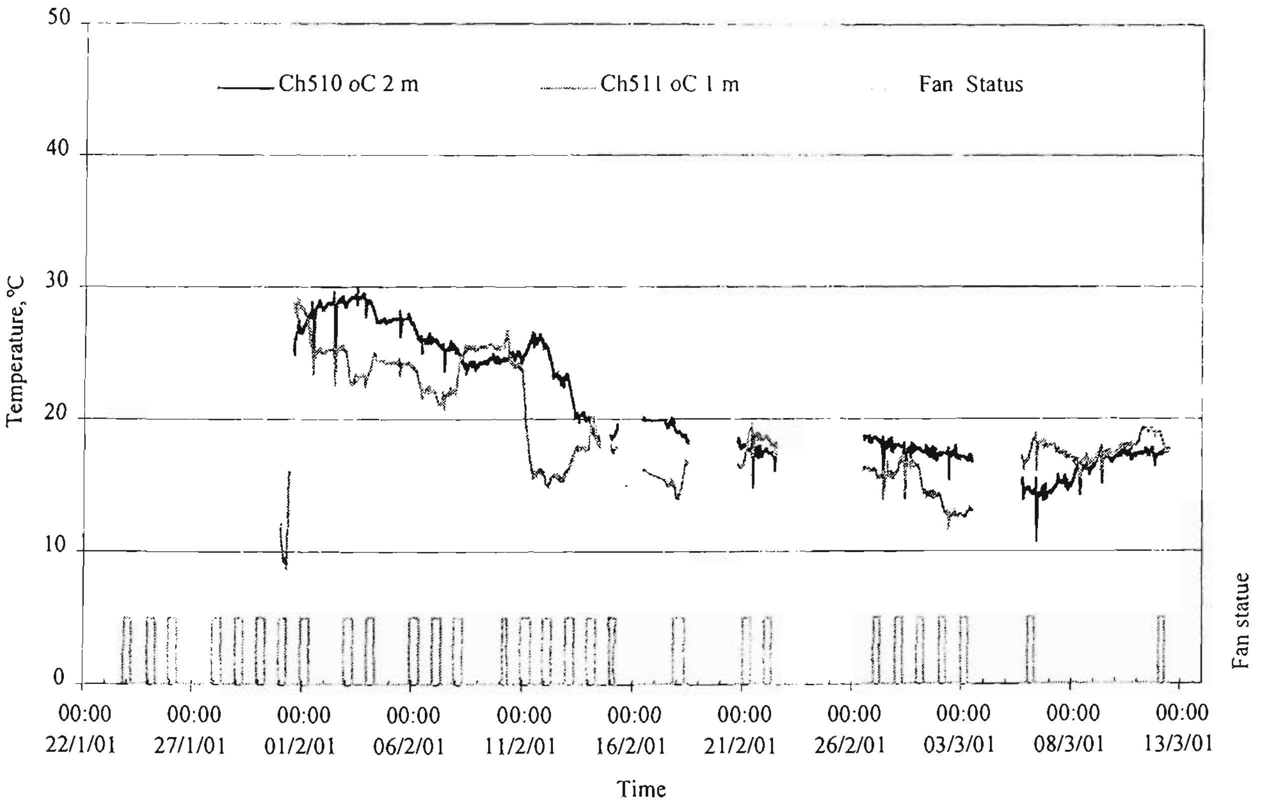

Figure 5.45 Grain temperatures at heights of 1m and 2m along the centerline of the silo containing canola

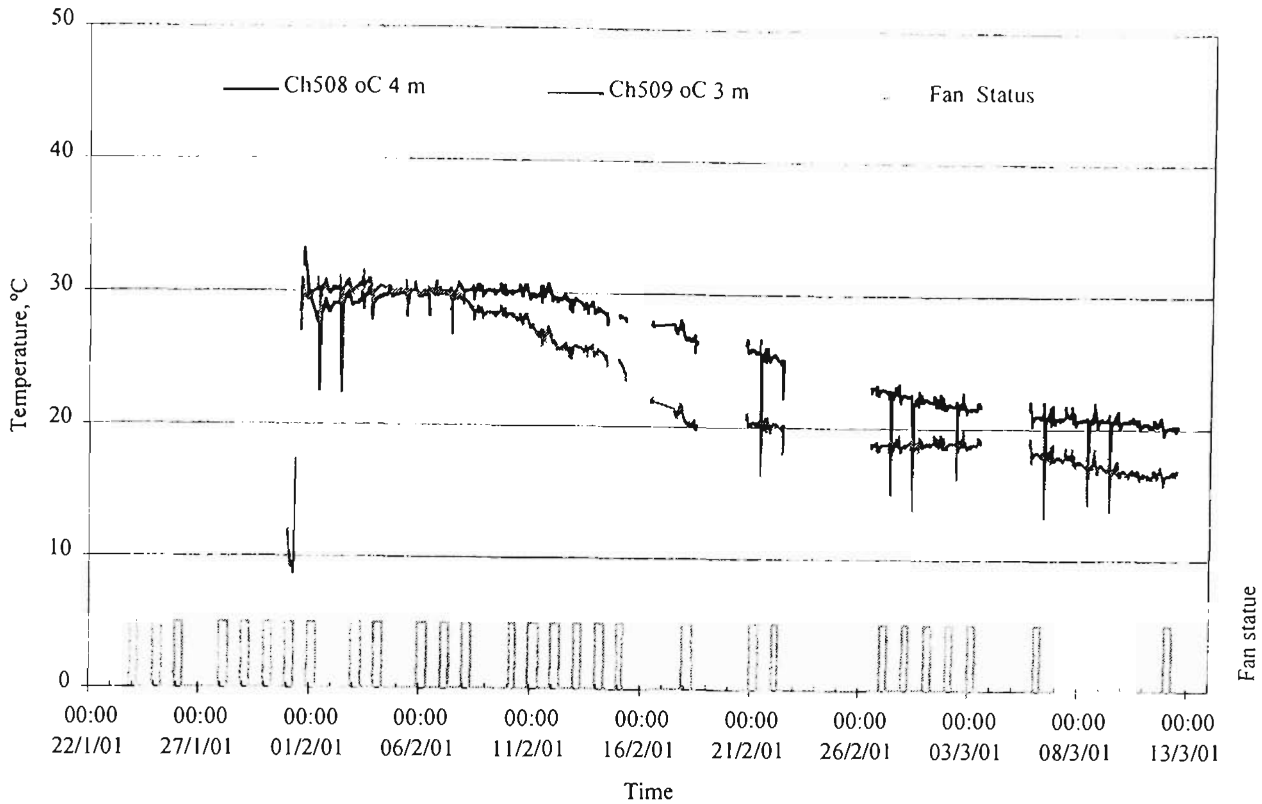

Figure 5.46 Grain temperatures at hights of 3m and 4m along the centerline of the silo containing canola

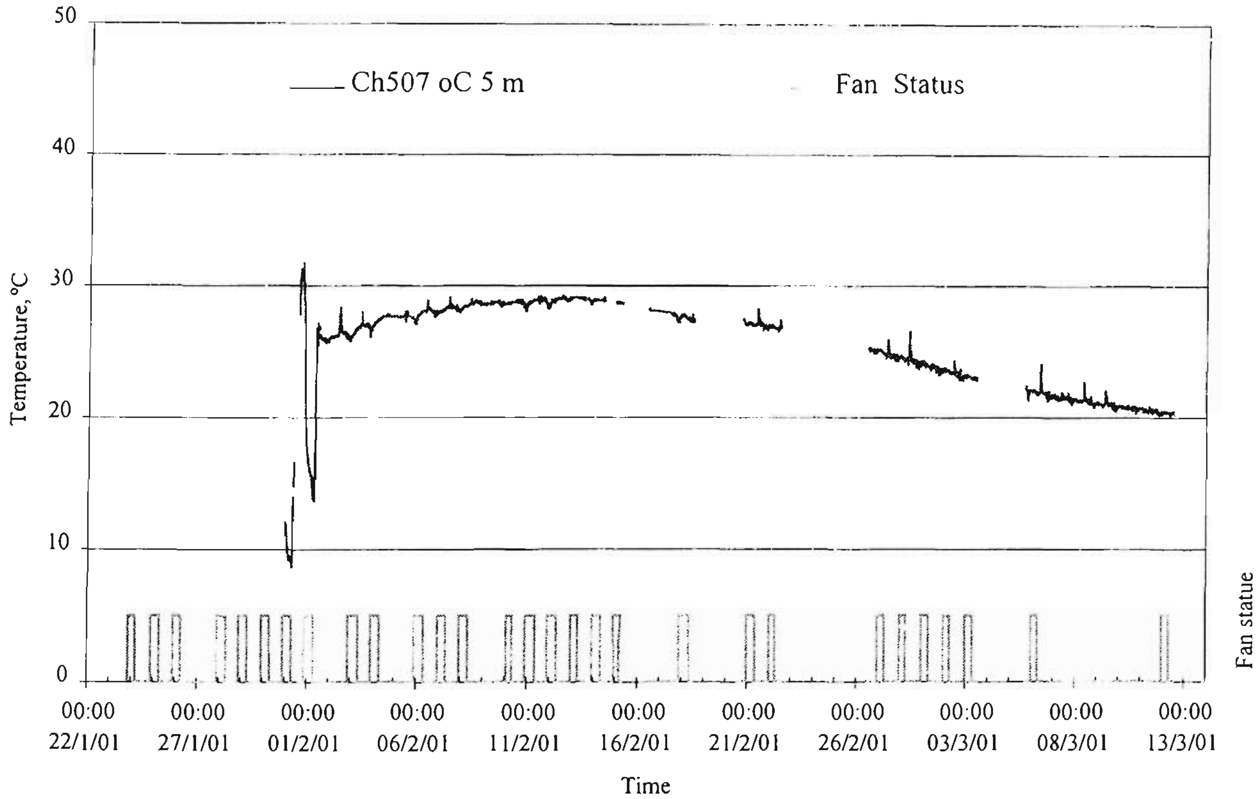

Figure 5.47 Grain temperatures at height of 5m along the centerline of the silo containing canola

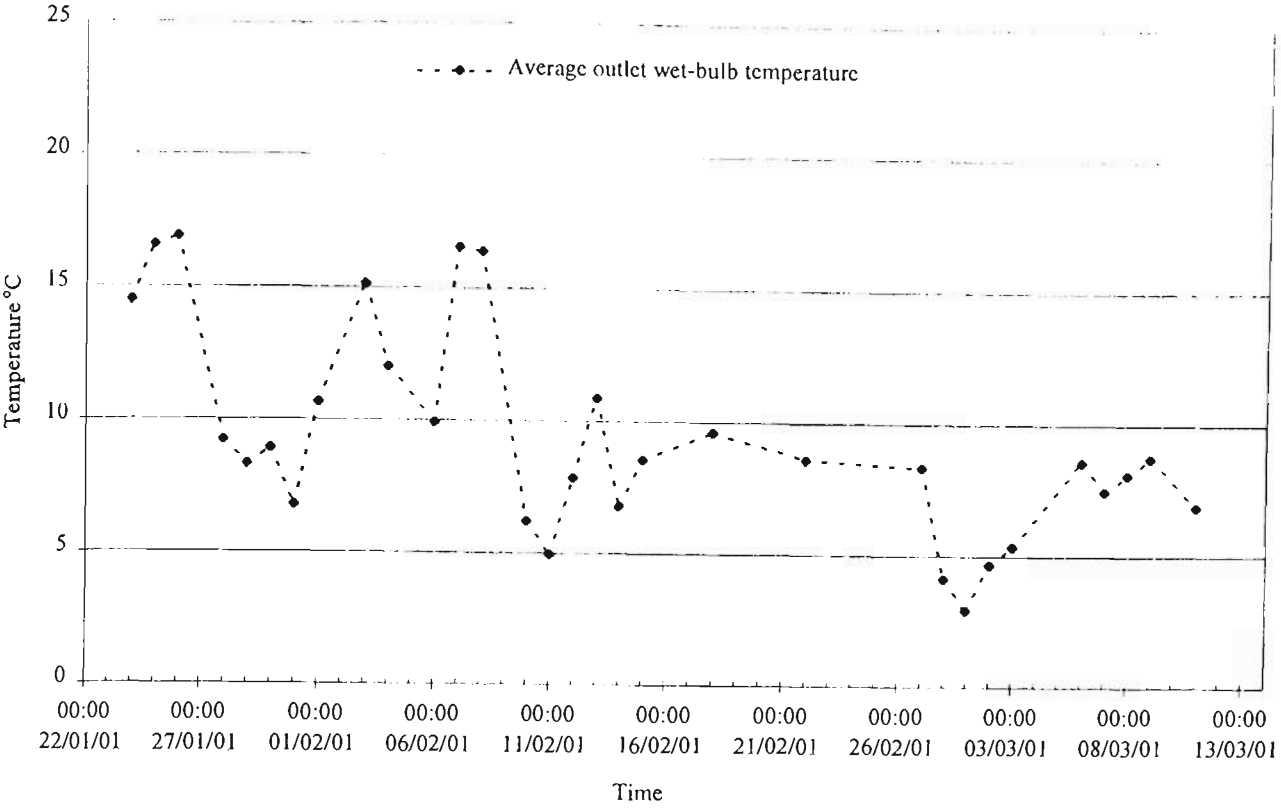

Figure 5.48 Average outlet wet-bulb temperatures of the desiccant unit at cooling processes

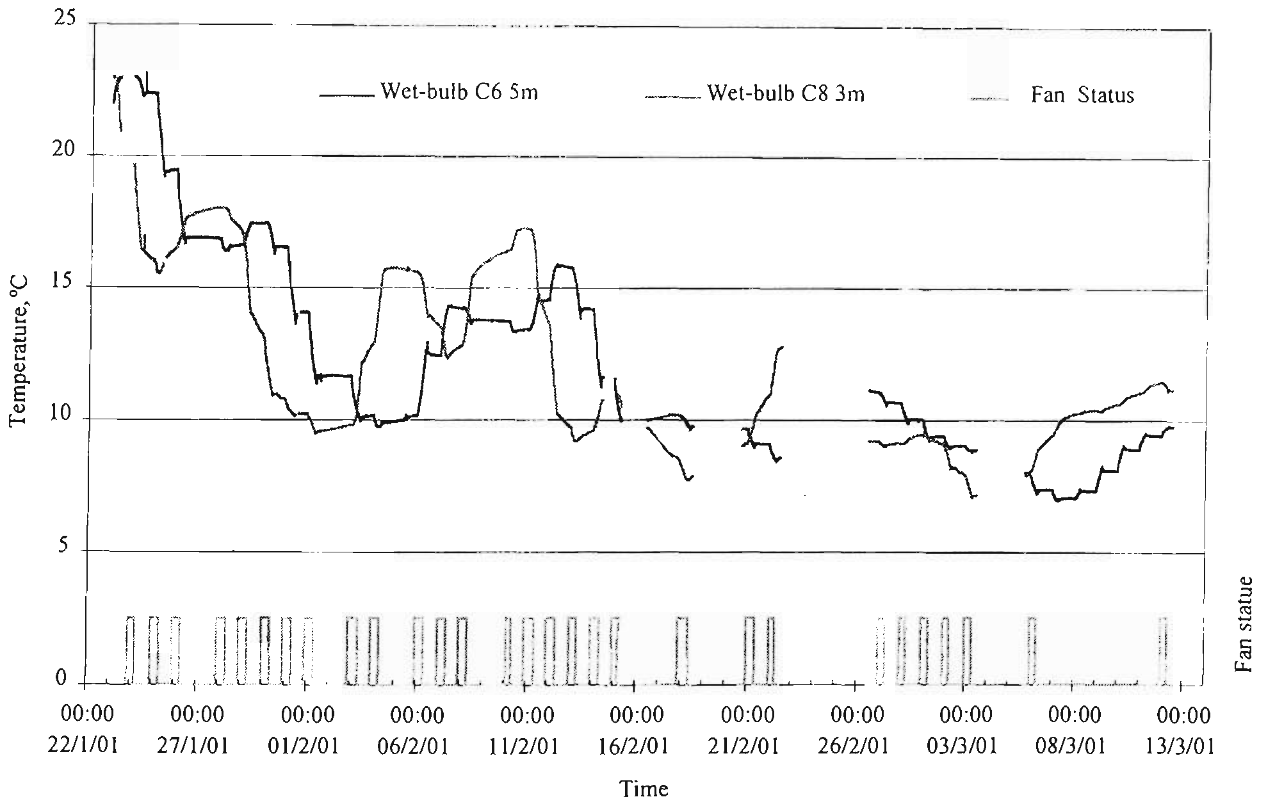

Figure 5.49 Grain wet-bulb temperatures at heights of 3m and 5m along the centerline of the silo containing wheat

We also noted that both wheat and canola that are at 1m high from the base of the silo responds most rapidly to the conditions of the inlet air, as shown in figure 5.48. The rate of response to the inlet air decreases with distance from the base of the silo, and the trend of inlet conditions is smoothed.

In figure 5.49, we plot the wet-bulb temperatures at 5m and 3m along centerline of wheat silo that the grain wet-bulb temperature calculated from the measured data by temperature and relative humidity sensors. The sensor of humidity and temperature transmitter at 7m developed a fault during the experiment so the results for the wet-bulb temperature are not reported here.

Comparing with the plots in figure 5.48, the wet-bulb temperatures of wheat in figure 5.49 captures the outlet trends of cooling unit well. The wet-bulb temperatures of the intergranular air near the top of the grain bulk are higher than those leaving the unit. One reason for this may be the ingress of heat through bulks of the silo and there is a delay between the conditions of the air at the base of silo and that at the top.

The average temperature of wheat fell to 17°C from its initial value 28°C and the average temperature of canola fell to 17.3°C from 28.3°C. The maximum reduction of wheat wet-bulb temperatures at heights 3m and 5m reached 15°C from its initial value, 22.5°C. However, re-warming features appeared in the both wheat and canola silos. This was caused by a sub-optimal operation schedule of the cooling unit that could not capture the coolest time during experimental period.

5.5 Calculations and future study

The experimental studies reported in this thesis have highlighted the fact that the desiccant cooling system does reduce the wet-bulb temperature of ambient air. Most importantly, this is reflected in the lower wet-bulb temperature of the intergranular air in the silos. Empirical relationships that describe the performance of the desiccant cooling system have been developed, but in future it is essential that this work be refined. It is therefore proposed that the research may be progressed by

- Formulating detailed mathematical models of the cooling device. This would permit design variables such as the widths of the desiccant beds and cooling channels to be changed, and their effects on performance to be evaluated;

- Devising new control algorithms to minimize the increasing grain temperature during periods of the warm weather.

CHAPTER 6

SIMULATION STUDY

In the previous five chapters, we have described the studies of mathematical modelling and field testing of the new cooling unit. In this chapter, we investigate a better control strategy for the desiccant cooling system by using the time-proportioning algorithm. The cooling degrees in the silos are calculated with the mathematical model.

According to the conclusions of chapter 4, the calculated grain temperatures had the poor agreement with the recorded data at wall boundary of the silo. We could use the measured values of the surface temperatures of the wall and the headspace but the variables selected in this prediction study with the mathematical model are only along the centerline in both silos. Those are regarded as being indicative of the overall performance of the cooling system, particularly for large bulks of grain. The initial conditions and ambient conditions of the field experiments are used in the study. The outlet conditions of the novel desiccant cooling during cooling trials were calculated with equations (5.2) and (5.3) and the results of the calculation represented the duct inlet conditions when the cooling fan was on.

6.1 Experimental simulation

To ensure that the calculated grain temperatures agree with the recorded experimental data points, the simulation of the experimental results with the mathematical model is the first process in this exercise on control strategies.

6.1.1 Simulated grain temperatures for the wheat silo

The initial conditions in the wheat silo are listed in table 6.1. The measured ambient conditions were used as the boundary conditions in the simulation process. The principal simulation positions selected were along the central line at the 3m, 5m and 7m heights that represented the grain condition at lower, middle and upper levels in the silo. In figure 6.1, to 6.3 we plot the simulation results comparing with the recorded data from the field experiments. It is clear that all of three simulation plots captured the experimental trends well.

Table 6.1 The initial temperature and moisture contents of wheat silo

Grid point	Height of grid point m	Temperature °C	Moisture content wet bases
1	0.00	26.75	11.0
2	0.25	26.75	11.0
3	0.76	26.23	11.0
4	1.26	26.23	11.0
5	1.77	29.65	10.7
6	2.27	29.65	10.7
7	2.77	31.19	10.0
8	3.28	31.19	10.0
9	3.78	30.96	9.0
10	4.29	30.96	9.0
11	4.79	25.45	11.0
12	5.30	25.45	11.0
13	5.80	24.29	8.8
14	6.31	24.29	8.8
15	6.81	30.29	9.6
16	7.32	30.29	9.6
17	7.82	25.39	10.5
18	8.33	25.39	10.5
19	8.58	25.13	10.5

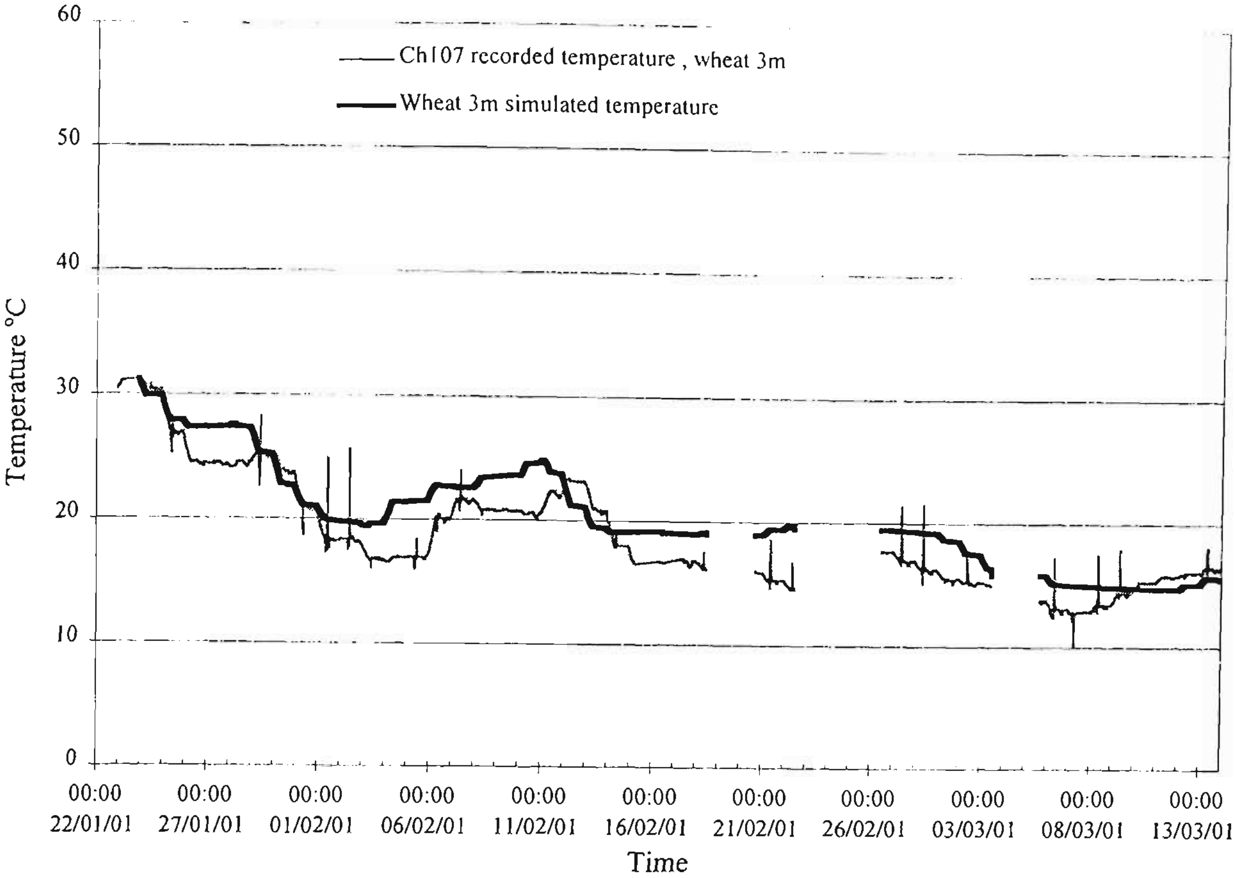

Figure 6.1 Simulated grain temperatures compared with the experimental recorded data at the height 3m along the centreline of wheat silo

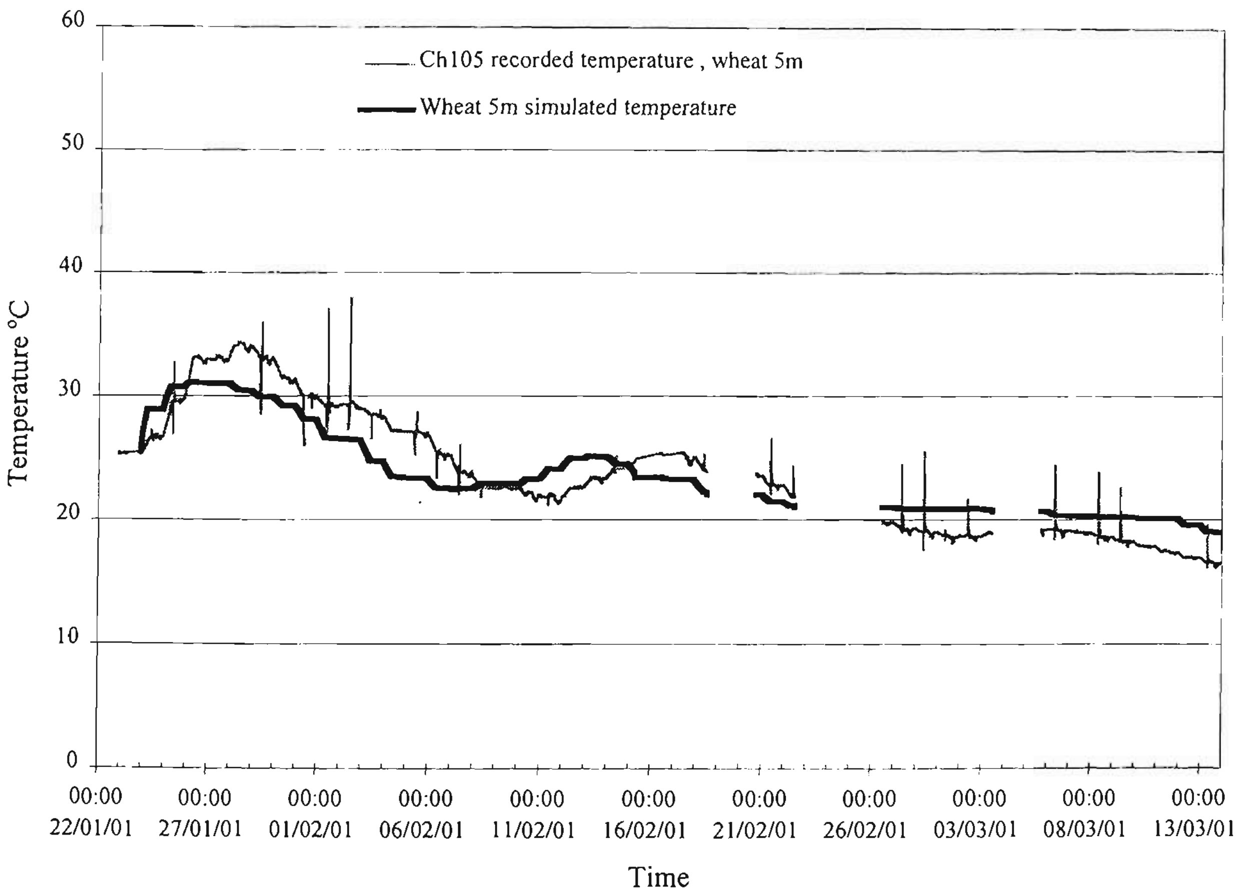

Figure 6.2 Simulated grain temperatures compared with the experimental recorded data at the height 5m along the centreline of wheat silo

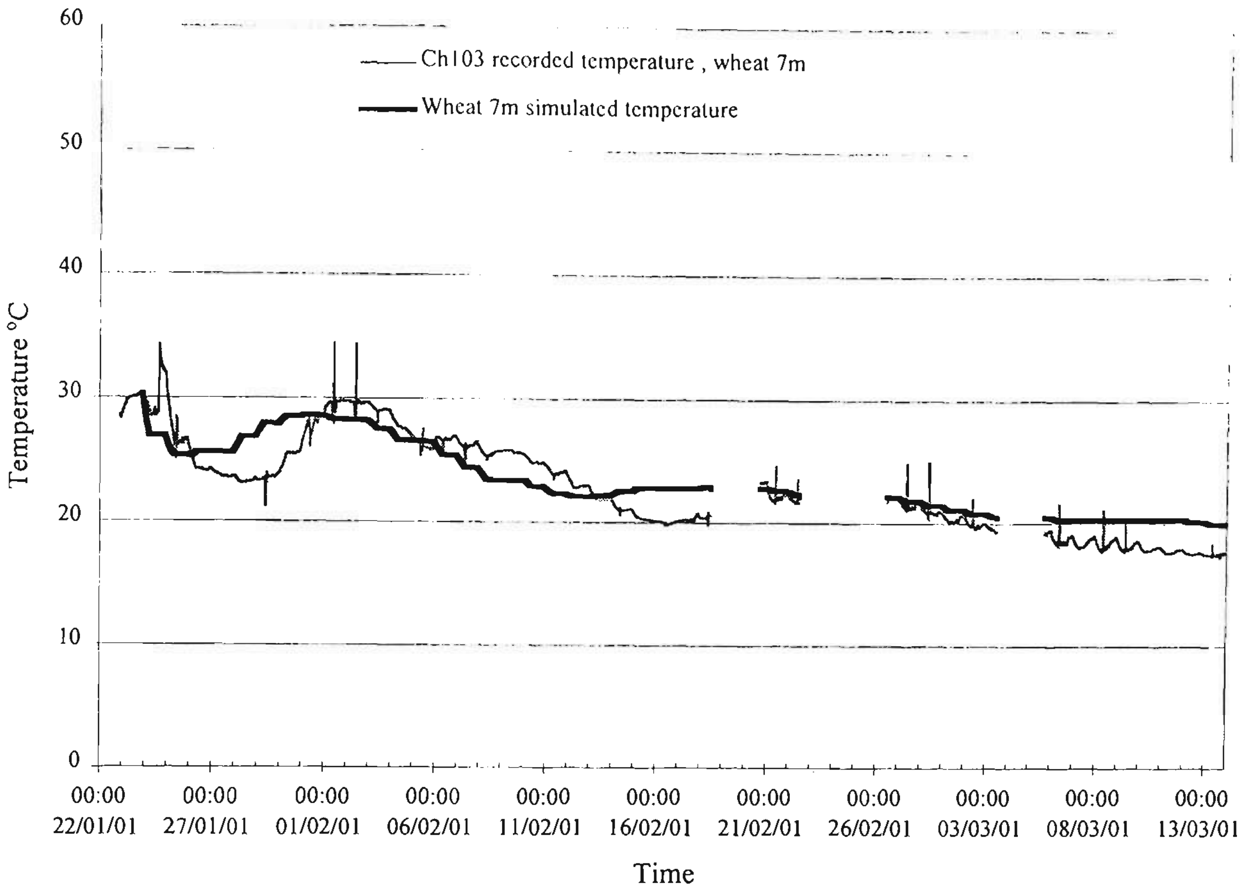

Figure 6.3 Simulated grain temperatures compared with the experimental recorded data at the height 7m along the centreline of wheat silo

The following features are observed from figures 6.1 to 6.3:

- The ranges of simulation temperatures are smaller than the experimental data ranges in those three levels of grains.
- In the middle and upper levels the trends of simulation temperatures occur earlier than the recorded temperatures.
- The simulations temperatures in the middle and upper levels do not decrease as fast as the recorded data in the last ten days of the experiment.
- The recorded grain temperatures changed slightly in all three levels during the days of no operation. However, the simulation indicated that the grain temperatures remained constant on those days.

6.1.2 Simulated grain temperatures for the canola silo

The initial conditions of canola silo are listed in table 6.2. The ambient condition of experimental recording was used as the boundary conditions in the simulation processing.

The principal simulation positions selected are along the central line at the heights of 1m, 3m and 5m from the bottom of the silo. In figures 6.4, 6.5 and 6.6 the simulation results comparing with the recorded data are plotted.

Table 6.2 The initial temperature and moisture contents of canola silo

Grid point	Height of grid point m	Temperature °C	Moisture content wet bases
1	0.00	25.22	5.2
2	0.18	25.22	5.2
3	0.52	25.22	5.2
4	0.88	25.22	5.2
5	1.23	25.22	5.2
6	1.58	28.06	4.7
7	1.93	28.06	4.7
8	2.28	28.06	4.7
9	2.63	29.88	4.6
10	2.98	29.88	4.6
11	3.33	29.88	4.6
12	3.69	27.97	3.1
13	4.04	27.97	3.1
14	4.39	27.97	3.1
15	4.75	26.83	5.1
16	5.10	26.83	5.1
17	5.45	32.12	5.1
18	5.80	32.12	5.1
19	5.96	32.12	5.1

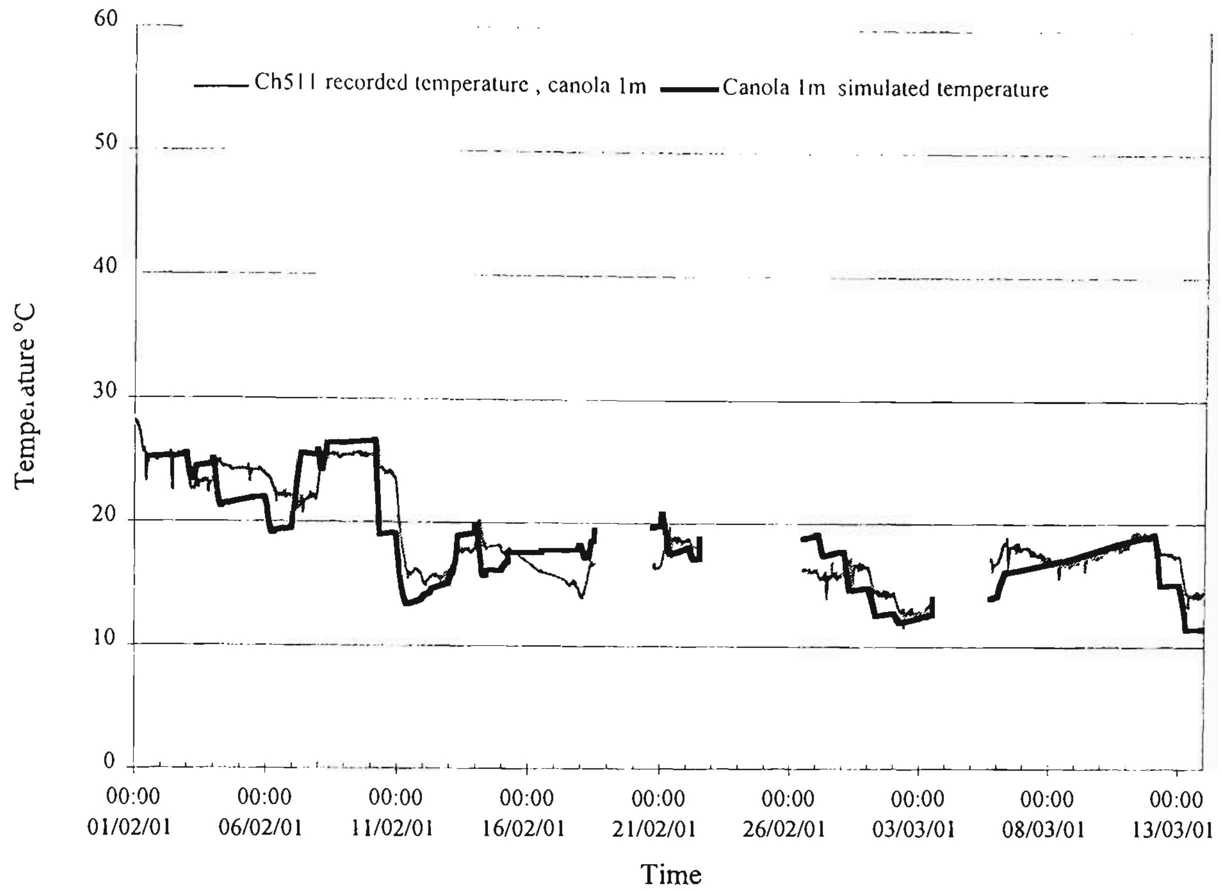

Figure 6.4 Simulated grain temperatures compared with the experimental recorded data at the height 1m along the centreline of canola silo

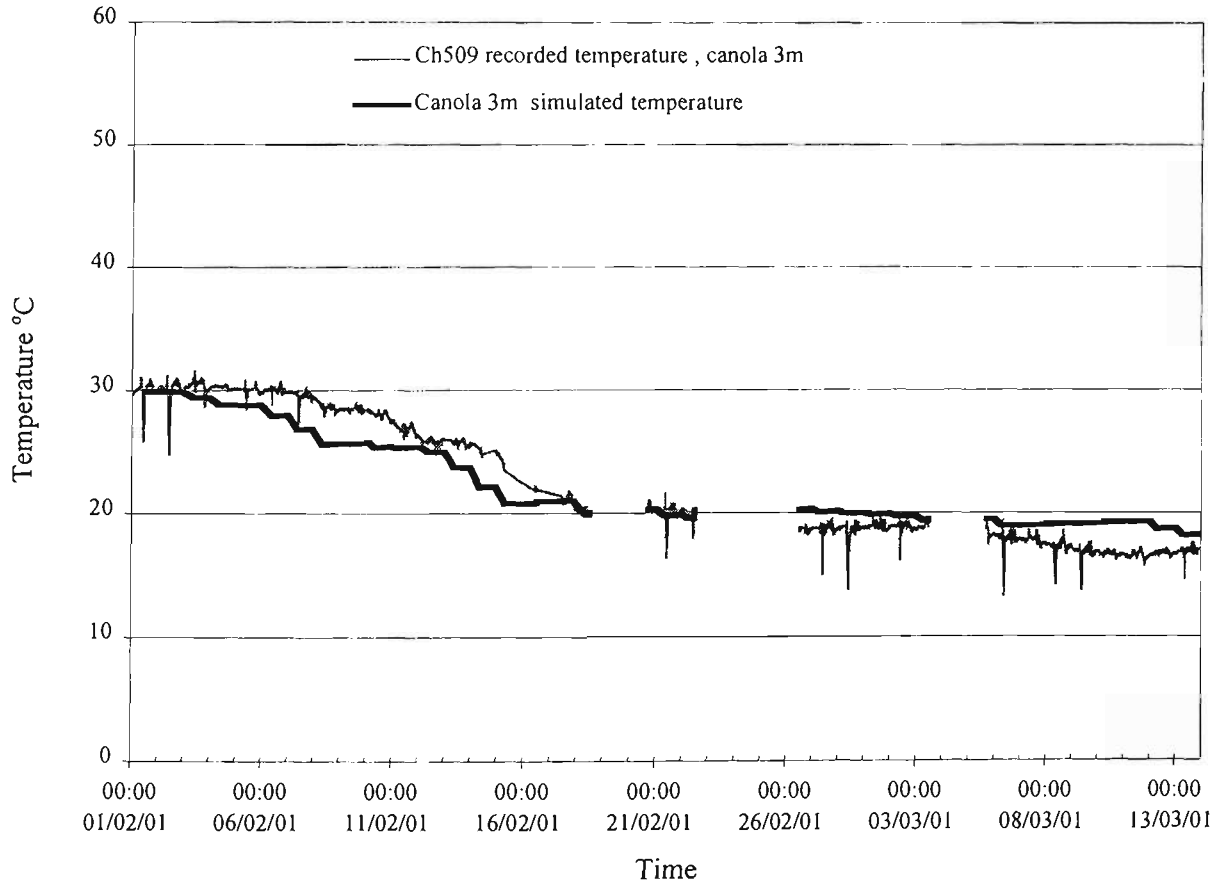

Figure 6.5 Simulated grain temperatures compared with the experimental recorded data at the height 3m along the centreline of canola silo

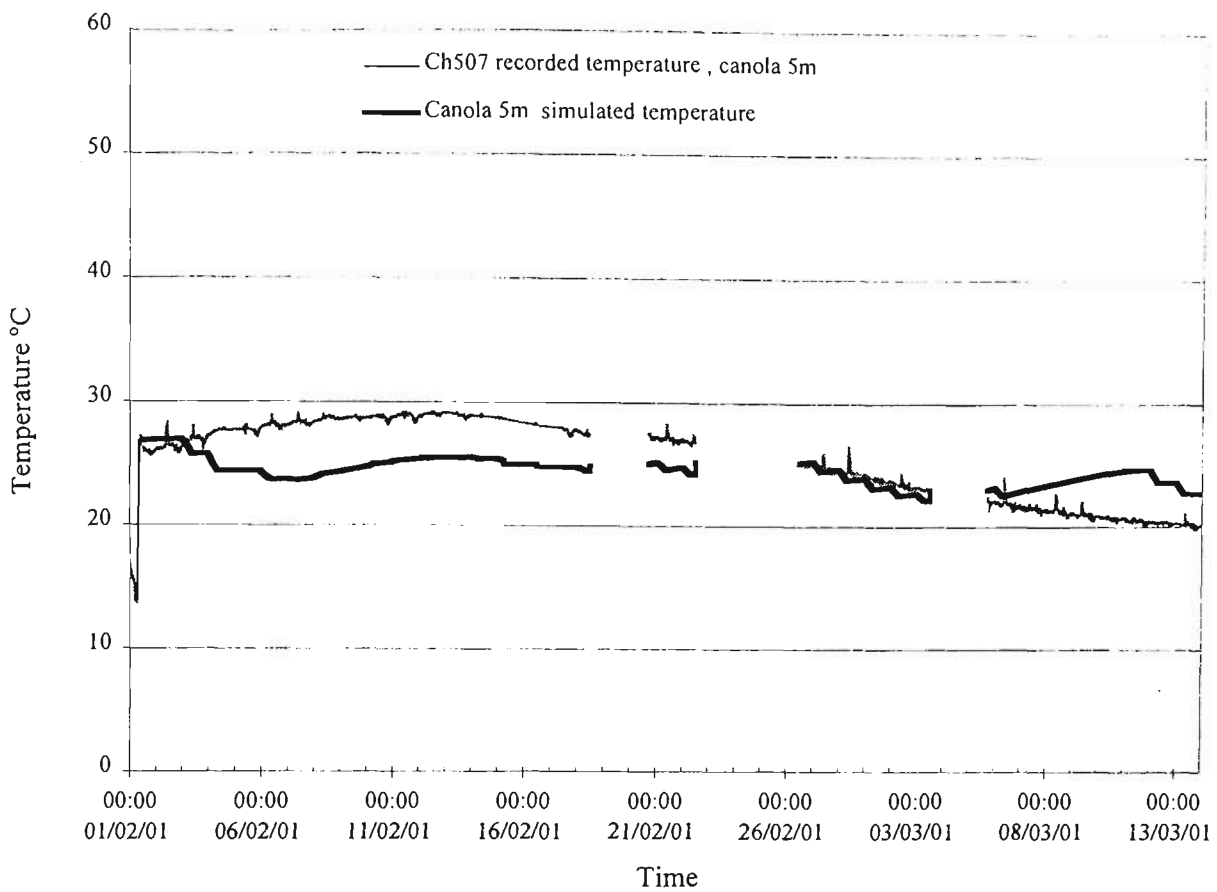

Figure 6.6 Simulated grain temperatures compared with the experimental recorded data at the height 5m along the centreline of canola silo

The comparisons of the simulation results and recorded experimental data allow us to draw the following conclusions:

- There are a few trends of experimental recorded temperatures in the lower level are not captured by the simulation plots.
- The ranges of simulation temperatures in the middle and upper levels are smaller than the recorded data.
- The simulation temperatures in the upper level do not follow the plots of recorded data very well.
- Compared with the steady simulation temperatures during the days of no operations the recorded grain temperatures slightly changed.

6.2 Simulated grain temperatures with calculated conditions of the air leaving the desiccant system

6.2.1 Calculated conditions of the air leaving the desiccant system during the cooling processes

In previous chapter we obtained the following empirical formulae to calculate the average outlet of desiccant system during the cooling processes

$$\Delta T_{WB_{cool}} = 0.0644\phi_{initial} - 5.5863 \tag{5.2}$$

$$\Delta T_{cool} = -0.0303\phi_{initial} + 2.5751 \tag{5.3}$$

where $\Delta T_{WB_{cool}}$ and ΔT_{cool} are the changes of wet-bulb and dry-bulb temperatures of the process air after cooling processes, and $\phi_{initial}$ is the initial relative humidity of the air leaving the desiccant unit during the cooling processes.

In this section we use this set of formulae to simulate the conditions of the air leaving the desiccant system during the cooling process. The calculated results are used as the inlet of the duct instead of the recorded data when the fan is on. The average relative humidity of the air leaving the cooling system was taken to be 25%. This relative humidity also indicted the average degree of regeneration of the desiccant.

The conditions of the air leaving the desiccant system were calculated by using equations (5.2) and (5.3). However, under some conditions those equations predicted relative humidity of the air leaving the system that were beyond possible physical bounds. When this occurred a relative humidity of the air of 25% was assumed. Furthermore, according to the mechanics of the desiccant, it is impossible to produce the air with a smaller relative humidity than the degree of regeneration of the desiccant. Similarly, a relative humidity of the air of 25% was assumed when the predicted relative humidity of the air leaving the system was smaller than 25%.

6.2.2 Simulated grain temperatures with the calculated condition of the air leaving desiccant system

In figures 6.6 to 6.12, the calculated grain temperatures in both wheat and canola silos are plotted. It is shown that the calculated grain temperatures agree with the recorded data plots very well. Hence, the empirical formulae (5.2) and (5.3) combined with the degree of regeneration of the desiccant can be used to calculate the condition of the air leaving the desiccant system during the cooling processes.

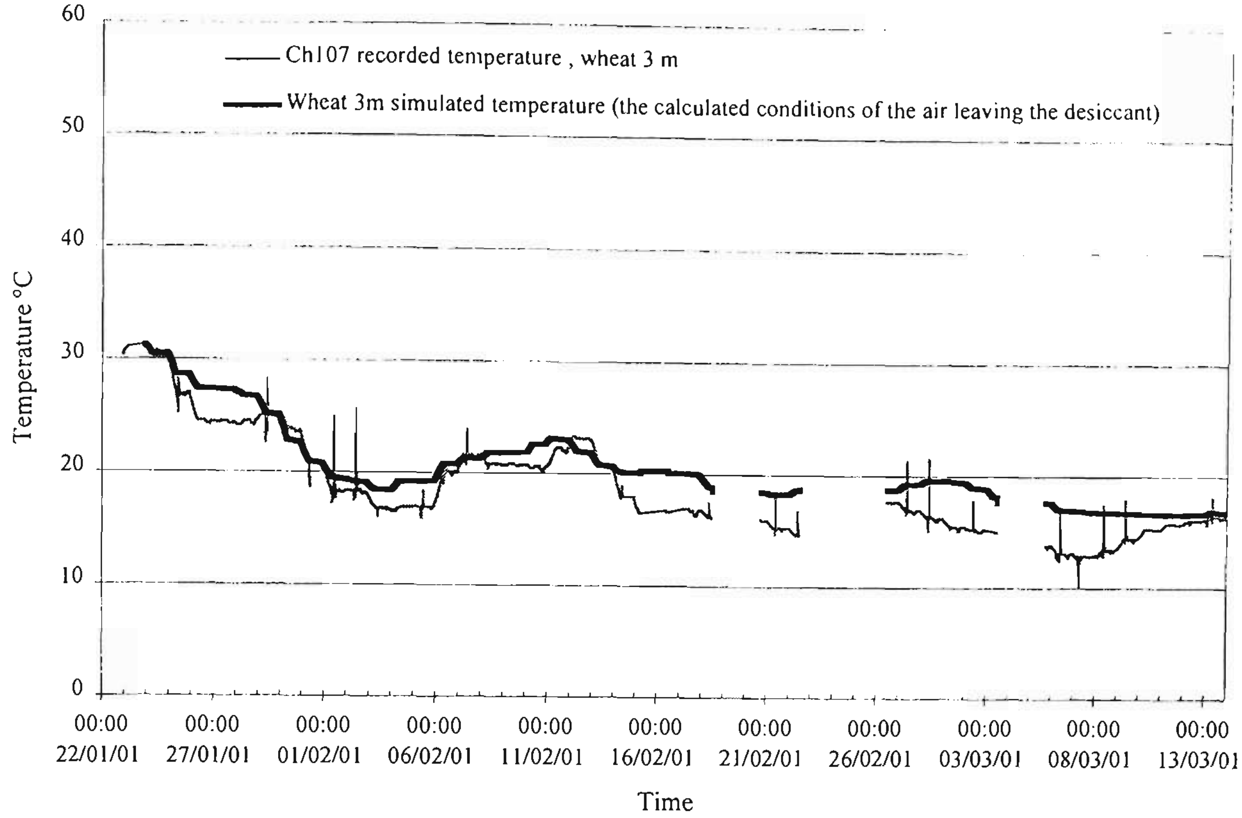

Figure 6.7 Simulated grain temperatures compared with experimental plots at the height 3m along the centreline of wheat silo, the calculated conditions of the air leaving the desiccant system are used when the fan was on

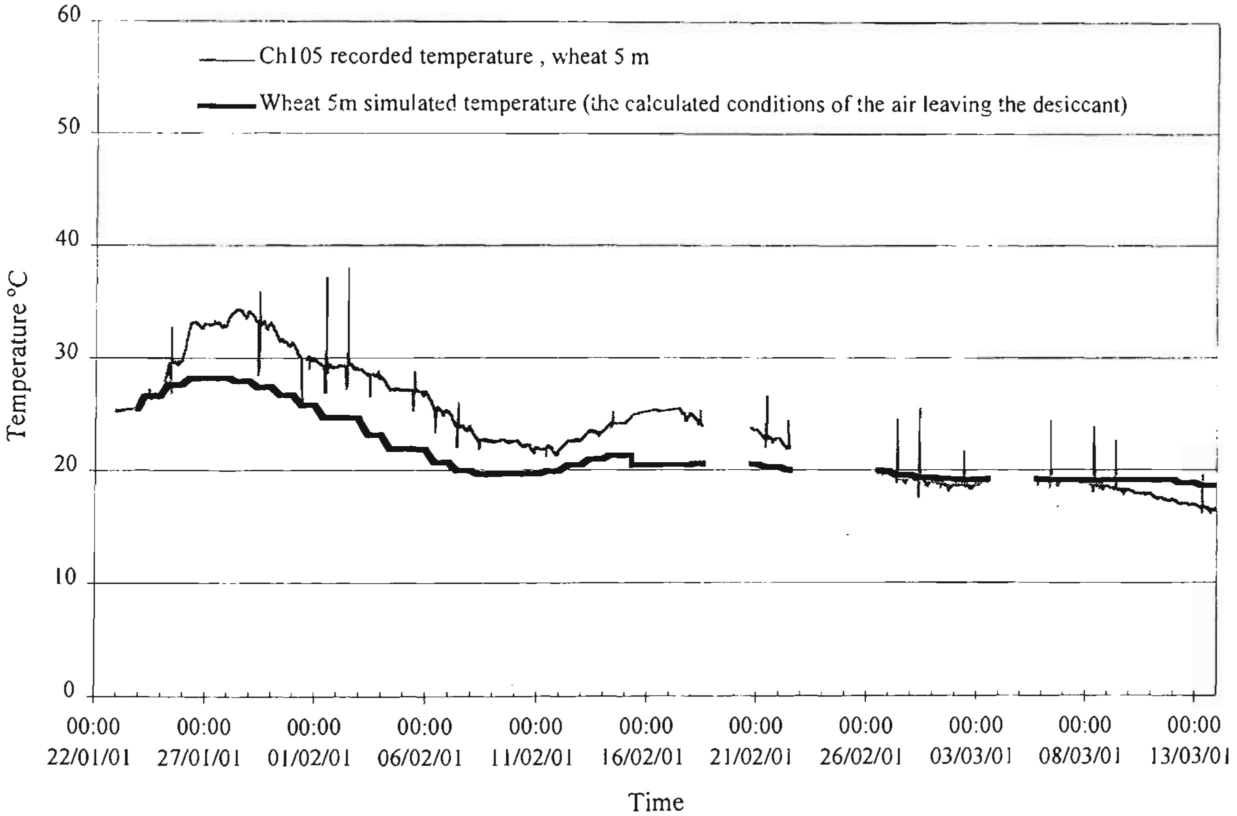

Figure 6.8 Simulated grain temperatures compared with experimental plots at the height 5m along the centreline of wheat silo, the calculated conditions of the air leaving the desiccant system are used when the fan was on

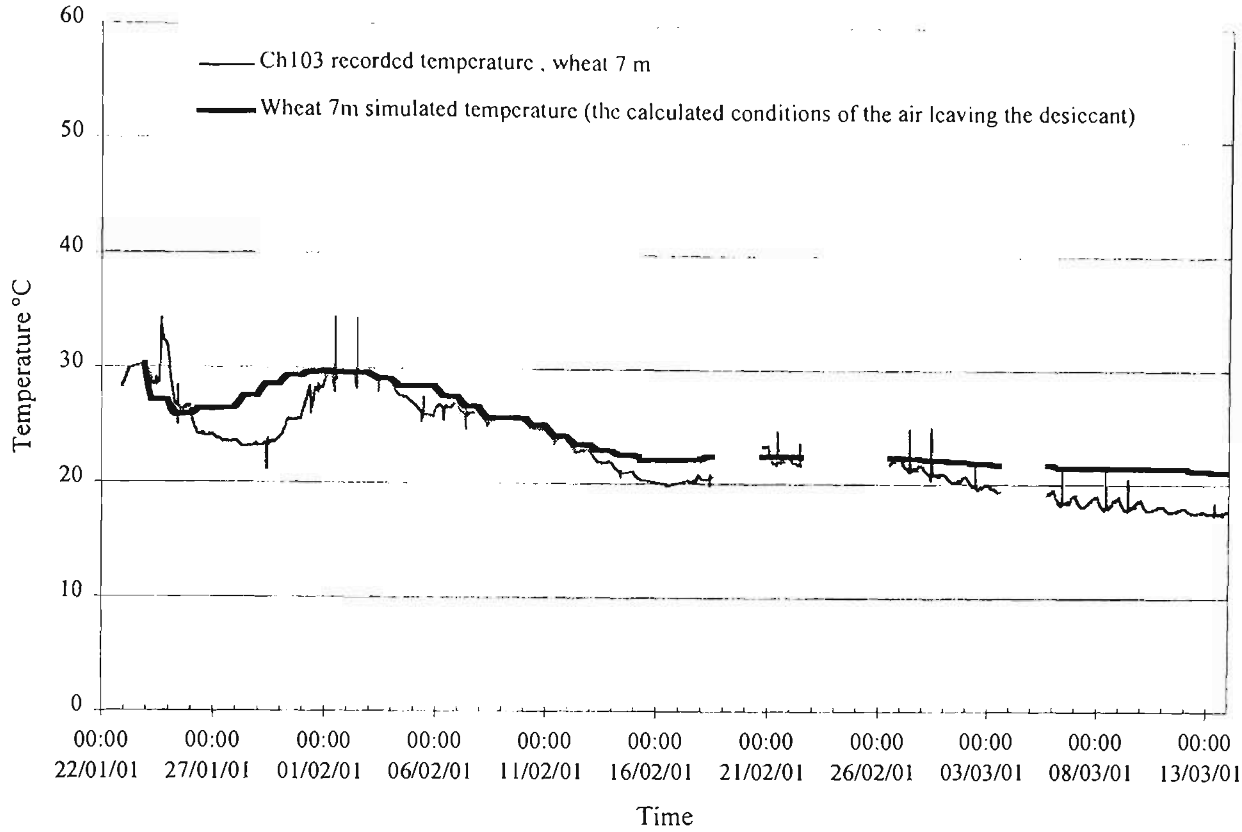

Figure 6.9 Simulated grain temperatures compared with exeprimental plots at the height 7m along the centerline of wheat silo, the calculated conditions of the air leaving the desiccant system are used when the fan was on

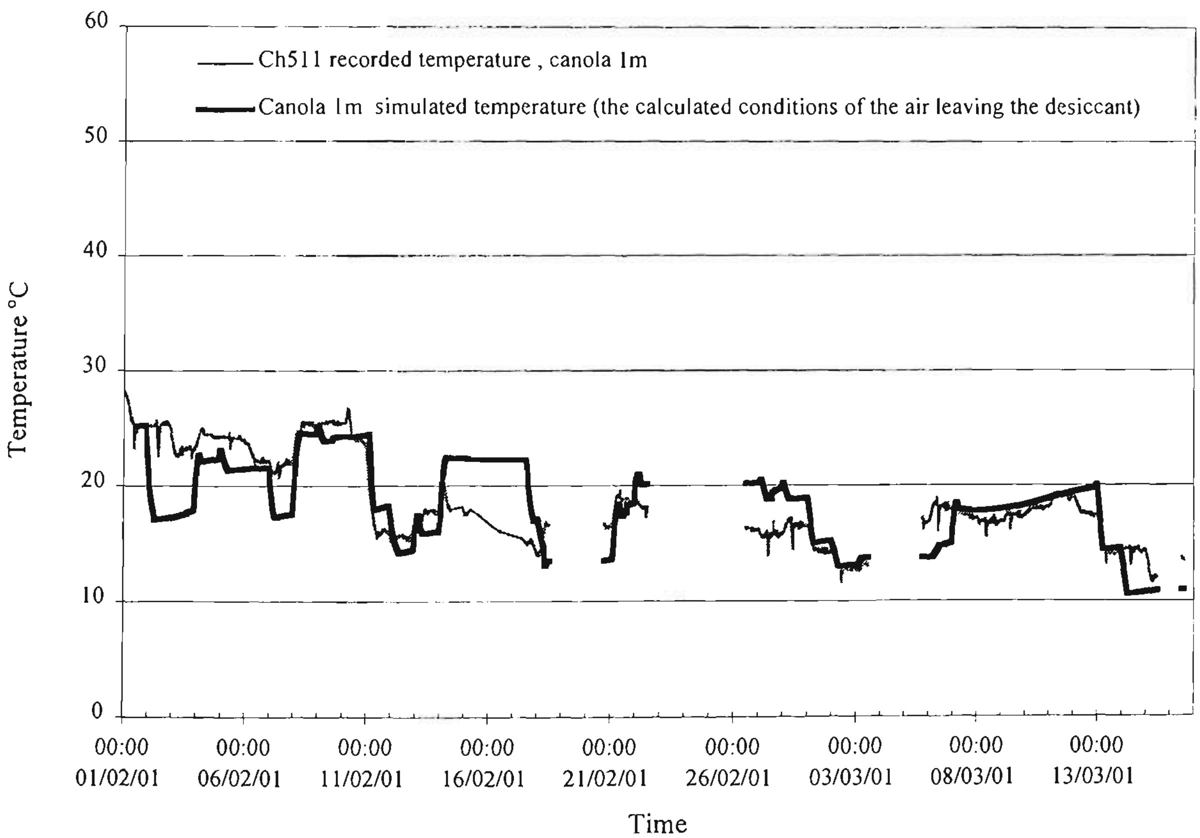

Figure 6.10 Simulated grain temperatures compared with experimental plots at the height 1m along the centerline of canola silo, the calculated conditions of the air leaving the desiccant system are used when the fan was on

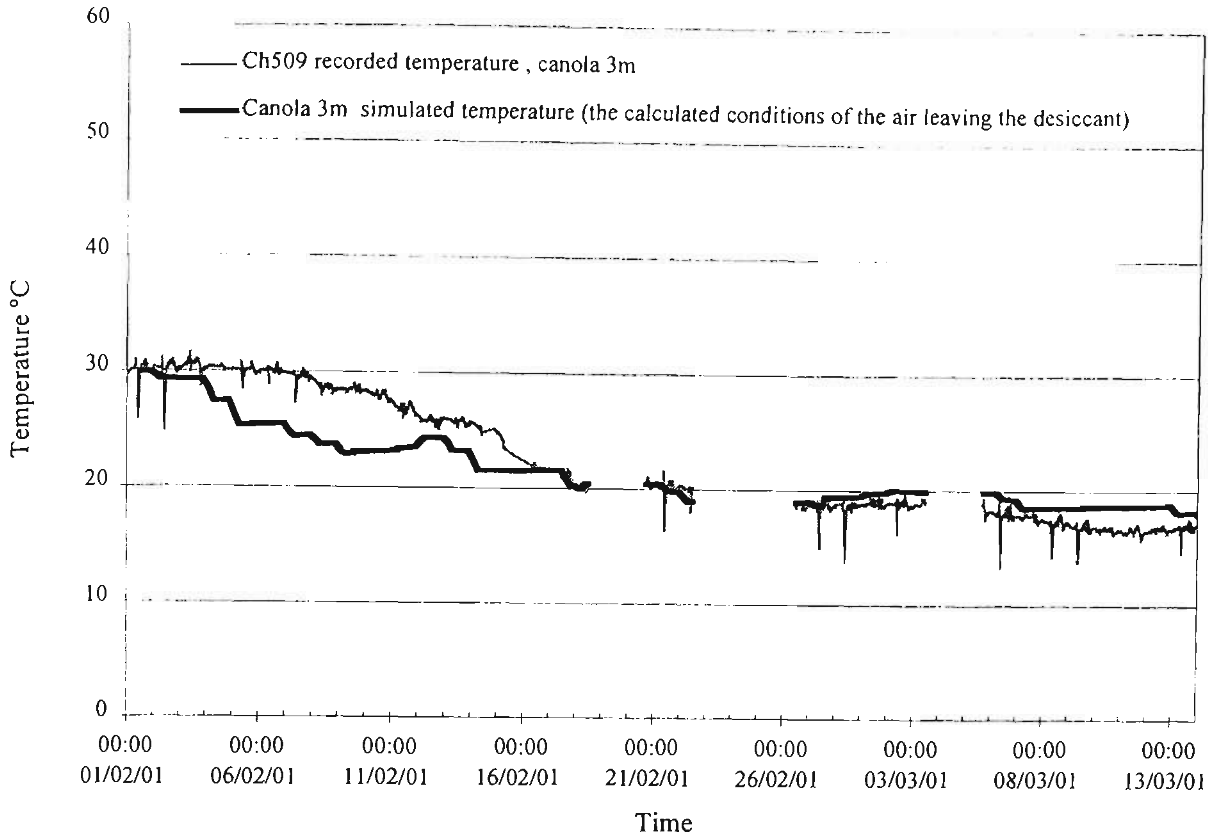

Figure 6.11 Simulated grain temperatures compared with experimental plots at the height 3m along the centerline of canola silo, the calculated conditions of the air leaving the desiccant system are used when the fan was on

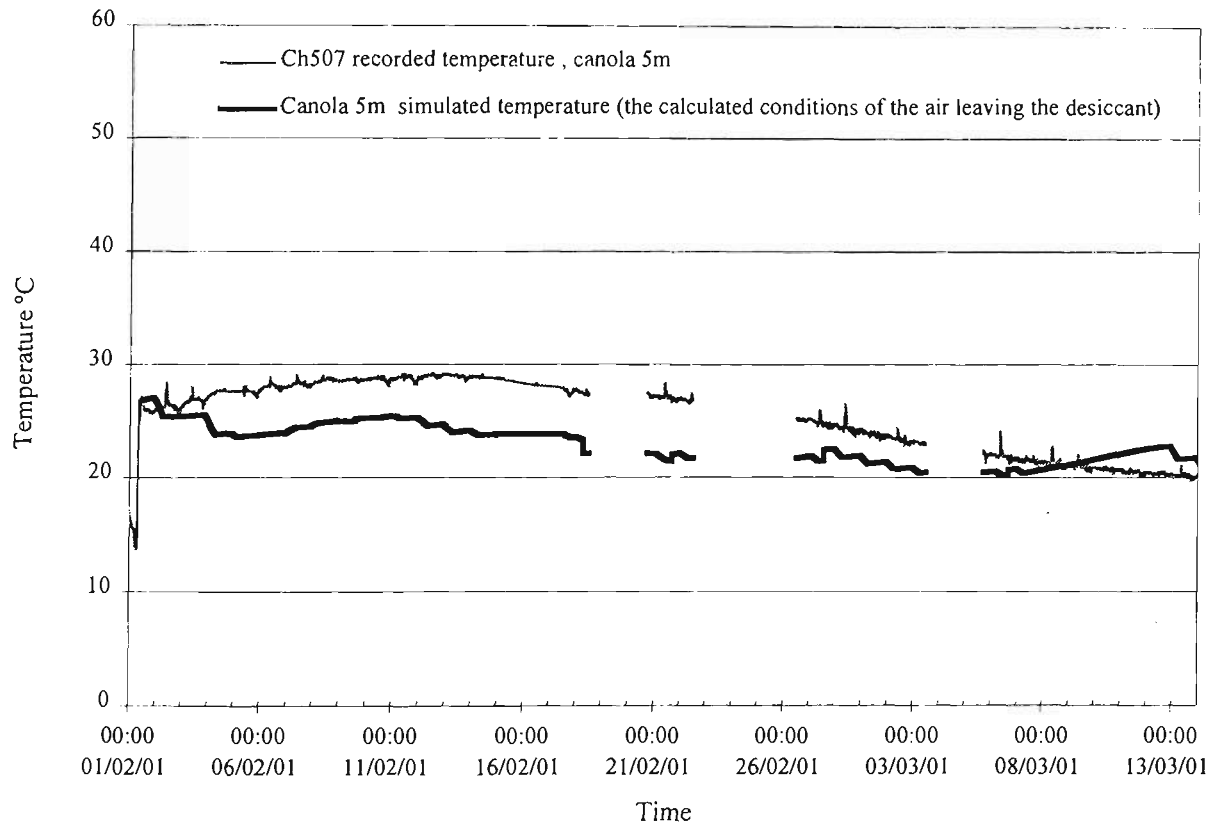

Figure 6.12 Simulated grain temperatures compared with experimental plots at the height 5m along the centerline of canola silo, the calculated conditions of the air leaving the desiccant system are used when the fan was on

6.3 Predicted grain temperatures

In the previous chapter we noted that both wheat and canola silos had the features that the grains were sometime warmed by the aeration air. This arose as a result of a very simple and unpractical operation schedule of the desiccant system, *i.e.* it comes controlled by a timer. In this section, we introduce an established operation method for cooling grain storage, namely time-proportioning control (Elder, 1972). A schedule of six-hour operation per day can be described mathematically as:

When the system is off

If $T_{amb} < T_{set}^{on}$, the system switches on

$$\text{where } T_{set}^{on} = T_{set}^{0} + \frac{3\times\Delta t}{24\times 3600} \tag{6.1}$$

When the system is on

If $T_{amb} > T_{set}^{off}$, the system switches off

$$\text{where } T_{set}^{off} = T_{set}^{0} - \frac{9\times\Delta t}{24\times 3600} \tag{6.2}$$

where T_{amb} is the actual ambient temperature, °C, Δt is the time step, s, T_{set}^{0} is the old value of the setpoint, °C, T_{set}^{on} is the new setpoint of the controller for switching on the system after a time Δt when the system is off, °C, and T_{set}^{off} is the new setpoint of the controller for switching off the system after a time Δt when the system is on, °C.

During the total operation period lasted 54 days a total of 205 hours of cooling resulted which is about 50 hours is less than the measured operation time. The average grain temperatures are reduced about 11°C.

The predicted grain temperatures are plotted in figures 6.13 to 6.18.

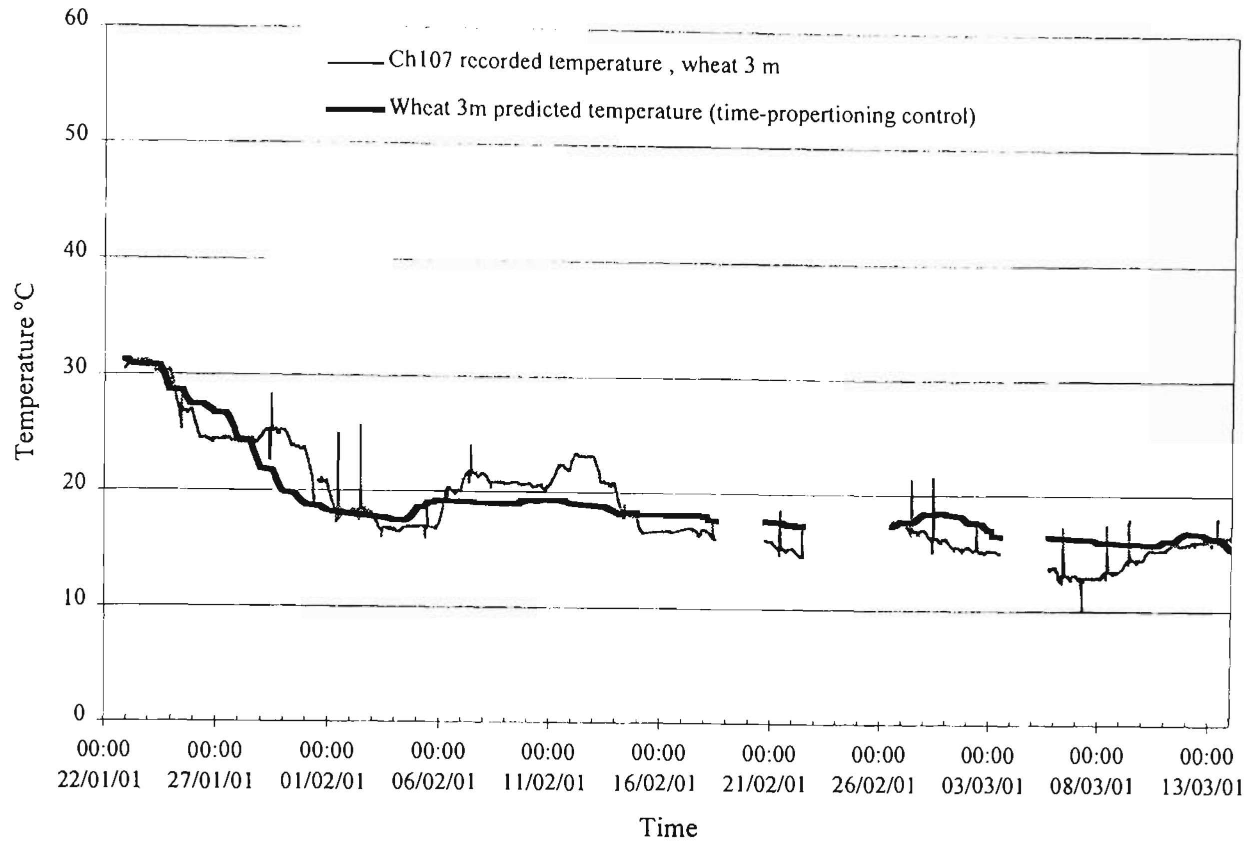

Figure 6.13 Predicted grain temperatures compared with experimental plots at the height 3m along the centerline of wheat silo, the desiccant system is operated using the time-proportioning control algorithm

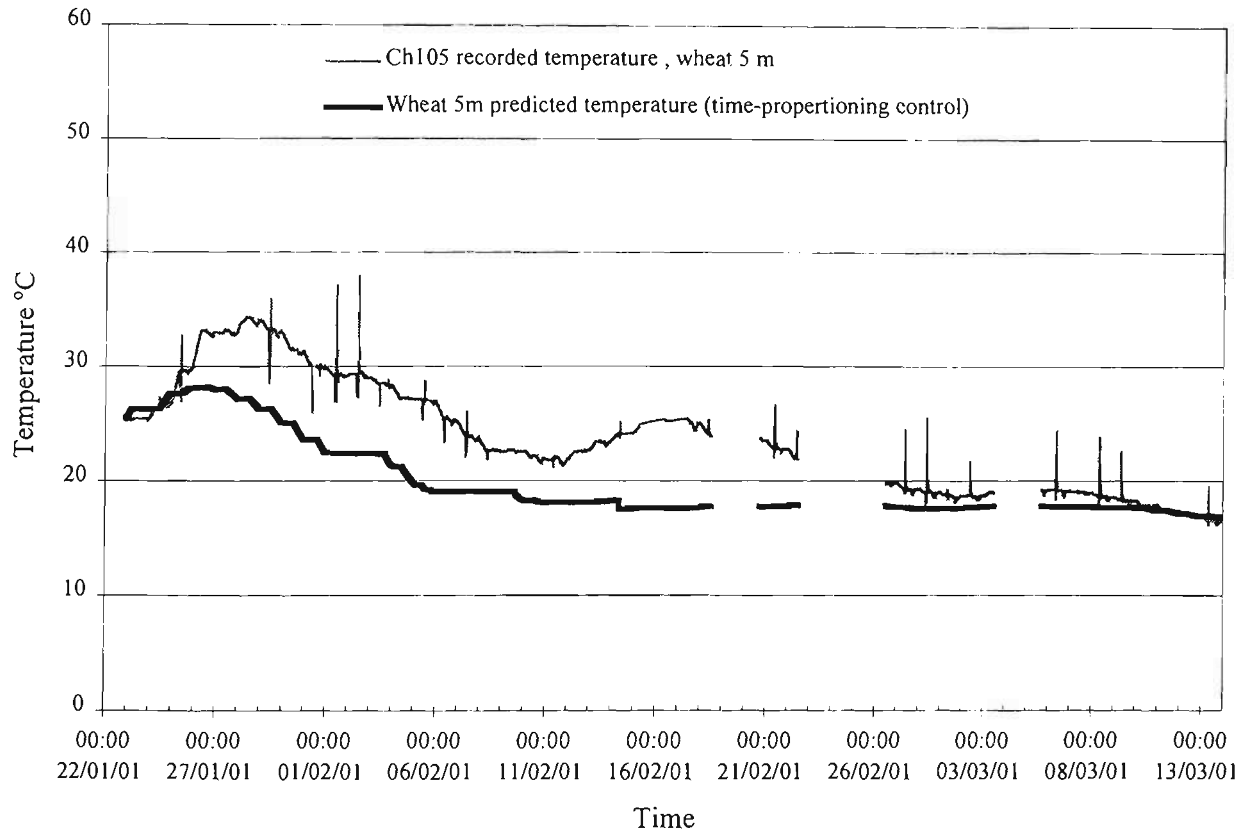

Figure 6.14 Predicted grain temperatures compared with experimental plots at the height 5m along the centerline of wheat silo, the desiccant system is operated using the time-proportioning control algorithm

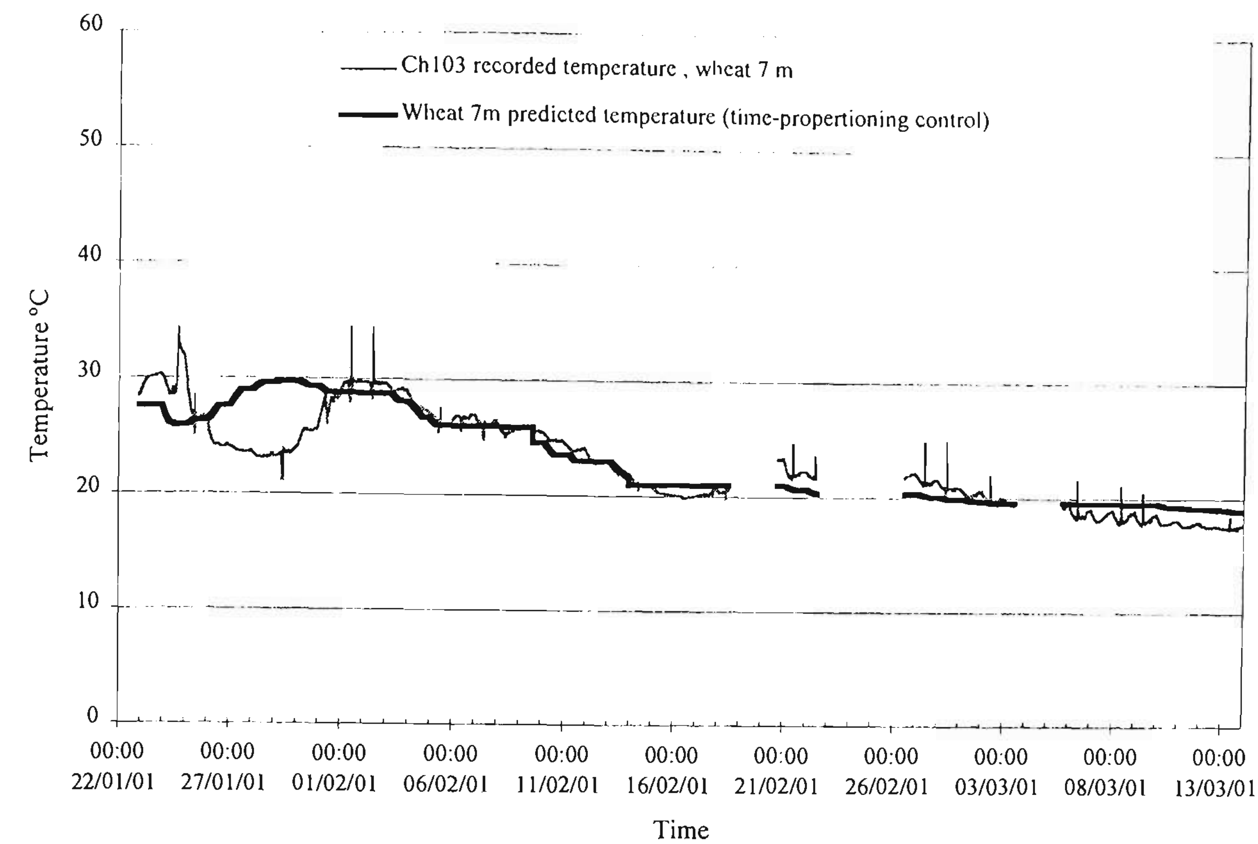

Figure 6.15 Predicted grain temperatures compared with experimental plots at the height 7m along the centerline of wheat silo, the desiccant system is operated using the time-proportioning control algorithm

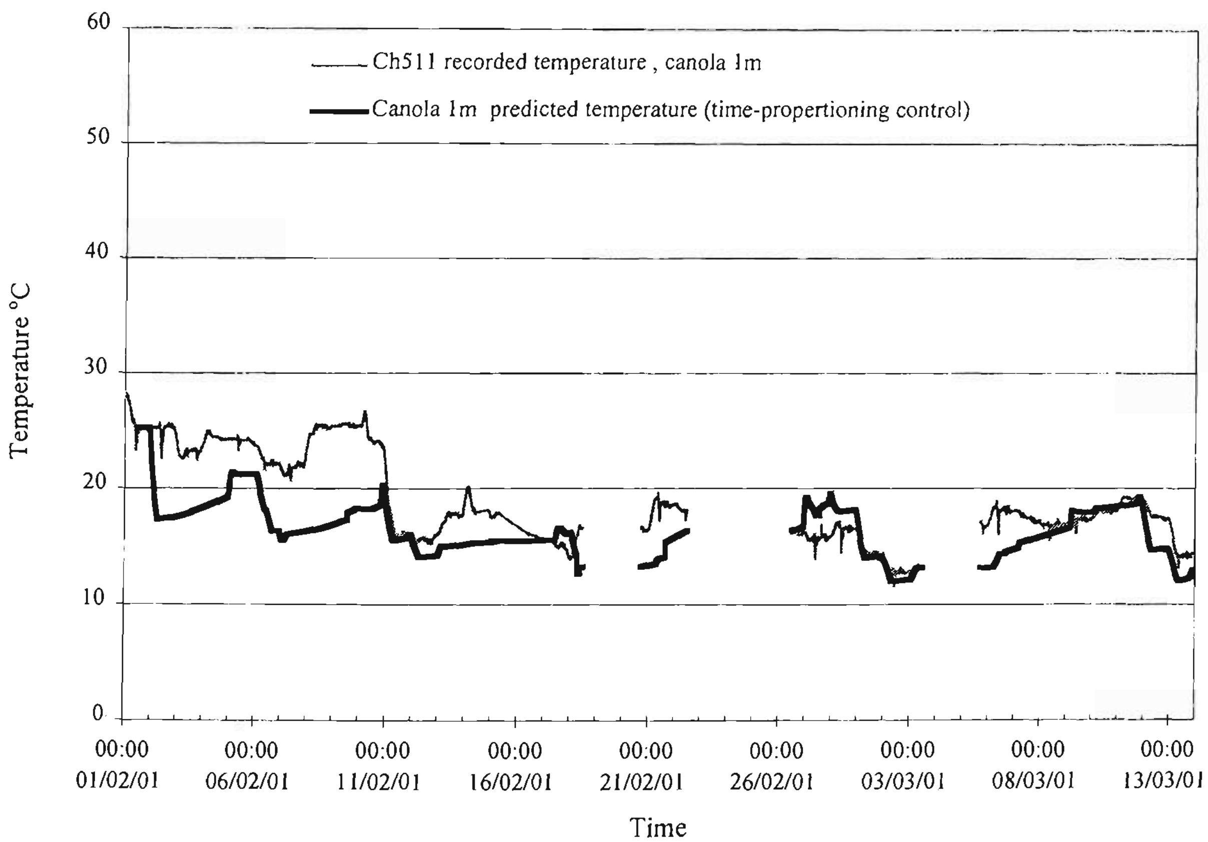

Figure 6.16 Predicted grain temperatures compared with experimental plots at the height 1m along the centerline of canola silo, the desiccant system is operated using the time-proportioning control algorithm

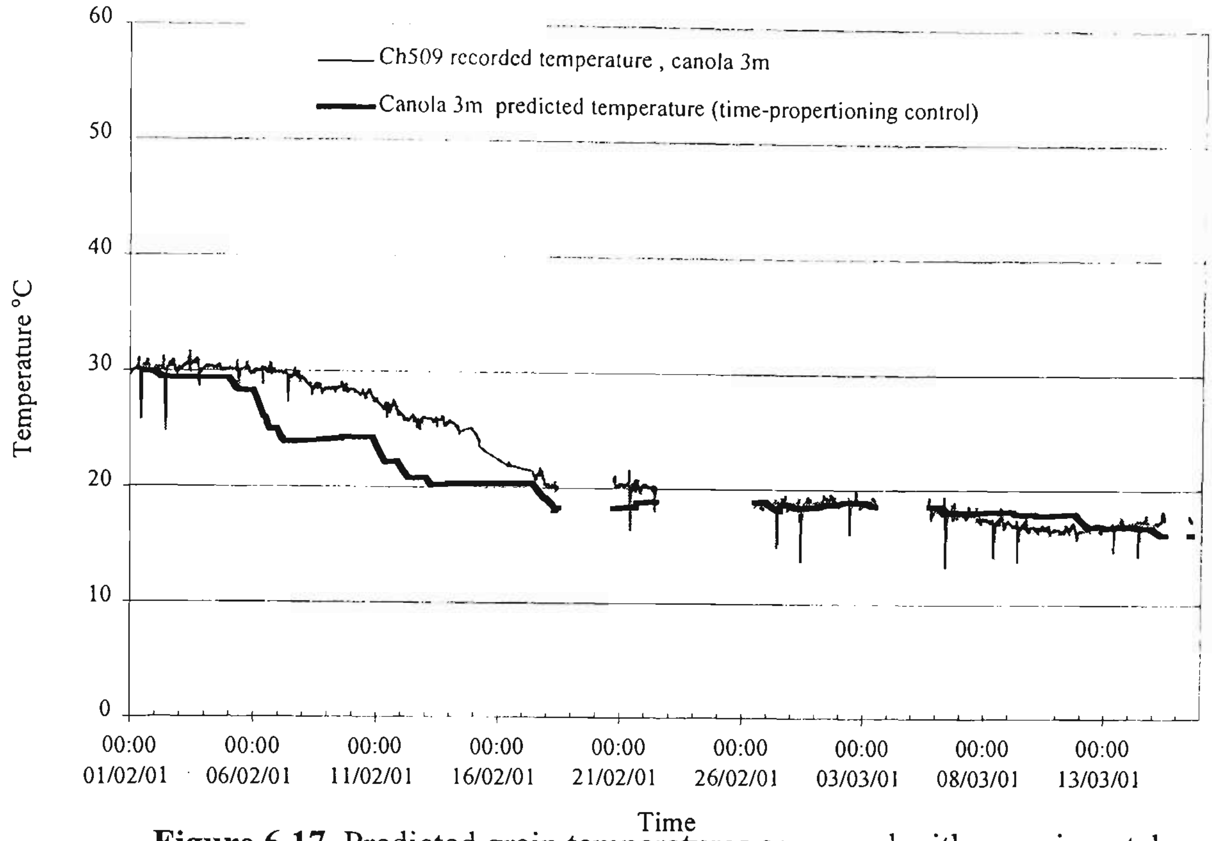

Figure 6.17 Predicted grain temperatures compared with experimental plots at the height 3m along the centerline of canola silo, the desiccant system is operated using the time-proportioning control algorithm

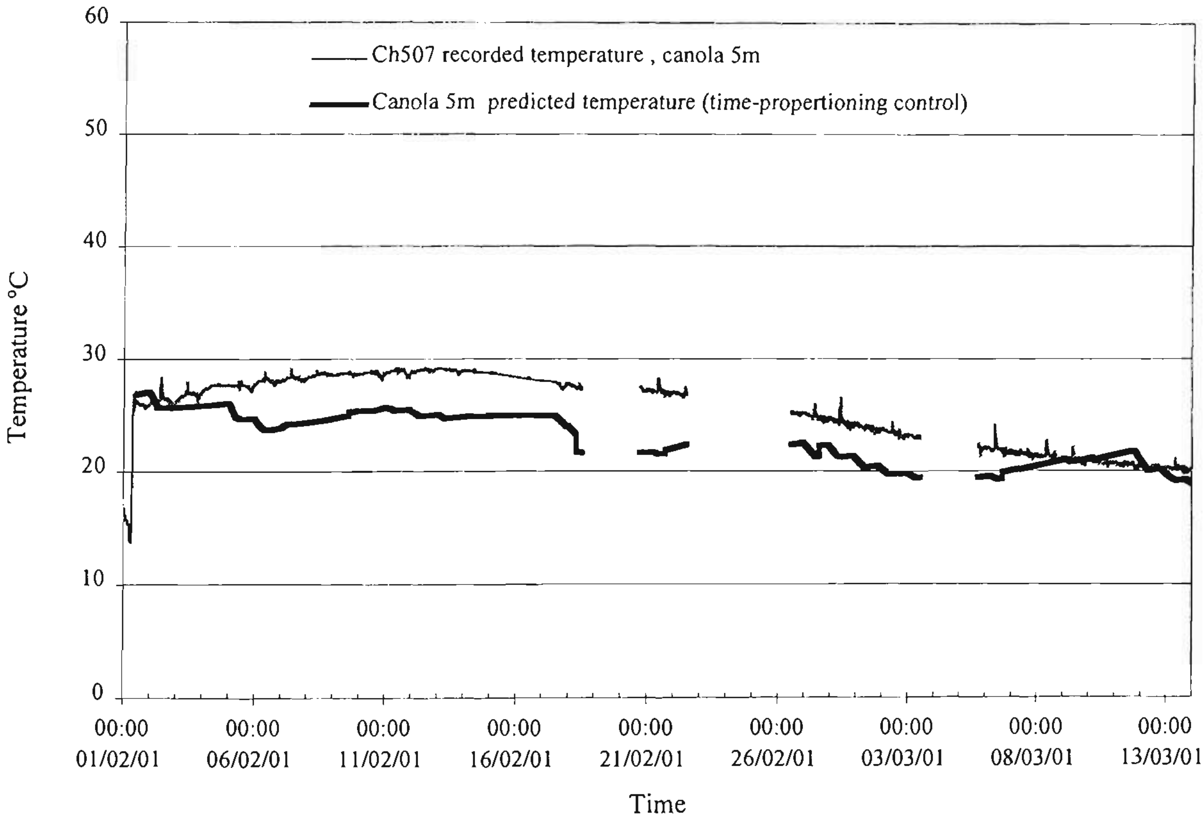

Figure 6.18 Predicted grain temperatures compared with experimental plots at the height 5m along the centerline of canola silo, the desiccant system is operated using the time-proportioning control algorithm

Comparing with the calculated plots in the figures 6.7 to 6.12, the following features are found in the figures 6.13 to 6.18:

- In general, the calculated grain temperatures of the time-proportioning control are lower than the calculated plots under the experimental regime in which the system was operated by a time clock.
- In both the wheat and canola silos, the re-warmed ranges of the grain temperature are smaller under the time-proportioning control than the experimental control.
- Under time-proportioning control, the range of the grain temperature in the lower level of the canola silo is smaller than the experimentally operated control.
- Under time-proportioning control, the calculated grain temperatures in the upper level in the both wheat and canola silos appeared only slightly improved. The situation can be explained by that the headspace conditions are the same under both the time-proportioning control and the experimental operate control that is one of the main influences on the grain temperatures on the upper level of the silo.

6.4 Conclusions

The simulation study permits one to draw the following conclusions:

- Simulated grain temperatures along the centerline of the silos agree with the trends of the recorded data plots very well.
- Combining with the degree of the regeneration of the desiccant the empirical formulae, equations (5.2) and (5.3), obtained in the previous chapter can be used to calculate the conditions of the air leaving the desiccant system during the cooling processes.
- Under time-proportioning control, the calculated grain temperatures were lower than those obtained under simply on/off control actuated by a timer, suggesting that a timer did not select the coldest available air.

CHAPTER 7

CONCLUSIONS

In this research we have explored how a novel desiccant cooling system can be used to cool stored grains with a combination of mathematical modeling and field studies. This particular cooling duty differs from those conventionally encountered in air conditioning applications because knowledge of the hygroscopic nature of foodgrains is required. The conclusions of this thesis are as follows:

- A detailed literature review has been presented on the application of the desiccant techniques to cooling grain silos.
- A mathematical model that governs the temperature and moisture transfer within a ventilated silo has been developed and boundary conditions discussed.
- The mathematical model has been converted to discretized equations with simple linearized algebraic forms, as well as the boundary conditions equations.
- The mathematical model has been compared with a set of field data. The comparison results showed that the calculated grain temperatures along the centerline of the silo captured the experimental recorded data very well. The calculated results at the wall were in poor agreement with the experimental recorded data. When the recorded data were used for the boundary conditions, the agreement of those calculated results with experimental data points at the wall boundary have been improved. It is essential that more accurate methods of simulating the temperatures of the silo wall and headspace be implemented in the mathematical model.
- A theoretical analysis of the performances of the desiccant cooling system

has been obtained both for cooling and for regeneration processes.

- Two prototypes of a novel desiccant cooling system were designed and built in Ararat, Victoria.
- A detailed experimental study including laboratory and field testing has been completed.
- Comparing with the ambient conditions, the wet-bulb temperature of the process air can be reduced by 5 ~ 7°C during the desiccant cooling processes.
- The desiccant device can be regenerated completely in six hours using an air regeneration temperature of 65°C.
- Regression analyses have been carried out for the recorded outlet data both of cooling and regeneration processes. The results indicate that the regeneration rate of the desiccant is the main cause of the changes of the dry-bulb temperature and wet-bulb temperature of the process air during the cooling processes and empirical formulae are obtained to calculate the average outlet of desiccant system during the cooling processes.
- In the field experiments, the average grain temperatures were reduced by 11°C in both wheat and canola silos.
- The calculated grain temperatures of the mathematical model along the centerline predicted by mathematical model agreed with recorded data of the field experimental study for both wheat and canola silos.
- The empirical formulae obtained from a regression study of the experimental recorded data can be used to calculated outlet recorded data for the desiccant cooling processes and the degree of regeneration of desiccant need to be combined to ensure the realistic calculated results.
- The method of the time-proportioning algorithm is used to control the desiccant cooling system has been studied and the degree of cooling in the both wheat and canola silos are predicted.

The main contributions of this thesis to the literature are as follows:

- A mathematical model has been developed especially for modelling the features of the thermophysical processes occurring in an aerated silo and the calculated grain temperatures of the mathematical model agreed with the recorded data very well along the centerline of the silo.

- The general patterns of the outlet have been obtained both for the cooling and regeneration processes of a novel desiccant device.
- A novel desiccant cooling system has been built and tested both in the laboratory the field in which two silos were aerated in the field.
- The recorded outlets of the desiccant cooling system agreed with the general patterns both in cooling and regeneration processes.
- An empirical method to calculate the conditions of the air leaving the desiccant device during the cooling process was established.

Future research should be carried out in the following areas:

- An accurate mathematical model for calculating the temperatures of the wall and headspace of the silo should be studied.
- A comprehensive mathematical model of grain cooling unit should be formulated. This will enable design feature to be investigated and the design optimized.
- The operating schedule of the desiccant cooling system should be improved to enable the system avoid operating the warm weather conditions. This needs a suitable model to control the system operation according to actual weather condition.

REFERENCES

1. Ahmad, M., Perera, M.D.C., and Thorpe, G.R. 1997. *Development of a novel solar desiccant cooling system for insect control in stored grain.* Department of Civil and Building Engineering, Victoria University. Melbourne. pp 90.

2. Ahmad, M. and Thorpe, G.R. 1998. *The performance of a solar thermal desiccant system for cooling farm-stored grains in the sub-tropics.* Department of Civil and Building Engineering , Victoria University. Melbourne. pp 93.

3. ASHRAE, 1992. *Desiccant cooling and dehumidification.* American Society of Heating, Refrigerating & Air-Conditioning Engineers, Inc. Atlanta, GA USA.

4. ASHRAE, 1994. *1994 ASHRAE Refrigeration Handbook(SI).* American Society of Heating, Refrigerating & Air-Conditioning Engineers, Inc. Atlanta, GA USA.

5. ASHRAE, 1995. *1995 ASHRAE Application Handbook(SI).* American Society of Heating, Refrigerating & Air-Conditioning Engineers, Inc. Atlanta, GA USA.

6. ASHRAE, 1996. "Chapter 22: Desiccant dehumification and pressure drying equipment". In: *1996 ASHRAE Systems and Equipment Handbook(SI).* American Society of Heating, Refrigerating & Air-Conditioning Engineers, Inc. Atlanta, GA USA. pp 22.1 - 22.10.

7. ASHRAE, 1997. "Chapter 6: Psychrometrics" In: *1997 ASHRAE Fundamentals Handbook(SI).* American Society of Heating, Refrigerating & Air-Conditioning Engineers, Inc. Atlanta, GA USA. pp 6.1 - 6.17.

8. Berezin, I.S. and Zhidkov, N.P., 1965a. *Computing methods: Volume 1.* Pergrmon Press Ltd., Oxford, U.K.. pp 464.

9. Berezin, I.S. and Zhidkov, N.P., 1965b. *Computing methods: Volume 2.* Pergrmon Press Ltd., Oxford, U.K.. pp 679.

10. Billiard, F., 1998. "New development in the food cold chain worldwide". In: *Refrigeration into the new millennium: Proceedings of the 20th international congress of refrigeration.* 20 - 25 September 1999. Sydney, Australia. paper No: 726. pp 14.

11. Brooker, D. E., 1961. "Pressure patterns in grain - drying systems established by numerical methods". Transactions of the American Society of Agricultural Engineers. Vol 4:1 pp72-74. 1961.

12. Brundrett, G.W., 1987. *Handbook of dehumidification technology.* Anchor Brendon Ltd, Tiptree, Esses, U.K. pp 299.

13. Bureau of Meteorology, Australia, 1988a. *Climatic averages Australia.* Commonwealth of Australia, Canberra, pp 532.

14. Bureau of Meteorology, Australia, 1988b. *Climatic atlas of Australia.* Bureau of meteorology: Australia, 1988.

15. Bureau of Meteorology, Australia (BOM), 2000. *Climatic average.* http://www.bom.gov.au/climate/average/, Bureau of meteorology: Australia, submitted at 23rd November 2000.

16. Carnahan, B., Luther, H. A. and Wilkes, J. O. 1969. *Applied numerical methods.* John Wiley &Sons, Inc., New York, USA. Pp 604

17. Cenkoski, S. and Zhang, Q. 1995. "Engineering proprerties og grains and oilseeds". In: *Stored-grain ecosystems.* Jayas, D. S., White, N. D. G. and Muir, W. E. edited. Marcel Dekker, Inc., New York, USA. pp. 411 - 463.

18. Chau, R.K. 1982. "Grain aeration with air conditioning by a desiccant". American Society of Agricultural Engineers. Paper No. 82-3031. St. Joseph, MI USA.

19. Chen, C.C. and Morey, R.V., 1989. "Comparison of four EMC/ERH equations". Transactions of the ASAE 1989. American Society of Agricultural Engineers,

1989, pp 983 – 990.

20. Chen, L. and Thorpe, G.R., 1999. "A novel system for cooling stored grains". In: *Refrigeration into the new millennium: Proceedings of the 20th international congress of refrigeration.* 20 - 25 September, 1999. Sydney, Australia. paper No: 184. pp 8.

21. Chen, L. and Thorpe, G.R., 2000. "Simulation of aerated grain silos". In: : *Proceedings of the AIRAH 2000 Conference.* 29 - 31 March, 2000. Melbourne Australia. pp 6

22. Close, D.J. and Banks, P.J., 1972. "Coupled equilibrium heat and single adsorbate transfer in fluid flow through a porous medium. II. Prediction for a silica-gel air-drier using characteristic charts". *Chemical Engineering and Science*, Vol 27, pp 1157 – 1169. 1972.

23. Darby, J., 1998. "Bunker aeration trial". In: Proceedings of Australian Postharvest Technical Conference 1998, Canberra, Australia. pp 245 ~ 251.

24. de Lucia, M. and Assennato, D., 1994. *Agricultural engineering in development - Post-harvest operations and management of foodgrains.* FAO Agricultural services bulletin No: 93. Food and Agriculture Organization of the United Nations (FAO), Rome, Italy.

25. Desmarchelier, J.M. 1993. *A Guide to Grain Aeration: Part 1. Strategy Manual.* Stored Grain Research Laboratory, CSIRO Division of Entomology, Canberra.

26. Downing, D., 1997. "Traverse techniques for air measurement". http://www.airflow.com/techtop/techi004.htm. Airflow technical products Inc. submitted on 8 March, 2000.

27. Driscoll, R. H. and Srzednicki, G.S., 1998. "Overseas perspective on aeration". In: Proceedings of Australian Postharvest Technical Conference 1998, Canberra, Australia. pp 221 ~ 226.

28. Duffie, J. A. and Beckman, W. A., 1980. *Solar engineering of thermal processes.* Wiley-Interscience Publication, New York, USA. pp. 762.

29. Elder, W. B. 1978. "The future of temperature controlled storages and heat treatment of grain." In: *Grist* Australia Grain Institute Research. Vol. 39, pp 8-10, 1978

30. Ergun, S. 1952. "Fluid flow through packed columns". *Chemical engineering progress*. Vol. 48:2, pp89-94. 1952

31. Ferziger, J.H. and Peric, M., 1996. *Computational methods for fluid dynamics*. Springer, Berlin, Germany. pp. 356.

32. Food and Agriculture Organization of the United Nations (FAO), 1998. *FAO yearbook - Production 1997*, Vol. 51. Food and Agriculture Organization of the United Nations (FAO), Rome, Italy. pp 300.

33. Forchheimer, P. H. (1901) – Wasserbeuregung durch boden, Zeit. Ver. Deutsch. Ing, **45**, 1782-1788.

34. Frisvad, J.C. 1995. "Mycotoxins and mycotoxingenic fungi in storage". In: *Stored-grain ecosystems*. Jayas, D. S., White, N. D. G. and Muir, W. E. edited. Marcel Dekker, Inc., New York USA. pp. 123 - 167.

35. Gibson, A. M., Eyles, M. J., Hocking, A. D., and Best, D. J. 1994. "Application of Mathematical modelling techniques for oredicting mould growth". In: *Stored product protection: Proceedings of the 6th International Working Conference on Stored-product Protection*. Highley, E., Wright, E.J., Banks, H.J., and Champ, B.R. (eds.) pp. 988-991.

36. Gas Research Institution (GRI), 2000 a. "Desiccant cycle" In: *Desiccant tutorial – Basic*. http://www.gri.org/pub/solutions/desiccant/tutorial/basic/des-cycle.html. submitted on 28 April, 2000.

37. Gas Research Institution (GRI), 2000 b. "Desiccant sorption" In: *Desiccant tutorial – Main*. http://www.gri.org/pub/solutions/desiccant/tutorial/des_sorption.html, submitted on 28 April, 2000.

38. Gwinner, J., Harnisch, R. and Mück, O., 1996. *Manual of the prevention of post-*

harvest grain losses. 2nd edition. Deutsche Gesellschaft fuer Technische Zusammenarbeit (GTZ) Gmbh, Eschborn, Germany. pp 338.

39. Harein, P.K. and Davis, R. 1992. "Control of stored-grain insects". In: *Storage of cereal grains and their products* (Fourth Edition). Saucer, D.B. (ed.) American Association of Cereal Chemists, Inc. St. Paul, Minnesota, USA. pp. 491-534.

40. Hukill, W. V. and Ives, N. C. (1955) "Radial are flow resistance of grain". *Agricultural Engineering*. Vol. 36:5, pp. 332-335.

41. Hunter, A. J., 1981, "A climatic model for predication of percentile statistic for ambient temperature". *International Monthly Weather Review*, Vol. 109, pp 722-728.

42. Hunter, A. J., 1983. "Pressure difference across an aerated seed bulk for some common duct and store cross-sections". *Journal of agricultural engineering research*, Vol. 28, pp 437 - 450.

43. ICMSF (International Commission on Microbiological Specification for Foods), 1996. *Microorganisms in foods - Characteristics of microbial pathogens*. Balckie Academic & Professional, London, U.K. pp. 513

44. Jin, Y. 1996. *Modelling the microclimate in a conical bottomed circular grain silo*. Thesis of Master's degree. Victoria University of Technology, Melbourne, Australia. pp 205.

45. Kozeny, J. (1927) - Über kapillare Leitung des Wassers im Boden. Ber. Wien Akad., 136A, pp 271 – 277.

46. Maier, D.E. 1994. "Chilled aeration and storage of US crops - a review." In: *Stored product protection: Proceedings of the 6th International Working Conference on Stored-product Protection*. Highley, E., Wright, E.J., Banks, H.J., and Champ, B.R. (eds.) pp. 300-311.

47. Maier, D.E. and Navarro, S. 1994. "Chilled of grain by refrigerated air." In: *The*

mechanics and physics of modern grain aeration management. Navarro, S. Noyes, R. T. (eds.). CRC Press, Boca Raton, USA pp. 672 .

48. Mathews, J.H., 1987. *Numerical methods for computer science, engineering, and mathematics.* Prentice-hall, Inc. Englewood Cliffs, New Jersey, USA. pp 507.

49. McCalla, T.R., 1967. *Introduction to numerical methods and FORTRAN programming.* JOHN Wiley & Sons, Inc. New York, New York, USA. pp 359.

50. Miller, W.M. 1984. "Solid desiccants for food drying and energy storage". American Society of Agricultural Engineers. Paper No. 84-6005. St. Joseph, MI USA.

51. Patankar, S.V. 1980. *Numerical heat transfer and fluid flow.* McGraw-Hill Book Co. pp 197.

52. Pedersen, J.R. 1992. "Insects: Identification, Damage, and Detection". In: *Storage of Cereal Grains and Their Products* (Fourth Edition). Saucer, D.B. (ed.) American Association of Cereal Chemists, Inc. St. Paul, Minnesota, USA

53. Pomeranz, Y., 1994. "Biochemical, functional, and nutritive change during storage". In: *Storage of cereal grains and their products* (Fourth Edition). Saucer, D.B. (ed.) American Association of Cereal Chemists, Inc. St. Paul, Minnesota, USA. pp. 55 - 141.

54. Rodda, E.D., and Rode, D.W. 1977. "Desiccant dehumidifiers for drying grain". American Society of Agricultural Engineers. Paper No. 77-3528. St. Joseph, MI USA

55. Samarskii, A. A. and Andreyev, V. B. (1963). "On a high-accuracy scheme for an elliptic equation with several space variables". *Journal of computational mathematics and mathematical physics.* Vol.3 pp 1371 – 1382. 1963 U.S.S.R.

56. Scheidegger, A. E., 1960. *The physics of flow through porous media.* Oxford University Press, London, U.K. pp. 313.

57. Shedd, C. K., 1953. "Resistance of grains and seeds to air flow". *Agricultural*

Engineering. Vol.34:9, pp. 616 – 619. 1953.

58. Singh, A.K. and Thorpe, G.R. 1993a. "The application of a grid generation technique to the numerical modeling of heat and moisture movement in peaked bulks of grain". *Journal of food Process Engineering*, Vol. 16, pp 127 – 145, 1993.

59. Singh, A.K. and Thorpe, G.R., 1993b. "Solution procedure for three-dimensional free convective flow in peaked bulks of grain". *Journal of Stored Products Research*, Vol. 28, pp 221 – 235, 1993.

60. Smith, G.D., 1985. *Numerical solution of partial differential equations – finite difference methods*. Third edition. Claredon press, Oxford, U.K.. pp337.

61. Sutherland, J.W., Banks, P.J. and Griffiths, H.J., 1971. "Equilibrium heat and moisture transfer in air flow through grains". *J. Agric. Eng. Res.* Vol. 16, pp 368 - 386.

62. Slayzak, S.J., Pesaran A.A. and Hancock, C.E., 1996. *Experimental evaluation of commercial desiccant dehumidifier wheels*. In: http://www.nrel.gov/desiccantcool/wheels.htm. Advanced desiccant cooling & dehumidification program, National Renewable Energy Laboratory, US Department of Energy. Boulder, USA. pp 14.

63. Stored Grain Research Laboratory (SGRL), CSIRO Division of Entomology. Canberra, 1999. *Stored grain aeration trial at Wongon Hills, West Australia, 1 November 1998 ~ 3 January 1999*. Stored Grain Research Laboratory, CSIRO Division of Entomology. Canberra. (personal exchanged information)

64. Tao, W. 1986. *Computational heat transfer* (Chinese vision). Xi'an Jiao-tong University Press, Xi'an, China. pp 721.

65. Techajunta, S., Chrirarattananon, S. and Exell, R.H.B., 1999. "Experiments in a solar simulator on solid desiccant regeneration and air humidification for air conditioning in a tropical humid climate". *Renewable Energy* (1999) vol. 17 pp 549 – 568.

66. Tipples, K.H. 1995. "Quality and nutritional changes in stored grain". In: *Stored-grain ecosystems*. Jayas, D. S., White, N. D. G. and Muir, W. E. (eds.). Marcel Dekker, Inc. New York USA. pp. 325-351

67. Thorpe, G.R. and Hunter, A.J. 1977. "Expressions for pressure and velocity distributions in non-uniformly aerated grain bulks". *Journal of agricultural engineering research.* Vol. 22, pp. 27 – 35.

68. Thorpe, G.R., 1985. "Some fundamental principles and benefits of aeration of stored grain". In: *Preserving Grain Quality by Aeration and in-store Drying.* Proceedings of an international seminar held at Kuala Lumper, Malaysia, 9 - 11 October, 1985.

69. Thorpe, G.R. and Whitaker, S., 1992a. "Local mass and thermal equilibria in ventilated grain bulks. part I: the development of heat and mass conservation equations". *J. stored Pro. Res.* Vol 28 No: 1 pp. 15-27, 1992.

70. Thorpe, G.R. and Whitaker, S., 1992b. "Local mass and thermal equilibria in ventilated grain bulks. part II: the development of constraints". *J. stored Pro. Res.* Vol 28 No: 1 pp. 29-54, 1992.

71. Thorpe, G.R., 1994a. "Modelling heat and mass transfer phenomena in bulks of respiring grains". *Proceedings of the 6th international working conference on stored-product protection.* CAB International , Oxford, U.K., Vol. 1, pp. 369 - 367.

72. Thorpe, G.R., 1994b. *Heating and mass transfer in ventilated bulks of respiring grains - a theoretical analysis and technological application.* Department of civil and building Engineering, Victoria University of Technology, Melbourne, Australia. Report 1/94. pp 90.

73. Thorpe, G.R., 1995a. "Modelling the ecosystem in ventilated farm grain silos". Department of civil and building Engineering, Victoria University of Technology, Melbourne, Australia. Report 1/95. pp 88.

74. Thorpe, G.R., 1995b. "More complete mathematical descriptions of heat and

moisture transfer in respiring bulks of grains". *Agricultureal Engineering Australia*. Vol. 21. 2 (1995), pp. 10 -15.

75. Thorpe, G.R., 1996. *Design of a novel desiccant grain cooling system.* Provisional Paten lodged November 1996.

76. Thorpe, G.R., 1997. "Modelling ecosystems in ventilated conical bottomed farm grain silos". *Ecological Modelling*. Vol. 94 (1997), pp 255 -286.

77. Thorpe, G.R., 1998a. "The modelling and potential applications of a simple solar regeneration grain cooling device". *Postharvest Biology and Technology* (1998) vol. 13 pp 151 - 168.

78. Thorpe, G.R., 1998b. "*siloCAD®* – design software for aerated grain silo" int. The Conference of Engineers in Agriculture, Perth, Australia, no: SEAg 98/045, 1998.

79. Thorpe, G.R., 2001a. "Chapter 4, Physical Basis of aeration". In: *The mechanics and physics of modern grain aeration management.* Shlomo, N. and Ronald, T.N. edited. CRC Press, Boca Raton USA.

80. Thorpe, G.R., 2001b. "Chapter 12, Airflow distribution in ventilated beds of grain". In: *The mechanics and physics of modern grain aeration management.* Shlomo, N. and Ronald, T.N. edited. CRC Press, Boca Raton USA.

81. Walpole, R.E. and Myers R.H. 1993. *Probability and statistics for engineers and scientists.* Fifth edition. MacMillan Publishing Company, New York USA. pp766.

82. White, N. D. G. 1995. "Insects, mite, and insecticides in stored-grain ecosystems". In: *Stored-grain ecosystems.* Jayas, D. S., White, N. D. G. and Muir, W. E. edited. Marcel Dekker, Inc., New York USA. pp. 123 - 167.

83. Wilson, D.M. and Abramson, D., 1992. "Mycotoxins". In: *Storage of cereal grains and their products* (Fourth Edition). Saucer, D.B. (ed.) American Association of Cereal Chemists, Inc. St. Paul, Minnesota, USA. pp. 491-534.

84. Wilson, M.T., 1999. "A model for predicting mould growth and subsequent heat generation in bulk stored grain". *Journal of Stored Products Research*. Vol. 35 (1999) pp 1 - 13.

85. Wilson, S.G. 1993. *A Guide to Grain Aeration: Part 2. Design and Use of Grain Aeration Systems in Warm temperate Climates*. Stored Grain Research Laboratory, CSIRO Division of Entomology. Canberra.

CORRECTION REPORT

One examiner expressed some disquiet about using pseudo wet-bulb temperature to estimate the rate of growth of insect population in stored grain (page 6,7 in thesis). The model that has been used, namely that of Desmarchelier, is probably one of the most reliable available models and we do not share the examiner's concern.

In Chapter 3, cylindrical co-ordinates could have been used but they would ultimately have limited the mathematical model to circular silos. The model presented in the thesis is formulated for arbitrary geometries. Furthermore, the mathematical technique used is quite standard and based on the procedure recommended by Patankar.

One examiner questioned the accuracy of the boundary conditions (page 72). It could be that the examiner has failed to appreciate the subtlety of boundary conditions. In fact they do account for natural convection external to the silo as well as solar radiation. Effectively, a sol-air temperature is used. The thermal diffusivity of steel is such that heat transfer through the steel occurs many orders of magnitude quickly than through the grain and a quasi steady state can be assumed.

In page 89, the data in figure 4.5 are purely empirical and do not relate to a climate model.

One examiner had reservations about not attempting to improve the boundary condition or to look for a physical reason for discrepancies (page 114). The problem of calculating the boundary conditions in the headspace is indeed formidable. It has not got been solved, although an excellent start has been made be Dr Mahesh Prakash, a VU PhD graduate, and the empirical approach used in the thesis is quite satisfactory.

Respiration heat has not included in the mathematical model since in an aerated silo, the respiration heat of grains is negligible and does not influence the temperature and moisture content of grain.

None of the experimental work on the desiccant cooler and silos was carried out by the staff of SGRL. The candidate played the key role in instrumentating the system and solely responsible for programming the data acquisition system.

The examiner made several comments on the thesis. Responses to the more significant ones are:

- Page 12: The check has made and it is right in the thesis that the speed of temperature front is about 100 times of the moisture front.
- Page 15: The examiner is correct in so far as the grain does dry out, but 0.5% is considered to a small amount.
- Page 16: Yes, it illustrates the passage of cooling wetting fronts.
- Page 18: The reason for both field trials was that there was too much silica gel in the system. As a result all of this gel had to be regenerated during the day, which was wasteful of energy.
- Page 33: The specific heat of moisture vapour is accounted separately.
- Page 39: Wilson provided an excellent source of data.
- Page 46: Equations 2.93 to 2.96 have been included for completeness.
- Page 52: Yes, the staggered grid still continuity balanced.
- Page 57: The examiner is strictly correct – we must consider conserved quantities. However, the treatment of the thermal energy balance in the thesis remains rigorously correct.
- Page 69: The examiner is correct – the integral heat of wetting is a function of temperature. Numerical experiments suggested it can be safely ignored.
- Page 89: The figure 4.5 is intelligible to a reader who read s the legend and caption carefully.
- Page 141: The regeneration process was stopped so that the cooling process could be initiated.

03/Jul/2003 1

HP VEE

ave File Name.

 File Format: 2.3

EE Revision: 5.01

ution mode: VEE 5 Compatibility

ram Explorer Overview

Untitled
- Main
  - Recording
  - Recording1
- Globals
  - global1
  - global2
  - range1
  - range10
  - range2
  - range3
  - range4
  - range5
  - range6
  - range7
  - range8
  - range9
  - sheet
  - sheet1

onfiguration

y configuration
- HP-IB0
  - datalogger(@(NOT LIVE))
- HP-IB7
  - dmm(hp34401a@(NOT LIVE))
  - dvm(hp3478a@(NOT LIVE))
  - fgen(hp3325b@(NOT LIVE))
  - funcgen(hp33120a@(NOT LIVE))
  - oscope(hp54600@(NOT LIVE))
  - scope(hp54504a@(NOT LIVE))
- Serial9
  - serial(@(NOT LIVE))
- VXI0
  - vxi(@(NOT LIVE))

(M): Detail View, Total Objects: 13

1 2 3 4 5 6 7

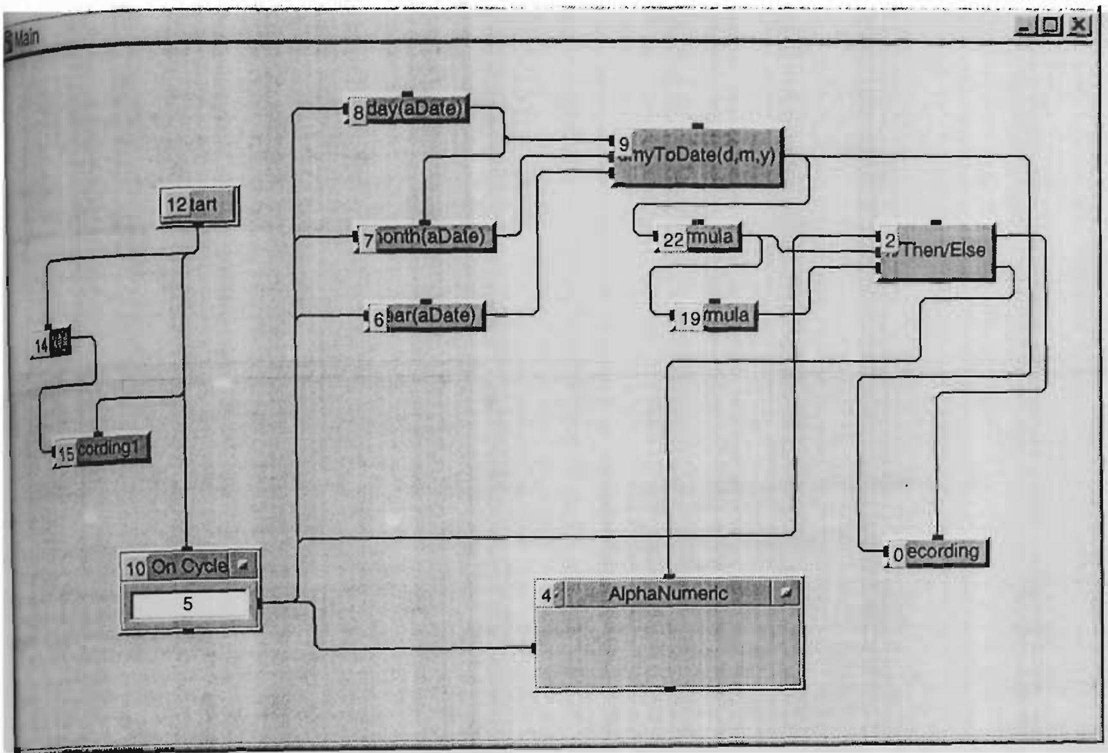

1 2 3 4 5 6 7

```
n "Main"
at: D7  UserObject "Recording"
at: B7  If/Then/Else "If/Then/Else"
If/Else cases: A>B AND A<C
at: D5  AlphaNumeric "AlphaNumeric"
at: B3  Formula "year(aDate)"
Formula: year(aDate)
at: B3  Formula "month(aDate)"
Formula: month(aDate)
at: A3  Formula "mday(aDate)"
Formula: mday(aDate)
at: A5  Formula "dmyToDate(d,m,y)"
Formula: dmyToDate(d,m,y)
 at: D2  On Cycle "On Cycle"
Cycle Time: 5
 at: A2  Start "Start"
 at: B1  Formula "now()"
Formula: now()
 at: C1  UserObject "Recording1"
 at: B5  Formula "Formula"
Formula: C+5
 at: B5  Formula "Formula"
Formula: C+12*3600
```

u 03/Jul/2003

in: Recording (M.0): Detail View, Total Objects: 43

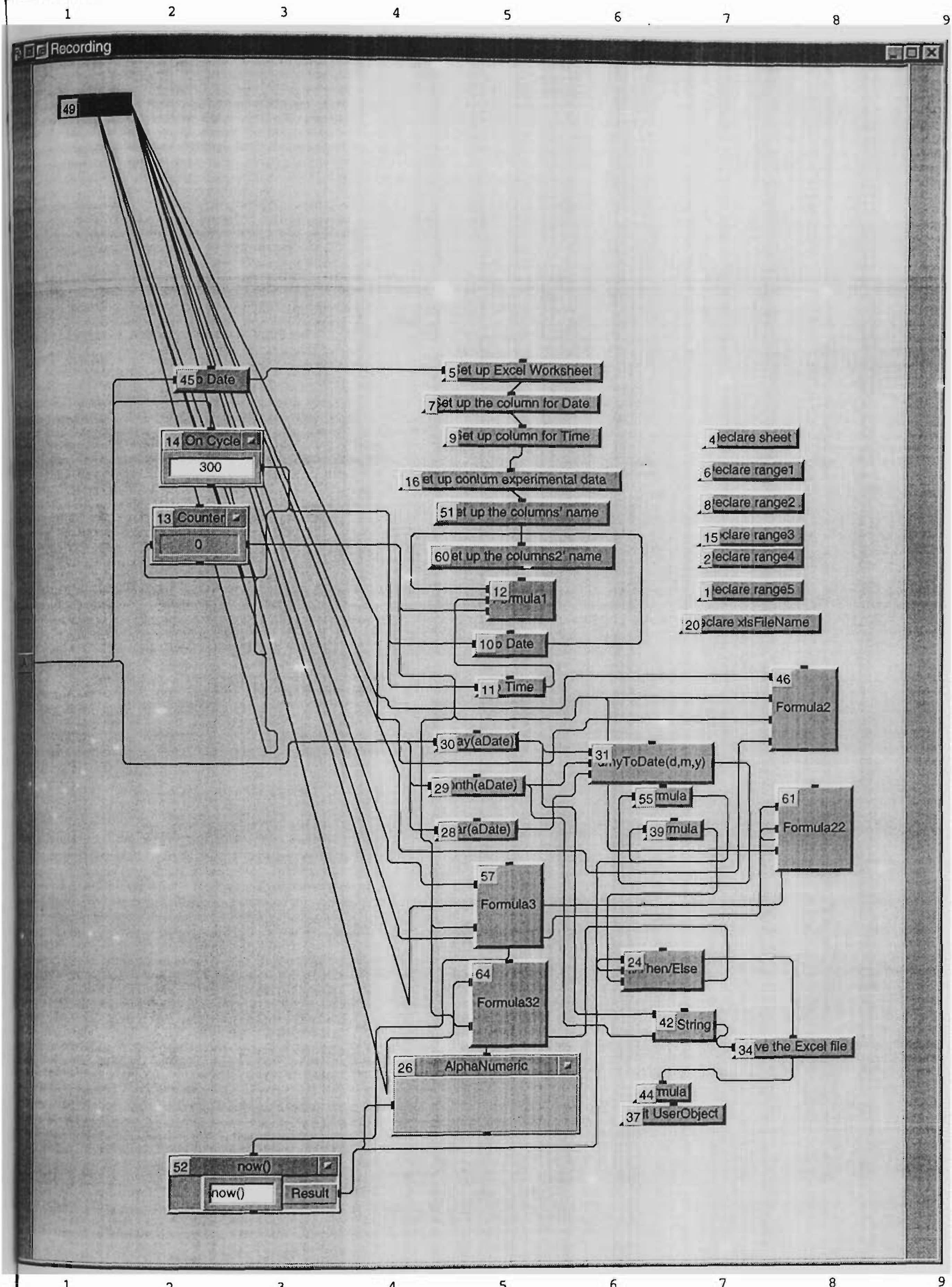


```
rObject  "Recording"
at: E7  Declare Variable "Declare range5"
Variable Scope: Global
Variable Name: "range5"
at: E7  Declare Variable "Declare range4"
Variable Scope: Global
Variable Name: "range4"
at: D7  Declare Variable "Declare sheet"
Variable Scope: Global
Variable Name: "sheet"
at: C5  Formula "Set up Excel Worksheet"
Formula: 5 lines.
 set sheet = CreateObject("Excel.Sheet").worksheets(1);
 sheet.Ap
```

```
 sheet.Application.Windows(1).Caption = "Experiment :"+A;

at: D7  Declare Variable "Declare range1"
Variable Scope: Global
Variable Name: "range1"
at: D5  Formula "Set up the column for Date"
Formula: 4 lines.
 set range1 = sheet.Range("C:C");
 range1.NumberFormat = "d-mmm-yy";

at: D7  Declare Variable "Declare range2"
Variable Scope: Global
Variable Name: "range2"
at: D5  Formula "Set up column for Time"
Formula: 3 lines.
 set range2 = sheet.Range("D:D");
 range2.NumberFormat = "hh:mm:ss";

at: F5  To String "To Date"
Transactions: WRITE TEXT a DATE:DMY EOL
at: F5  To String "To Time"
Transactions: WRITE TEXT a TIME:HMS:H24 EOL
at: E5  Formula "Formula1"
Formula: 5 lines.
 sheet.Cells(C+5,1) = C;
 sheet.Cells(C+5,2) = "Ararat";
 sheet.Cells(C+5,3) = A;
 sheet.Cells(C+5,4)  = B;

at: E2  Counter "Counter"
at: D2  On Cycle "On Cycle"
Cycle Time: 300
at: E7  Declare Variable "Declare range3"
Variable Scope: Global
Variable Name: "range3"
at: D5  Formula "Set up conlum experimental data"
Formula: 3 lines.
 set range3 = sheet.Range("E:CR");
 range3.NumberFormat = "#0.00";

at: F7  Declare Variable "Declare xlsFileName"
Variable Scope: Global
Variable Name: "global1"
at: I6  If/Then/Else "If/Then/Else"
If/Else cases: A>=C AND A<B
at: J5  AlphaNumeric "AlphaNumeric"
at: G5  Formula "year(aDate)"
Formula: year(aDate)
at: G5  Formula "month(aDate)"
Formula: month(aDate)
at: G5  Formula "mday(aDate)"
Formula: mday(aDate)
at: G6  Formula "dmyToDate(d,m,y)"
Formula: dmyToDate(d,m,y)
at: I8  Formula "Save the Excel file"
Formula: sheet.SaveAs(A);
at: J6  Exit UserObject "Exit UserObject"
at: G6  Formula "Formula"
Formula: 2 lines.
 A-300

at: I7  To String "To String"
Transactions: WRITE TEXT b+"m"+a+"d" STR
at: J6  Formula "Formula"
Formula: sheet.Application.Quit();
at: C2  To String "To Date"
Transactions: WRITE TEXT a DATE:DMY EOL
at: F8  Formula "Formula2"
Formula: 38 lines.
 sheet.Cells(B+5,5) = C[0];
 sheet.Cells(B+5,6) = C[1];
 sheet.Cells(B+5,7) = C[2];
 sheet.Cells(B+5,8) = C[3];
 sheet.Cells(B+5,9) = C[4];
 sheet.Cells(B+5,10) = C[5];
 sheet.Cel
```

```
sheet.Cells(B+5,12) = C[7];
sheet.Cells(B+5,13) = C[8];
sheet.Cells(B+5,14) = C[9];
sheet.Cells(B+5,15) = C[10];
sheet.Cells(B+5,16) = NW[0];
sheet.Cells(B+5,17) = NW[1];
sheet.Cells(B+5,18) = NW[2];
sheet.Cells(B+5,19) = NW[3];
sheet.Cells(B+5,20) = NW[4];
sheet.Cells(B+5,21) = NW[5];
sheet.Cells(B+5,22) = NW[6];
sheet.Cells(B+5,23) = NW[7];
sheet.Cells(B+5,24) = NW[8];
sheet.Cells(B+5,25) = NW[9];
sheet.Cells(B+5,26) = NW[10];
sheet.Cells(B+5,27) = NW[11];
sheet.Cells(B+5,95) = NW[12];
sheet.Cells(B+5,28) = SE[0];
sheet.Cells(B+5,29) = SE[1];
sheet.Cells(B+5,30) = SE[2];
sheet.Cells(B+5,31) = SE[3];
sheet.Cells(B+5,32) = SE[4];
sheet.Cells(B+5,33) = SE[5];
sheet.Cells(B+5,34) = SE[6];
sheet.Cells(B+5,35) = SE[7];
sheet.Cells(B+5,36) = SE[8];
sheet.Cells(B+5,37) = SE[9];
sheet.Cells(B+5,38) = SE[10];
sheet.Cells(B+5,39) = SE[11];

8 at: A1  Unknown "Parse Error"
9 at: A1  Unknown "Parse Error"
0 at: A1  Unknown "Parse Error"
1 at: E5  Formula "Set up the columns' name"
Formula: 214 lines.
sheet.Cells(1,1) = "record No:";
sheet.Cells(1,2) = "Location:";
sheet.Cells(1,3) = "Date:";
sheet.Cells(1,4) = "Time";
sheet.Cells(1,5) = "Ch100";
sheet.Cells(2,5) = "oC";
sheet.Cells(3,5) = "C0";
sheet.Cells(4,5) = "9.25 m";
sheet.Cells(1,6) = "Ch101";
sheet.Cells(2,6) = "oC";
sheet.Cells(3,6) = "C1";
sheet.Cells(4,6) = "9 m";
sheet.Cells(1,7) = "Ch102";
sheet.Cells(2,7) = "oC";
sheet.Cells(3,7) = "C2";
sheet.Cells(4,7) = "8 m";
sheet.Cells(1,8) = "Ch103";
sheet.Cells(2,8) = "oC";
sheet.Cells(3,8) = "C3";
sheet.Cells(4,8) = "7 m";
sheet.Cells(1,9) = "Ch104";
sheet.Cells(2,9) = "oC";
sheet.Cells(3,9) = "C4";
sheet.Cells(4,9) = "6 m";
sheet.Cells(1,10) = "Ch105";
sheet.Cells(2,10) = "oC";
sheet.Cells(3,10) = "C5";
sheet.Cells(4,10) = "5 m";
sheet.Cells(1,11) = "Ch106";
sheet.Cells(2,11) = "oC";
sheet.Cells(3,11) = "C6";
sheet.Cells(4,11) = "4 m";
sheet.Cells(1,12) = "Ch107";
sheet.Cells(2,12) = "oC";
sheet.Cells(3,12) = "C7";
sheet.Cells(4,12) = "3 m ";
sheet.Cells(1,13) = "Ch108";
sheet.Cells(2,13) = "oC";
sheet.Cells(3,13) = "C8";
sheet.Cells(4,13) = "2 m";
sheet.Cells(1,14) = "Ch109";
```

```
sheet.Cells(2,14) = "oC";
sheet.Cells(3,14) = "C9";
sheet.Cells(4,14) = "1 m";
sheet.Cells(1,15) = "Ch110";
sheet.Cells(2,15) = "oC";
sheet.Cells(3,15) = "C10";
sheet.Cells(4,15) = "0 m";
sheet.Cells(1,16) = "Ch200";
sheet.Cells(2,16) = "oC";
sheet.Cells(3,16) = "NWT1";
sheet.Cells(4,16) = "1 m";
sheet.Cells(1,17) = "Ch201";
sheet.Cells(2,17) = "oC";
sheet.Cells(3,17) = "NWT2";
sheet.Cells(4,17) = "0.5 m";
sheet.Cells(1,18) = "Ch202";
sheet.Cells(2,18) = "oC";
sheet.Cells(3,18) = "NWT3";
sheet.Cells(4,18) = "0.2 m";
sheet.Cells(1,19) = "Ch203";
sheet.Cells(2,19) = "oC";
sheet.Cells(3,19) = "NWT4";
sheet.Cells(4,19) = "0.1 m";
sheet.Cells(1,20) = "Ch204";
sheet.Cells(2,20) = "oC";
sheet.Cells(3,20) = "NWT5";
sheet.Cells(4,20) = "0.05 m";
sheet.Cells(1,21) = "Ch205";
sheet.Cells(2,21) = "oC";
sheet.Cells(3,21) = "NWT6";
sheet.Cells(4,21) = "0.0 m";
sheet.Cells(1,22) = "Ch206";
sheet.Cells(2,22) = "oC";
sheet.Cells(3,22) = "NWL1";
sheet.Cells(4,22) = "1.0 m";
sheet.Cells(1,23) = "Ch207";
sheet.Cells(2,23) = "oC";
sheet.Cells(3,23) = "NWL2";
sheet.Cells(4,23) = "0.5 m";
sheet.Cells(1,24) = "Ch208";
sheet.Cells(2,24) = "oC";
sheet.Cells(3,24) = "NWL3";
sheet.Cells(4,24) = "0.2 m";
sheet.Cells(1,25) = "Ch209";
sheet.Cells(2,25) = "oC";
sheet.Cells(3,25) = "NWL4";
sheet.Cells(4,25) = "0.1 m";
sheet.Cells(1,26) = "Ch210";
sheet.Cells(2,26) = "oC";
sheet.Cells(3,26) = "NWL5";
sheet.Cells(4,26) = "0.05 m";
sheet.Cells(1,27) = "Ch211";
sheet.Cells(2,27) = "oC";
sheet.Cells(3,27) = "NWL6";
sheet.Cells(4,27) = "0.0 m";
sheet.Cells(1,28) = "Ch300";
sheet.Cells(2,28) = "oC";
sheet.Cells(3,28) = "SET1";
sheet.Cells(4,28) = "1.0 m";
sheet.Cells(1,29) = "Ch301";
sheet.Cells(2,29) = "oC";
sheet.Cells(3,29) = "SET2";
sheet.Cells(4,29) = "0.5 m";
sheet.Cells(1,30) = "Ch302";
sheet.Cells(2,30) = "oC";
sheet.Cells(3,30) = "SET3";
sheet.Cells(4,30) = "0.2 m";
sheet.Cells(1,31) = "Ch303";
sheet.Cells(2,31) = "oC";
sheet.Cells(3,31) = "SET4";
sheet.Cells(4,31) = "0.1 m";
sheet.Cells(1,32) = "Ch304";
sheet.Cells(2,32) = "oC";
sheet.Cells(3,32) = "SET5";
sheet.Cells(4,32) = "0.05 m";
sheet.Cells(1,33) = "Ch305";
sheet.Cells(2,33) = "oC";
sheet.C
```

```
sheet.Cells(4,33) = "0.0 m";
sheet.Cells(1,34) = "Ch306";
sheet.Cells(2,34) = "oC";
sheet.Cells(3,34) = "SEL1";
sheet.Cells(4,34) = "1.0 m";
sheet.Cells(1,35) = "Ch307";
sheet.Cells(2,35) = "oC";
sheet.Cells(3,35) = "SEL2";
sheet.Cells(4,35) = "0.5 m";
sheet.Cells(1,36) = "Ch308";
sheet.Cells(2,36) = "oC";
sheet.Cells(3,36) = "SEL3";
sheet.Cells(4,36) = "0.2 m";
sheet.Cells(1,37) = "Ch309";
sheet.Cells(2,37) = "oC";
sheet.Cells(3,37) = "SEL4";
sheet.Cells(4,37) = "0.1 m";
sheet.Cells(1,38) = "Ch310";
sheet.Cells(2,38) = "oC";
sheet.Cells(3,38) = "SEL5";
sheet.Cells(4,38) = "0.05 m";
sheet.Cells(1,39) = "Ch311";
sheet.Cells(2,39) = "oC";
sheet.Cells(3,39) = "SEL6";
sheet.Cells(4,39) = "0.0 m";
sheet.Cells(1,40) = "Ch400";
sheet.Cells(2,40) = "oC";
sheet.Cells(3,40) = "C1";
sheet.Cells(4,40) = "9 m";
sheet.Cells(1,41) = "Ch401";
sheet.Cells(2,41) = "% rh";
sheet.Cells(3,41) = "C1";
sheet.Cells(4,41) = "9 m";
sheet.Cells(1,42) = "Ch402";
sheet.Cells(2,42) = "oC";
sheet.Cells(3,42) = "C4";
sheet.Cells(4,42) = "7 m";
sheet.Cells(1,43) = "Ch403";
sheet.Cells(2,43) = "% rh";
sheet.Cells(3,43) = "C4";
sheet.Cells(4,43) = "7 m";
sheet.Cells(1,44) = "Ch404";
sheet.Cells(2,44) = "oC";
sheet.Cells(3,44) = "C6";
sheet.Cells(4,44) = "5 m";
sheet.Cells(1,45) = "Ch405";
sheet.Cells(2,45) = "% rh";
sheet.Cells(3,45) = "C6";
sheet.Cells(4,45) = "5 m";
sheet.Cells(1,46) = "Ch406";
sheet.Cells(2,46) = "oC";
sheet.Cells(3,46) = "C8";
sheet.Cells(4,46) = "3 m";
sheet.Cells(1,47) = "Ch407";
sheet.Cells(2,47) = "% rh";
sheet.Cells(3,47) = "C8";
sheet.Cells(4,47) = "3 m";
sheet.Cells(1,48) = "Ch408";
sheet.Cells(2,48) = "oC";
sheet.Cells(3,48) = "NWT5";
sheet.Cells(4,48) = "0.05 m";
sheet.Cells(1,49) = "Ch409";
sheet.Cells(2,49) = "% rh";
sheet.Cells(3,49) = "NWT5";
sheet.Cells(4,49) = "0.05 m";
sheet.Cells(1,50) = "Ch410";
sheet.Cells(2,50) = "oC";
sheet.Cells(3,50) = "NWL5";
sheet.Cells(4,50) = "0.05 m";
sheet.Cells(1,51) = "Ch411";
sheet.Cells(2,51) = "% rh";
sheet.Cells(3,51) = "NWL5";
sheet.Cells(4,51) = "0.05 m";
sheet.Cells(1,52) = "Ch412";
sheet.Cells(2,52) = "oC";
sheet.Cells(3,52) = "SET5";
sheet.Cells(4,52) = "0.05 m";
sheet.Cel
```

```
sheet.Cells(2,53) = "% rh";
sheet.Cells(3,53) = "SET5";
sheet.Cells(4,53) = "0.05 m";
sheet.Cells(1,54) = "Ch414";
sheet.Cells(2,54) = "oC";
sheet.Cells(3,54) = "SEL5";
sheet.Cells(4,54) = "0.05 m";
sheet.Cells(1,55) = "Ch415";
sheet.Cells(2,55) = "% rh";
sheet.Cells(3,55) = "SEL5";
sheet.Cells(4,55) = "0.05 m";
```

```
52 at: K3  Formula "now()"
Formula: now()
55 at: G6  Formula "Formula"
Formula: 2 lines.
  A+36*3600

56 at: A1  Unknown "Parse Error"
57 at: H5  Formula "Formula3"
Formula: 17 lines.
  sheet.Cells(B+5,40) = RH[0]*100-40;
  sheet.Cells(B+5,41) = RH[1]*100;
  sheet.Cells(B+5,42) = RH[2]*100-40;
  sheet.Cells(B+5,43) = RH[3]*100;
  sheet.Cells(B+5,44) = RH[4]*100-40;
  sheet.Cells(B+5,45) = RH[5]*100;
  sheet.Cells(B+5,46) = RH[6]*100-40;
  sheet.Cells(B+5,47) = RH[7]*100;
  sheet.Cells(B+5,48) = RH[8]*100-40;
  sheet.Cells(B+5,49) = RH[9]*100;
  sheet.Cells(B+5,50) = RH[10]*100-40;
  sheet.Cells(B+5,51) = RH[11]*100;
  sheet.Cells(B+5,52) = RH[12]*100-40;
  sheet.Cells(B+5,53) = RH[13]*100;
  sheet.Cells(B+5,54) = RH[14]*100-40;
  sheet.Cells(B+5,55) = RH[15]*100;

0 at: E5  Formula "Set up the columns2' name"
Formula: 169 lines.
  sheet.Cells(1,56) = "Ch505:";
  sheet.Cells(2,56) = "oC";
  sheet.Cells(3,56) = "Small 1";
  sheet.Cells(4,56) = "7 m";
  sheet.Cells(1,57) = "Ch506";
  sheet.Cells(2,57) = "oC";
  sheet.Cells(3,57) = "Small 2";
  sheet.Cells(4,57) = "6  m";
  sheet.Cells(1,58) = "Ch507";
  sheet.Cells(2,58) = "oC";
  sheet.Cells(3,58) = "Small 3";
  sheet.Cells(4,58) = "5 m";
  sheet.Cells(1,59) = "Ch508";
  sheet.Cells(2,59) = "oC";
  sheet.Cells(3,59) = "Small 4";
  sheet.Cells(4,59) = "4 m";
  sheet.Cells(1,60) = "Ch509";
  sheet.Cells(2,60) = "oC";
  sheet.Cells(3,60) = "Small 5";
  sheet.Cells(4,60) = "3 m";
  sheet.Cells(1,61) = "Ch510";
  sheet.Cells(2,61) = "oC";
  sheet.Cells(3,61) = "Small 6";
  sheet.Cells(4,61) = "2 m";
  sheet.Cells(1,62) = "Ch511";
  sheet.Cells(2,62) = "oC";
  sheet.Cells(3,62) = "Small 7";
  sheet.Cells(4,62) = "1 m";
  sheet.Cells(1,63) = "Ch600";
  sheet.Cells(2,63) = "oC";
  sheet.Cells(3,63) = "  ";
  sheet.Ce
```

```
sheet.Cells(1,64) = "Ch601";
sheet.Cells(2,64) = "oC";
sheet.Cells(3,64) = "  ";
sheet.Cells(4,64) = "  ";
sheet.Cells(1,65) = "Ch602";
sheet.Cells(2,65) = "oC";
sheet.Cells(3,65) = "  ";
sheet.Cells(4,65) = "  ";
sheet.Cells(1,66) = "Ch603";
sheet.Cells(2,66) = "oC";
sheet.Cells(3,66) = "  ";
sheet.Cells(4,66) = "  ";
sheet.Cells(1,67) = "Ch604";
sheet.Cells(2,67) = "oC";
sheet.Cells(3,67) = "  ";
sheet.Cells(4,67) = "  ";
sheet.Cells(1,68) = "Ch605";
sheet.Cells(2,68) = "oC";
sheet.Cells(3,68) = "  ";
sheet.Cells(4,68) = "  ";
sheet.Cells(1,69) = "Ch606";
sheet.Cells(2,69) = "oC";
sheet.Cells(3,69) = "  ";
sheet.Cells(4,69) = "  ";
sheet.Cells(1,70) = "Ch607";
sheet.Cells(2,70) = "oC";
sheet.Cells(3,70) = "  ";
sheet.Cells(4,70) = "  ";
sheet.Cells(1,71) = "Ch608";
sheet.Cells(2,71) = "oC";
sheet.Cells(3,71) = "  ";
sheet.Cells(4,71) = "  ";
sheet.Cells(1,72) = "Ch609";
sheet.Cells(2,72) = "oC";
sheet.Cells(3,72) = "  ";
sheet.Cells(4,72) = "  ";
sheet.Cells(1,73) = "Ch610";
sheet.Cells(2,73) = "oC";
sheet.Cells(3,73) = "  ";
sheet.Cells(4,73) = "  ";
sheet.Cells(1,74) = "Ch611";
sheet.Cells(2,74) = "oC";
sheet.Cells(3,74) = "  ";
sheet.Cells(4,74) = "  ";
sheet.Cells(1,75) = "Ch612";
sheet.Cells(2,75) = "oC";
sheet.Cells(3,75) = "  ";
sheet.Cells(4,75) = "  ";
sheet.Cells(1,76) = "Ch613";
sheet.Cells(2,76) = "oC";
sheet.Cells(3,76) = "  ";
sheet.Cells(4,76) = "  ";
sheet.Cells(1,77) = "Ch614";
sheet.Cells(2,77) = "oC";
sheet.Cells(3,77) = "  ";
sheet.Cells(4,77) = "  ";
sheet.Cells(1,78) = "Ch615";
sheet.Cells(2,78) = "oC";
sheet.Cells(3,78) = "  ";
sheet.Cells(4,78) = "  ";
sheet.Cells(1,79) = "Ch700";
sheet.Cells(2,79) = "oC";
sheet.Cells(3,79) = "  ";
sheet.Cells(4,79) = " ";
sheet.Cells(1,80) = "Ch701";
sheet.Cells(2,80) = "% rh";
sheet.Cells(3,80) = "  ";
sheet.Cells(4,80) = "  ";
sheet.Cells(1,81) = "Ch702";
sheet.Cells(2,81) = "oC";
sheet.Cells(3,81) = "  ";
sheet.Cells(4,81) = "  ";
sheet.Cells(1,82) = "Ch703";
sheet.Cells(2,82) = "% rh";
sheet.Cells(3,82) = "  ";
sheet.Cells(4,82) = " ";
sheet.Cells(1,83) = "Ch704";
sheet.Cells(2,83) = "oC";
```

```
sheet.Cells(3,83) = "  ";
sheet.Cells(4,83) = "  ";
sheet.Cells(1,84) = "Ch705";
sheet.Cells(2,84) = "% rh";
sheet.Cells(3,84) = "  ";
sheet.Cells(4,84) = "  ";
sheet.Cells(1,85) = "Ch706";
sheet.Cells(2,85) = "oC";
sheet.Cells(3,85) = "  ";
sheet.Cells(4,85) = "  ";
sheet.Cells(1,86) = "Ch707";
sheet.Cells(2,86) = "% rh";
sheet.Cells(3,86) = "  ";
sheet.Cells(4,86) = "  ";
sheet.Cells(1,87) = "Ch708";
sheet.Cells(2,87) = "oC";
sheet.Cells(3,87) = "  ";
sheet.Cells(4,87) = "  ";
sheet.Cells(1,88) = "Ch709";
sheet.Cells(2,88) = "% rh";
sheet.Cells(3,88) = "  ";
sheet.Cells(4,88) = "  ";
sheet.Cells(1,89) = "Ch710";
sheet.Cells(2,89) = "oC";
sheet.Cells(3,89) = "   ";
sheet.Cells(4,89) = "  ";
sheet.Cells(1,90) = "Ch711";
sheet.Cells(2,90) = "% rh";
sheet.Cells(3,90) = "  ";
sheet.Cells(4,90) = "  ";
sheet.Cells(1,91) = "Ch712";
sheet.Cells(2,91) = "oC";
sheet.Cells(3,91) = "  ";
sheet.Cells(4,91) = "  ";
sheet.Cells(1,92) = "Ch713";
sheet.Cells(2,92) = "% rh";
sheet.Cells(3,92) = "  ";
sheet.Cells(4,92) = "  ";
sheet.Cells(1,93) = "Ch714";
sheet.Cells(2,93) = "oC";
sheet.Cells(3,93) = "  ";
sheet.Cells(4,93) = " ";
sheet.Cells(1,94) = "Ch715";
sheet.Cells(2,94) = "% rh";
sheet.Cells(3,94) = "  ";
sheet.Cells(4,94) = "  ";
sheet.Cells(1,95) = "Ch212";
sheet.Cells(2,95) = "oC";
sheet.Cells(3,95) = " Channel ";
sheet.Cells(4,95) = "  ";
```

l at: G8 Formula "Formula22"
Formula: 26 lines.

```
sheet.Cells(B+5,56) = small[0];
sheet.Cells(B+5,57) = small[1];
sheet.Cells(B+5,58) =small[2];
sheet.Cells(B+5,59) = small[3];
sheet.Cells(B+5,60) = small[4];
sheet.Cells(B+5,61) = small[5];
sheet.Cells(B+5,62) = small[6];
sheet.Cells(B+5,63) = Card6[0];
sheet.Cells(B+5,64) = Card6[1];
sheet.Cells(B+5,65) = Card6[2];
sheet.Cells(B+5,66) = Card6[3];
sheet.Cells(B+5,67) = Card6[4];
sheet.Cells(B+5,68) = Card6[5];
sheet.Cells(B+5,69) = Card6[6];
sheet.Cells(B+5,70) = Card6[7];
sheet.Cells(B+5,71) = Card6[8];
sheet.Ce
```

```
sheet.Cells(B+5,73)  =  Card6[10];
sheet.Cells(B+5,74)  =  Card6[11];
sheet.Cells(B+5,75)  =  Card6[12];
sheet.Cells(B+5,76)  =  Card6[13];
sheet.Cells(B+5,77)  =  Card6[14];
sheet.Cells(B+5,78)  =  Card6[15];
```

```
at: A1  Unknown "Parse Error"
at: A1  Unknown "Parse Error"
at: I5  Formula "Formula32"
Formula: 17 lines.
sheet.Cells(B+5,79)  =  RH[0]*100-40;
sheet.Cells(B+5,80)  =  RH[1]*100;
sheet.Cells(B+5,81)  =  RH[2]*100-40;
sheet.Cells(B+5,82)  =  RH[3]*100;
sheet.Cells(B+5,83)  =  RH[4]*100-40;
sheet.Cells(B+5,84)  =  RH[5]*100;
sheet.Cells(B+5,85)  =  RH[6]*100-40;
sheet.Cells(B+5,86)  =  RH[7]*100;
sheet.Cells(B+5,87)  =  RH[8]*100-40;
sheet.Cells(B+5,88)  =  RH[9]*100;
sheet.Cells(B+5,89)  =  RH[10]*100-40;
sheet.Cells(B+5,90)  =  RH[11]*100;
sheet.Cells(B+5,91)  =  RH[12]*100-40;
sheet.Cells(B+5,92)  =  RH[13]*100;
sheet.Cells(B+5,93)  =  RH[14]*100-40;
sheet.Cells(B+5,94)  =  RH[15]*100;
```

```
at: A1  Unknown "Parse Error"
```

Jul/2003

t Recording: Panel View

200 300 400 500 600 700

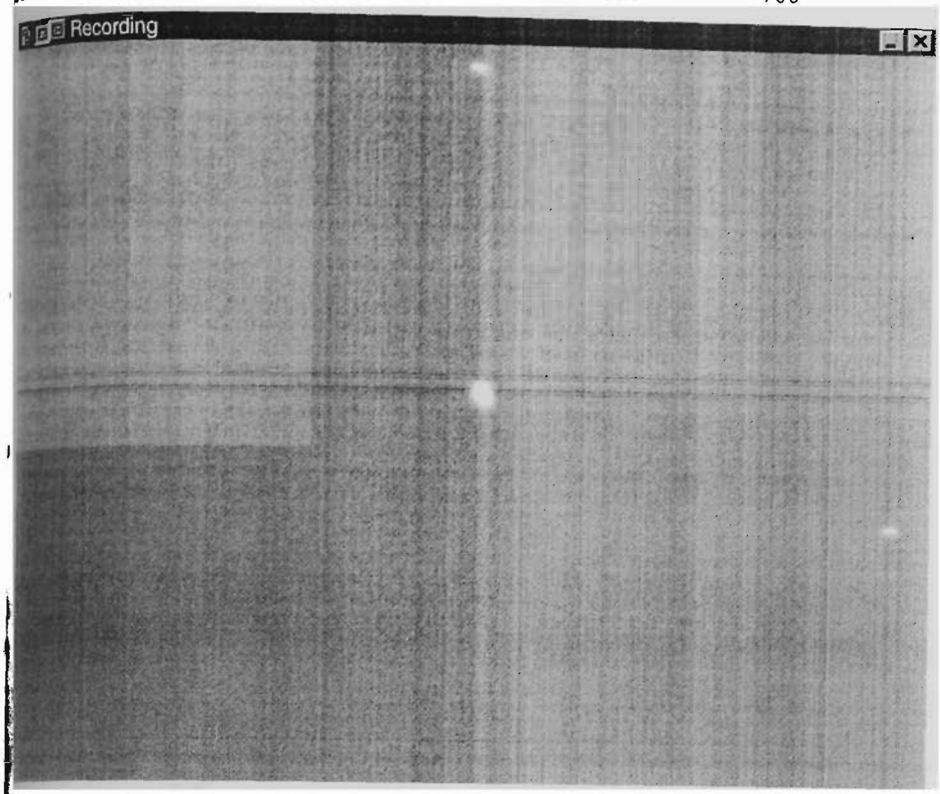

PanelView "Recording" (w=410, h=300)

200 300 400 500 600 700

1 2 3 4 5 6 7 8

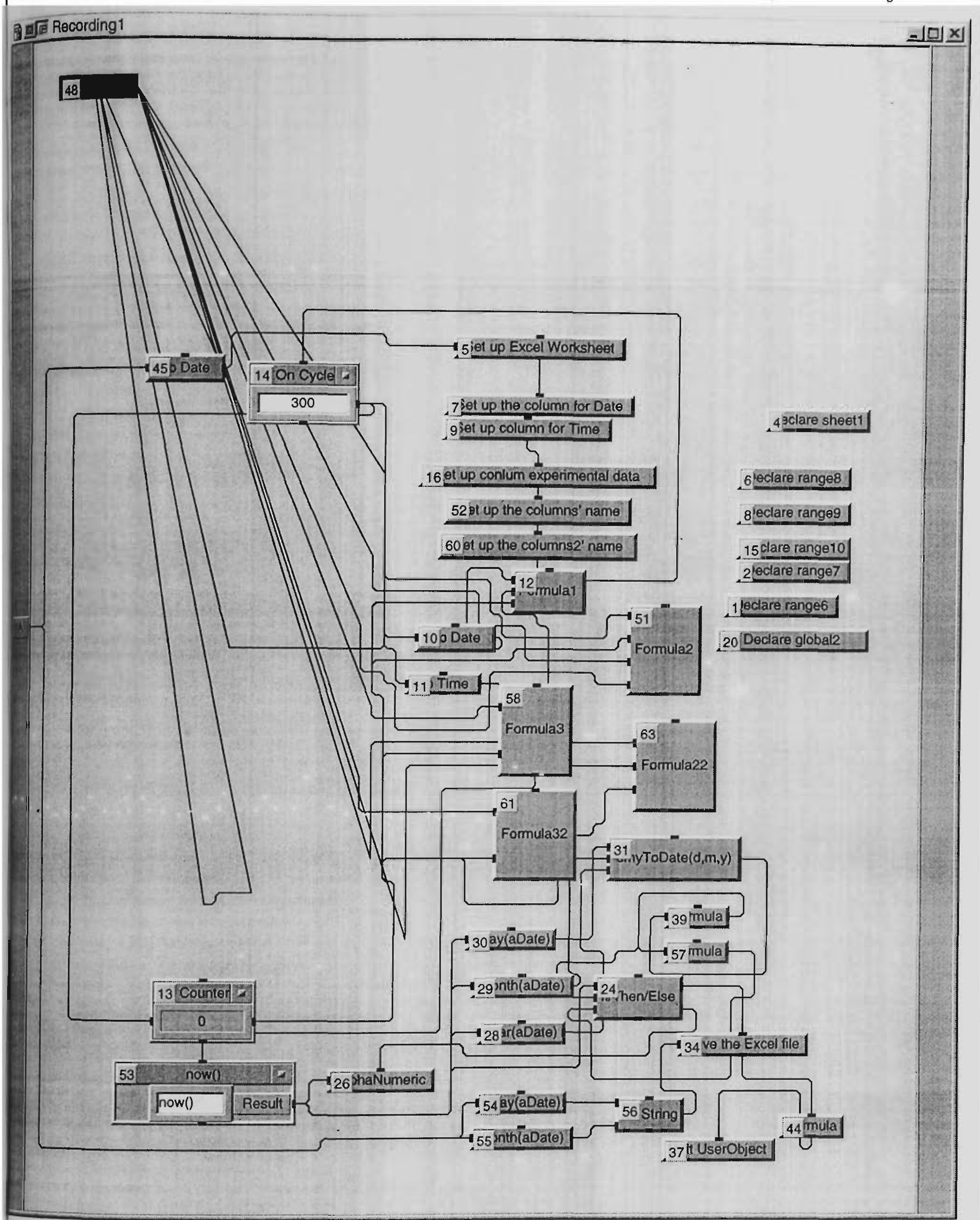

1 2 3 4 5 6 7 8

```
rObject  "Recording1"
 at: E7  Declare Variable "Declare range6"
 Variable Scope: Global
 Variable Name: "range6"
 at: E7  Declare Variable "Declare range7"
 Variable Scope: Global
 Variable Name: "range7"
 at: D7  Declare Variable "Declare sheet1"
 Variable Scope: Global
 Variable Name: "sheet1"
 at: C5  Formula "Set up Excel Worksheet"
 Formula: 5 lines.
  set sheet = CreateObject("Excel.Sheet").worksheets(1);
  sheet.Application.Visible = TRUE;
  sheet.Application.Windows(1).Caption = "Experiment :"+A;


 at: D7  De
 Variable Sc
```

```
 Variable Name: "range8"
7 at: D5  Formula "Set up the column for Date"
 Formula: 4 lines.
   set range1 = sheet.Range("C:C");
   range1.NumberFormat = "d-mmm-yy";


8 at: D7  Declare Variable "Declare range9"
 Variable Scope: Global
 Variable Name: "range9"
9 at: D5  Formula "Set up column for Time"
 Formula: 3 lines.
   set range2 = sheet.Range("D:D");
   range2.NumberFormat = "hh:mm:ss";

10 at: F4  To String "To Date"
 Transactions: WRITE TEXT a DATE:DMY EOL
11 at: F4  To String "To Time"
 Transactions: WRITE TEXT a TIME:HMS:H24 EOL
12 at: E5  Formula "Formula1"
 Formula: 5 lines.
   sheet.Cells(C+5,1) = C;
   sheet.Cells(C+5,2) = "Ararat";
   sheet.Cells(C+5,3) = A;
   sheet.Cells(C+5,4)  = B;

13 at: I2  Counter "Counter"
14 at: C3  On Cycle "On Cycle"
 Cycle Time: 300
15 at: E7  Declare Variable "Declare range10"
 Variable Scope: Global
 Variable Name: "range10"
16 at: D5  Formula "Set up conlum experimental data"
 Formula: 3 lines.
   set range3 = sheet.Range("E:CR");
   range3.NumberFormat = "#0.00";

20 at: F7  Declare Variable "Declare global2"
 Variable Scope: Global
 Variable Name: "global2"
24 at: I6  If/Then/Else "If/Then/Else"
 If/Else cases: A>=C AND A<B
26 at: I4  AlphaNumeric "AlphaNumeric"
28 at: I5  Formula "year(aDate)"
 Formula: year(aDate)
9 at: I5  Formula "month(aDate)"
 Formula: month(aDate)
0 at: H5  Formula "mday(aDate)"
 Formula: mday(aDate)
1 at: G6  Formula "dmyToDate(d,m,y)"
 Formula: dmyToDate(d,m,y)
4 at: I7  Formula "Save the Excel file"
 Formula: sheet.SaveAs(A);
7 at: J7  Exit UserObject "Exit UserObject"
9 at: H6  Formula "Formula"
 Formula: 2 lines.
   A+12*3600

4 at: J7  Formula "Formula"
 Formula: sheet.Application.Quit();
5 at: C2  To String "To Date"
 Transactions: WRITE TEXT a DATE:DMY EOL
6 at: A1  Unknown "Parse Error"
7 at: A1  Unknown "Parse Error"
8 at: A1  Unknown "Parse Error"
1 at: F6  Formula "Formula2"
 Formula: 38 lines.
   sheet.Cells(B+5,5) = C[0];
   sheet.Cells(B+5,6) = C[1];
   sheet.Cells(B+5,7) = C[2];
   sheet.Cells(B+5,8) = C[3];
   sheet.Cells(B+5,9) = C[4];
   sheet.Cells(B+5,10) = C[5];
   sheet.Cells(B+5,11) = C[6];
   sheet.Cells(B+5,12) = C[7];
   sheet.Cells(B+5,13) = C[8];
   sheet.Cells(B+5,14) = C[9];
```

```
sheet.Cells(B+5,15) = C[10];
sheet.Cells(B+5,16) = NW[0];
sheet.Cells(B+5,17) = NW[1];
sheet.Cells(B+5,18) = NW[2];
sheet.Cells(B+5,19) = NW[3];
sheet.Cells(B+5,20) = NW[4];
sheet.Cells(B+5,21) = NW[5];
sheet.Cells(B+5,22) = NW[6];
sheet.Cells(B+5,23) = NW[7];
sheet.Cells(B+5,24) = NW[8];
sheet.Cells(B+5,25) = NW[9];
sheet.Cells(B+5,26) = NW[10];
sheet.Cells(B+5,27) = NW[11];
sheet.Cells(B+5,95) = NW[12];
sheet.Cells(B+5,28) = SE[0];
sheet.Cells(B+5,29) = SE[1];
sheet.Cells(B+5,30) = SE[2];
sheet.Cells(B+5,31) = SE[3];
sheet.Cells(B+5,32) = SE[4];
sheet.Cells(B+5,33) = SE[5];
sheet.Cells(B+5,34) = SE[6];
sheet.Cells(B+5,35) = SE[7];
sheet.Cells(B+5,36) = SE[8];
sheet.Cells(B+5,37) = SE[9];
sheet.Cells(B+5,38) = SE[10];
sheet.Cells(B+5,39) = SE[11];

52 at: D5  Formula "Set up the columns' name"
Formula: 217 lines.
sheet.Cells(1,1) = "record No:";
sheet.Cells(1,2) = "Location:";
sheet.Cells(1,3) = "Date:";
sheet.Cells(1,4) = "Time";
sheet.Cells(1,5) = "Ch100";
sheet.Cells(2,5) = "oC";
sheet.Cells(3,5) = "C0";
sheet.Cells(4,5) = "9.25 m";
sheet.Cells(1,6) = "Ch101";
sheet.Cells(2,6) = "oC";
sheet.Cells(3,6) = "C1";
sheet.Cells(4,6) = "9 m";
sheet.Cells(1,7) = "Ch102";
sheet.Cells(2,7) = "oC";
sheet.Cells(3,7) = "C2";
sheet.Cells(4,7) = "8 m";
sheet.Cells(1,8) = "Ch103";
sheet.Cells(2,8) = "oC";
sheet.Cells(3,8) = "C3";
sheet.Cells(4,8) = "7 m";
sheet.Cells(1,9) = "Ch104";
sheet.Cells(2,9) = "oC";
sheet.Cells(3,9) = "C4";
sheet.Cells(4,9) = "6 m";
sheet.Cells(1,10) = "Ch105";
sheet.Cells(2,10) = "oC";
sheet.Cells(3,10) = "C5";
sheet.Cells(4,10) = "5 m";
sheet.Cells(1,11) = "Ch106";
sheet.Cells(2,11) = "oC";
sheet.Cells(3,11) = "C6";
sheet.Cells(4,11) = "4 m";
sheet.Cells(1,12) = "Ch107";
sheet.Cells(2,12) = "oC";
sheet.Cells(3,12) = "C7";
sheet.Cells(4,12) = "3 m ";
sheet.Cells(1,13) = "Ch108";
sheet.Cells(2,13) = "oC";
sheet.Cells(3,13) = "C8";
sheet.Cells(4,13) = "2 m";
sheet.Cells(1,14) = "Ch109";
sheet.Cells(2,14) = "oC";
sheet.Cells(3,14) = "C9";
sheet.Cells(4,14) = "1 m";
sheet.Cells(1,15) = "Ch110";
sheet.Cells(2,15) = "oC";
sheet.Cells(3,15) = "C10";
sheet.Cel
```

```
sheet.Cells(1,16) = "Ch200";
sheet.Cells(2,16) = "oC";
sheet.Cells(3,16) = "NWT1";
sheet.Cells(4,16) = "1 m";
sheet.Cells(1,17) = "Ch201";
sheet.Cells(2,17) = "oC";
sheet.Cells(3,17) = "NWT2";
sheet.Cells(4,17) = "0.5 m";
sheet.Cells(1,18) = "Ch202";
sheet.Cells(2,18) = "oC";
sheet.Cells(3,18) = "NWT3";
sheet.Cells(4,18) = "0.2 m";
sheet.Cells(1,19) = "Ch203";
sheet.Cells(2,19) = "oC";
sheet.Cells(3,19) = "NWT4";
sheet.Cells(4,19) = "0.1 m";
sheet.Cells(1,20) = "Ch204";
sheet.Cells(2,20) = "oC";
sheet.Cells(3,20) = "NWT5";
sheet.Cells(4,20) = "0.05 m";
sheet.Cells(1,21) = "Ch205";
sheet.Cells(2,21) = "oC";
sheet.Cells(3,21) = "NWT6";
sheet.Cells(4,21) = "0.0 m";
sheet.Cells(1,22) = "Ch206";
sheet.Cells(2,22) = "oC";
sheet.Cells(3,22) = "NWL1";
sheet.Cells(4,22) = "1.0 m";
sheet.Cells(1,23) = "Ch207";
sheet.Cells(2,23) = "oC";
sheet.Cells(3,23) = "NWL2";
sheet.Cells(4,23) = "0.5 m";
sheet.Cells(1,24) = "Ch208";
sheet.Cells(2,24) = "oC";
sheet.Cells(3,24) = "NWL3";
sheet.Cells(4,24) = "0.2 m";
sheet.Cells(1,25) = "Ch209";
sheet.Cells(2,25) = "oC";
sheet.Cells(3,25) = "NWL4";
sheet.Cells(4,25) = "0.1 m";
sheet.Cells(1,26) = "Ch210";
sheet.Cells(2,26) = "oC";
sheet.Cells(3,26) = "NWL5";
sheet.Cells(4,26) = "0.05 m";
sheet.Cells(1,27) = "Ch211";
sheet.Cells(2,27) = "oC";
sheet.Cells(3,27) = "NWL6";
sheet.Cells(4,27) = "0.0 m";
sheet.Cells(1,28) = "Ch300";
sheet.Cells(2,28) = "oC";
sheet.Cells(3,28) = "SET1";
sheet.Cells(4,28) = "1.0 m";
sheet.Cells(1,29) = "Ch301";
sheet.Cells(2,29) = "oC";
sheet.Cells(3,29) = "SET2";
sheet.Cells(4,29) = "0.5 m";
sheet.Cells(1,30) = "Ch302";
sheet.Cells(2,30) = "oC";
sheet.Cells(3,30) = "SET3";
sheet.Cells(4,30) = "0.2 m";
sheet.Cells(1,31) = "Ch303";
sheet.Cells(2,31) = "oC";
sheet.Cells(3,31) = "SET4";
sheet.Cells(4,31) = "0.1 m";
sheet.Cells(1,32) = "Ch304";
sheet.Cells(2,32) = "oC";
sheet.Cells(3,32) = "SET5";
sheet.Cells(4,32) = "0.05 m";
sheet.Cells(1,33) = "Ch305";
sheet.Cells(2,33) = "oC";
sheet.Cells(3,33) = "SET6";
sheet.Cells(4,33) = "0.0 m";
sheet.Cells(1,34) = "Ch306";
sheet.Cells(2,34) = "oC";
sheet.Cells(3,34) = "SEL1";
sheet.Cells(4,34) = "1.0 m";
sheet.Cells(1,35) = "Ch307";
sheet.Ce
```

```
sheet.Cells(3,35) = "SEL2";
sheet.Cells(4,35) = "0.5 m";
sheet.Cells(1,36) = "Ch308";
sheet.Cells(2,36) = "oC";
sheet.Cells(3,36) = "SEL3";
sheet.Cells(4,36) = "0.2 m";
sheet.Cells(1,37) = "Ch309";
sheet.Cells(2,37) = "oC";
sheet.Cells(3,37) = "SEL4";
sheet.Cells(4,37) = "0.1 m";
sheet.Cells(1,38) = "Ch310";
sheet.Cells(2,38) = "oC";
sheet.Cells(3,38) = "SEL5";
sheet.Cells(4,38) = "0.05 m";
sheet.Cells(1,39) = "Ch311".
sheet.Cells(2,39) = "oC";
sheet.Cells(3,39) = "SEL6";
sheet.Cells(4,39) = "0.0 m";
sheet.Cells(1,40) = "Ch400";
sheet.Cells(2,40) = "oC";
sheet.Cells(3,40) = "C1";
sheet.Cells(4,40) = "9 m";
sheet.Cells(1,41) = "Ch401";
sheet.Cells(2,41) = "% rh";
sheet.Cells(3,41) = "C1";
sheet.Cells(4,41) = "9 m";
sheet.Cells(1,42) = "Ch402";
sheet.Cells(2,42) = "oC";
sheet.Cells(3,42) = "C4";
sheet.Cells(4,42) = "7 m";
sheet.Cells(1,43) = "Ch403";
sheet.Cells(2,43) = "% rh";
sheet.Cells(3,43) = "C4";
sheet.Cells(4,43) = "7 m";
sheet.Cells(1,44) = "Ch404";
sheet.Cells(2,44) = "oC";
sheet.Cells(3,44) = "C6";
sheet.Cells(4,44) = "5 m";
sheet.Cells(1,45) = "Ch405";
sheet.Cells(2,45) = "% rh";
sheet.Cells(3,45) = "C6";
sheet.Cells(4,45) = "5 m";
sheet.Cells(1,46) = "Ch406";
sheet.Cells(2,46) = "oC";
sheet.Cells(3,46) = "C8";
sheet.Cells(4,46) = "3 m";
sheet.Cells(1,47) = "Ch407";
sheet.Cells(2,47) = "% rh";
sheet.Cells(3,47) = "C8";
sheet.Cells(4,47) = "3 m";
sheet.Cells(1,48) = "Ch408";
sheet.Cells(2,48) = "oC";
sheet.Cells(3,48) = "NWT5";
sheet.Cells(4,48) = "0.05 m";
sheet.Cells(1,49) = "Ch409";
sheet.Cells(2,49) = "% rh";
sheet.Cells(3,49) = "NWT5";
sheet.Cells(4,49) = "0.05 m";
sheet.Cells(1,50) = "Ch410";
sheet.Cells(2,50) = "oC";
sheet.Cells(3,50) = "NWL5";
sheet.Cells(4,50) = "0.05 m";
sheet.Cells(1,51) = "Ch411";
sheet.Cells(2,51) = "% rh";
sheet.Cells(3,51) = "NWL5";
sheet.Cells(4,51) = "0.05 m";
sheet.Cells(1,52) = "Ch412";
sheet.Cells(2,52) = "oC";
sheet.Cells(3,52) = "SET5";
sheet.Cells(4,52) = "0.05 m";
sheet.Cells(1,53) = "Ch413";
sheet.Cells(2,53) = "% rh";
sheet.Cells(3,53) = "SET5";
sheet.Cells(4,53) = "0.05 m";
sheet.Cells(1,54) = "Ch414";
sheet.Cells(2,54) = "oC";
sheet.Ce
```

```
sheet.Cells(4,54) = "0.05 m";
sheet.Cells(1,55) = "Ch415";
sheet.Cells(2,55) = "% rh";
sheet.Cells(3,55) = "SEL5";
sheet.Cells(4,55) = "0.05 m";
```

```
53 at: I2  Formula "now()"
Formula: now()
54 at: J5  Formula "mday(aDate)"
Formula: mday(aDate)
55 at: J5  Formula "month(aDate)"
Formula: month(aDate)
56 at: J6  To String "To String"
Transactions: WRITE TEXT b+"m"+a+"d-new" STR
57 at: H6  Formula "Formula"
Formula: A-300
58 at: F5  Formula "Formula3"
Formula: 17 lines.
 sheet.Cells(B+5,40) = RH[0]*100-40;
 sheet.Cells(B+5,41) = RH[1]*100;
 sheet.Cells(B+5,42) = RH[2]*100-40;
 sheet.Cells(B+5,43) = RH[3]*100;
 sheet.Cells(B+5,44) = RH[4]*100-40;
 sheet.Cells(B+5,45) = RH[5]*100;
 sheet.Cells(B+5,46) = RH[6]*100-40;
 sheet.Cells(B+5,47) = RH[7]*100;
 sheet.Cells(B+5,48) = RH[8]*100-40;
 sheet.Cells(B+5,49) = RH[9]*100;
 sheet.Cells(B+5,50) = RH[10]*100-40;
 sheet.Cells(B+5,51) = RH[11]*100;
 sheet.Cells(B+5,52) = RH[12]*100-40;
 sheet.Cells(B+5,53) = RH[13]*100;
 sheet.Cells(B+5,54) = RH[14]*100-40;
 sheet.Cells(B+5,55) = RH[15]*100;

59 at: A1  Unknown "Parse Error"
60 at: E5  Formula "Set up the columns2' name"
Formula: 169 lines.
 sheet.Cells(1,56) = "Ch505:";
 sheet.Cells(2,56) = "oC";
 sheet.Cells(3,56) = "Small 1";
 sheet.Cells(4,56) = "7 m";
 sheet.Cells(1,57) = "Ch506";
 sheet.Cells(2,57) = "oC";
 sheet.Cells(3,57) = "Small 2";
 sheet.Cells(4,57) = "6  m";
 sheet.Cells(1,58) = "Ch507";
 sheet.Cells(2,58) = "oC";
 sheet.Cells(3,58) = "Small 3";
 sheet.Cells(4,58) = "5 m";
 sheet.Cells(1,59) = "Ch508";
 sheet.Cells(2,59) = "oC";
 sheet.Cells(3,59) = "Small 4";
 sheet.Cells(4,59) = "4 m";
 sheet.Cells(1,60) = "Ch509";
 sheet.Cells(2,60) = "oC";
 sheet.Cells(3,60) = "Small 5";
 sheet.Cells(4,60) = "3 m";
 sheet.Cells(1,61) = "Ch510";
 sheet.Cells(2,61) = "oC";
 sheet.Cells(3,61) = "Small 6";
 sheet.Cells(4,61) = "2 m";
 sheet.Cells(1,62) = "Ch511";
 sheet.Cells(2,62) = "oC";
 sheet.Cells(3,62) = "Small 7";
 sheet.Cells(4,62) = "1 m";
 sheet.Cells(1,63) = "Ch600";
 sheet.Cells(2,63) = "oC";
 sheet.Cells(3,63) = "  ";
 sheet.Ce
```

```
sheet.Cells(1,64) = "Ch601";
sheet.Cells(2,64) = "oC";
sheet.Cells(3,64) = "   ";
sheet.Cells(4,64) = "   ";
sheet.Cells(1,65) = "Ch602";
sheet.Cells(2,65) = "oC";
sheet.Cells(3,65) = "   ";
sheet.Cells(4,65) = "   ";
sheet.Cells(1,66) = "Ch603";
sheet.Cells(2,66) = "oC";
sheet.Cells(3,66) = "   ";
sheet.Cells(4,66) = "   ";
sheet.Cells(1,67) = "Ch604";
sheet.Cells(2,67) = "oC";
sheet.Cells(3,67) = "   ";
sheet.Cells(4,67) = "   ";
sheet.Cells(1,68) = "Ch605";
sheet.Cells(2,68) = "oC";
sheet.Cells(3,68) = "   ";
sheet.Cells(4,68) = "   ";
sheet.Cells(1,69) = "Ch606";
sheet.Cells(2,69) = "oC";
sheet.Cells(3,69) = "   ";
sheet.Cells(4,69) = "   ";
sheet.Cells(1,70) = "Ch607";
sheet.Cells(2,70) = "oC";
sheet.Cells(3,70) = "   ";
sheet.Cells(4,70) = "   ";
sheet.Cells(1,71) = "Ch608";
sheet.Cells(2,71) = "oC";
sheet.Cells(3,71) = "   ";
sheet.Cells(4,71) = "   ";
sheet.Cells(1,72) = "Ch609";
sheet.Cells(2,72) = "oC";
sheet.Cells(3,72) = "   ";
sheet.Cells(4,72) = "   ";
sheet.Cells(1,73) = "Ch610";
sheet.Cells(2,73) = "oC";
sheet.Cells(3,73) = "   ";
sheet.Cells(4,73) = "   ";
sheet.Cells(1,74) = "Ch611";
sheet.Cells(2,74) = "oC";
sheet.Cells(3,74) = "   ";
sheet.Cells(4,74) = "   ";
sheet.Cells(1,75) = "Ch612";
sheet.Cells(2,75) = "oC";
sheet.Cells(3,75) = "   ";
sheet.Cells(4,75) = "   ";
sheet.Cells(1,76) = "Ch613";
sheet.Cells(2,76) = "oC";
sheet.Cells(3,76) = "   ";
sheet.Cells(4,76) = "   ";
sheet.Cells(1,77) = "Ch614";
sheet.Cells(2,77) = "oC";
sheet.Cells(3,77) = "   ";
sheet.Cells(4,77) = "   ";
sheet.Cells(1,78) = "Ch615";
sheet.Cells(2,78) = "oC";
sheet.Cells(3,78) = "   ";
sheet.Cells(4,78) = "   ";
sheet.Cells(1,79) = "Ch700";
sheet.Cells(2,79) = "oC";
sheet.Cells(3,79) = "   ";
sheet.Cells(4,79) = " ";
sheet.Cells(1,80) = "Ch701";
sheet.Cells(2,80) = "% rh";
sheet.Cells(3,80) = "   ";
sheet.Cells(4,80) = "   ";
sheet.Cells(1,81) = "Ch702";
sheet.Cells(2,81) = "oC";
sheet.Cells(3,81) = "   ";
sheet.Cells(4,81) = "   ";
sheet.Cells(1,82) = "Ch703";
sheet.Cells(2,82) = "% rh";
sheet.Cells(3,82) = "   ";
sheet.Cells(4,82) = " ";
sheet.Cells(1,83) = "Ch704";
sheet.Cel
```

```
sheet.Cells(3,83) = "  ";
sheet.Cells(4,83) = "  ";
sheet.Cells(1,84) = "Ch705";
sheet.Cells(2,84) = "% rh";
sheet.Cells(3,84) = "  ";
sheet.Cells(4,84) = "  ";
sheet.Cells(1,85) = "Ch706";
sheet.Cells(2,85) = "oC";
sheet.Cells(3,85) = "  ";
sheet.Cells(4,85) = "  ";
sheet.Cells(1,86) = "Ch707";
sheet.Cells(2,86) = "% rh";
sheet.Cells(3,86) = "  ";
sheet.Cells(4,86) = "  ";
sheet.Cells(1,87) = "Ch708";
sheet.Cells(2,87) = "oC";
sheet.Cells(3,87) = "  ";
sheet.Cells(4,87) = "  ";
sheet.Cells(1,88) = "Ch709";
sheet.Cells(2,88) = "% rh";
sheet.Cells(3,88) = "  ";
sheet.Cells(4,88) = "  ";
sheet.Cells(1,89) = "Ch710";
sheet.Cells(2,89) = "oC";
sheet.Cells(3,89) = "   ";
sheet.Cells(4,89) = "  ";
sheet.Cells(1,90) = "Ch711";
sheet.Cells(2,90) = "% rh";
sheet.Cells(3,90) = "  ";
sheet.Cells(4,90) = "  ";
sheet.Cells(1,91) = "Ch712";
sheet.Cells(2,91) = "oC";
sheet.Cells(3,91) = "  ";
sheet.Cells(4,91) = "  ";
sheet.Cells(1,92) = "Ch713";
sheet.Cells(2,92) = "% rh";
sheet.Cells(3,92) = "  ";
sheet.Cells(4,92) = "  ";
sheet.Cells(1,93) = "Ch714";
sheet.Cells(2,93) = "oC";
sheet.Cells(3,93) = "  ";
sheet.Cells(4,93) = " ";
sheet.Cells(1,94) = "Ch715";
sheet.Cells(2,94) = "% rh";
sheet.Cells(3,94) = "  ";
sheet.Cells(4,94) = "  ";
sheet.Cells(1,95) = "Ch212";
sheet.Cells(2,95) = "oC";
sheet.Cells(3,95) = " Channel ";
sheet.Cells(4,95) = "  ";
```

```
at: G5  Formula "Formula32"
Formula: 17 lines.
sheet.Cells(B+5,79) = RH[0]*100-40;
sheet.Cells(B+5,80) = RH[1]*100;
sheet.Cells(B+5,81) = RH[2]*100-40;
sheet.Cells(B+5,82) = RH[3]*100;
sheet.Cells(B+5,83) = RH[4]*100-40;
sheet.Cells(B+5,84) = RH[5]*100;
sheet.Cells(B+5,85) = RH[6]*100-40;
sheet.Cells(B+5,86) = RH[7]*100;
sheet.Cells(B+5,87) = RH[8]*100-40;
sheet.Cells(B+5,88) = RH[9]*100;
sheet.Cells(B+5,89) = RH[10]*100-40;
sheet.Cells(B+5,90) = RH[11]*100;
sheet.Cells(B+5,91) = RH[12]*100-40;
sheet.Cells(B+5,92) = RH[13]*100;
sheet.Cells(B+5,93) = RH[14]*100-40;
sheet.Cells(B+5,94) = RH[15]*100;
```

```
62 at: A1  Unknown "Parse Error"
63 at: G6  Formula "Formula22"
└ Formula: 26 lines.
  ├ sheet.Cells(B+5,56) = small[0];
  ├ sheet.Cells(B+5,57) = small[1];
  ├ sheet.Cells(B+5,58) =small[2];
  ├ sheet.Cells(B+5,59) = small[3];
  ├ sheet.Cells(B+5,60) = small[4];
  ├ sheet.Cells(B+5,61) = small[5];
  ├ sheet.Cells(B+5,62) = small[6];
  ├ sheet.Cells(B+5,63) = Card6[0];
  ├ sheet.Cells(B+5,64) = Card6[1];
  ├ sheet.Cells(B+5,65) = Card6[2];
  ├ sheet.Cells(B+5,66) = Card6[3];
  ├ sheet.Cells(B+5,67) = Card6[4];
  ├ sheet.Cells(B+5,68) = Card6[5];
  ├ sheet.Cells(B+5,69) = Card6[6];
  ├ sheet.Cells(B+5,70) = Card6[7];
  ├ sheet.Cells(B+5,71) = Card6[8];
  ├ sheet.Cells(B+5,72) = Card6[9];
  ├ sheet.Cells(B+5,73) = Card6[10];
  ├ sheet.Cells(B+5,74) = Card6[11];
  ├ sheet.Cells(B+5,75) = Card6[12];
  ├ sheet.Cells(B+5,76) = Card6[13];
  ├ sheet.Cells(B+5,77) = Card6[14];
  ├ sheet.Cells(B+5,78) = Card6[15];
  ├
  ├
  └
64 at: A1  Unknown "Parse Error"
65 at: A1  Unknown "Parse Error"
```

u 03/Jul/2

ain: Recording1: Panel View

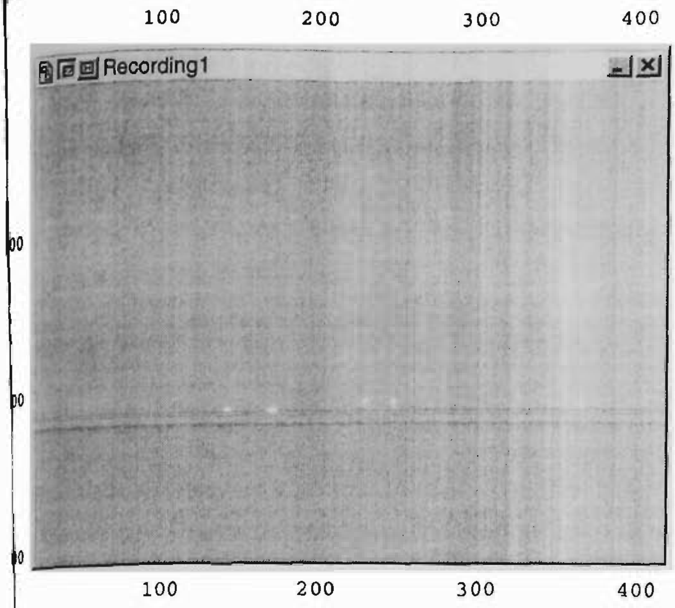

PanelView "Recording1" (w=410, h=300)

dex Page